EPRG-PRCI-APGA
23rd Joint Technical Meeting
Edinburgh, Scotland
6–10 June 2022

EPRG-PRCI-APGA
23rd Joint Technical Meeting
Edinburgh, Scotland • 6–10 June 2022

A COMPARISON OF REMOTE SENSING TECHNOLOGIES FOR SLOPE MONITORING
PAPER NUMBER: 35

Martin Derby*, GeoStabilization International
Mark Saunders, Golder Associates Inc.

* presenting author

ABSTRACT

Unstable slopes and landslides are having an increasing impact on our infrastructure in the United States. Infrastructure, such as natural gas pipelines, are sometimes located in difficult terrain with poor soil conditions, which are susceptible to potential slope movement (i.e., creep) and landslides. Recent increases and intensity of weather/precipitation have impacted the integrity of pipelines on unstable slopes by the increased soil saturation and porewater pressure in the slope soils. Numerous methods have been developed to monitor both infrastructure and the adjacent slope soils. In-situ or geotechnical instrumentation, such as inclinometers, and extensometers have been utilized to measure soil and rock movement for decades. Potential movement of pipelines and other structures are typically measured by strain gauges. In-situ measuring data can be obtained manually at pre-selected intervals or in "near real-time" with web-based deliverables. Recent advances with remote sensing techniques (spatial) and lasers have made it possible to obtain measurements in soil and rock surfaces without in-situ instrumentation. LiDAR (Light Detecting and Ranging) is an airborne method that scans a surface with a laser and measures distance by analyzing the reflected light. Ground-based (GB) InSAR (Interferometric Synthetic Aperture Radar) has been widely used in the mining industry to monitor slopes for movement and can quantify slope displacement over an extensive area. GBInSAR utilizes microwave technology to continuously scan a slope and monitor displacement and velocity in real time. InSAR is a satellite-based, remote sensing technology that can measure ground displacement over large regions. InSAR images can be obtained from orbiting satellites approximately every 14 days.

This research project will focus on a comparison of several in-situ methods and two remote sensing technologies, GBInSAR and InSAR. Survey points and extensometers were used to measure the changes in surface movements (i.e., tension cracks) over time, and then compared to GBInSAR data for accuracy. Increased moisture content (pore water pressure) plays an important role in the reduction of soil cohesion and soil strength within the slope. Monitoring precipitation and soil moisture are important factors in determining the root cause of slope movement and failures. This research project includes a comparison of spatial and in-situ monitoring systems that was performed on a steep slope with natural gas pipeline located in the Appalachian region of the United States. The overall objective of the comparison research is to determine the reliability of the remote sensing methods (GBInSAR and InSAR) compared with in-situ instrumentation for slope monitoring, that will ultimately reduce risk and increase pipeline infrastructure integrity.

DISCLAIMER

These Proceedings and any of the Papers included herein are for the exclusive use of EPRG, PRCI and APGA-RSC member companies and their designated representatives and others specially authorised to attend the JTM and receive the Proceedings. The Proceedings and Papers may not be copied or circulated to organisations or individuals not authorised to attend the JTM. The Proceedings and the Papers shall be treated as confidential documents and may not be cited in papers or reports except those published under the auspices of EPRG, PRCI or APGA-RSC.

1. EXECUTIVE SUMMARY

Geohazards, including unstable slopes and landslides, are having an increasing impact on our infrastructure in the United States and globally. Infrastructure, such as natural gas pipelines, are sometimes located in difficult terrain with poor soil conditions, which are susceptible to potential slope movement (i.e., creep) and landslides. Numerous methods have been developed to monitor both infrastructure and the adjacent soils and bedrock. Survey point (SP) or monuments, obtained manually or with Global Navigation Satellite System (GNSS), are typically used to measure surface movement of a slope. In-situ or geotechnical instrumentation, such as inclinometers, extensometers and piezometers have been utilized to measure soil and rock movement and pore pressure for decades. Potential movement of pipelines and other structures is typically measured by strain gauges or tilt meters. In-situ measuring data can be obtained manually at pre-selected intervals or in near "real-time" with web-based deliverables.

Recent advances with remote sensing techniques have made it possible to obtain measurements in soil and rock surfaces in three dimensions without in-situ instrumentation. Ground based (GB) InSAR (Interferometric Synthetic Aperture Radar) has been widely used in the mining industry to monitor slopes for movement and can quantify displacement over a region. GBInSAR utilizes microwave technology to continuously scan a slope and monitor displacement and velocity in near real time. Satellite based InSAR is a remote sensing technology for slope monitoring that has not been fully utilized by oil and gas operators due primarily to economics. Recent advances utilizing algorithms, and the launching of new satellites, have made the retrieval of satellite data more economical for end-users, including oil and gas operators.

The research field site was located at a previously identified unstable slope along a pipeline ROW in eastern Ohio. The research was carried out over the course of a five-month monitoring period which included a post-construction monitoring period along with an InSAR data report. The primary objective of this project was to perform a comparison study utilizing the GBInSAR and InSAR remote sensing techniques and in-situ instrumentation and determine the reliability of the GBInSAR data, and in-situ instrumentation data to the original GNSS survey measurements.

Based on the results observed from the SP's and GBInSAR displacements it was decided to categorize the agreements based on three levels. The levels of agreement include 1, 2, and 3 and are summarized below:

Level 1 – agreement indicates the survey point movement direction and displacement matches with the GBInSAR cell movement direction and displacement.

Level 2 – agreement indicates either the survey point movement direction or displacement matches with the GBInSAR cell movement direction or displacement.

Level 3 - neither the survey point movement direction or displacement matches with the GBInSAR cell movement direction and displacement.

The level analysis includes 19 SP's. Level 1 agreement includes six (6) SP's where the movement direction and displacement value match well against the GBInSAR data. Level 2 agreement contains 11 of the 19 SP's and is based on good agreement between either the movement direction or displacement between the SP and GBInSAR data. Level 3 contains only two (2) SP's showing poor correlation between the SP and GBInSAR movement direction and displacement.

For the pre-construction period, the GBInSAR data showed good agreement between the displacement time series and SP. There are several points that did not show good correlation, and this can mostly be attributed to high vegetation on the slope during monitoring. The high irregular vegetation causes low amplitude and inconsistent radar reflections reducing the reflected amplitude. Rain data and soil moisture probe data show good agreement with each other; however, no discernible correlation was observed with the GBInSAR data. This may be related to the amount of rainfall not being significant enough to cause movement at this site or infiltration rates are low. This is evident as the soil moisture probes responded to rain events, but the units were only buried approximately 15.24cm (6 inches) in the ground. Overall, the amount of rainfall observed over the three-month monitoring period was not considered significant with the largest single event at 4.57cm (1.8 inches). The extensometer data set showed elongation between 1.52cm and 2.54cm (0.6 inches and 1 inch. This amount of displacement over the monitoring period is relatively small and correlates well with the localized minimal movement of the GBInSAR data near these locations.

Interferometric synthetic aperture radar (InSAR) is a satellite-based remote sensing technology that is used to monitor ground displacement/movement, generally over large geographic regions. 3vGeomatics (3vG) was subcontracted to provide satellite images and analysis of the site, before, during, and after the research monitoring period. A total of 19 descending (west-looking) images, and 6 (six) ascending (east-looking) images were acquired. 3vG concluded that the InSAR data shows strong displacement on the slope of interest, which has been occurring since early 2020. Displacement amounts ranging from -5.1cm/yr up to -25.4cm (-2 inches/year up to -10 inches/year) (movement away from the satellite) were observed in the InSAR data.

The GBInSAR and InSAR data both showed displacement over the site. In general, the InSAR data showed good results and correlation with the GBInSAR. The InSAR displacement map shows clear movement between 5.1cm to 25.4cm/year (2 to 10 in/year) over the field site, in correlation with observed GBInSAR values with an average between 12.7cm to 25.4cm (5-10 inches) near SP 5 and SP 8.

In conclusion, this project has attempted to integrate multiple in-situ instruments along with two state of the art remote sensing monitoring systems, GBInSAR and InSAR. The project was a unique opportunity to examine and monitor an unstable slope both during and after construction remediation activities. In general, the remote sensing technologies were able to capture movement over the area of interest and show displacement trends in the data over their respective time series. There was not a general one to one correlation between the in-situ measurements and the remote sensing measurements as the in-situ measurements are point source monitoring. However, both the GBInSAR and InSAR datasets measured slope movement trends over their respective time series. Both GBInSAR and InSAR were affected by slope vegetation to varying degrees. Based on these results both remote sensing technologies can serve to collect meaningful and reliable data along unstable slopes on pipeline ROWs, for both short-term (high-risk slopes) and long-term monitoring.

2. INTRODUCTION

One of the most common geohazards that affects natural gas pipelines is unstable slopes [1]. A significant factor causing pipeline failures in the United States is landslides [2]. Landslides are generally caused by a downward movement of soil and rock as a response to a gravitational force and intense precipitation [3]. Landslides and unstable slopes are having an increasing impact on our infrastructure (e.g., pipelines) in the US, including the Appalachian Plateau region. Natural gas pipelines are located in difficult terrain (i.e., steep slopes) with poor soils and rock conditions, which are susceptible to potential slope movement. Slope movement can potentially be a threat to the pipeline integrity if the threats are not investigated and properly remediated [4]. Slow earth flow or slump are the most common types of landslides within the Appalachian Plateaus Province (see Figure 1), which is the most severe for landsliding in the US [5]. Precipitation in the Appalachian region ranges from 890 to 1140 mm per year (35 to 45 inches per year), which generally occurs in late winter and early spring, which then contributes to an area of major landslide severity [6].

Figure 1 - Appalachian Plateau physiographic province (hatched area) [6]

The Marcellus Shale, which is located within the Appalachian Plateau and Basin, is an organic rich formation (see Figure 2) that has been extensively explored and drilled and is currently a vital natural gas producing formation in the United States [7]. The natural gas wells within the Marcellus Shale region require a pipeline or a "gathering line" to transport the natural gas to an offsite location/compressor station and are often located in remote areas with steep terrain. As more natural gas wells are drilled, more pipelines will be required. Slope monitoring with instrumentation is important for observing changing slope conditions that could potentially lead to total pipeline failure [8].

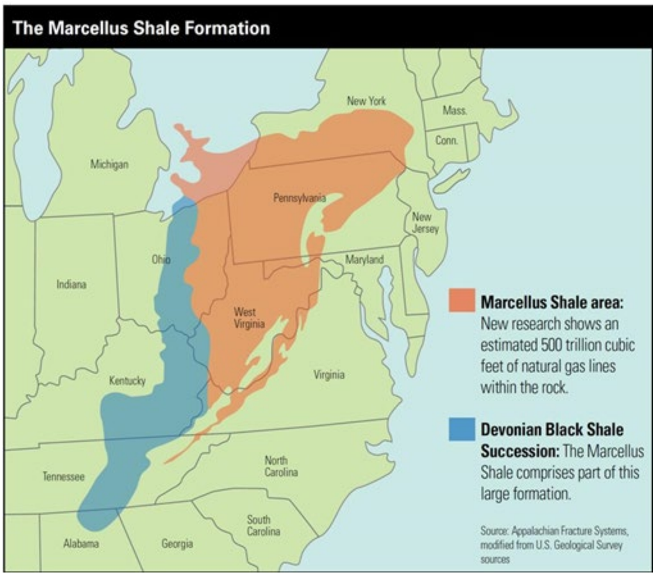

Figure 2 - The Marcellus Shale Formation (USGS)

Cawood [9], explains that monitoring of slopes gives advanced warning before slope failure, but it also depends on the ability of the monitoring system. Many types of infrastructure, not just pipelines and pipeline facilities, have been impacted by landslides/unstable slopes throughout the Appalachian Basin region.

Modern technologies are assisting in the location of future landslides, which can be difficult to predict [10]. A geohazard assessment or analysis is typically performed on the pipeline corridor and prior to construction to determine potential existing integrity issues. A geohazard assessment is used to characterize the landslide/unstable slopes (and other types of geohazards) to determine the potential impact on a given infrastructure. Geohazard assessments follow a phased approach, beginning with a desktop analysis [11]. The desk-top review includes bedrock maps, landslide maps, LiDAR data and aerial photography.

Once the landslides are defined and delineated within a given area, then a Phase II program is performed (a site-specific visit to confirm the observations from the Phase I program). The Phase II program includes the identification/mapping of scarps, tension cracks, seeps, hummocky terrain, toe area, and flanks. Once the landslide/unstable slope characteristics have been identified, then a Phase III program can be performed (subsurface investigation). However, it may be deemed that monitoring with instrumentation may be more appropriate for the site/pipeline. A pipeline corridor or right-of-way (ROW) typically ranges from 30.5m to 45.7m (100 to 150 feet) wide, and the length of a geohazard analysis will typically vary from a few kilometers (miles) to a few hundred kilometers (miles). Typical landslide observations include (from the top of the slope proceeding downward): crown, scarp, right and left flanks, rupture surface, transverse or tension cracks zone of depletion, zone of accumulation and the toe of the slope.

This research focused on the utilization of some well-established monitoring in-situ techniques (i.e., survey points, extensometers, etc.), and the addition of remote sensing techniques (i.e., GBInSAR and InSAR) for this detailed research project.

The centerpiece of the monitoring research project is the GBInSAR. InSAR has been used previously in landslide research to determine movement/displacement rates of slow-moving landslides. Girven [12] compared and corelated satellite InSAR deformation data of high spatial and temporal resolution of four slow-moving landslides in Berkeley Hills, CA. The research concluded that InSAR can be used to determine landslide deformation rates over time and that significant acceleration occurs as a result of precipitation, with an observed time lag (approximately 30 days).

There have been several studies focused on utilizing GBInSAR for both slope monitoring and understanding landslide characteristics. For example, Romeo et al. [13], performed a detailed study on the comparison of GBInSAR to extensometers, but did not include the monitoring with inclinometers or the effects on precipitation. This research will include a more comprehensive look at surface slope movement, effects on precipitation, and the reliability of the GBInSAR to monitor high risk slopes containing natural gas pipelines.

Introduction to Slope Monitoring Methods

There are numerous methods for monitoring slope movement along pipeline right-of-way's (ROW). Well established in-situ methods such as survey points and inclinometers can monitor and measure discrete movement of the slope soils. Strain gauges are typically used to monitor pipeline lateral and horizontal movements along with stress on the pipeline. Measurements can be made manually at pre-selected intervals or in real-time. However, in-situ monitoring data, which obtained at a given point source, does not give an overall view of the slope geodynamics.

Recent advances in remote sensing technologies such as aerial-based LiDAR have greatly increased the ability to observe landslide movement within and around pipeline corridors. The LiDAR technology uses pulsed laser light to illuminate a known target and then measures the return of the reflected light or pulses [14]. The LiDAR technology is able remove the vegetation and produce an earth digital elevation model or map. LiDAR is usually obtained from a fixed wing aircraft and more recently by unmanned aerial vehicles (UAVs). InSAR (interferometric synthetic aperture radar) is a satellite-based technology, that uses two (or more) SAR images to generate maps that may indicate ground surface movement or deformation. InSAR images from a given site are based on the satellite orbits and can range from 4 to 14 days. Both remote sensing technologies can be utilized from "pre-selected" dates and are not in "near real-time".

One technology that could provide "near real-time" data for monitoring a slope is with a ground based InSAR system or what is commonly known as GBInSAR (or Terrestrial InSAR/TInSAR). GBInSAR has been used extensively for monitoring mine slopes for more than a decade, in locations around the globe. Additionally, the GBInSAR system has been recently used to monitor high-risk slopes relating to the transportation industry.

Early discussions were held several years ago with a GBInSAR manufacture on the potential for monitoring high-risk slopes for the pipeline industry. A research idea/vision was developed after the principal investigator spoke with pipeline operators, university research professionals, research organizations (the PRCI) and various geohazard professionals.

Initial discussions with the PRCI occurred in 2018, which was then followed by several subsequent presentations to the Surveillance, Operations and Monitoring (SOM) section of the PRCI. Each presentation furthered detailed the research and how the research was going to be conducted. The general purpose of this research (May 15, 2019) emerged as follows:

"To conduct a comparison of slope (geohazard) monitoring methods using both in-situ and remote sensing technologies, and the ultimate goal for operators to choose the most appropriate geohazard monitoring technology for a given site, that can be based on accuracy, reliability and economics."

This research project will provide pipeline owners and operators the ability to use another potential monitoring tool for monitoring high-risk slopes that will ultimately reduce risk and increase pipeline integrity. This report will include: the purpose and site history including the site geology; the research approach; the monitoring instrumentation; data analysis and results; conclusions and future recommendations.

Site History

Following a geohazard monitoring research presentation (October 2019), a member of the PRCI approached the principal investigator with a potential site. After further discussion with the PRCI, it was determined that the site in question would be a suitable site to conduct the geohazard monitoring research. The agreement with the PRCI and Golder was signed in May 2020, and the initial site visit was conducted shortly thereafter.

The GBInSAR was mobilized to the site on June 9, 2020, and commenced with collection of data on June 11th. Ten reflectors were installed throughout the slope on June 12th, and the site rain gage, moisture point sensors (3), and extensometers (4) were set up on June 17th. Weekly to bi-weekly visits were made to the site to download the rain gage data, obtain extensometer measurements, check on the GBInSAR (including the solar panels), and to check on the general slope conditions (i.e., tension cracks, etc.). Survey/GNSS data were obtained once a week from the 19 SP's, (from an independent licensed surveyor). Figure 3 shows an overview of the slope and identified landslide of the site. Figure 4 shows a view from the GBInSAR looking east towards the slope. Figure 5 is a photograph of the slope looking west with a radar reflector in the foreground.

The owner/operator of the site indicated to the research team that the slope was going to mitigation, and construction would commence on September 11, 2020. The last day of measurements occurred on September 10, 2020. During the mitigation period, the owner/operator indicated that they would like the research team to collect data after the construction was completed (hereinafter referred to as post-construction monitoring period). Post-construction commenced on November 30, 2020, and was completed on January 24, 2021. During the course of the post-construction monitoring, the research team was notified that an InSAR dataset was available to the project team. In June 2021, Golder was issued a change order to include the InSAR data, and a report was provided by 3vG which is summarized in this report.

LEGEND

- Identified Landslide Area
- Natural Gas Pipeline
- Limits of Disturbance and Permanent Easement (Right-of-Way)

0 40 80
1 " = 40 FEET
FEET

REFERENCE(S)

1. GOLDER ASSOCIATES INC. (IDENTIFIED LANDSLIDE AREA)
2. MOTT MCDONALD (STATIONING, LOD, ROW)
3. CONFIDENTIAL CLIENT (NATURAL GAS PIPELINE)
4. OGRIP (OSIP III 2020 AERIAL IMAGERY)
5. COORDINATE SYSTEM: NAD83 2011 UTM ZONE 17N FT

CONSULTANT

GOLDER

YYYY-MM-DD	2021-02-24
DESIGNED	TL
PREPARED	TL
REVIEWED	MS
APPROVED	MD

CLIENT

PIPELINE RESEARCH COUNCIL INTERNATIONAL, INC. ("PRCI")
15059 CONFERENCE CENTER DRIVE, SUITE 130,
CHANTILLY, VA 20151

PROJECT

A COMPARISON BETWEEN IN-SITU INSTRUMENTATION AND REMOTE SENSING METHODS FOR SLOPE MONITORING WITHIN A PIPELINE RIGHT-OF-WAY
PROJECT NO. PR635-203904
CONTRACT NO. GHZ-2-05

TITLE

SITE OVERVIEW MAP
PRE-CONSTRUCTION

PROJECT NO.	PHASE	REV.	FIGURE
20144586	006	A	3

IF THIS MEASUREMENT DOES NOT MATCH WHAT IS SHOWN, THE SHEET SIZE HAS BEEN MODIFIED FROM: ANSI B

1 in

Figure 4 - Site overview from the GBInSAR (looking east)

Figure 5 - Site overview from the top of the slope – with a reflector (looking west)

Ground-Based InSAR Introduction

GBInSAR

Monitoring ground displacements with the GBInSAR technology has been more widely accepted in the past several years [15]. GBInSAR is the primary slope monitoring method to be studied for this research report. The attributes of the GBInSAR technology include a proactive and early warning system in near real-time [16]. This technically advanced and innovative monitoring system, commonly known as GBInSAR (or sometimes called terrestrial SAR or TInSAR) is a slope monitoring system that measures both velocity and displacement in near real-time (readings approximately every 4 minutes – scan to processed data). The TInSAR and the terrestrial laser scanner are non-contact technologies for ground remote sensing [17]. GBInSAR monitoring systems have been utilized throughout the mining industry since 2010 and recently started to make traction in the transportation sector.

Equipment and Installation

The GBInSAR monitoring system (see Figure 6) for this research project is the IBIS-Rover by IDS GeoRadar. IDS designed the IBIS-Rover for a real time monitoring system that uses synthetic aperture radar [18]. This system includes an advanced atmospheric correction algorithm and provides displacement data to be accurate within a millimeter [18]. Some of the hardware features of the IBIS monitoring system include high spatial resolution (0.75m x 8.8m resolution cell at 1000m); long operating range (from 10m to 2,500m); rapid scan time (90 seconds); broad area coverage (14,000m2 at 2,500m); fully remote operation (wireless radio link); and self-powered option using solar panels, generator, and batteries.

Software and Data Output

The Guardian software package includes the following: zero delays in data processing and alarm generation, user defined built-in geotechnical analysis tools, georeferenced with 3D interactive data handling, and multiple alarm generation [18].

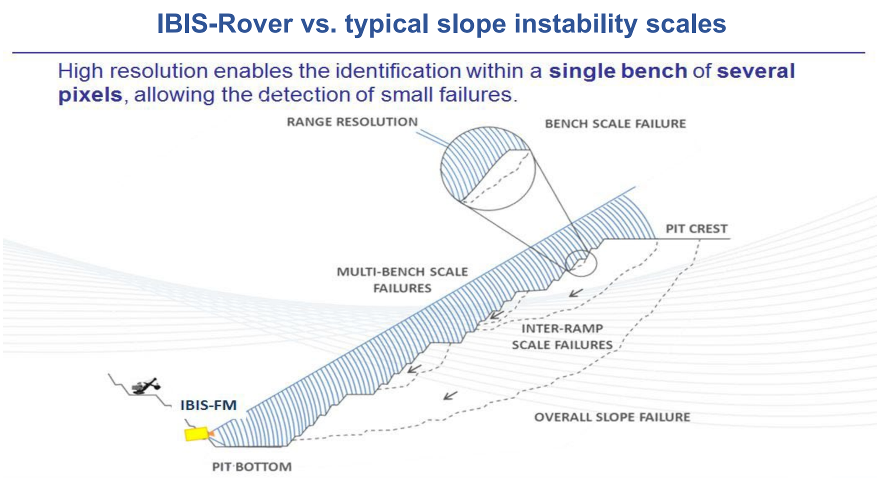

Figure 6 - IBIS-Rover located at the base of the slope with the range resolution (from IDS GeoRadar)

Slope movement trends that can be identified by the Guardian software include progressive (accelerating) displacement, steady movement, and regressive displacement [16]. A data comparison was performed on the results of each remote sensing dataset (i.e., GBInSAR) and with the RTK GNSS survey data, which is further defined in section 5.

Corner reflectors (Figure 7) were placed to assist in the signal assessment of a specific location and provide a validation of the microwave energy at that specific point. An array (ten) of corner reflectors were installed for triangulation for the sole purpose of increasing point accuracy.

Figure 7 - Corner Reflectors on a slope that is being monitored with GBInSAR

The data acquisition period with the GBInSAR was approximately three (3) months. Data were transmitted in real-time and downloaded on a daily basis.

GBInSAR has been utilized in the mining industry as an advanced movement and early warning system since 2010. The system is capable of continuous (24x7) sub-millimetric accuracy at distances of up to 4.5 km. The system can provide near real-time displacement and velocity images to track and monitor movement through the lifecycle of a project.

For this project the same technology was introduced to monitor a landslide over a pipeline ROW on a vegetated slope. The GBInSAR used for this research project was the IBIS Rover Radar unit from IDS GeoRadar North America as shown in Figure 8. IBIS stands for Image By Interferometric Survey. The unit consists of dual radar antennas positioned on a single sensor head which is mounted on a 1m (3.3 feet) long track. The sensor head progresses back and forth across the track to simulate radar units at two different positions.

Figure 8 - Set up of the IBIS-Rover at the field site

Past GBInSAR research for PRCI

A previous PRCI project, Catalog No. PR-271-143717-R01 was submitted by C-CORE titled "Ground Based Radar Monitoring of Pipeline Infrastructure" in June 2015. The project used GBInSAR to monitor the movement of a building and pipeline located within a compressor station in California, USA. The study also compared the movement of the GBInSAR with traditional satellite InSAR analysis. The results of the GBInSAR data accurately monitored the movement within 1 mm accuracy.

3. VALUE TO MEMBERS

This landslide monitoring research is a comparison of traditional survey data, in-situ instrumentation, GBInSAR, and InSAR data. The research will present the accuracy and supporting data of using near "real-time" GBInSAR data and satellite InSAR remote monitoring technology and for monitoring active slopes with pipelines. This research data will give owners and operators the ability to select an appropriate landslide monitoring technology that can be based on accuracy, reliability and economics.
If a landslide is deemed as a high risk to a pipeline or a pipeline facility, which is based on the geohazard assessment or pipeline data (i.e., strain gauges and/or In-Line Inspection [ILI] data), then near "real-time" monitoring utilizing the GBInSAR technology may be appropriate. The GBInSAR will be able to monitor velocity and acceleration and produce displacement maps which may aid in determining if and when the landslide may impact the integrity of the asset (i.e., pipeline or pipeline facility).

This research also includes the presentation of satellite based InSAR data, along with a data comparison of GBInSAR to satellite InSAR.

4. APPROACH

4.1. Study Area

Regional/Site Geology and Slope Conditions
The Appalachian Plateaus Province or Appalachian Region is comprised of continental and oceanic fragments (from early and mid-Paleozoic geologic age – 475 to 375 million years) [19]. During this time period, thick deposits of carbonate rock were deposited beneath shallow seas, which was followed by receding shallow seas and the deposition of sedimentary strata [20].

The project site is located in eastern Ohio and within the Marcellus Shale region. The area in Ohio is known for steep and narrow valleys which makes it difficult to construct pipelines. According to the USGS geologic map, the site is underlain by the Conemaugh Group. The Ohio Geological Survey [21] defines the Conemaugh Group (Pc) of Pennsylvanian age and consisting of shale, siltstone, and mudstone. The group also contains minor amounts of sandstone (see Figure 9 for a field example), limestone, and coal. The strata adjacent the Conemaugh Group is the Monongahela Group (Pm).

Figure 9 - Bedrock Outcrop (sandstone) – Southeastern portion of the site

The Conemaugh Group (Pc) contains the well-known Pittsburgh red beds, which have a relative susceptibility to landsliding [22]. Pomeroy also classified the risks of landslides as "moderately high to severe". The red clays that originate from the Conemaugh Group have a relatively low permeability, with a relatively high porosity (as much as 40%), and a shear strength that decreases with excessive pore pressure [22].

The research study site includes a natural gas pipeline. The natural gas pipeline was installed in the slope in 2017. "In 2018, the testing results of the ILI data, indicated that potential lateral movement was occurring within the pipeline along the slope" [23].

Nineteen survey points (SP) and five inclinometers were installed in November 2019 and survey data collected once a week and tabulated. Prior to May 2020, the slope was moving at a rate of approximately one inch per week. This rate of movement makes this an ideal research site to monitor and collect geospatial slope movement data with both in-situ instruments and GBInSAR.

4.2. Pre-Construction Instrumentation

The instrumentation field data collection was performed over a three-month timeframe at the site. Instrumentation used in this portion of the study consisted of both in-situ and remote sensing slope monitoring. The following is a breakdown of the instrumentation used for the research project:

- GBInSAR
- Survey Points
- Extensometer Set Points
- Soil moisture Probes/Rain Gauge
- Inclinometers
- InSAR

Figure 10 shows the layout of each of the in-situ monitoring points across the field site to provide a reference for instrumentation across the site.

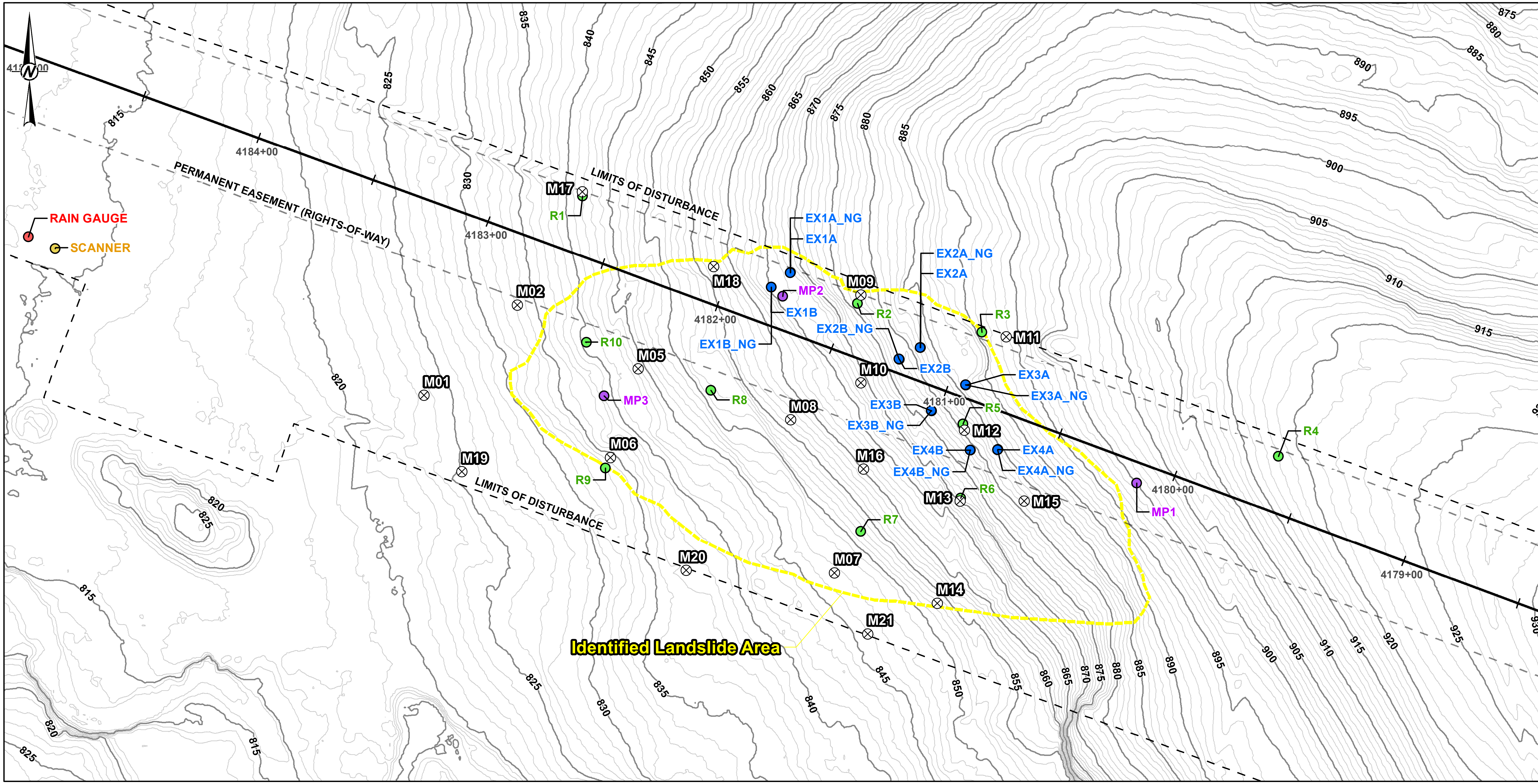

LEGEND

- ⊗ Pre-Construction Monitoring Point Location (2020-06-10)
- Extensometer
- Moisture Point
- Rain Gauge
- Reflector
- Scanner
- Identified Landslide Area
- Natural Gas Pipeline
- Limits of Disturbance and Permanent Easement (Right-of-Way)
- Elevation contour (5 ft Interval)
- Elevation contour (1 ft Interval)

0 40 80

1 " = 40 FEET FEET

REFERENCE(S)

1. GOLDER ASSOCIATES INC. (IDENTIFIED LANDSLIDE AREA, INSTRUMENT LOCATION, MONITORING POINT)
2. MOTT MCDONALD (STATIONING, LOD, ROW)
3. CONFIDENTIAL CLIENT (NATURAL GAS PIPELINE, CONTOUR)
4. COORDINATE SYSTEM: NAD83 2011 UTM ZONE 17N FT
5. SERVICE LAYER CREDITS: © OPENSTREETMAP (AND) CONTRIBUTORS, CC-BY-SA

CLIENT

PIPELINE RESEARCH COUNCIL INTERNATIONAL, INC. ("PRCI")
15059 CONFERENCE CENTER DRIVE, SUITE 130,
CHANTILLY, VA 20151

PROJECT

A COMPARISON BETWEEN IN-SITU INSTRUMENTATION AND REMOTE SENSING METHODS FOR SLOPE MONITORING WITHIN A PIPELINE RIGHT-OF-WAY
PROJECT NO. PR635-203904
CONTRACT NO. GHZ-2-05

CONSULTANT

GOLDER

YYYY-MM-DD	2021-02-24
DESIGNED	TL
PREPARED	TL
REVIEWED	MS
APPROVED	MD

TITLE

SITE MONITORING POINT OVERVIEW
PRE-CONSTRUCTION

PROJECT NO.	PHASE	REV.	FIGURE
20144586	006	A	10

IF THIS MEASUREMENT DOES NOT MATCH WHAT IS SHOWN, THE SHEET SIZE HAS BEEN MODIFIED FROM: ANSI B

GBInSAR

The GBInSAR was mobilized to the site on June 9, 2020, and commenced with collection of data on June 11 through September 10, 2020. IDS GeoRadar assisted Golder in the initial setup of the system hardware and software, and verified the system was operating correctly and transmitting the data to the IDS server in Golden, Colorado for processing and storage. The unit was setup in a stable location outside the influence of the slope movement. The trailer was secured and leveled prior to system initialization. Figure 11 shows the setup of the GBInSAR system and its orientation to the slope. Ten (10) corner reflectors were installed across the site as control points for the GBInSAR system. The reflectors provided a high reflectivity surface and shape to serve as control points for radar reflectivity or amplitude. The GBInSAR unit collected data continuously 24 hours a day and seven days a week at a scan frequency of approximately 90 seconds. The data were saved and transmitted to the offsite processing computer after each sample run. Alarms were set up on the offsite field processing computer to alert the team if the unit experienced a disruption from near real-time processing by email. The ability to remote login into the field computer controlling the data acquisition was also established to check on the status of the equipment such as solar charging input and fuel level. Once the system was running and confirmed collecting data, the GBInSAR was "hands-free" until the end of the monitoring session.

Figure 11 - Photograph of the GBInSAR with the slope in the background

Survey Points

The SP's (labeled as M on Figure 10) were installed by the site owner-operator in November 2019, prior to Golder implementing the GBInSAR data collection. The SP's were installed using traditional survey nails and surveyed using an RTK-GNSS system. SP's were surveyed approximately weekly until September 9th, 2020, when the site was shut down in preparation of construction activities. A total of 19 SP's were used in the analysis for in-situ slope monitoring. GNSS surveyed points indicate true 3D movement as the slope is moving. These points were used as the ground control basis for the GBInSAR comparison. Since operation of the GBInSAR did not commence until June 11, the June 10, 2020, survey date was used as the baseline measurement to correlate movement through the three-month monitoring period.

Extensometer Readings

A Geokon Model 1610 Tape Extensometer was used to measure the distance between two fixed rods at the site. The rods were approximately 1m (3 feet) in length and were inserted into the ground roughly 0.5m to 0.6m (1.6 – 2 foot) as vertical as possible with the subsurface conditions. The rods were threaded with an eyelet near the top to connect the two ends of the extensometer and take measurements. Four sets of rods were embedded across identified tension cracks on site to measure movement between the two fixed ends. The locations were named Extensometer-1AB, Extensometer-2AB, Extensometer-3AB, and Extensometer-4AB (see Figure 10). Figure 12 below shows an example of one of the extensometer setups in the field and measurement being recorded.

Figure 12 - Example of an extensometer reading

Soil Moisture Probes/Rain Gauge

As part of the in-situ instrumentation three (3) soil moisture probes were installed at the site with the purposes of attempting to monitor soil moisture conditions throughout the project. Onset HOBOnet Soil Moisture Temp Sensors were installed on the site. These units are solar powered wireless units that communicate with a sensor master device which collects each node sensor data every hour and then transmits that data cellularly to a cloud server every six hours.

The sensor probes were installed by digging a small 25cm (10-inch) hole and inserting the sensor into the side wall of the hole at a depth of approximately 15-20cm (6-8 inches). The hole was backfilled with soil and the units control box was mounted on a temporary PVC pole (the wireless control unit can be seen in Figure 12 above with black tape wrapped along the PVC pipe). Sensor communication was established through wireless line of sight, and cellular communication was confirmed before placing the sensor master. Data communications and uploads were confirmed before leaving the field.

An AcuRite digital rain gauge was installed at the site adjacent to the GBInSAR trailer. The unit is a self-emptying unit that can store daily rainfall amounts for retrieval at a later date. The unit was checked, and data were recorded at each visit to the site. The data are used to compare with the soil moisture probes and provide an overall record of rainfall for the site.

InSAR

InSAR is a remote sensing method using satellite-based acquisition systems capable of measuring displacement over time. InSAR analysis is performed by comparing two different time sequenced events to create a phase difference interferogram. The interferogram represents the difference in displacement between the two-time series. There are numerous satellite systems available to commercial users each with different frequencies each with specific advantages and disadvantages. For example, the ALOS-2 satellite collects data at a wavelength of 22.9 cm and is effective at capturing quality data through vegetation due to its longer wavelength when compared to other satellites.

It was voted by the PRCI committee to include a InSAR monitoring component into this research on June 30, 2021. A change order was issued and 3vG was contracted by Golder to provide InSAR data and report for the field site over the monitoring period. A summary of the report will be outlined in section 5 and included in Appendix D.

4.3. Post-Construction Instrumentation

Instrumentation used in the post-construction study consisted of both in-situ and remote sensing slope monitoring. Figure 13 shows the location of the post-construction monitoring equipment. The following is a breakdown of the instrumentation used for the research project. In many cases the setup was similar to the pre-construction setup and will not be repeated in this section.

- GBInSAR
- Survey Points
- Extensometer Readings
- Soil moisture Probes/Rain Gauge

GBInSAR

The dates of operation of the GBInSAR data collection were from November 30, 2020 – January 24, 2021. The initial setup of the system was the same for the pre-construction monitoring period. There were several periods of inactivity due to generator issues that occured during cold weather temperatures. Modifications were made to winterize the generator in the field in an attempt to supplement the lower solar input, which was not an issue during the summer months. It was decided to continue monitoring past the original 30 days to accommodate the loss in days due to the generator shutdown. A total of 40 days of monitoring were completed during the post-mitigation session. The missing dates are:

December 03, 2020 – December 05, 2020
December 15, 2020 – December 23, 2020; and
December 26, 2020 – December 30, 2021.

Survey Points

The SP's were installed by the site owner-operator on November 24, 2020. They were installed using traditional survey nails and surveyed using an RTK-GNSS system. SP's were surveyed approximately twice per week until January 19th, 2021, when the site was shut down due to survey completion. A total of 12 SP's with baseline movement greater than 0.15m (0.5 feet) were chosen in the analysis for movement control. GNSS surveyed points indicate true 3D movement as the slope is moving. These points were used as the ground control basis for the GBInSAR comparison.

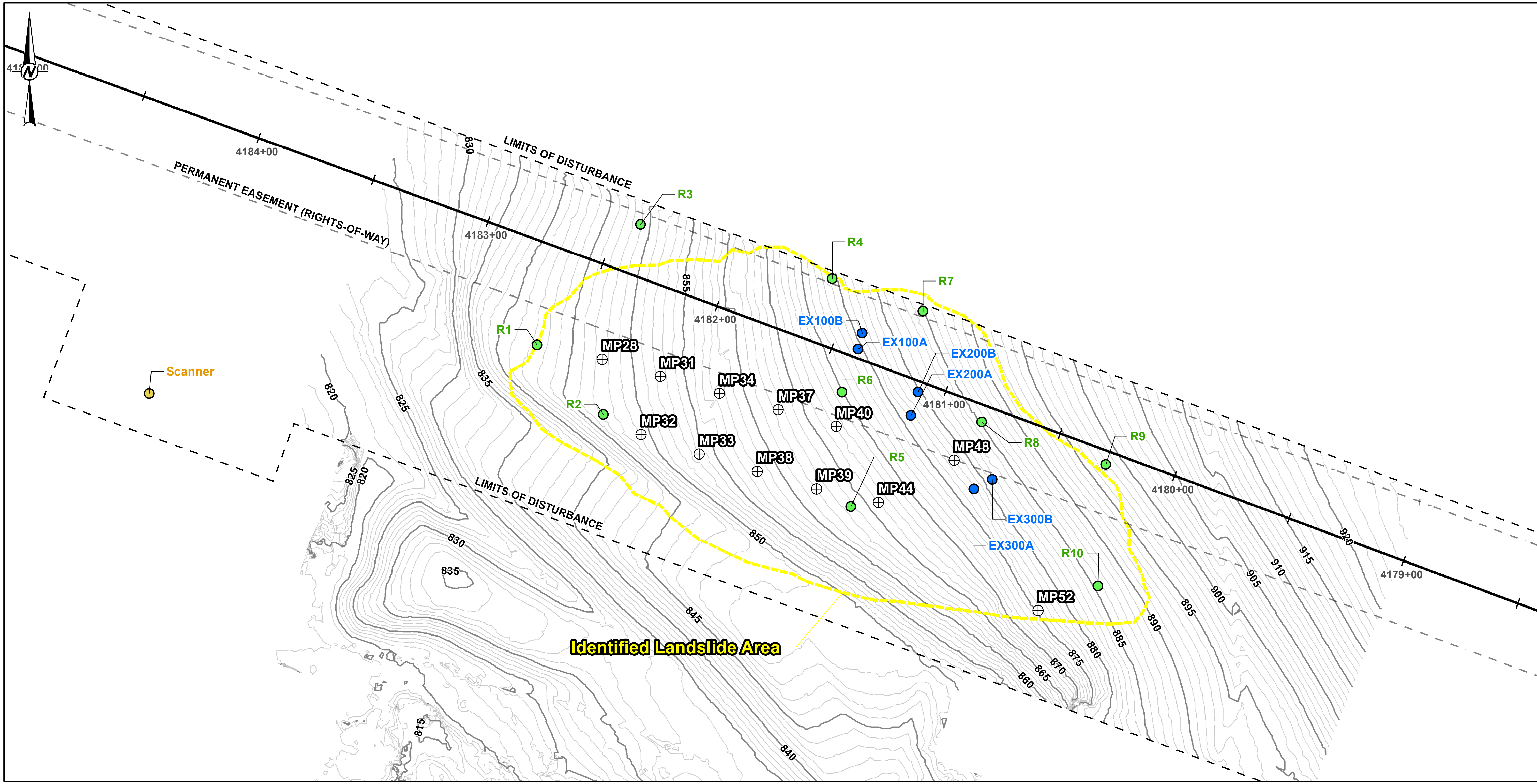

LEGEND

- ⊕ Post-Consturction Monitoring Point Location (2020-11-24)
- Extensometer
- Reflector
- Scanner
- Identified Landslide Area
- Natural Gas Pipeline
- Limits of Disturbance and Permanent Easement (Right-of-Way)
- Elevation contour (5 ft Interval)
- Elevation contour (1 ft Interval)

0 40 80

1 " = 40 FEET FEET

REFERENCE(S)

1. GOLDER ASSOCIATES INC. (IDENTIFIED LANDSLIDE AREA, INSTRUMENT LOCATION, MONITORING POINT)
2. MOTT MCDONALD (STATIONING, LOD, ROW)
3. CONFIDENTIAL CLIENT (NATURAL GAS PIPELINE, CONTOUR)
4. COORDINATE SYSTEM: NAD83 2011 UTM ZONE 17N FT
5. SERVICE LAYER CREDITS: © OPENSTREETMAP (AND) CONTRIBUTORS, CC-BY-SA

CONSULTANT

GOLDER

YYYY-MM-DD	2021-06-08
DESIGNED	TL
PREPARED	TL
REVIEWED	MS
APPROVED	MD

CLIENT

PIPELINE RESEARCH COUNCIL INTERNATIONAL, INC. ("PRCI")
15059 CONFERENCE CENTER DRIVE, SUITE 130,
CHANTILLY, VA 20151

PROJECT

A COMPARISON BETWEEN IN-SITU INSTRUMENTATION AND REMOTE SENSING METHODS FOR SLOPE MONITORING WITHIN A PIPELINE RIGHT-OF-WAY
PROJECT NO. PR635-203904
CONTRACT NO. GHZ-2-05

TITLE

SITE MONITORING POINT OVERVIEW
POST-CONSTRUCTION

PROJECT NO.	PHASE	REV.	FIGURE
20144586	007	A	13

Extensometer Readings

The post-construction extensometer instrumentation were installed on November 23, 2020. Three sets were established across visible tension cracks on the slope and are shown on Figure 14. The installation method was the same as in the pre-construction instrumentation surveying. Figure 14 below shows an example of the extensometer 300AB set up across an identified tension crack.

Figure 14 - Photo of Extensometer 300AB across tension crack

Soil Moisture Probes/Rain Gauge

The same soil moisture probes were used as in the pre-construction surveying and installed in a similar method. However, during the initial couple of days of operation, soil probe 1 stopped operating, and therefore only two soil moisture probes were used for post-construction monitoring.

An AcuRite digital rain gauge was installed at the site adjacent to the GBInSAR trailer. The unit is a self-emptying unit that can store daily rainfall amounts for later retrieval. The unit was checked and data were recorded at each visit to the site. The data are used to compare with the soil moisture probes and track overall precipitation.

5. INSTRUMENTATION RESULTS

The following section details the results from the in-situ and remote monitoring that occurred onsite during the pre and post-construction activities. The sections are separated based on pre and post-construction activities. Based on the number of individual comparisons performed only select example data set comparisons are provided in the sections below, and the remaining figures are located within their corresponding appendices.

Pre-Construction Results

The pre-construction field work commenced on June 10, 2021, and was completed on September 10, 2020. The following presents the results of pre-construction monitoring activities.

Comparison of GBInSAR and Survey Points

The results of the GBInSAR and the SPs are presented and compared together as traditional in-situ measurements and remote sensing GBInSAR data.

The SP data are used as a method to track survey control movement against the GBInSAR displacement data. Figure 15 presents a vector arrow map of the magnitude of the SP movement over the survey timeframe. Based on the data received from the survey company the movement of the SP's over the monitoring period ranged from 0.25- 9.65cm (0.1 – 3.8 inches).

The GBInSAR data processing for the radar cells takes place in the IDS Guardian software in which discussions on this process are available from published sources and will not be discussed in this report. Two main displays of the GBInSAR software analysis data include reflectivity amplitude and displacement. The reflectivity amplitude map shown in Figure 16 indicates the radar signal strength of the reflected signal in decibels (dB). The highest return signals are from the ten reflectors placed across the site. The area closest to the radar and the central portion of the site, in general, had good amplitude reflectivity. The high amplitude reflectivity was the sandstone rock outcrop in the bottom portion of the amplitude map (highlighted with white circle). This is a typical response when observing stable rock faces.

Figure 17 shows the total displacement map for the GBInSAR data over the monitoring period with the SP's plotted. The colorized cells correspond to displacement (inches) from the GBInSAR data. Negative displacement is movement away from the radar unit and positive displacement is movement toward the radar. Some general observations from this figure are as follows:

- Central portion of the ROW shows in general a movement trend away from the radar.
- The edges of the ROW are bounded by high displacement directly caused by high vegetation.
- Areas of movement are observed in the ROW that indicate movement toward the radar.

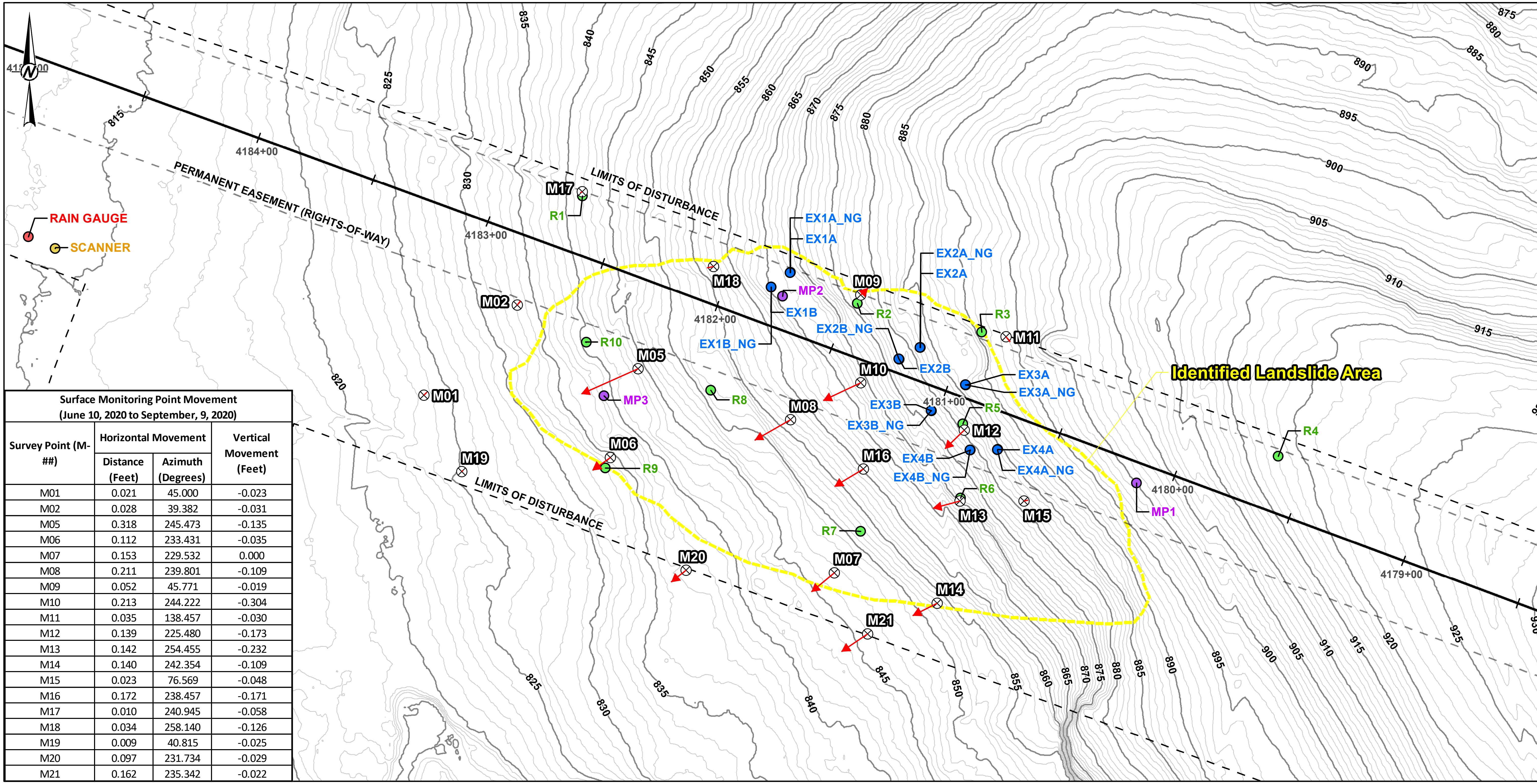

Surface Monitoring Point Movement (June 10, 2020 to September, 9, 2020)			
Survey Point (M-##)	Horizontal Movement		Vertical Movement (Feet)
	Distance (Feet)	Azimuth (Degrees)	
M01	0.021	45.000	-0.023
M02	0.028	39.382	-0.031
M05	0.318	245.473	-0.135
M06	0.112	233.431	-0.035
M07	0.153	229.532	0.000
M08	0.211	239.801	-0.109
M09	0.052	45.771	-0.019
M10	0.213	244.222	-0.304
M11	0.035	138.457	-0.030
M12	0.139	225.480	-0.173
M13	0.142	254.455	-0.232
M14	0.140	242.354	-0.109
M15	0.023	76.569	-0.048
M16	0.172	238.457	-0.171
M17	0.010	240.945	-0.058
M18	0.034	258.140	-0.126
M19	0.009	40.815	-0.025
M20	0.097	231.734	-0.029
M21	0.162	235.342	-0.022

LEGEND

- ⊗ Pre-Construction Monitoring Point Location (2020-06-10)
- Monitoring Point Movement - Direction and Proportional Distance (See Notes)
- Extensometer
- Moisture Point
- Rain Gauge
- Reflector
- Scanner
- Identified Landslide Area
- Natural Gas Pipeline
- Limits of Disturbance and Permanent Easement (Right-of-Way)
- Elevation contour (5 ft Interval)
- Elevation contour (1 ft Interval)

0 40 80
1 " = 40 FEET FEET

NOTE(S)

1. LENGTH OF SURVEY POINT MOVEMENT ARROWS (RED) ARE 80-TIMES LONGER THAN ACTUAL MEASUREMENTS (IE. 0.5 FT FIELD MEAURE SHOWS AS 40 FT ON THIS MAP, OR 1" = 0.5 FT OF MOVEMENT).

REFERENCE(S)

1. GOLDER ASSOCIATES INC. (IDENTIFIED LANDSLIDE AREA, INSTRUMENT LOCATION, MONITORING POINT, VECTOR MOVEMENT)
2. MOTT MCDONALD (STATIONING, LOD, ROW)
3. CONFIDENTIAL CLIENT (NATURAL GAS PIPELINE, CONTOUR)
4. COORDINATE SYSTEM: NAD83 2011 UTM ZONE 17N FT
5. SERVICE LAYER CREDITS: © OPENSTREETMAP (AND) CONTRIBUTORS, CC-BY-SA

CLIENT

PIPELINE RESEARCH COUNCIL INTERNATIONAL, INC. ("PRCI")
15059 CONFERENCE CENTER DRIVE, SUITE 130,
CHANTILLY, VA 20151

PROJECT

A COMPARISON BETWEEN IN-SITU INSTRUMENTATION AND REMOTE SENSING METHODS FOR SLOPE MONITORING WITHIN A PIPELINE RIGHT-OF-WAY
PROJECT NO. PR635-203904
CONTRACT NO. GHZ-2-05

CONSULTANT

GOLDER

YYYY-MM-DD	2021-02-25
DESIGNED	TL
PREPARED	TL
REVIEWED	MS
APPROVED	MD

TITLE

SITE MONITORING VECTOR MOVEMENT PRE-CONSTRUCTION

PROJECT NO.	PHASE	REV.	FIGURE
20144586	006	A	15

IF THIS MEASUREMENT DOES NOT MATCH WHAT IS SHOWN, THE SHEET SIZE HAS BEEN MODIFIED FROM: ANSI B

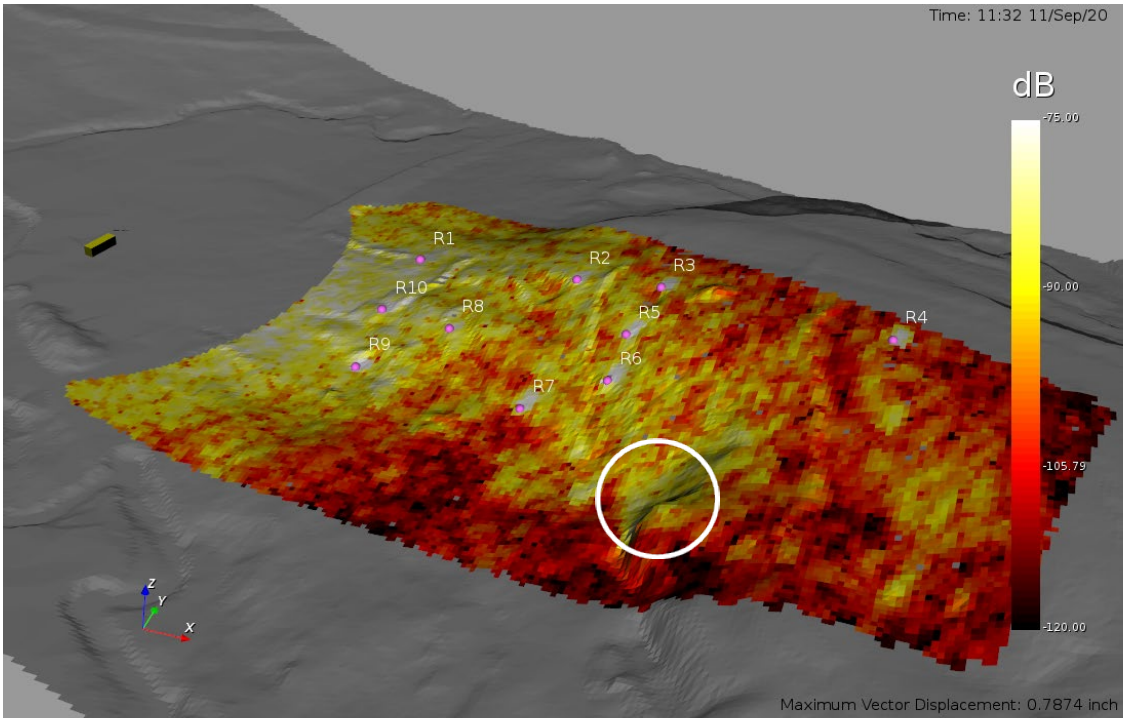

Figure 16 - Reflectivity amplitude of GBInSAR (north is in direction of Y axis – white circle indicates sandstone outcrop)

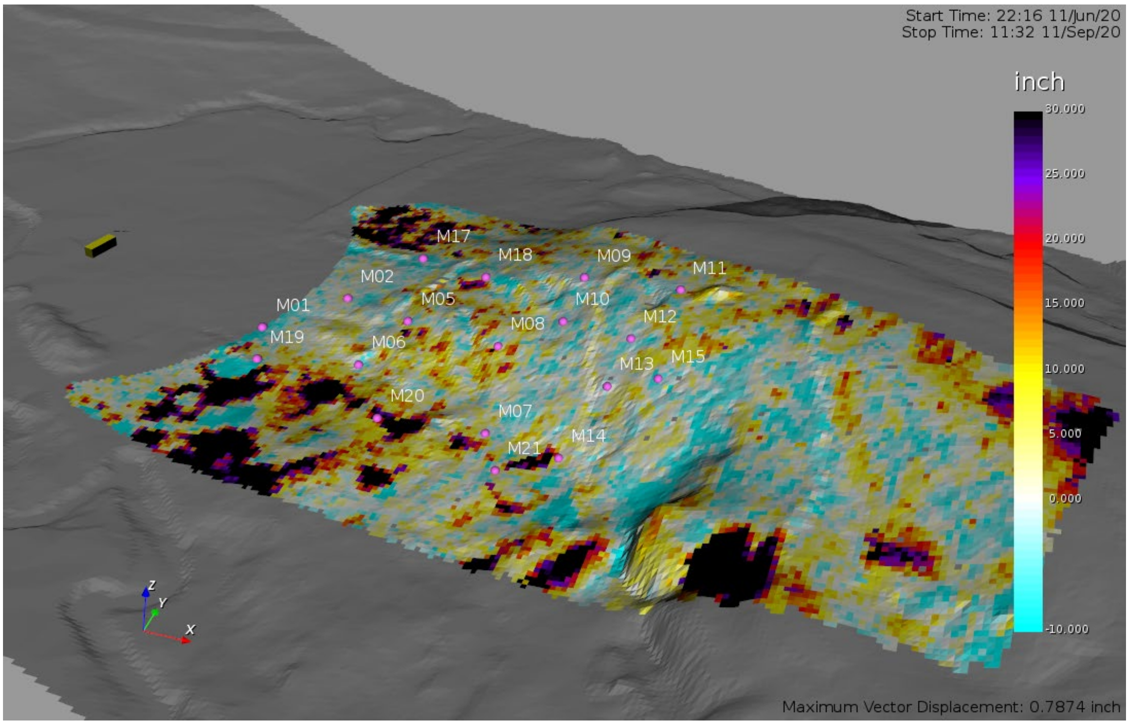

Figure 17 - Total displacement map over the monitoring period (north is in direction of Y axis)

GBInSAR data are plotted as a time series displacement graph with positive displacement as being representative of movement toward the radar and negative displacement as movement away from the radar unit. The GBInSAR data analysis was performed using the following methodology:

- Plot the baseline location of the SP on the radar displacement cell map.
- At the cell location where the SP plotted, a time series graph was extracted for that single cell. The time series graph shows the displacement over time of that particular radar cell.
- Based on the analysis of the single cell data it was decided to perform a secondary analysis on the radar data using a grid of 3x5 cells. For each SP time series graphs were extracted for each surrounding cell in the 3x5 array. The average of the 15 cells was calculated to create a single time series graph representing the average of the 15 nearest cells to the SP location.

The 15-cell average method was utilized to include the adjacent cells in the analysis to extend the footprint beyond just a single cell comparison. This was a consistent way to examine the data across all SP's. Figure 18 below presents an example of what this single and multiple cell analysis look like in the Guardian Software.

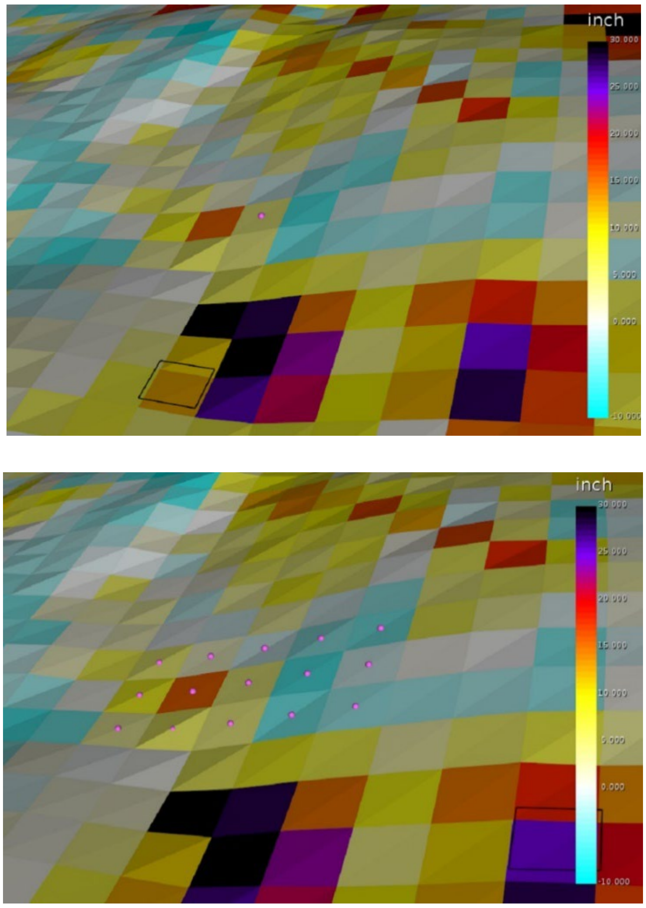

Figure 18 - Example of single cell (top) and multiple cell (bottom) analysis (pink dots)

Based on the results observed from the survey points and GBInSAR displacements it was decided to categorize the agreements based on three levels. The levels of agreement include 1, 2, and 3 and summarized below in Table 1.

Level ID	Description
Level 1	agreement indicates the SP movement direction and displacement matches with the GBInSAR cell movement direction and displacement
Level 2	agreement indicates either the SP movement direction or displacement matches with the GBInSAR cell movement direction or displacement
Level 3	neither the SP movement direction or displacement matches with the GBInSAR cell movement direction and displacement

Table 1 - Comparison Agreement Levels established between Survey Points and GBInSAR

Using this categorization to rank each SP agreement level against the corresponding radar data, the following sets of figures are presented next to show one example from each level. The remaining comparison figures are presented in Appendix B. Please note the locational information is faded purposely on each graph as to keep the site confidential.

Based on the level analysis the 19 SP's are distributed across the three different levels as shown in Table 2. Level 1 agreement includes six (6) SP's where the SP movement direction and displacement value match well against the GBInSAR data. Level 2 agreement contains 11 of the 19 SP's and is based on good agreement between either the movement direction or displacement between the SP's and GBInSAR data. Level 3 contains only two (2) SP's showing poor correlation between the SP and GBInSAR movement direction and displacement.

Using this categorization to rank each SP agreement level against the corresponding radar data, the following sets of figures are presented next to show one example from each level. The remaining comparison figures are presented in Appendix B. Please note the locational information is faded purposely on each graph as to keep the site confidential.

Based on the level analysis the 19 SP's are distributed across the three different levels as shown in Table 2. Level 1 agreement includes six (6) SP's where the SP movement direction and displacement value match well against the GBInSAR data. Level 2 agreement contains 11 of the 19 SP's and is based on good agreement between either the movement direction or displacement between the SP's and GBInSAR data. Level 3 contains only two (2) SP's showing poor correlation between the SP and GBInSAR movement direction and displacement.

Level 1 (6)
M02
M05
M09
M11
M15
M21
Level 2 (11)
M06
M07
M08
M10
M12
M13
M14
M16
M18
M19
M20
Level 3 (2)
M01
M17

Table 2 - Breakdown of Survey Point Rank Levels

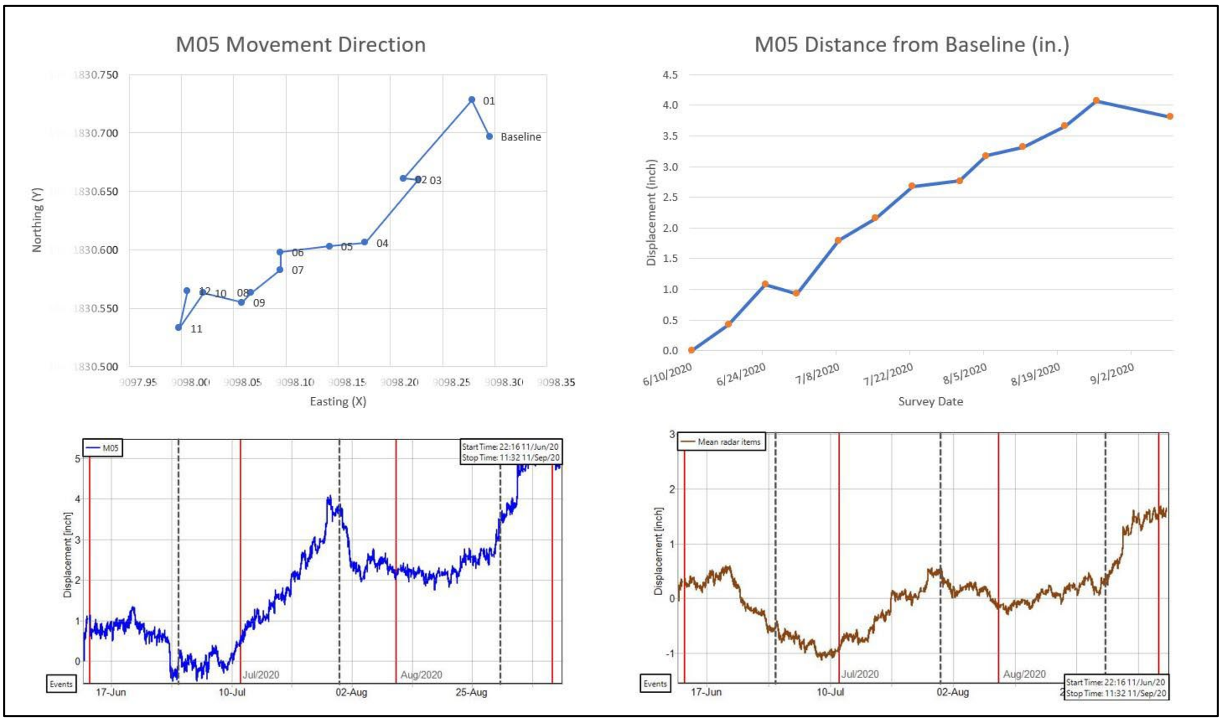

Figure 19 - Level 1 SP05 Survey Point and GBInSAR Comparison. SP movement from baseline to last reading (top left), cumulative SP movement (top right), single cell GBInSAR displacement image (bottom left), 15-point average GBInSAR displacement image (bottom right).

Level 1

Figure 19 presents the results for SP05 categorized as a Level 1. The movement direction of the SP indicates southwesterly movement (top left image) and the total offset distance the SP moved from the baseline reading is 9.65cm (3.8 in) (top right). The bottom left image indicates the single cell analysis from the GBInSAR data showing a positive displacement at approximately 12.45cm (4.9 inches). The bottom right image shows the 15-point average indicating a 4.1cm (1.6-inch) displacement. These results show good agreement in the movement direction of the SP and the radar results as well as a good agreement for the total displacement amount.

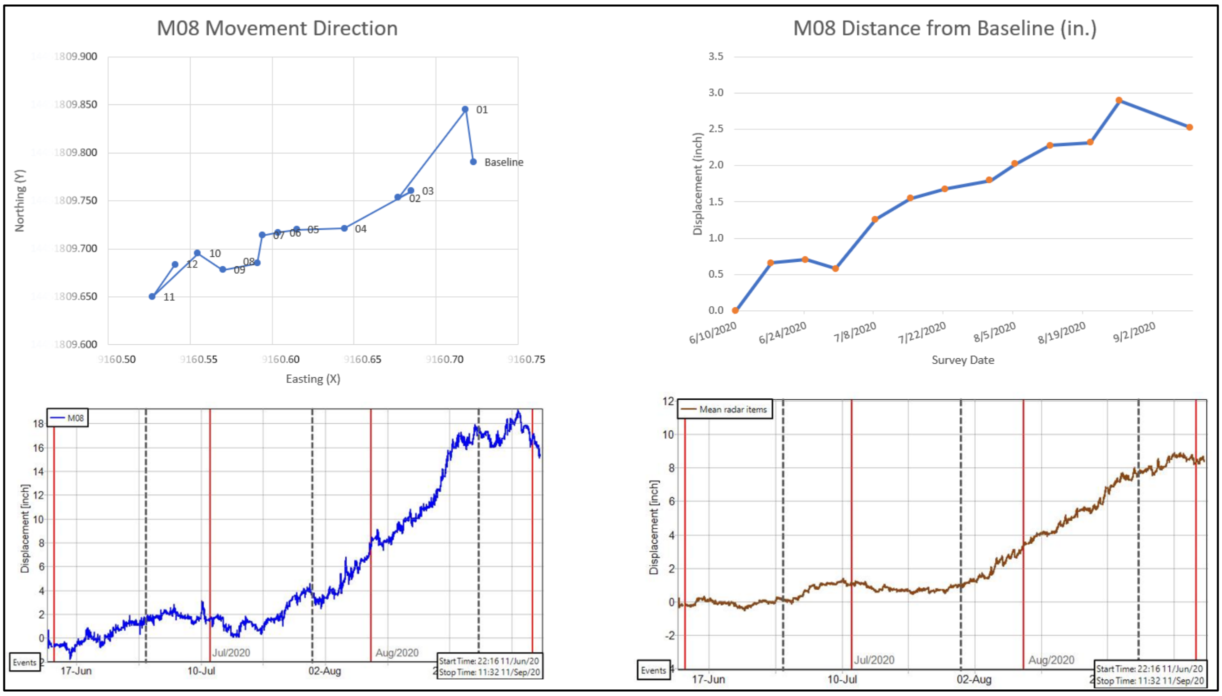

Figure 20 - Level 2 SP08 Survey Point and GBInSAR Comparison. SP movement from baseline to last reading (top left), cumulative SP movement (top right), single cell GBInSAR displacement image (bottom left), 15-point average GBInSAR displacement image (bottom right).

Level 2

Figure 20 presents the results for SP08 categorized as a Level 2. The movement direction of the SP indicates southwesterly movement (top left image) and the total offset distance the SP moved from the baseline reading is 6.35cm (2.5 inches) (top right). The bottom left image indicates the single cell analysis from the GBInSAR data showing a positive displacement at approximately 40.6cm (16 inches). The bottom right image shows the 15-point average indicating a 20.8cm (8.2-inch) displacement. These results show good agreement in the movement direction; however, the radar displacement results show poor agreement for the total displacement amount. The radar shows a larger displacement than the SP displacement, however, the general trend agreement is good.

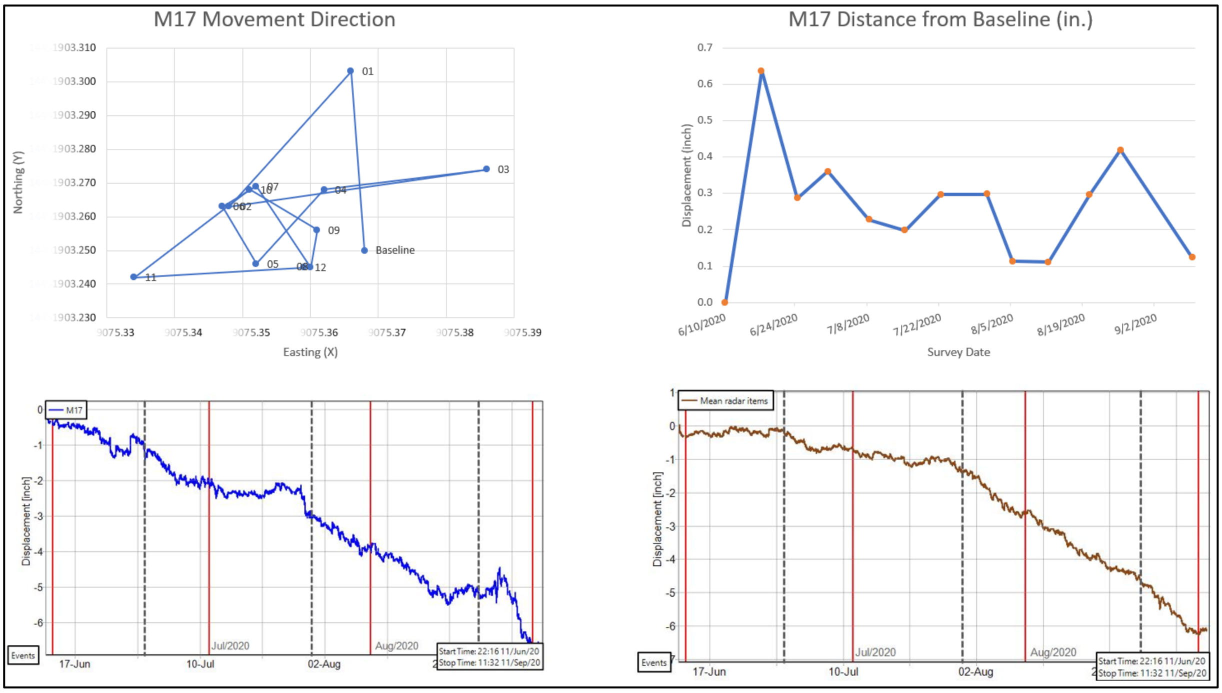

Figure 21 - Level 3 SP17 Survey Point and GBInSAR Comparison. SP movement from baseline to last reading (top left), cumulative SP movement (top right), single cell GBInSAR displacement image (bottom left), 15-point average GBInSAR displacement image (bottom right).

Level 3

Figure 21 presents the results for SP17 categorized as a Level 3. The movement direction of the SP indicates an overall southwesterly movement (top left image) and the total offset distance the SP moved from the baseline reading is 0.25cm (0.1 inch) (top right). The bottom left image indicates the single cell analysis from the GBInSAR data showing a negative displacement direction (away from radar) at approximately 15cm (6 inches). The bottom right image shows the 15-point average indicating a 15cm (6-inch) displacement. These results show poor agreement in the movement direction and the total displacement amount. SP17 is located near the edge of the ROW and most likely was influenced by thicker vegetation.

The previous three figures illustrated the comparison method using Levels 1-3. The remainder of these figures are presented in Appendix B.

Extensometer Readings

The data collected from the four sets of pre-construction extensometer points are presented in tabular format below. Extensometers sets 1AB – 4AB (Tables 3-6 respectively) each showed elongation across the two fixed rods of between 15 and 28 mm (0.6 inches and 1 inch). Extensometer set 4AB is approximately eight feet from SP12 and measures a displacement of 15cm (0.6 inches) compared with 4.1cm (1.6 inches) from SP12. This indicates agreement between the two different data types in this location. These two points were the only instance where an extensometer set was within 3m (10 feet) of a SP.

Date	Serial #	Temp °F	Temp °C	Reading (mm)	Time	Difference from prior read (mm)	Difference from prior read (in)
6/19/2020	2004219	75	24	2986.13	12:30 PM	--	--
6/24/2020	2004219	82	28	2991.00	3:00 PM	4.87	0.19
7/2/2020	2004219	85	29	2994.66	11:15 AM	3.66	0.14
7/10/2020	2004219	75	24	2996.16	9:00 AM	1.50	0.06
7/17/2020	2004219	84	29	2998.10	3:00 PM	1.94	0.08
7/23/2020	2004219	74	23	2998.55	10:10 AM	0.45	0.02
8/5/2020	2004219	72	22	3001.70	3:05 PM	3.15	0.12
8/20/2020	2004219	78	26	3001.85	1:35 PM	0.15	0.01
9/3/2020	2004219	74	23	3006.41	10:10 AM	4.56	0.18
9/11/2020	2004219	69	21	3007.49	10:05 AM	1.08	0.04
Difference from Baseline Reading						21.36	0.84

Table 3 – Extensometer 1AB Results

Date	Serial #	Temp °F	Temp °C	Reading (mm)	Time	Difference from prior read (mm)	Difference from prior read (in)
6/19/2020	2004219	75	24	3180.71	12:05 PM	--	--
6/24/2020	2004219	82	28	3185.71	2:45 PM	5.00	0.20
7/2/2020	2004219	85	29	3186.70	10:55 AM	0.99	0.04
7/10/2020	2004219	75	24	3191.42	9:55 AM	4.72	0.19
7/17/2020	2004219	84	29	3195.53	2:50 PM	4.11	0.16
7/23/2020	2004219	74	23	3198.76	9:55 AM	3.23	0.13
8/5/2020	2004219	72	22	3202.28	2:50 PM	3.52	0.14
8/20/2020	2004219	78	26	3206.10	1:10 PM	3.82	0.15
9/3/2020	2004219	74	23	3206.37	10:00 AM	0.27	0.01
9/11/2020	2004219	69	21	3208.49	9:55 AM	2.12	0.08
			Difference from Original Reading			27.78	1.09

Table 4 - Extensometer 2AB Results

Date	Serial #	Temp °F	Temp °C	Reading (mm)	Time	Difference from prior read (mm)	Difference from prior read (in)
6/19/2020	2004219	75	24	6052.89	12:20 PM	--	--
6/24/2020	2004219	82	28	6049.96	2:30 PM	-2.93	-0.12
7/2/2020	2004219	85	29	6058.59	10:40 AM	8.63	0.34
7/10/2020	2004219	75	24	6063.10	9:40 AM	4.51	0.18
7/17/2020	2004219	84	29	6066.37	2:40 PM	3.27	0.13
7/23/2020	2004219	74	23	6068.41	9:35 AM	2.04	0.08
8/5/2020	2004219	72	22	6071.23	2:35 PM	2.82	0.11
8/20/2020	2004219	78	26	6072.73	12:50 PM	1.50	0.06
9/3/2020	2004219	74	23	6072.74	9:50 AM	0.01	0.00
9/11/2020	2004219	69	21	6073.01	9:45 AM	0.27	0.01
			Difference from Original Reading			20.12	0.79

Table 5 - Extensometer 3AB Results

Date	Serial #	Temp °F	Temp °C	Reading (mm)	Time	Difference from prior read (mm)	Difference from prior read (in)
6/19/2020	2004219	75	24	3718.01	11:45 AM	--	--
6/24/2020	2004219	82	28	3715.64	2:15 PM	-2.37	-0.09
7/2/2020	2004219	85	29	3716.61	10:25 AM	0.97	0.04
7/10/2020	2004219	75	24	3717.81	9:20 AM	1.20	0.05
7/17/2020	2004219	84	29	3718.66	2:30 PM	0.85	0.03
7/23/2020	2004219	74	23	3720.68	9:20 AM	2.02	0.08
8/5/2020	2004219	72	22	3723.73	2:20 PM	3.05	0.12
8/20/2020	2004219	78	26	3730.02	12:30 PM	6.29	0.25
9/3/2020	2004219	74	23	3731.10	9:40 AM	1.08	0.04
9/11/2020	2004219	69	21	3733.17	9:35 AM	2.07	0.08
			Difference from Original Reading			15.16	0.60

Table 6 - Extensometer 4AB Results

Soil Moisture Probes/Rain Gauge

Soil moisture probe data are presented together with rainfall data over the duration of the field project and are shown in Figure 22. The soil moisture probe data shows good correlation with the rain gauge rainfall events. In general, there is an increase in the soil probe moisture content when there is a rainfall event at the site. The GBInSAR data were examined for correlations in displacement across rain events and increase in soil moisture content and there was no identified increase in movement observed in the time frames around precipitation on site. Long-term analysis of surface water infiltration and groundwater recharge should be performed in order to assess the interactions between the groundwater and slope movement/shear zone. Since piezometers could not be installed due to time constraints, it was thought that the soil moisture probes could potentially provide insight or correlation between precipitation, surface water infiltration and slope movement. However, the short monitoring duration (three months) was insufficient to provide conclusive data of the interaction.

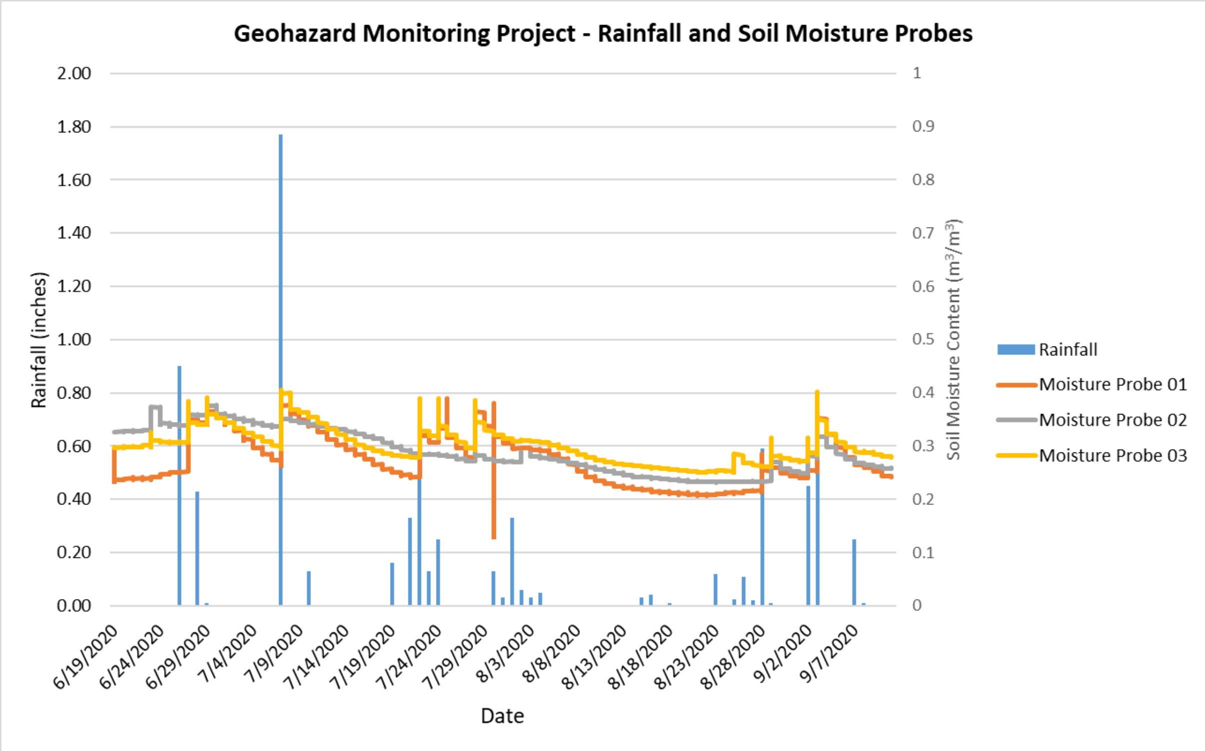

Figure 22 - Rainfall and Soil Moisture Probe Results - Pre-Construction

InSAR Summary and Results

Interferometric synthetic aperture radar or InSAR is a satellite-based remote sensing technology that is used to monitor ground displacement/movement, generally over large geographic regions. 3vG was subcontracted to provide satellite images and analysis of the site, before, during and after the research monitoring period. A total of 19 descending (west-looking) images acquiring from March 2020 to May 2021, and 6 (six) ascending (east-looking) images acquired from February 2021 to June 2021.

The following information are excerpts from the 3vG report and provide an overview of the InSAR investigation and analysis. The report is provided in Appendix D.

SAR Satellite: ALOS-2, long wavelength

Landscape: Rolling hills in Ohio with focus on the west facing slope

Product types: Displacement time series data, average displacement rate maps, signal-to-noise ratio (SNR) confidence contours, and new object detection products using amplitude data

Number of Images: 19 descending and 6 ascending

Reporting Period: March 15, 2020, to June 19, 2021

The displacement measurements were derived from the phase component of the satellite radar through interferometric image processing. InSAR does not require the deployment of personnel or equipment to the site or area of interest (AOI). According to 3vG, the quality of the InSAR data/images were reduced by thick vegetation at the site but was improved by using a satellite with a long wavelength (the Japanese ALOS-2 satellite).

InSAR monitoring is not affected by cloud cover, time of day, and site access obstacles. Each time a satellite passes over a defined AOI, typically every 4 to 14 days, a SAR image is acquired that is thousands of square miles in size (specific size depends on each satellite's footprint and the specified resolution). Algorithms are used to analyze millions of data points for each image obtained over to precisely measure displacement of the ground and infrastructure [24].

The raw data were collected from a satellite sensor called ALOS-2 (Advanced Land Observing Satellite - 2) which is on the PALSAR-2 satellite which is owned/operated by the Japanese Space Agency or JAXA. The raw data were purchased and processed by 3vG. The timeline for ascending and descending data are presented on Figure 23.

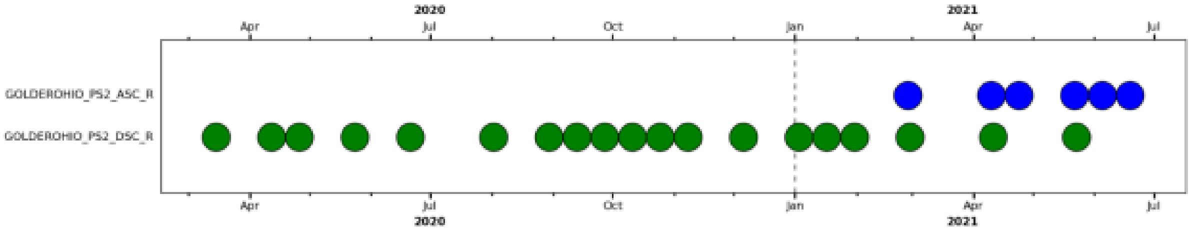

Figure 23 - Timeline of the ascending and descending data

Dual-Look Geometry

A dual-look geometry is created when both ascending and descending SAR images are combined. The dual-look product geometry provides a more accurate displacement and better coverage over the AOI. The ascending and descending displacement vectors can then be co-projected along the solved vector, not only providing directional information, but also increasing the displacement magnitude appropriately [24] (see Figure 24).

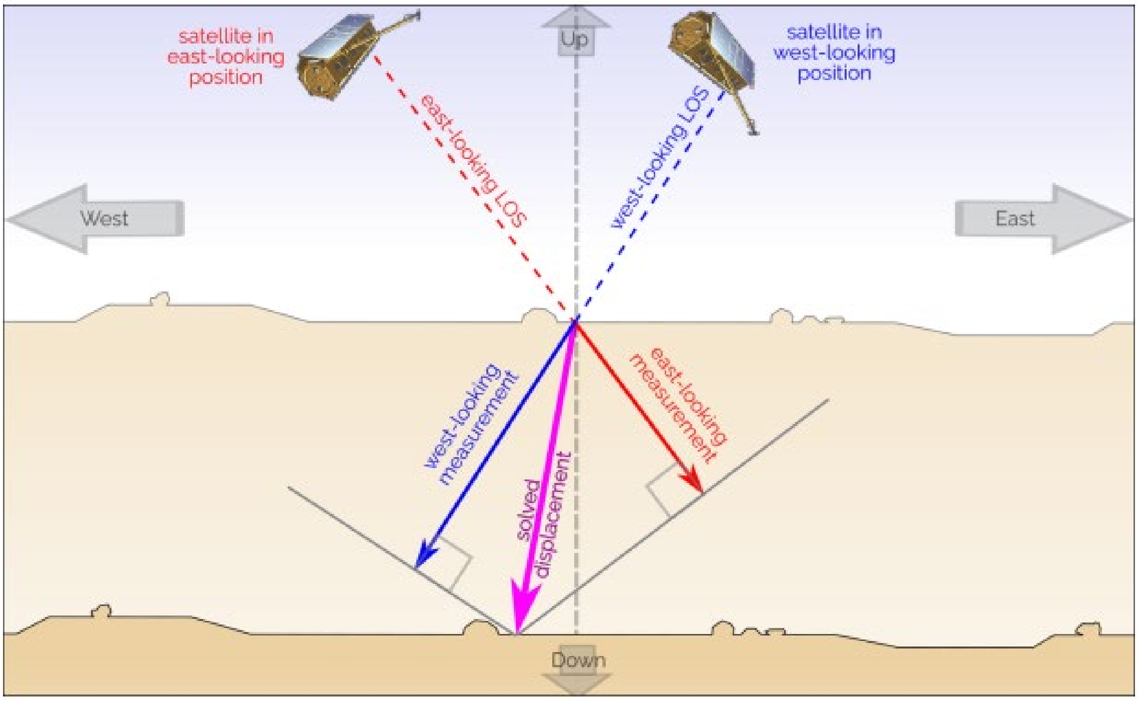

Figure 24 - Using both ascending and descending satellite acquisitions, it is possible to solve for the displacement vector. This includes the up-down components as well as the east-west components [24]

The results of the InSAR data consist of three product components, which are listed below:

- Displacement rate maps – Raster files of the average displacement rate in all measurable parts of the AOI.
- Signal to Noise Ratio (SNR): Vector files showing the extent of high confidence displacement areas.
- Time series data: Histories of cumulative displacement as noted from the descending line of sight over time

An example of a displacement map derived from the InSAR data over the selected time frame is shown in Figure 25. The displacement observed in the image ranges from -5.1cm/yr to -25.4cm/yr (-2 inches/year to -10 inches/year). Negative displacement indicates movement away from the satellite.

Figure 25 - Displacement derived from InSAR data over field site

In summary, 3vG concludes that the InSAR data shows strong displacement on the slope of interest, which has been occurring since early 2020. While the dual-look product is sensitive to displacement in more directions, it could only be produced for a shorter time period when images were available from both look directions. The single-look west looking analysis, while dimensionally restricted in displacement direction sensitivity, has measurements from earlier in 2020, and has a sufficient amount of quality data to time series graphs of cumulative displacement over time. Displacement amounts ranging from -5.1cm/yr up to -25.4cm (-2 inches/year up to -10 inches/year) (movement away from the satellite) were observed in the InSAR data.

Post-Construction Results

The post-construction field work commenced on November 30, 2020, and was completed on January 24, 2021. The following presents the results of post-construction monitoring activities.

Comparison of GBInSAR and Survey Points

Figure 26 shows the vector movement of the post-construction SP's. Since the points were selected to include only offset distances greater than 15.2cm (6 inches) the vector movement map shows relatively consistent offset for each SP. The same comparison methodology was applied in the post-construction analysis as during pre-construction activities. The same categorization to rank each SP agreement level against the corresponding radar data as in the pre-construction data analysis was performed. The comparison figures are presented in Appendix C. Please note the locational information is faded purposely on each graph as to keep the site confidential.

Two main displays of the GBInSAR software analysis data include reflectivity amplitude and displacement. The reflectivity amplitude map shown in Figure 27 indicates the radar signal strength of the reflected signal in decibels (dB). The highest return signals are from the reflectors placed across the site. The high amplitude area closest to the radar represents the new rock buttress and displayed high amplitude reflectivity. This is a typical response when observing stable rock faces.

Figure 28 shows the total displacement map for the GBInSAR data over the monitoring period. The colorized cells correspond to displacement (inches) from the GBInSAR data. Negative displacement is movement away from the radar unit and positive displacement is movement toward the radar. Some general observations from this figure are as follows:

- Overall displacement was measured to be low for the monitored area.
- Several isolated areas of positive and negative movement can be observed indicating more prevalent movement in these areas compared to others. This can be observed with Extensometer set 300AB (see below discussion on extensometers).

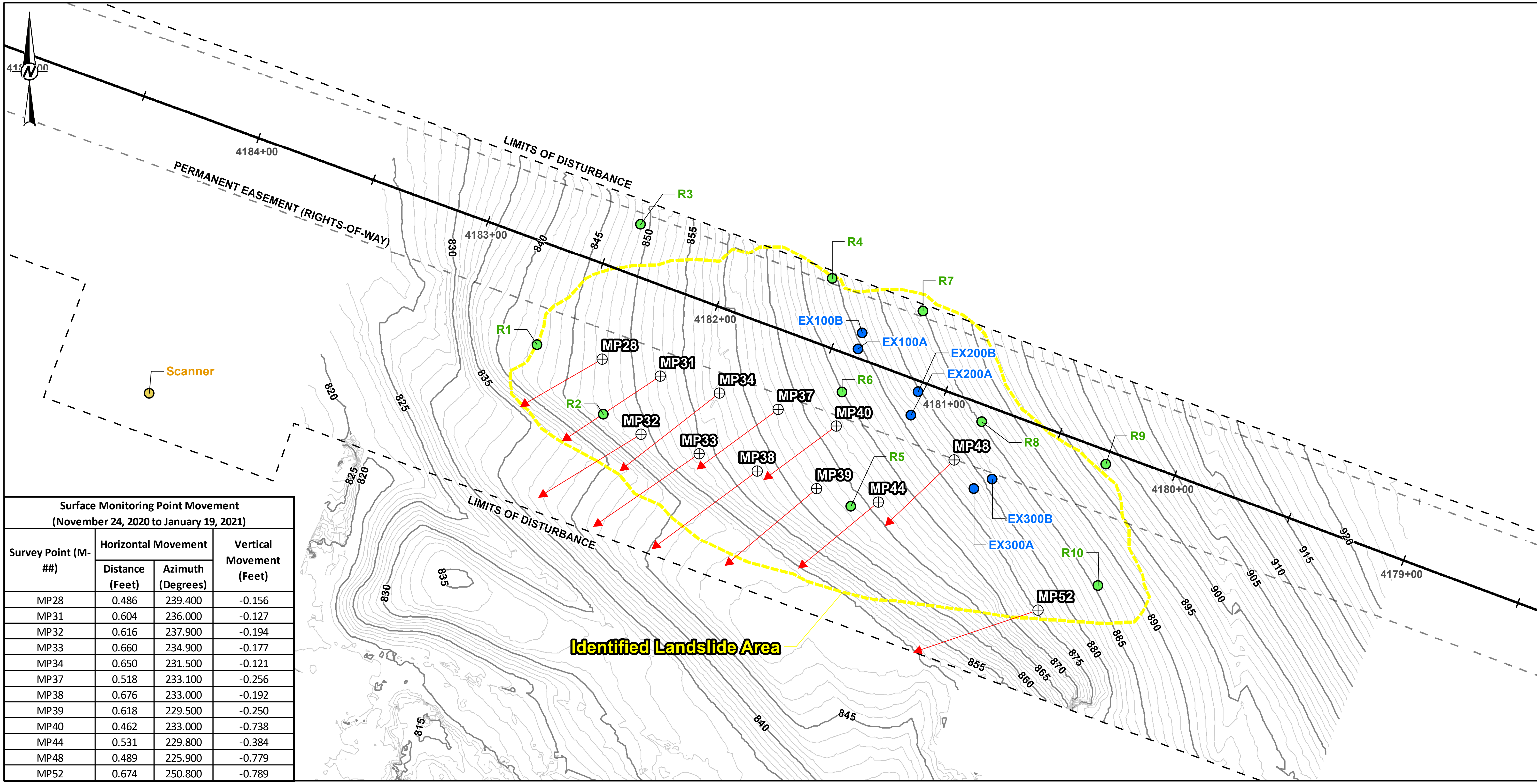

Surface Monitoring Point Movement (November 24, 2020 to January 19, 2021)			
Survey Point (M-##)	Horizontal Movement		Vertical Movement (Feet)
	Distance (Feet)	Azimuth (Degrees)	
MP28	0.486	239.400	-0.156
MP31	0.604	236.000	-0.127
MP32	0.616	237.900	-0.194
MP33	0.660	234.900	-0.177
MP34	0.650	231.500	-0.121
MP37	0.518	233.100	-0.256
MP38	0.676	233.000	-0.192
MP39	0.618	229.500	-0.250
MP40	0.462	233.000	-0.738
MP44	0.531	229.800	-0.384
MP48	0.489	225.900	-0.779
MP52	0.674	250.800	-0.789

LEGEND

- Post-Consturction Monitoring Point Location (2020-11-24)
- Monitoring Point Movement - Direction and Proportional Distance (See Notes)
- Extensometer
- Reflector
- Scanner
- Identified Landslide Area
- Natural Gas Pipeline
- Limits of Disturbance and Permanent Easement (Right-of-Way)
- Elevation contour (5 ft Interval)
- Elevation contour (1 ft Interval)

0 40 80
1 " = 40 FEET FEET

NOTE(S)

1. LENGTH OF SURVEY POINT MOVEMENT ARROWS (RED) ARE 80-TIMES LONGER THAN ACTUAL MEASUREMENTS (IE. 0.5 FT FIELD MEAURE SHOWS AS 40 FT ON THIS MAP, OR 1" = 0.5 FT OF MOVEMENT).

REFERENCE(S)

1. GOLDER ASSOCIATES INC. (IDENTIFIED LANDSLIDE AREA, INSTRUMENT LOCATION, MONITORING POINT, VECTOR MOVEMENT)
2. MOTT MCDONALD (STATIONING, LOD, ROW)
3. CONFIDENTIAL CLIENT (NATURAL GAS PIPELINE, CONTOUR)
4. COORDINATE SYSTEM: NAD83 2011 UTM ZONE 17N FT
5. SERVICE LAYER CREDITS: © OPENSTREETMAP (AND) CONTRIBUTORS, CC-BY-SA

CLIENT

PIPELINE RESEARCH COUNCIL INTERNATIONAL, INC. ("PRCI")
15059 CONFERENCE CENTER DRIVE, SUITE 130,
CHANTILLY, VA 20151

PROJECT

A COMPARISON BETWEEN IN-SITU INSTRUMENTATION AND REMOTE SENSING METHODS FOR SLOPE MONITORING WITHIN A PIPELINE RIGHT-OF-WAY
PROJECT NO. PR635-203904
CONTRACT NO. GHZ-2-05

CONSULTANT

GOLDER

YYYY-MM-DD	2021-06-08
DESIGNED	TL
PREPARED	TL
REVIEWED	MS
APPROVED	MD

TITLE

SITE MONITORING VECTOR MOVEMENT POST-CONSTRUCTION

PROJECT NO.	PHASE	REV.	FIGURE
20144586	007	A	26

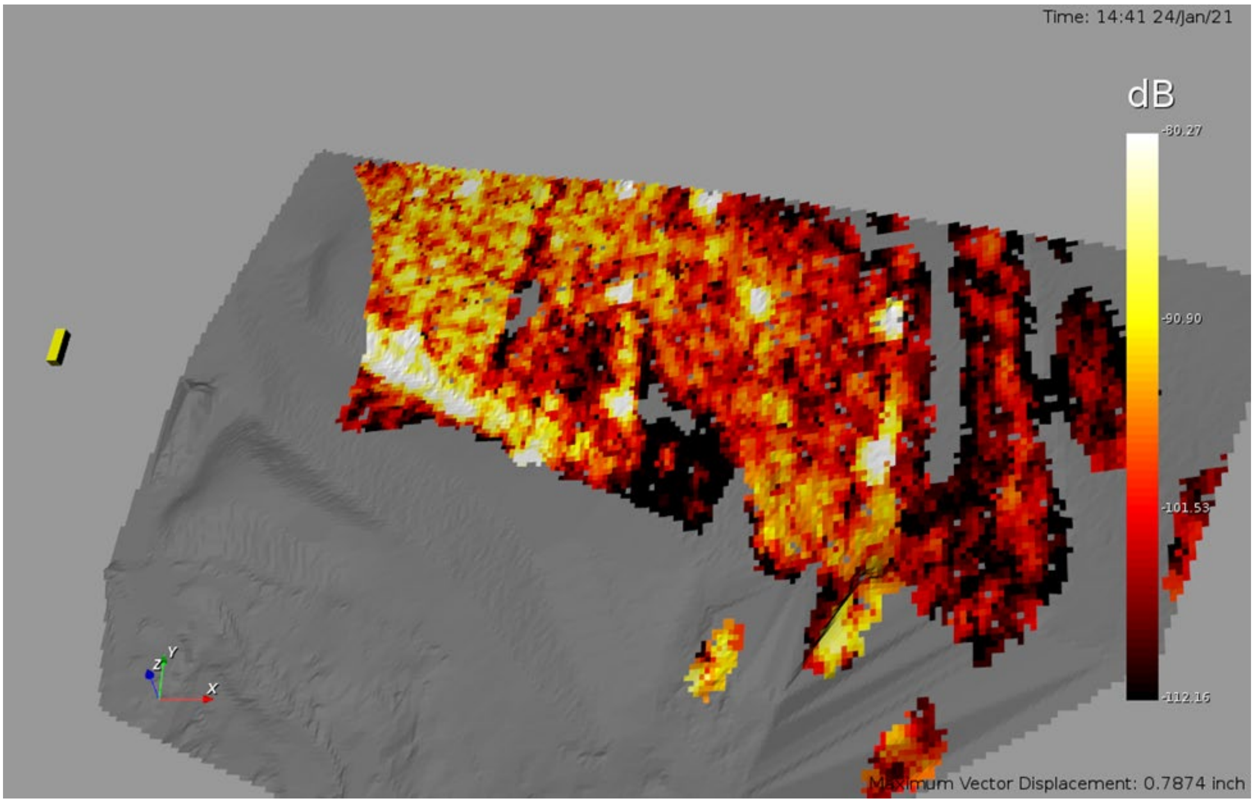

Figure 27 - Reflectivity amplitude of GBInSAR post-construction (north is in direction of Y axis)

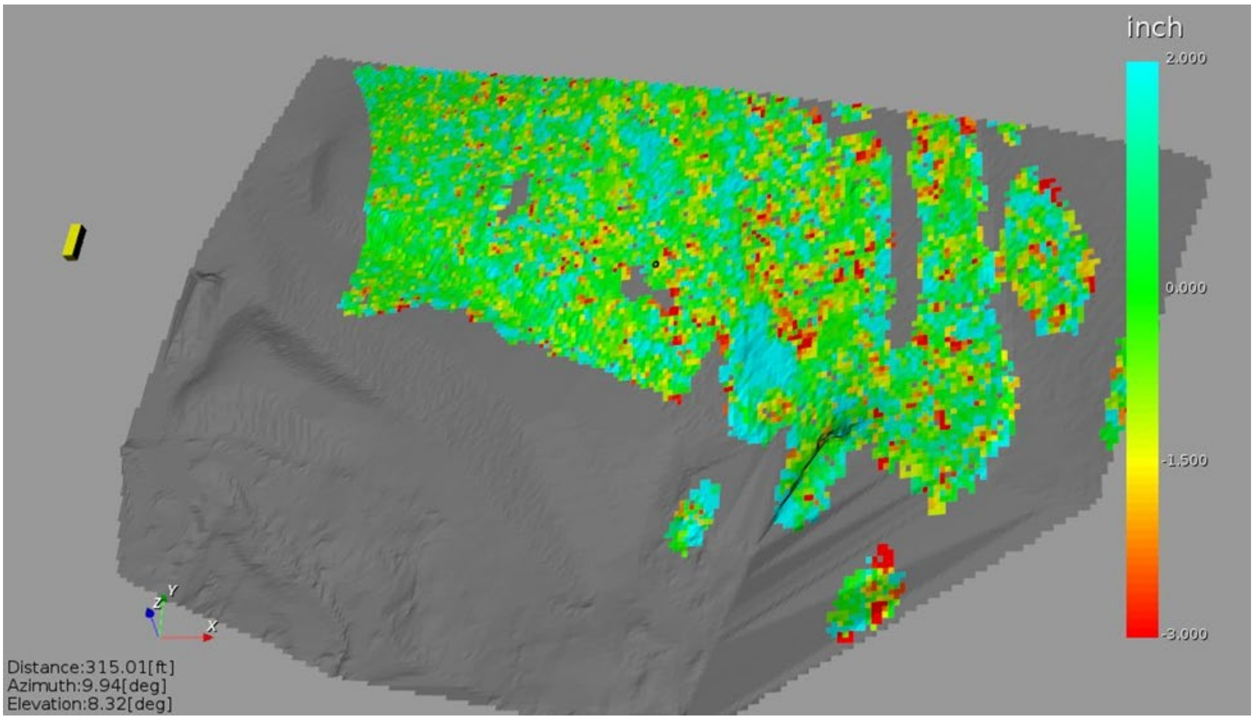

Figure 28 - Total displacement map over the post-construction monitoring period (north is in direction of Y axis)

As mentioned earlier in section 4.3, 12 SP's were used for the comparison between SP and GBInSAR movement direction and displacement as they were the only 12 SPs with displacements greater than 15.2cm (6 inches). Based on the level analysis the 12 SP's are distributed across the three different levels as shown in Table 7 (note the average method was used as the factor to indicate total offset movement and direction of the radar data). There were no Level 1 agreements observed during the analysis. Ten Level 2 SP's were classified as having good correlation with either movement direction or total offset. Two Level 3 SP's were identified during the analysis as having poor agreement with offset direction and distance. Most of the offsets observed from the post-construction GBInSAR data are less than 2.54cm (1 inch).

Level 2 (10)
M28
M31
M32
M33
M34
M37
M40
M44
M48
M52
Level 3 (2)
M38
M39

Table 7 - Breakdown of ranked Level analysis – Post-Construction

Extensometer Readings

The data collected from the three sets of post-construction extensometer points are presented in tabular format below. Extensometers sets 100AB – 300AB (Tables 8-10 respectively) showed variability in shortening and elongation across the two fixed rods of each set. Extensometer set 100AB and 200AB showed a small amount of shortening at 4.6cm and 2.54cm (1.8 and 1 inch) respectively, while set 300AB showed 17.5cm (6.9 inches) of elongation. The elongation on set 300AB shows gradual lengthening between the two set points over the two months of monitoring. Set 300AB was installed over the largest tension crack observed at site. The difference between the three sets of extensometer points could be related to the complex nature of the slope and movement.

Date	Serial #	Temp °F	Temp °C	Reading (mm)	Time	Difference from prior read (mm)	Difference from prior read (in)
11/23/2020	2004219	35	2	2065.35	3:30 PM	baseline	baseline
11/30/2020	2004219	38	3	2065.55	8:30 AM	0.2	0.0
12/15/2020	2004219	36	2	2020.20	5:45 PM	-45.4	-1.8
12/30/2020	2004219	50	10	2025.95	2:30 PM	5.8	0.2
1/9/2021	2004219	28	-2	2018.87	8:05 AM	-7.1	-0.3
1/14/2021	2004219	38	3	2010.11	--	-8.8	-0.3
1/23/2021	2004219	24	-4	2019.01	1:15:PM	8.9	0.4
Difference from Baseline Reading						-46.3	-1.8

Table 8 - Extensometer 100AB Results

Date	Serial #	Temp °F	Temp °C	Reading (mm)	Time	Difference from prior read (mm)	Difference from prior read (in)
11/23/2020	2004219	35	2	3095.64	3:30 PM	baseline	baseline
11/30/2020	2004219	38	3	3148.63	8:30 AM	53.0	2.1
12/15/2020	2004219	36	2	3133.47	5:35 PM	-15.2	-0.6
12/30/2020	2004219	50	10	3112.25	2:30 PM	-21.2	-0.8
1/9/2021	2004219	32	27	3101.04	8:05 AM	-11.2	-0.4
1/14/2021	2004219	-	-	Missing Data	-	-	-
1/23/2021	2004219	24	-4	3071.27	1:25 PM	-29.8	-1.2
Difference from Baseline Reading						-24.4	-1.0

Table 9 - Extensometer 200AB Results

Date	Serial #	Temp °F	Temp °C	Reading (mm)	Time	Difference from prior read (mm)	Difference from prior read (in)
11/23/2020	2004219	35	2	2716.70	3:30 PM	baseline	baseline
11/30/2020	2004219	38	3	2753.79	8:30 AM	37.1	1.5
12/15/2020	2004219	36	2	2796.95	5:45 PM	43.2	1.7
12/30/2020	2004219	50	10	2839.33	2:30 PM	42.4	1.7
1/9/2021	2004219	32	27	2865.10	8:05 AM	25.8	1.0
1/14/2021	2004219	38	3	2875.64	-	10.5	0.4
1/23/2021	2004219	24	-4	2891.52	1:15 PM	15.9	0.6
Difference from Baseline Reading						174.8	6.9

Table 10 - Extensometer 300AB Results

Soil Moisture Probes/Rain Gauge

Soil moisture probe data are presented together with rainfall data over the duration of the field project and are shown in Figure 29. Please note that rain gauge data was supplemented with local historical precipitation data as the cold temperatures may have affected rain gauge readings. Soil moisture probe 03 shows good correlation with the rain gauge and supplemental historical precipitation data. In general, there is an increase in the soil moisture probe moisture content when there is a rainfall event at the site. Moisture probe 02 remained relatively consistent throughout the monitoring event at approximately 0.36m^3/m^3.

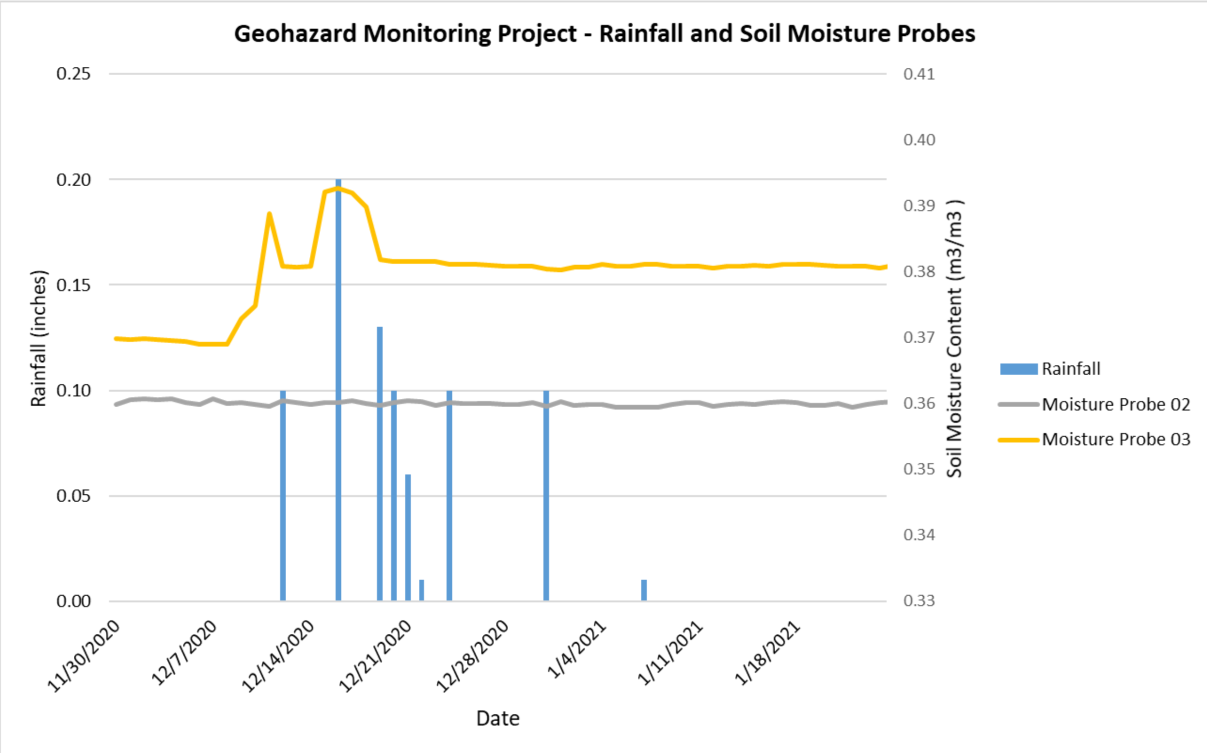

Figure 29 - Rainfall and Soil Moisture Probe Results - Post-Construction

6. CONCLUSIONS

Based on the results of this research project, the GBInSAR is a viable technology to add to a slope monitoring toolbox for oil and gas operations. Along with traditional satellite InSAR these two remote sensing technologies can supplement any geohazard monitoring program to monitor and provide continuous updates to a geohazard risk database. The addition of GBInSAR and InSAR to a traditional in-situ slope monitoring program, is a method to remotely monitor a slope over time to determine slope movement trends.

Based on the results of the in-situ and remote monitoring datasets the following conclusions are presented:

Pre-construction

- GBInSAR data showed good agreement between the displacement time series and SP's. There are several points that did not show good correlation, and this can mostly be attributed to high vegetation on the slope during monitoring. The high irregular vegetation causes low amplitude and inconsistent radar reflections reducing the reflected amplitude.
- Rain data and soil moisture probe data show good agreement with each other; however, no discernible correlation was observed with the GBInSAR data. This may be related to the amount of rainfall not being significant enough to cause movement at this site or infiltration rates are low. This is evident as the soil moisture probes responded to rain events, but the units were only buried approximately 15.2cm (6 inches) in the ground. Overall, the amount of rainfall observed over the three-month monitoring period was not considered significant with the largest single event at 4.6cm (1.8 inches).
- The extensometer data set showed elongation between 1.5cm (0.6 inches) and 2.5cm (1 inch). This amount of displacement over the monitoring period is small and correlates well with the localized minimal movement of the GBInSAR data near these locations.
- The GBInSAR and InSAR data both showed displacement over the site. In general, the InSAR data showed better than expected results and correlation with the GBInSAR. The InSAR displacement map shows clear movement between 5.1cm to 25.4cm/year (2 -10 in/year) over the field site in correlation with observed GBInSAR values on average between 12.7cm to 25.4cm (5-10 inches) near SP 5 and SP 8.

Post-construction

- The GBInSAR data from the post-construction monitoring phase overall showed a lower amount of displacement compared to the SP's. Amplitude reflectivity was good for the area of interest. It is unclear at this time what caused this discrepancy.
- Rain data and soil moisture probe data show good agreement with each other; however, no discernible correlation was observed with the GBInSAR data over this short monitoring time. This may be related to the amount of rainfall not being significant enough to cause movement at this site or infiltration rates are low. This is evident as the soil moisture probes responded to rain events, but the units were only buried approximately 15.2cm (6 inches) in the ground. Overall, the amount of rainfall observed over the three months was small with the largest single event at 0.5cm (0.2 inches). Two sets of extensometer data showed small amounts of shortening and the third set showed elongation of 17.8cm (7 inches). This amount of displacement over the monitoring period is relatively small and correlates with the localized movement of the GBInSAR data near this location. GBInSAR values were negative (away from the radar) but the displacement amount is approximately 7.6cm (3 inches) compared to the offset of 17.8cm (7 inches) measured from the extensometer showing good displacement trending information.

To summarize, this project has attempted to integrate multiple in-situ instruments along with two, state of the art remote sensing monitoring systems, GBInSAR and InSAR. The project was a unique opportunity to examine and monitor an unstable slope both during and after construction remediation activities. In general, the remote sensing technologies were able to capture movement over the area of interest and show displacement trends in the data over their respective time series. There was not a general one to one correlation between the in-situ measurements and the remote sensing measurements as the in-situ measurements are point source monitoring. However, both the GBInSAR and InSAR datasets measured slope movement trends over their respective time series. Both GBInSAR and InSAR were affected by slope vegetation to varying degrees. Based on these results both remote sensing technologies can serve to collect meaningful data along unstable slopes on pipeline ROWs, for both short-term (high-risk slopes) and long-term monitoring.

7. RECOMMENDATIONS

In summary, the results of the research project were overall of good quality. Adding the GBInSAR to a slope monitoring program, and later using the InSAR data for further comparison can benefit a site by allowing the owner/operator to quickly deploy a remote monitoring solution. We recommend the following points for consideration in deploying the GBInSAR and InSAR at a given slope monitoring site:

- Deployment of an automated total station adjacent to the GBInSAR for automated survey control. The purpose is to establish a suitable number of reflector monuments across critical parts of the slope to provide true movement and ground truth to the GBInSAR. The points would be auto surveyed using the total station multiple times per day to establish a strong baseline with a high density of measurement points which is at a much higher frequency than what was collected for this project. This total station data would be connected into the GBInSAR software allowing both to be uploaded and examined in near real-time. The benefits of this are to create more data sampling on the reflector monuments to compare movement trends directly with the highly sampled GBInSAR data, it would also prevent the need to have personnel on the slope on a weekly basis to survey the monuments.
- Deploy instrument in-line with the slope movement.
- Vegetation management of the slope is required to control backscatter of the radar signal. Vegetation growth can cause inaccurate slope radar returns. The GBInSAR manufacturer is currently working on enhancing algorithms that may be able to deal with vegetation, however, this is still in the developing stages.
- Attempt to coordinate monitoring around the early springtime months. This has two potential benefits, the first is vegetation is usually at a low level and second springtime is typically the time when the highest amount of precipitation occurs from winter snow melt and early spring rains. Most landslides directly involve water as a main mechanism for slope movement.
- Utilize the latest in GBInSAR technology with the ArcSAR unit. The unit has additional features that include a built in GNSS system, and the ability to create automatic DTM of the site. It is also fully capable of integrating seamlessly the IBIS radar, total station, and GNSS in one solution.
- InSAR has provided data to support the use of monitoring slopes over large geographic regions. InSAR is a reliable method for long-term monitoring of low or medium risk slopes. A possible scenario for the integration of InSAR data would be to select low to medium risk landslide and integrate an InSAR monitoring schedule (perhaps twice per year) to continually monitor and update an evolving landslide threat assessment database. If a slope requires near real-time data due to an elevated threat level (i.e., high risk), then GBInSAR is an appropriate technology to provide high data density in near real-time within the constraints listed above.

8. ACKNOWLEDGEMENT

Golder would like to thank the PRCI as well as the owners and operators for funding this geohazard monitoring research project. In particular, Golder would like to thank Ms. Carrie Greaney, Project Director of PRCI for her direction and unrelenting perseverance of making this a successful research project. Golder would also give thanks to all the owners and operators who funded this project, as well as their time and technical expertise – without their contributions, this research project would not be possible. We would also like to thank IDS GeoRadar for providing the GBInSAR, and their mechanical and technical insights at all hours of the day and night, and 3vGeomatics for their data analysis and report. Lastly, I would like to thank my co-author, Mark Saunders, for his vision, data collection assistance, data reduction, analysis, and overall management of the project.

9. REFERENCED PUBLICATIONS

1. Nadim, Farrokh and Lacasse, Suzanne. 2005. *Terrain and geohazard challenges facing onshore oil and gas pipelines, Mapping of landslide hazard and risk along a pipeline route, pages 117-128*. Published for the Organizing Committee by Thomas Telford Publishing, Thomas Telford Ltd, 1 Heron Quay, London E14 4JD.
2. INGAA, Interstate Natural Gas Association of America. 2020. *Guidelines for Management of Landslides Hazards for Pipelines*. The INGAA Foundation and a Group of Sponsors.
3. Sharma, M., and Lasker, S. 2017. *Landslide Mapping, Monitoring and Modeling Techniques: A New Approach using DOFS*. Proceedings of Second International Conference on Circuits, Controls and Communication. DOI: 10.1109 CCUBE.2017.8394149.
4. Golder, Associates Inc. 2016. *Mitigation of Land Movement in Steep and Rugged Terrain for Pipeline Projects: Lessons Learned from Constructing Pipelines in West Virginia*. The INGAA Foundation, Inc., Final Report No. 2015-03.
5. Gray, R.E., Hamel, J.V., and Adams. 2011. *Landslides in the Vicinity of Pittsburgh, Pennsylvania*. The Geological Society of America, Field Guide 20, pages 61-85, doi: 10.1130/2011.0020(04), 2011.
6. Gray, R.E., Ferguson, H.F., and Hamel J.V. 1979. *Slope Stability in the Appalachian Plateau, Pennsylvania and West Virginia, USA*. In Developments in Geotechnical Engineering, 14B, Rockslides and Avalanches, edited by B. Vought. New York. American Elsevier Publishing Company.
7. EIA, US Energy Information Administration. 2017. *Marcellus Shale Play, Geology Review. Independent Statistics and Analysis*. US Department of Energy, Washington, D.C.
8. Hunt, Roy F. 2004. *Geotechnical Investigation Manual, Second Edition, John Wiley, and Sons*.
9. Cawood, F.T., Stacey, T.R. 2006. "Survey and Geotechnical Slope Monitoring Considerations." *The Journal of the South African Institute of Mining and Metallurgy by the South African Institute of Mining and Metallurgy*, ISSN 0038-223X/3.00.
10. Davies, Tim. 2015. *Landslides Hazards, Risks and Disasters*. Oxford, UK, Elsevier.
11. Derby, Martin and Theriault, Bailey. 2019. *Assessing and Managing Geologic Hazards in the Appalachian Region of the United States*. Paper presented at the Proceedings of the International Pipeline Geotechnical (IPG) Conference, American Society of Mechanical Engineers. ISBN No.: 978-0-7918-5577-5.
12. Girven, Erin. 2019. *Statistical and Geospatial Analysis of InSAR Data for Characterization of Processes Controlling Motion of the Slow-Moving Berkeley Landslides. M.S. Thesis*. University at Buffalo, ProQuest Dissertations Publishing, http://search.proquest.com/docview/2305530395/.
13. Romeo, S, Kieffer, D., and Matteo, L. 2015. *Reliability of GBInSAR Monitoring in Ingelsberg Landslide Area (Bad Hofgastien, Austria)*. Geotechnical Safety and Rick V, IOS Press. DOI: 10.3233/978-1-61499-580-7-803.
14. Johnson, C., Markley, C., M Derby, B. Theriault, and J. and deLaChapelle. 2019. *An Overview of Current Methods for Monitoring Landslide Ground Movement to Better Understand Potential Hazards of Buried Pipelines.* Paper presented at the Proceedings to the Conference of Asset Integrity Management Pipeline – Integrity Management Under Geohazard Conditions, American Society of Mechanical Engineers.
15. Lombardi, L., Nocentini, M, Frodella, W., Nolesini, T., Bardi, F., Intieri, E., Carla, T., Solari, L., Dotta, G., Ferrigno, F., and Casegli, N. 2017. *The Calatabiano landslide (southern Italy): preliminary GB-InSAR monitoring data and remote 3D mapping, Landslides. Springer*, DOI: 10.1007/s10346-016-0767-6.
16. Borron, Steven and Derby, Martin. 2019. *Ground Based Interferometric Synthetic Aperture Radar Combined with a Critical Slope Monitoring Program Will Provide Early Detection of Slope Movement Along Pipeline Corridors*. Paper presented at the Proceedings of the International Pipeline Geotechnical (IPG) Conference, American Society of Mechanical Engineers. ISBN No. 978-0-7918-5577-5.
17. Mazzanti, Paolo. 2011. "Displacement Monitoring by Terrestrial SAR Interferometry for Geotechnical Purposes." *Geotechnical News*.
18. IDS GeoRadar, part of Hexagon. 2018. *Critical Slope Monitoring*. Marketing and information sheet.

19. Savigny, K.W., and Isherwood, A.E. 2005. "Terrain and Geohazard Challenges to Pipelines in Canada." pages 403-416. Published for the Organizing Committee by Thomas Telford Publishing, Thomas Telford Ltd, 1 Heron Quay, London E14 4JD. ISBN 0 7277 3278 1.
20. Ohio, Department of Natural Resources. 2011. "A Brief Summary of the Geologic History of Ohio." *Geofacts Brief No. 23*.
21. Slucher, E.R., Swinford, E.M, Larson, G.E., Powers, D.M. 2006. "Bedrock Geologic Map of Ohio: Ohio Division of Geological Survey." Map BG01, version 6.0; Scale 1:500,000.
22. Pomeroy, J.S. 1982. *Landslides in the Greater Pittsburgh Region, Pennsylvania*. Department of the Interior, US Geological Survey Professional Paper 1229, Washington. ISBN13: 9781287010531.
23. Confidential, Operator. 2019. *Confidential e-mail from the Owner Representative, Site History and Geology*. April 6.
24. Down, Murray and Brown, Jacob. 2021. *Archive InSAR Analysis of Slope Displacement in Muskingum County, Ohio*. Prepared for Golder Associates and the Pipeline Research Council International. July 9.

APPENDIX A DEFINITIONS

Appendix A - Definitions

Owner/Operator – Owner or operating company responsible for the operation and safety of the pipeline asset.

APPENDIX B PRE-CONSTRUCTION RESULTS

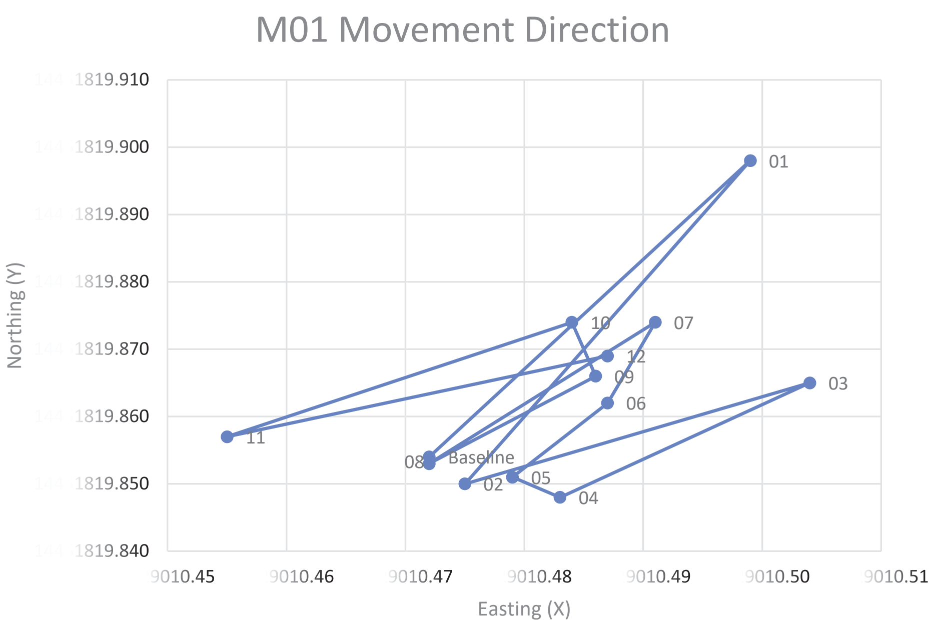

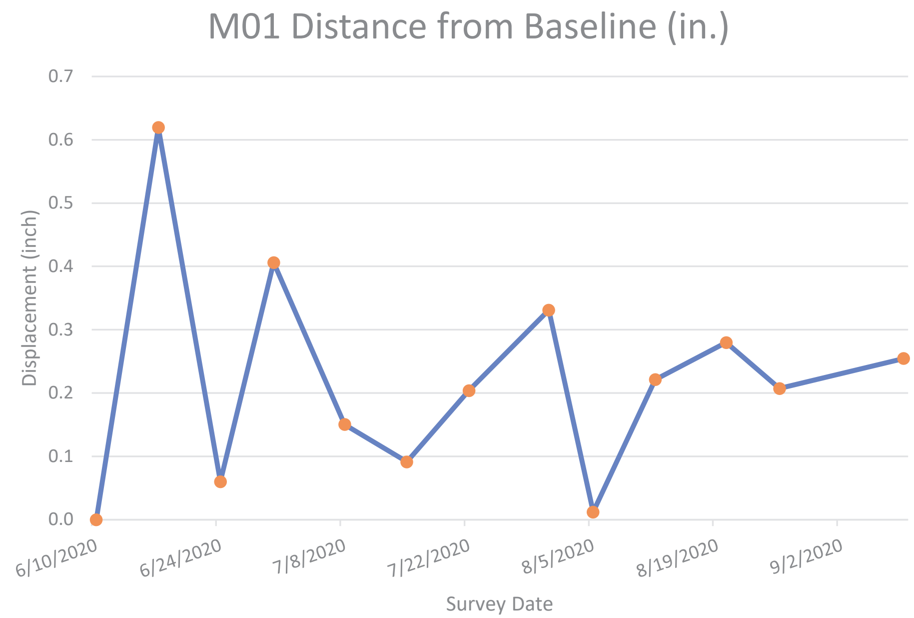

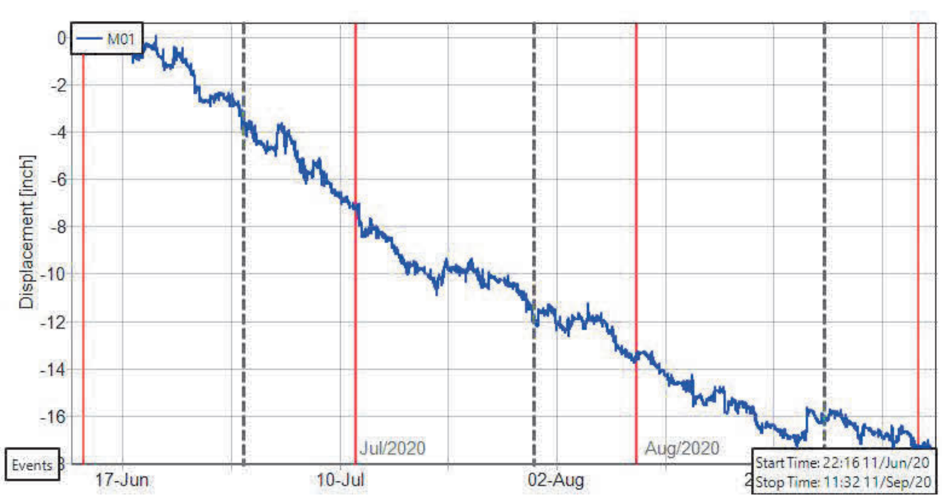

No 15-pixel average data not enough pixels

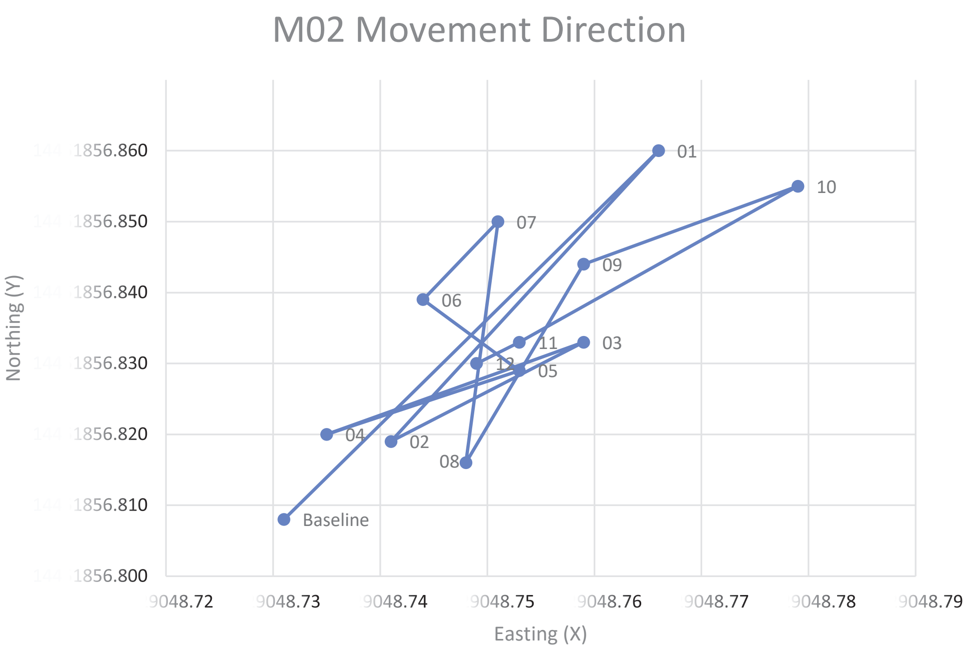
M02 Movement Direction
Northing (Y)
Easting (X)
1856.860
1856.850
1856.840
1856.830
1856.820
1856.810
1856.800
9048.72
9048.73
9048.74
9048.75
9048.76
9048.77
9048.78
9048.79
01
02
03
04
05
06
07
08
09
10
11
12
Baseline

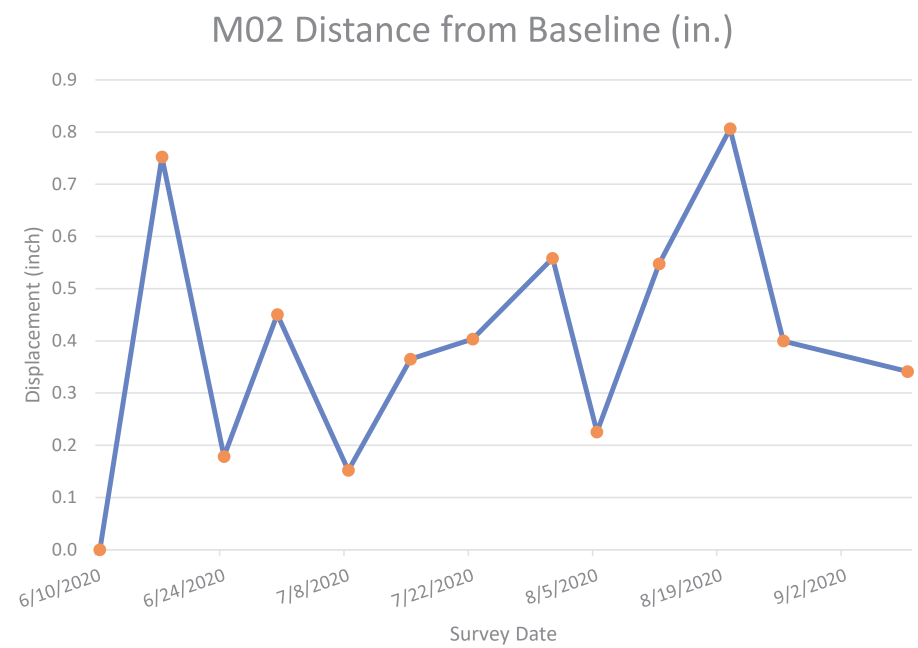
M02 Distance from Baseline (in.)
Displacement (inch)
Survey Date
0.0
0.1
0.2
0.3
0.4
0.5
0.6
0.7
0.8
0.9
6/10/2020
6/24/2020
7/8/2020
7/22/2020
8/5/2020
8/19/2020
9/2/2020

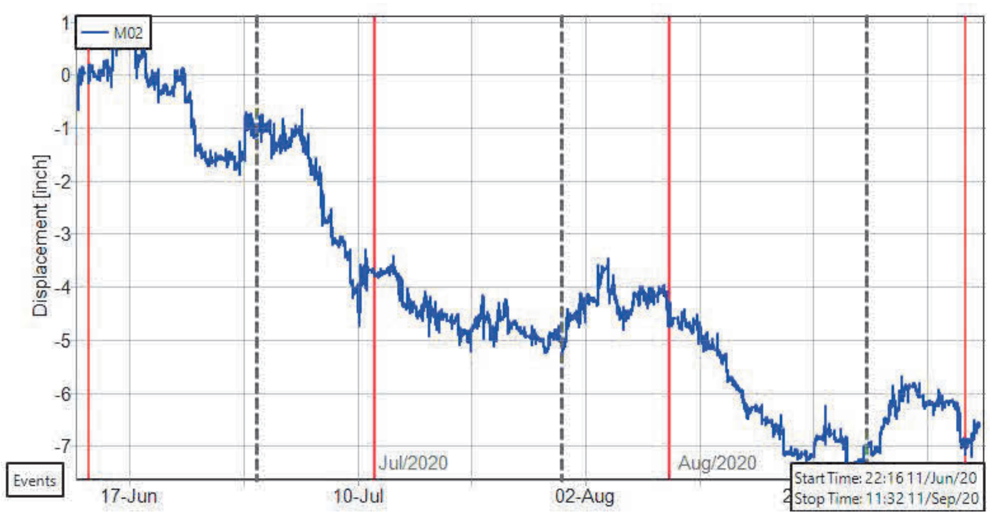
M02
Displacement [inch]
Events
17-Jun
10-Jul
02-Aug
Jul/2020
Aug/2020
Start Time: 22:16 11/Jun/20
Stop Time: 11:32 11/Sep/20

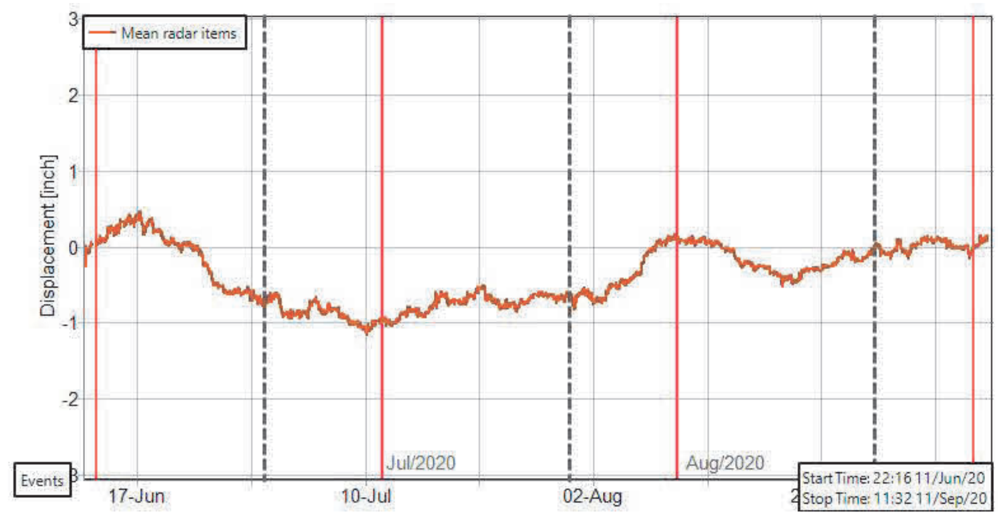
Mean radar items
Displacement [inch]
Events
17-Jun
10-Jul
02-Aug
Jul/2020
Aug/2020
Start Time: 22:16 11/Jun/20
Stop Time: 11:32 11/Sep/20

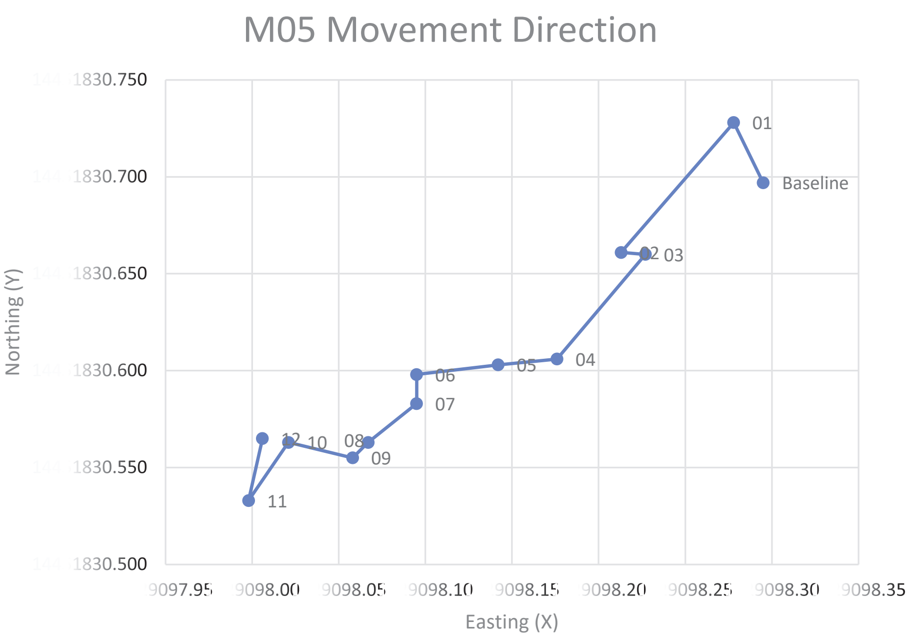

M05 Movement Direction
Northing (Y)
Easting (X)
1830.750
1830.700
1830.650
1830.600
1830.550
1830.500
9097.95
9098.00
9098.05
9098.10
9098.15
9098.20
9098.25
9098.30
9098.35
01
Baseline
03
04
05
06
07
08
09
10
11

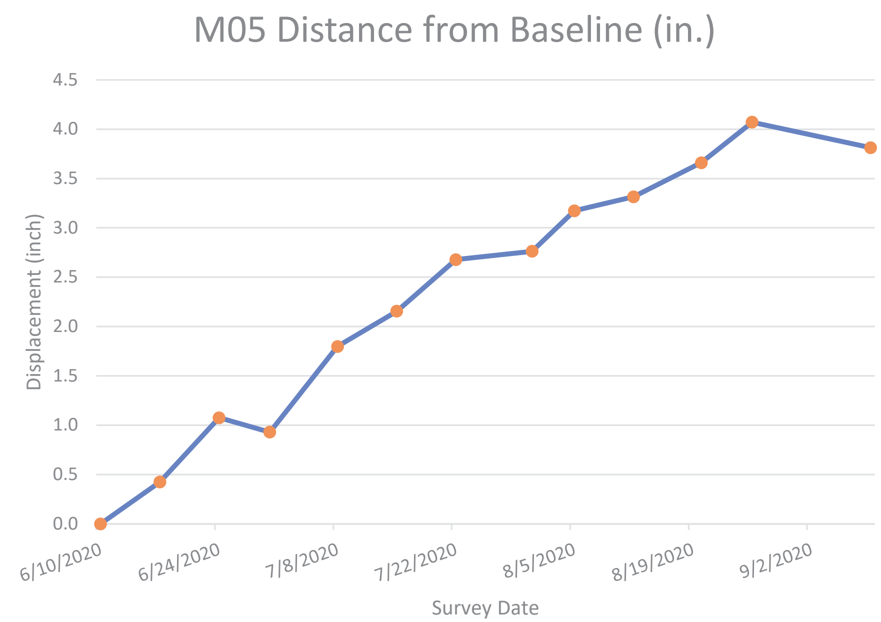

M05 Distance from Baseline (in.)
Displacement (inch)
Survey Date
4.5
4.0
3.5
3.0
2.5
2.0
1.5
1.0
0.5
0.0
6/10/2020
6/24/2020
7/8/2020
7/22/2020
8/5/2020
8/19/2020
9/2/2020

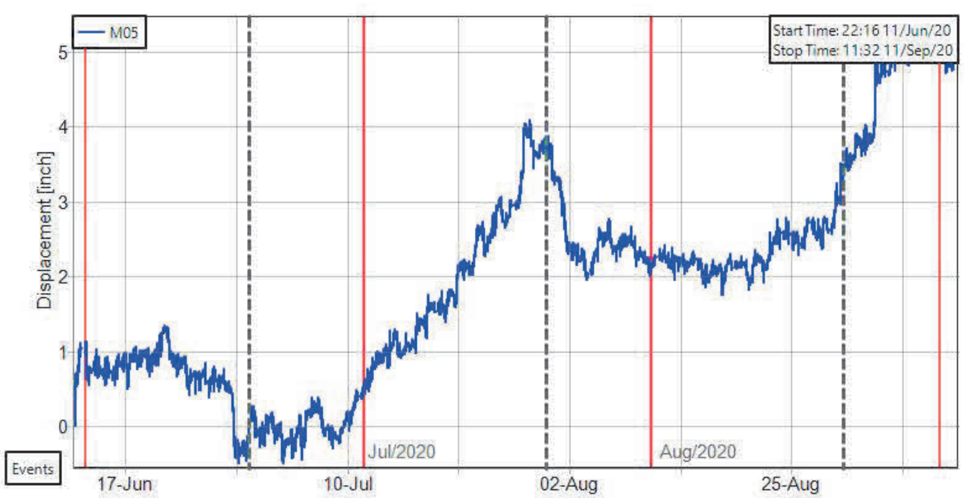

M05
Start Time: 22:16 11/Jun/20
Stop Time: 11:32 11/Sep/20
Displacement [inch]
Events
Jul/2020
Aug/2020
17-Jun
10-Jul
02-Aug
25-Aug

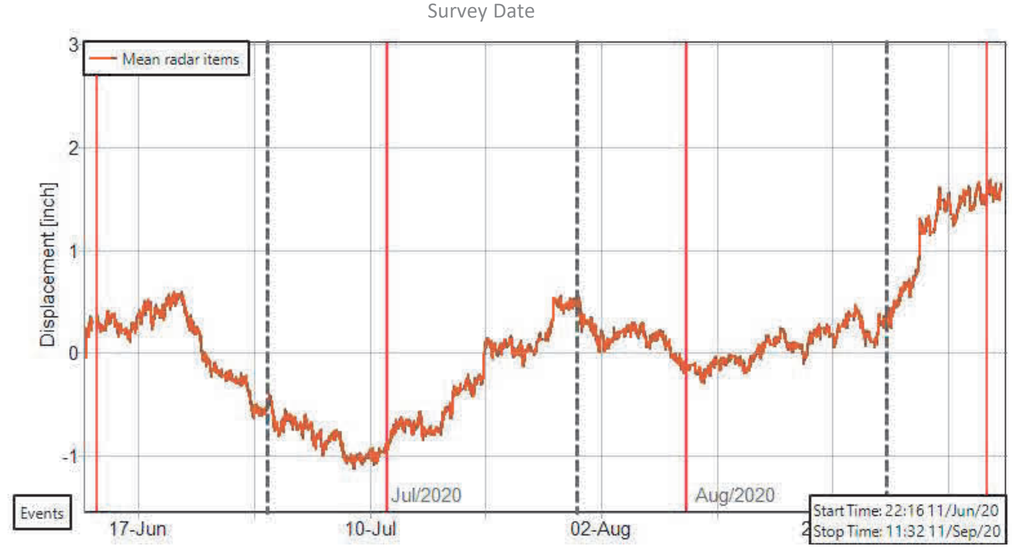

Mean radar items
Displacement [inch]
Events
Jul/2020
Aug/2020
17-Jun
10-Jul
02-Aug
Start Time: 22:16 11/Jun/20
Stop Time: 11:32 11/Sep/20

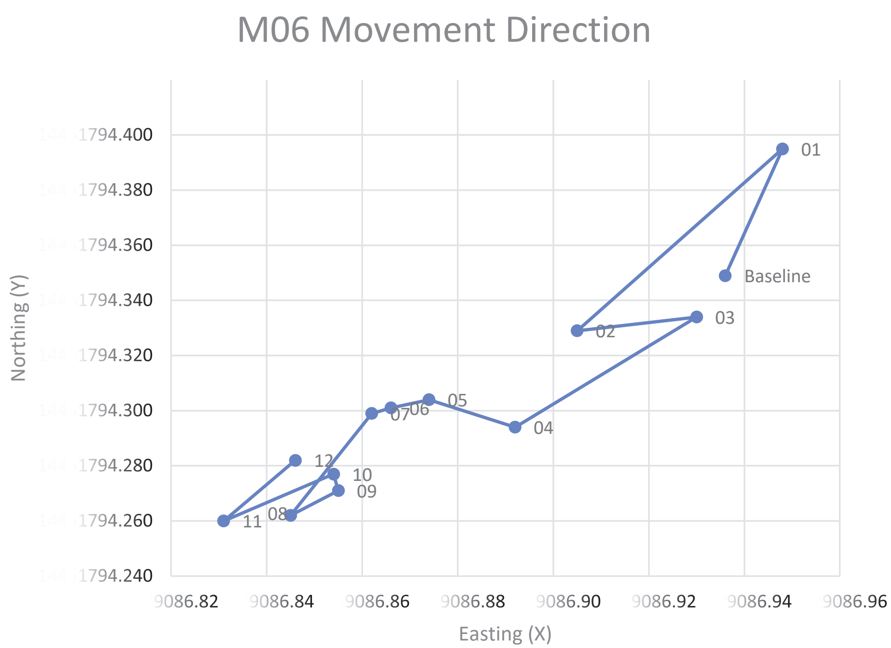
M06 Movement Direction
Northing (Y)
1794.400
1794.380
1794.360
1794.340
1794.320
1794.300
1794.280
1794.260
1794.240
9086.82
9086.84
9086.86
9086.88
9086.90
9086.92
9086.94
9086.96
Easting (X)
01
Baseline
02
03
04
05
06
07
08
09
10
11
12

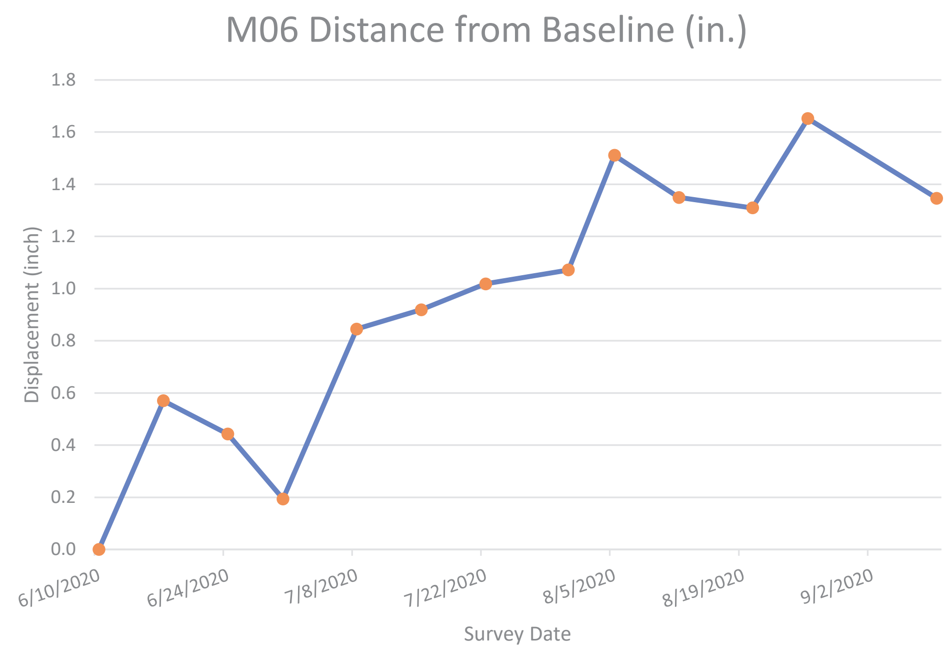
M06 Distance from Baseline (in.)
Displacement (inch)
1.8
1.6
1.4
1.2
1.0
0.8
0.6
0.4
0.2
0.0
6/10/2020
6/24/2020
7/8/2020
7/22/2020
8/5/2020
8/19/2020
9/2/2020
Survey Date

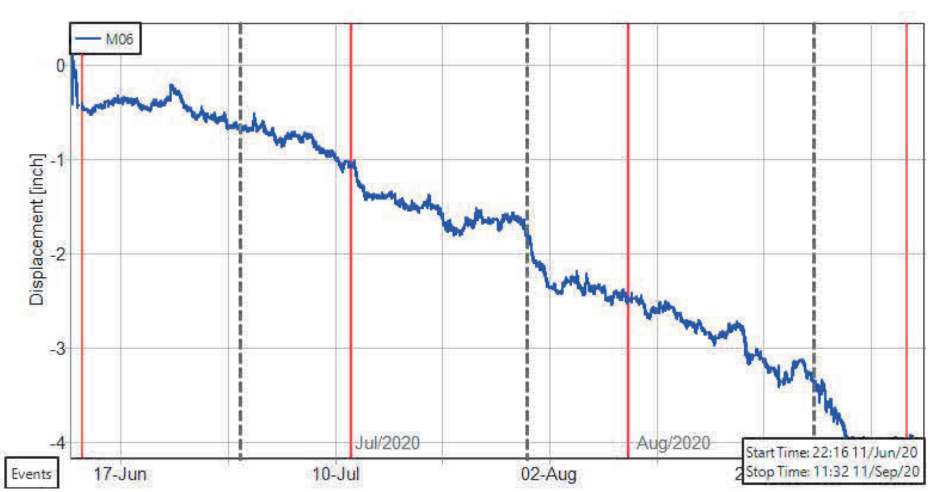
M06
Displacement [inch]
0
-1
-2
-3
-4
Jul/2020
Aug/2020
Events
17-Jun
10-Jul
02-Aug
Start Time: 22:16 11/Jun/20
Stop Time: 11:32 11/Sep/20

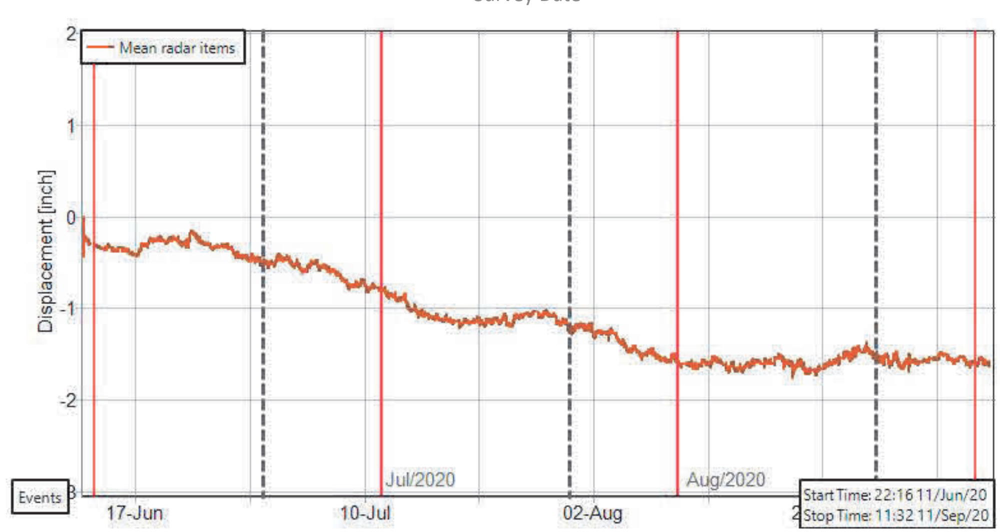
Mean radar items
Displacement [inch]
2
1
0
-1
-2
Jul/2020
Aug/2020
Events
17-Jun
10-Jul
02-Aug
Start Time: 22:16 11/Jun/20
Stop Time: 11:32 11/Sep/20

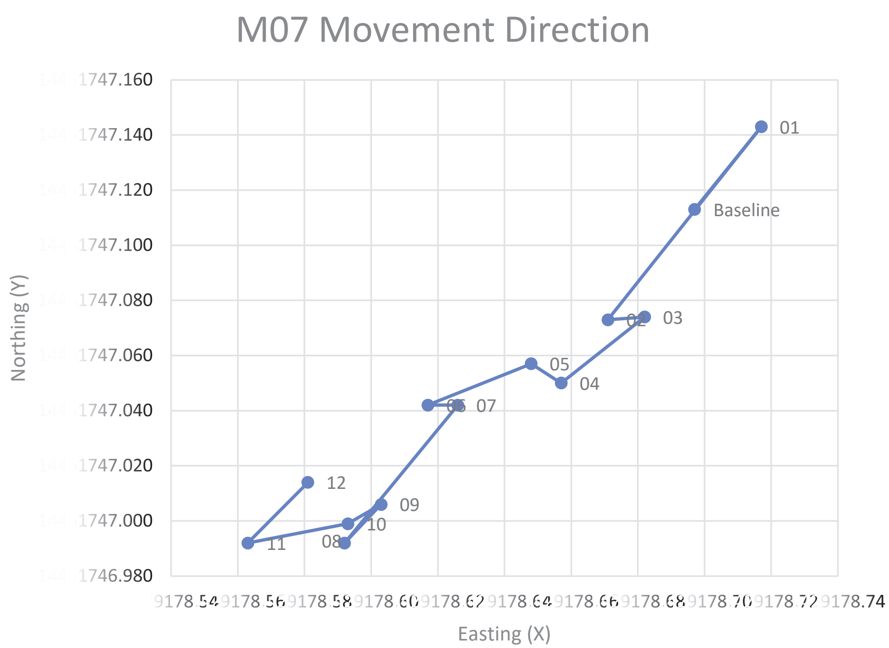
M07 Movement Direction
Northing (Y)
Easting (X)
1747.160
1747.140
1747.120
1747.100
1747.080
1747.060
1747.040
1747.020
1747.000
1746.980
01
Baseline
02
03
04
05
06
07
08
09
10
11
12

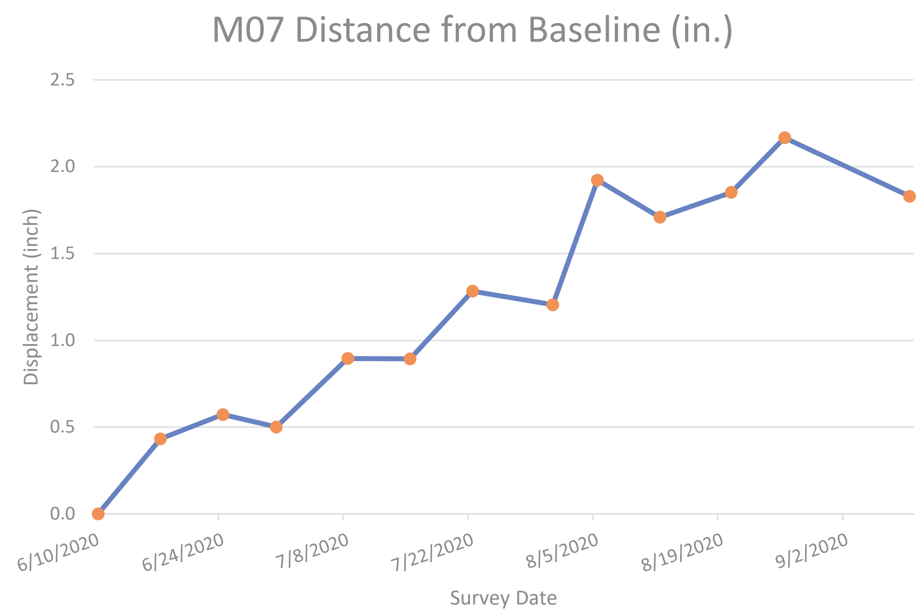
M07 Distance from Baseline (in.)
Displacement (inch)
Survey Date
2.5
2.0
1.5
1.0
0.5
0.0
6/10/2020
6/24/2020
7/8/2020
7/22/2020
8/5/2020
8/19/2020
9/2/2020

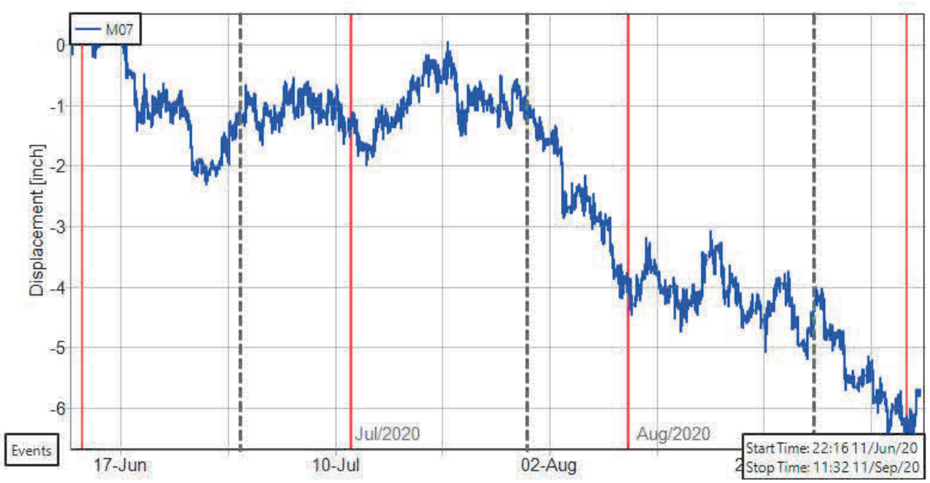
M07
Displacement [inch]
0
-1
-2
-3
-4
-5
-6
Events
17-Jun
10-Jul
02-Aug
Jul/2020
Aug/2020
Start Time: 22:16 11/Jun/20
Stop Time: 11:32 11/Sep/20

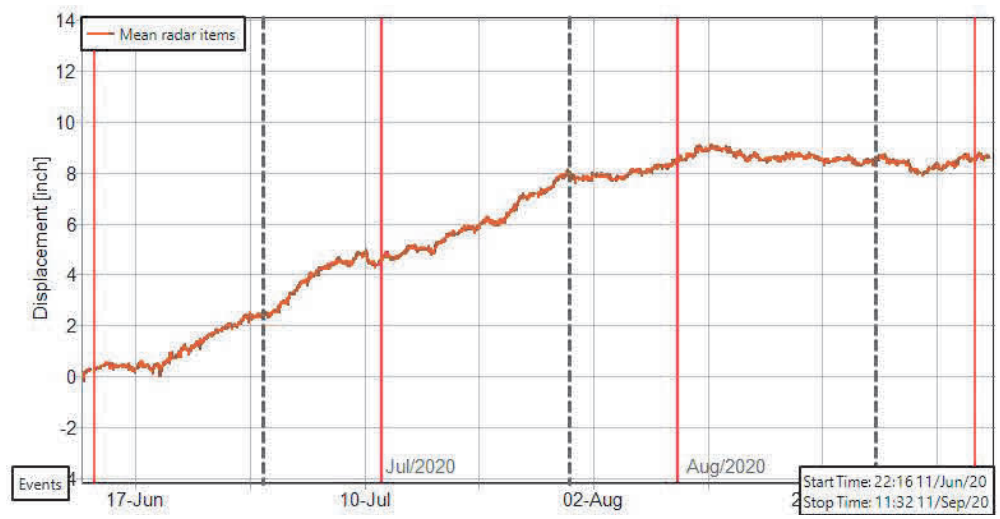
Mean radar items
Displacement [inch]
14
12
10
8
6
4
2
0
-2
Events
17-Jun
10-Jul
02-Aug
Jul/2020
Aug/2020
Start Time: 22:16 11/Jun/20
Stop Time: 11:32 11/Sep/20

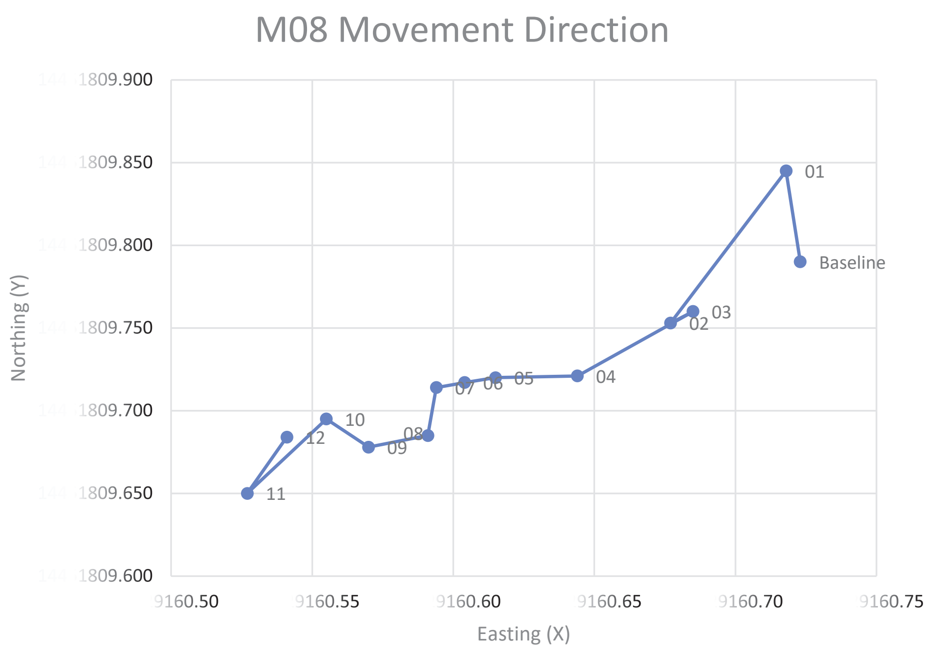

M08 Movement Direction
Northing (Y)
Easting (X)
1809.900
1809.850
1809.800
1809.750
1809.700
1809.650
1809.600
9160.50
9160.55
9160.60
9160.65
9160.70
9160.75
01
Baseline
02
03
04
05
06
07
08
09
10
11
12

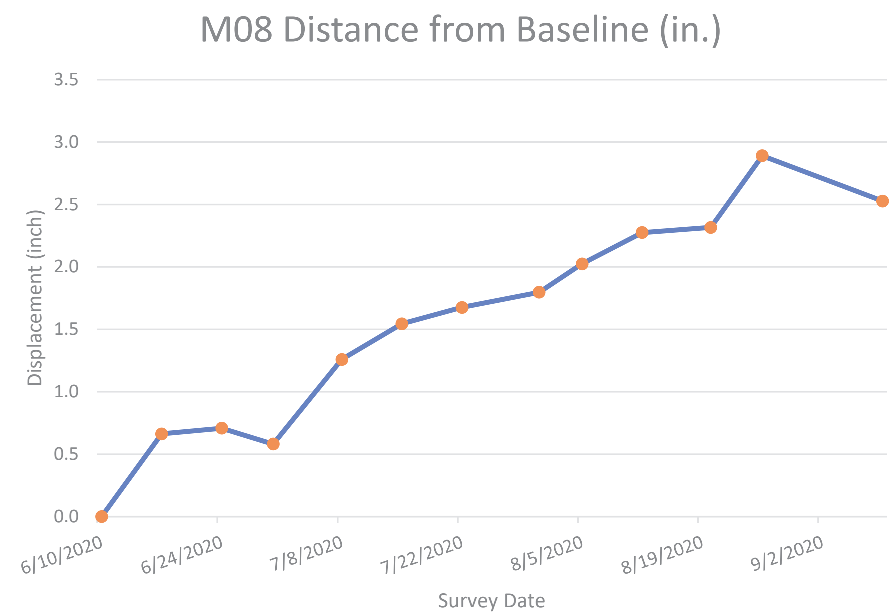

M08 Distance from Baseline (in.)
Displacement (inch)
Survey Date
3.5
3.0
2.5
2.0
1.5
1.0
0.5
0.0
6/10/2020
6/24/2020
7/8/2020
7/22/2020
8/5/2020
8/19/2020
9/2/2020

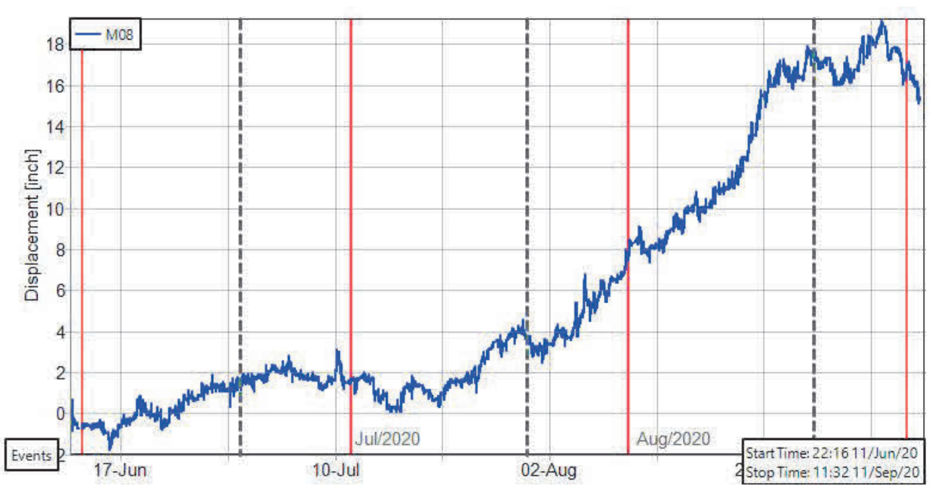

M08
Displacement [inch]
18
16
14
12
10
8
6
4
2
0
Events
17-Jun
10-Jul
02-Aug
Jul/2020
Aug/2020
Start Time: 22:16 11/Jun/20
Stop Time: 11:32 11/Sep/20

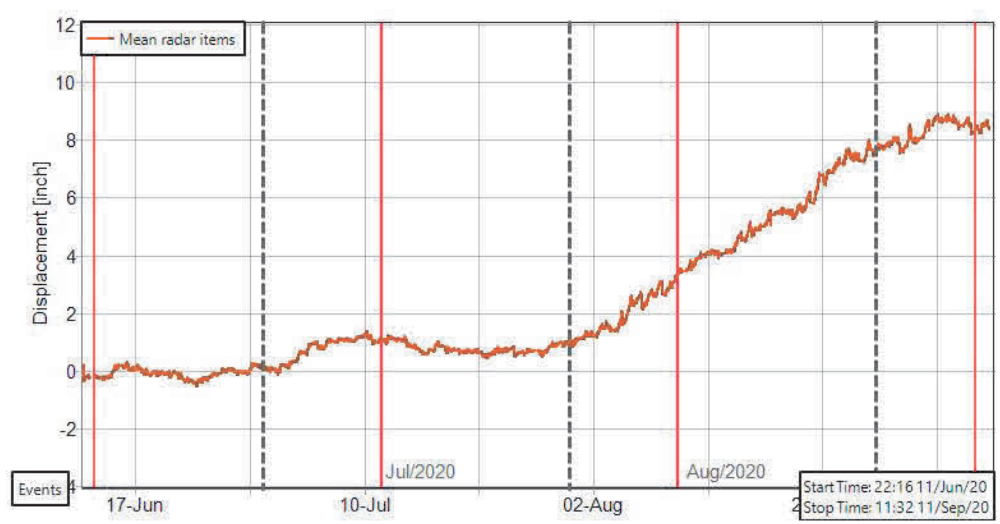

Mean radar items
Displacement [inch]
12
10
8
6
4
2
0
-2
Events
17-Jun
10-Jul
02-Aug
Jul/2020
Aug/2020
Start Time: 22:16 11/Jun/20
Stop Time: 11:32 11/Sep/20

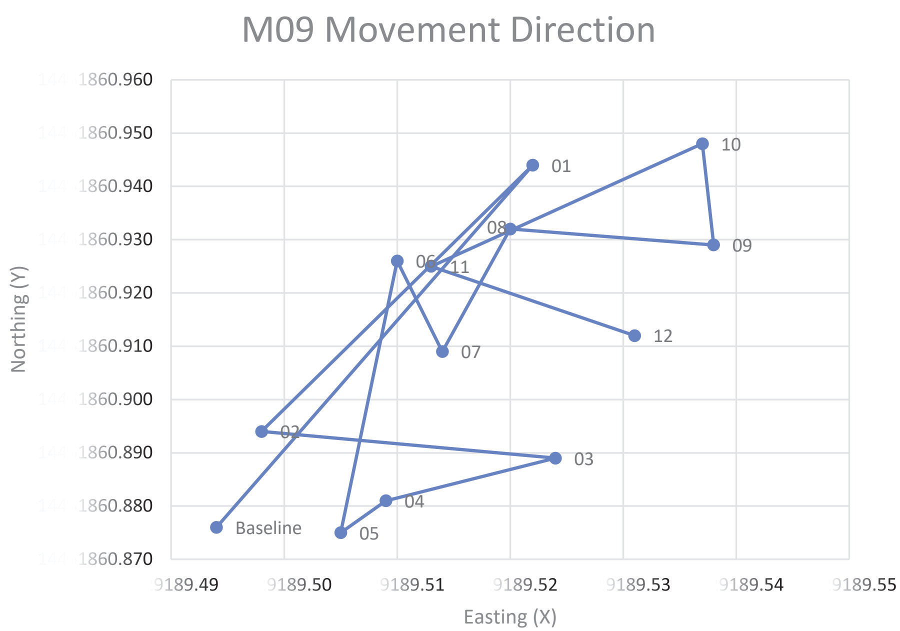

M09 Movement Direction
Northing (Y)
Easting (X)
Baseline
01
02
03
04
05
06
07
08
09
10
11
12

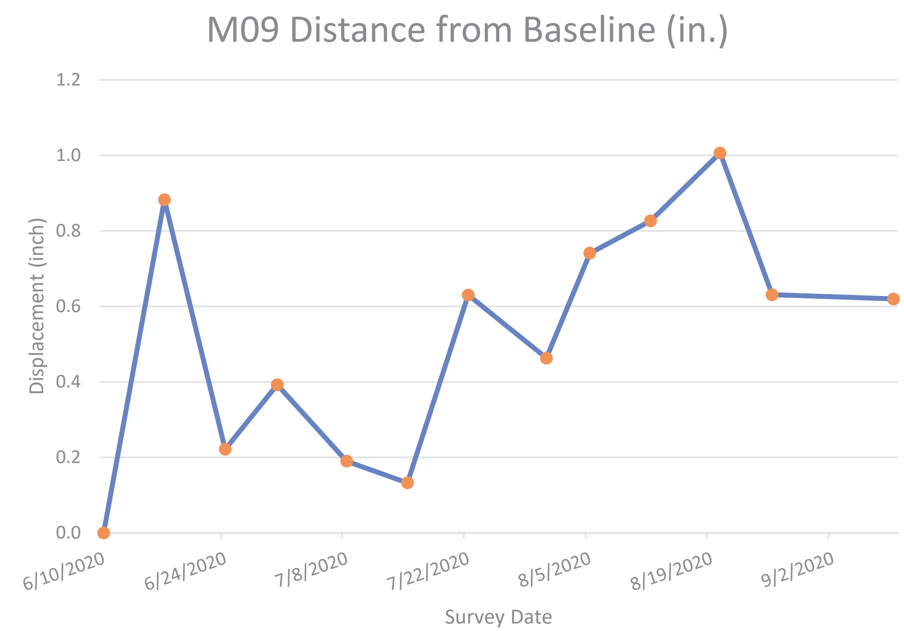

M09 Distance from Baseline (in.)
Displacement (inch)
Survey Date

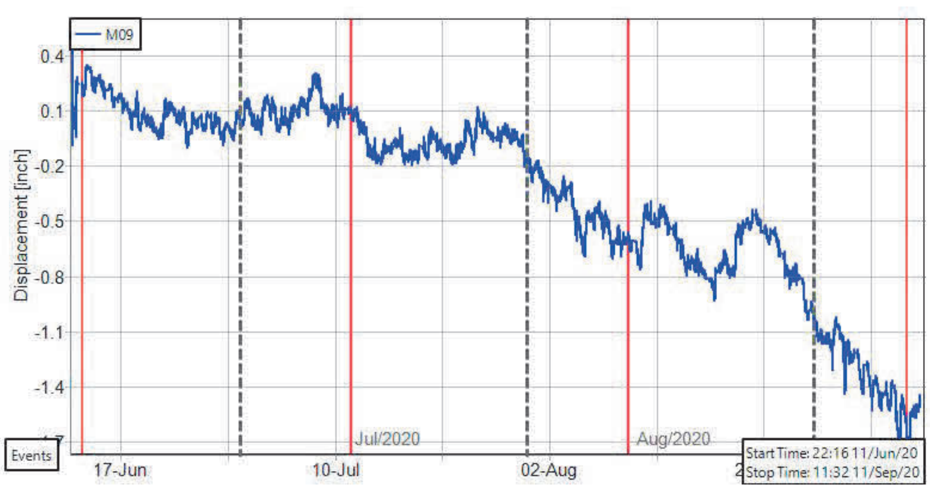

M09
Displacement [inch]
Events
Jul/2020
Aug/2020
17-Jun
10-Jul
02-Aug
Start Time: 22:16 11/Jun/20
Stop Time: 11:32 11/Sep/20

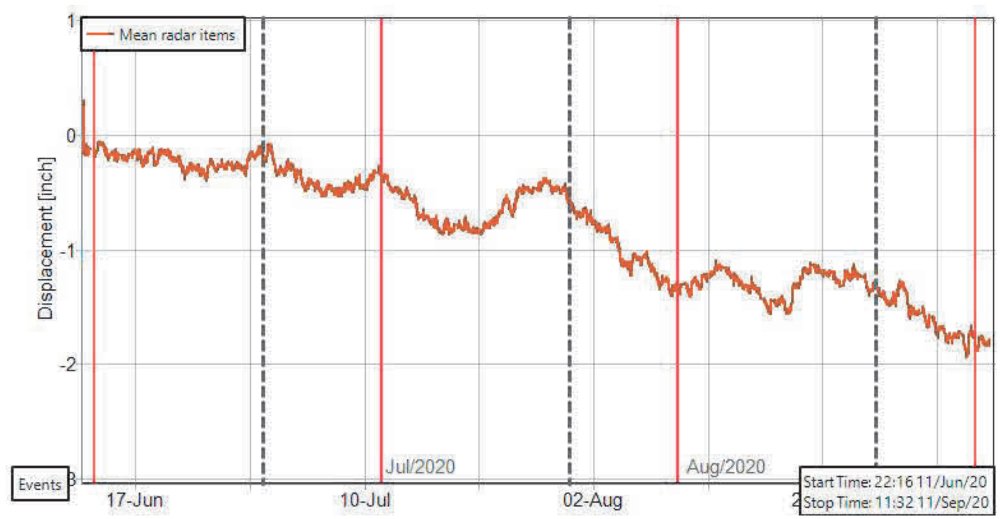

Mean radar items
Displacement [inch]
Events
Jul/2020
Aug/2020
17-Jun
10-Jul
02-Aug
Start Time: 22:16 11/Jun/20
Stop Time: 11:32 11/Sep/20

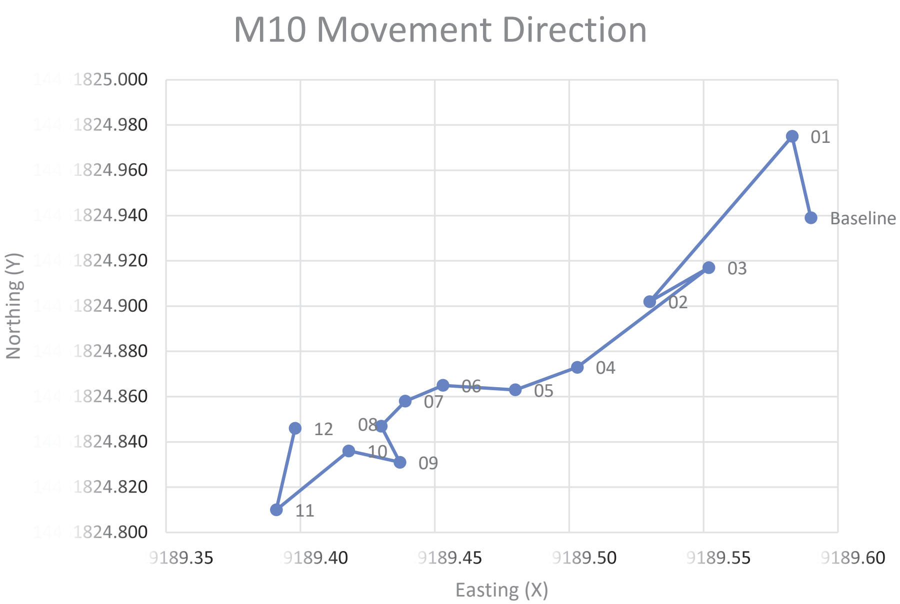
M10 Movement Direction
Northing (Y)
1825.000
1824.980
1824.960
1824.940
1824.920
1824.900
1824.880
1824.860
1824.840
1824.820
1824.800
9189.35
9189.40
9189.45
9189.50
9189.55
9189.60
Easting (X)
01
Baseline
03
02
04
05
06
07
08
10
09
12
11

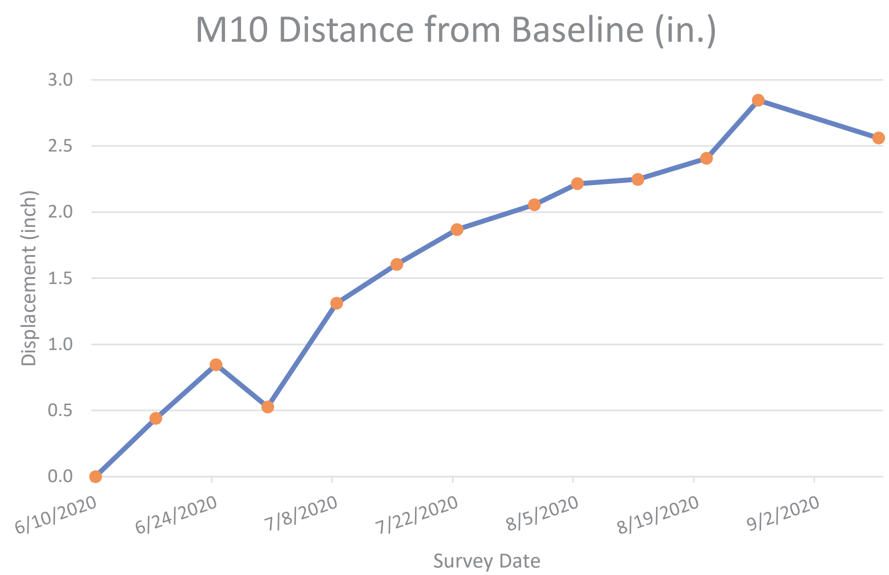
M10 Distance from Baseline (in.)
Displacement (inch)
3.0
2.5
2.0
1.5
1.0
0.5
0.0
6/10/2020
6/24/2020
7/8/2020
7/22/2020
8/5/2020
8/19/2020
9/2/2020
Survey Date

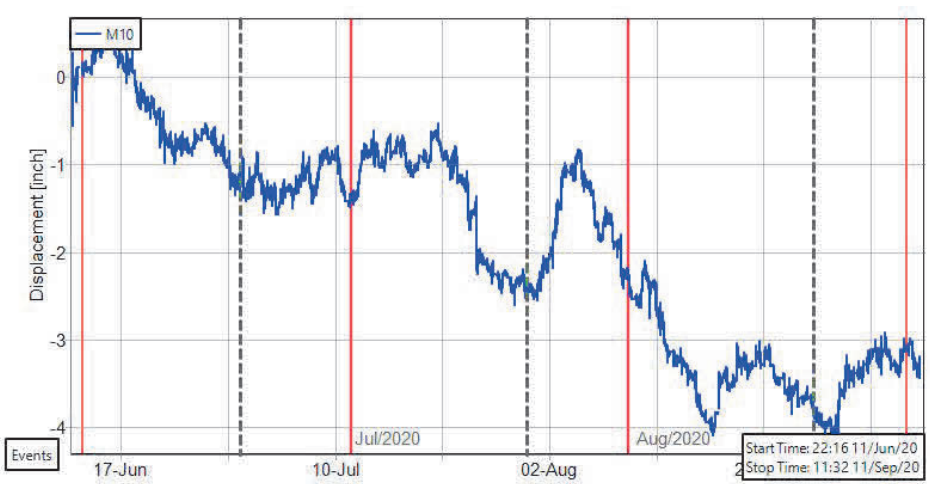
M10
Displacement [inch]
0
-1
-2
-3
-4
Events
Jul/2020
Aug/2020
17-Jun
10-Jul
02-Aug
Start Time: 22:16 11/Jun/20
Stop Time: 11:32 11/Sep/20

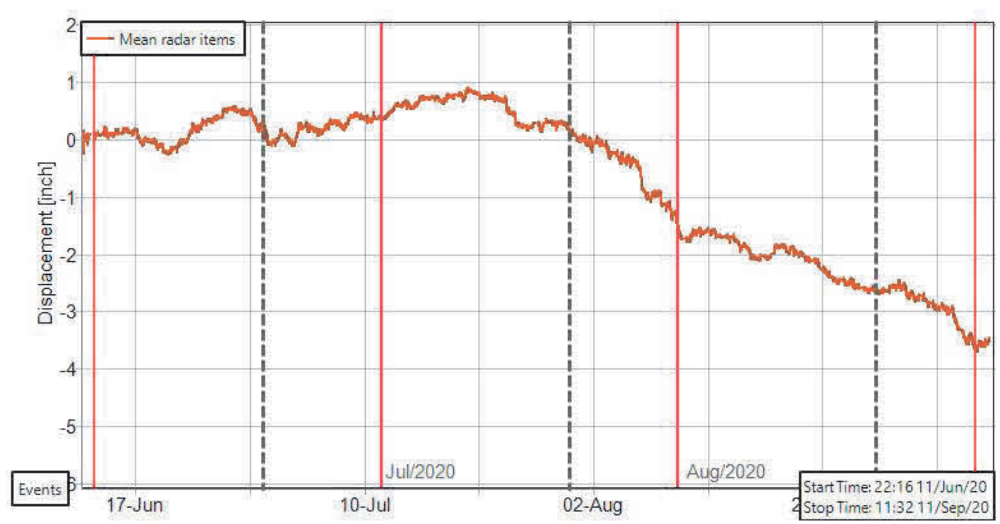
Mean radar items
Displacement [inch]
2
1
0
-1
-2
-3
-4
-5
Events
Jul/2020
Aug/2020
17-Jun
10-Jul
02-Aug
Start Time: 22:16 11/Jun/20
Stop Time: 11:32 11/Sep/20

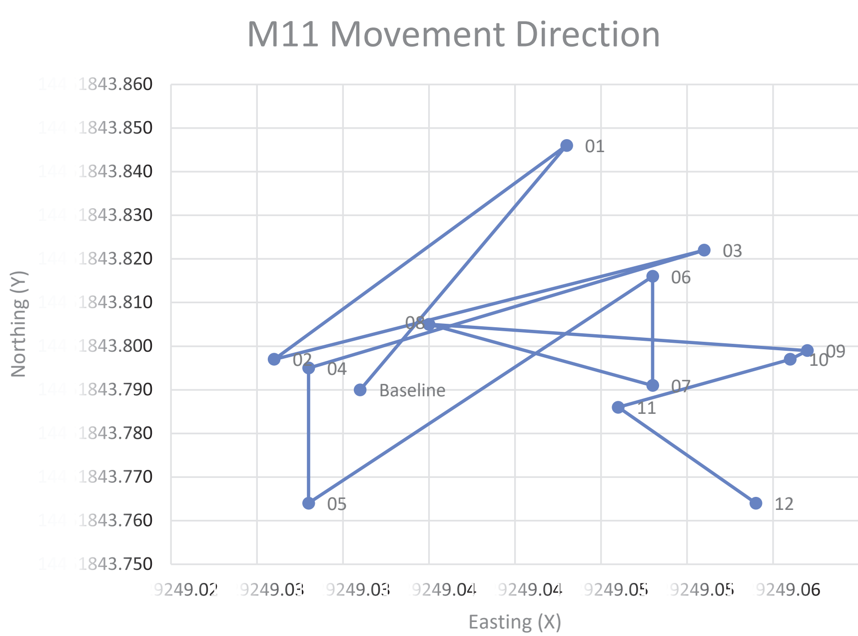
M11 Movement Direction
Northing (Y)
Easting (X)
1843.860
1843.850
1843.840
1843.830
1843.820
1843.810
1843.800
1843.790
1843.780
1843.770
1843.760
1843.750
Baseline
01
02
03
04
05
06
07
08
09
10
11
12

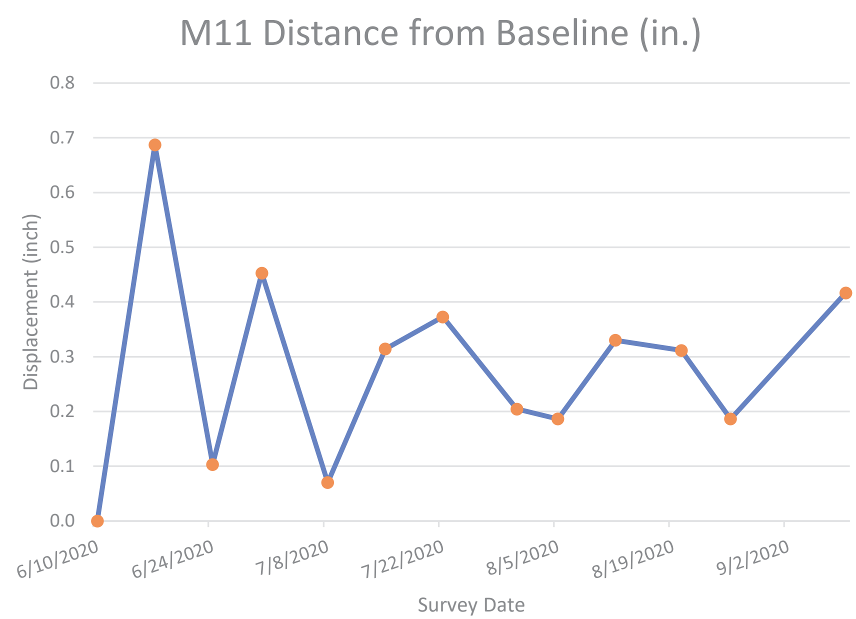
M11 Distance from Baseline (in.)
Displacement (inch)
Survey Date
0.8
0.7
0.6
0.5
0.4
0.3
0.2
0.1
0.0
6/10/2020
6/24/2020
7/8/2020
7/22/2020
8/5/2020
8/19/2020
9/2/2020

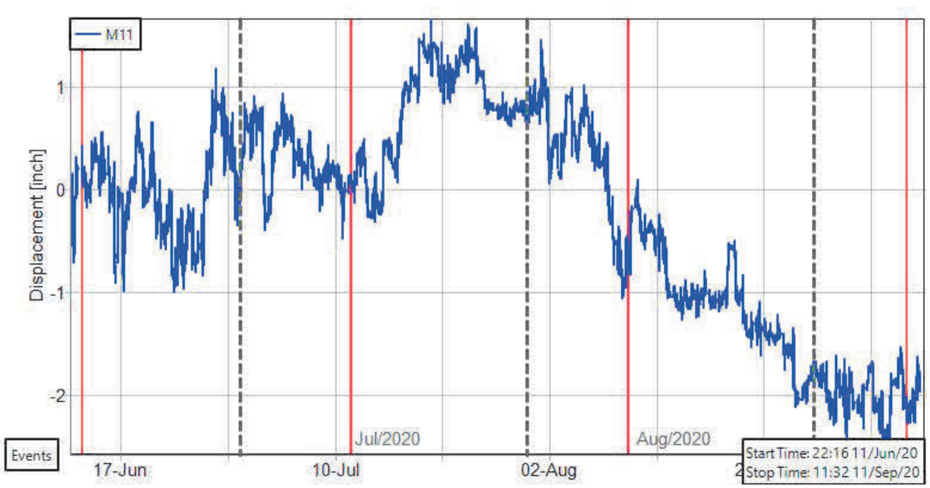
M11
Displacement [inch]
Events
17-Jun
10-Jul
02-Aug
Jul/2020
Aug/2020
Start Time: 22:16 11/Jun/20
Stop Time: 11:32 11/Sep/20

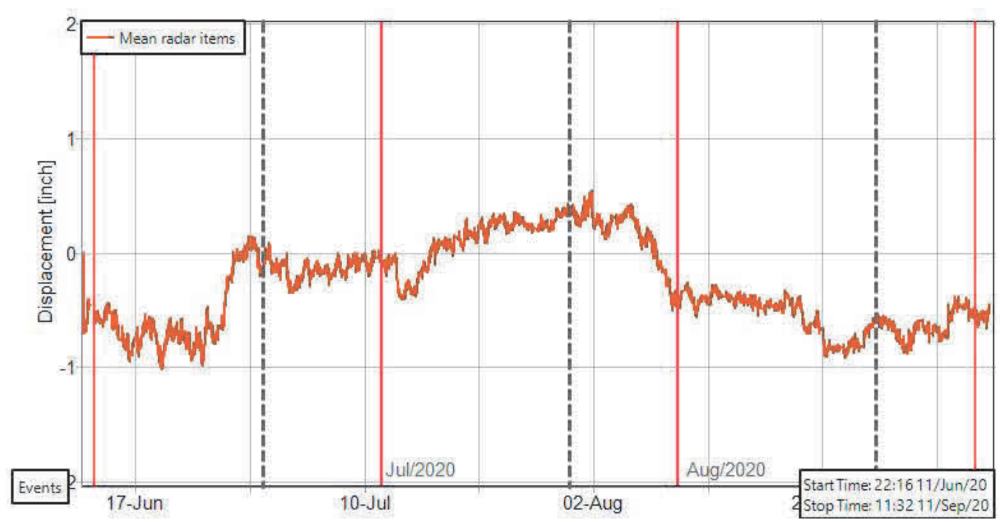
Mean radar items
Displacement [inch]
Events
17-Jun
10-Jul
02-Aug
Jul/2020
Aug/2020
Start Time: 22:16 11/Jun/20
Stop Time: 11:32 11/Sep/20

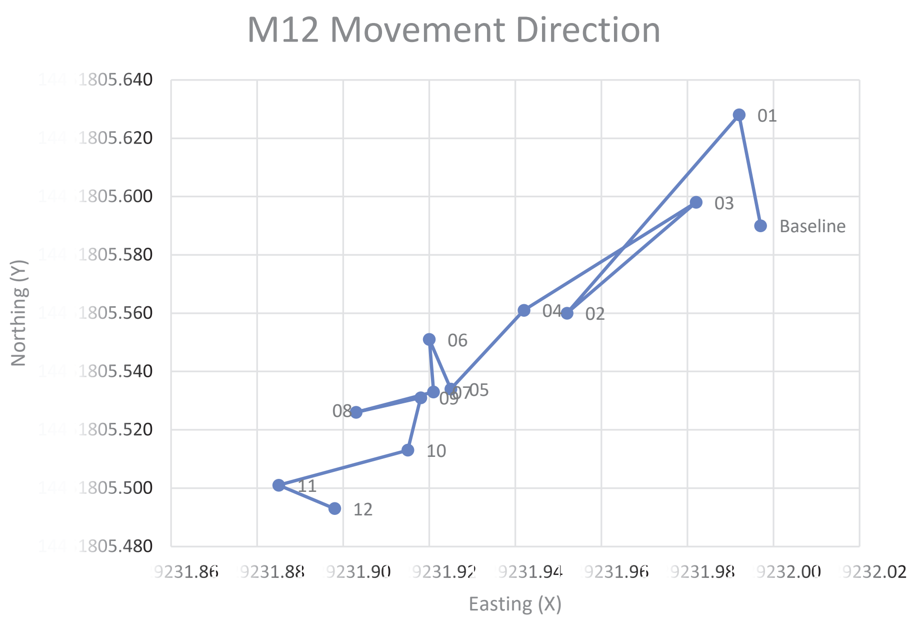
M12 Movement Direction
1805.640
1805.620
1805.600
1805.580
1805.560
1805.540
1805.520
1805.500
1805.480
Northing (Y)
9231.86
9231.88
9231.90
9231.92
9231.94
9231.96
9231.98
9232.00
9232.02
Easting (X)
01
03
Baseline
04
02
06
05
07
09
08
10
11
12

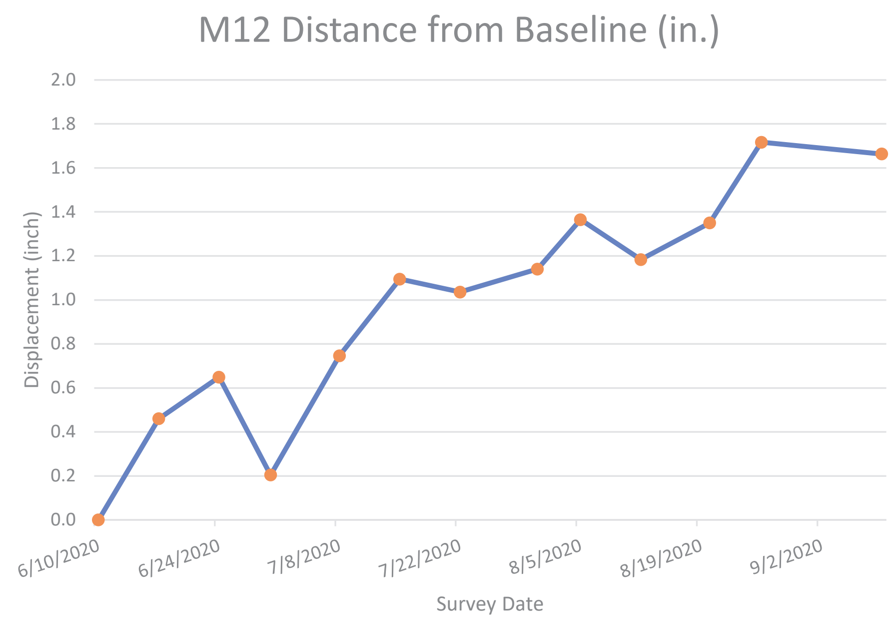
M12 Distance from Baseline (in.)
2.0
1.8
1.6
1.4
1.2
1.0
0.8
0.6
0.4
0.2
0.0
Displacement (inch)
6/10/2020
6/24/2020
7/8/2020
7/22/2020
8/5/2020
8/19/2020
9/2/2020
Survey Date

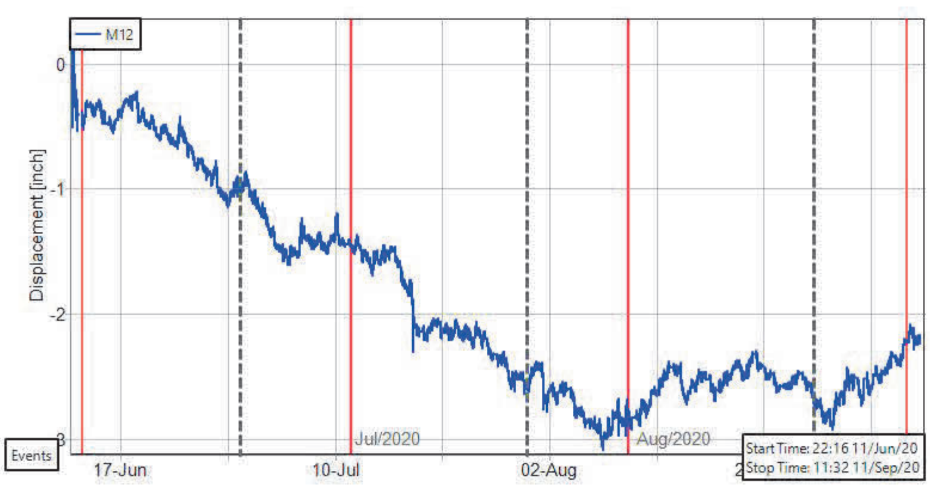
M12
0
-1
-2
Displacement [inch]
Events
17-Jun
10-Jul
02-Aug
Jul/2020
Aug/2020
Start Time: 22:16 11/Jun/20
Stop Time: 11:32 11/Sep/20

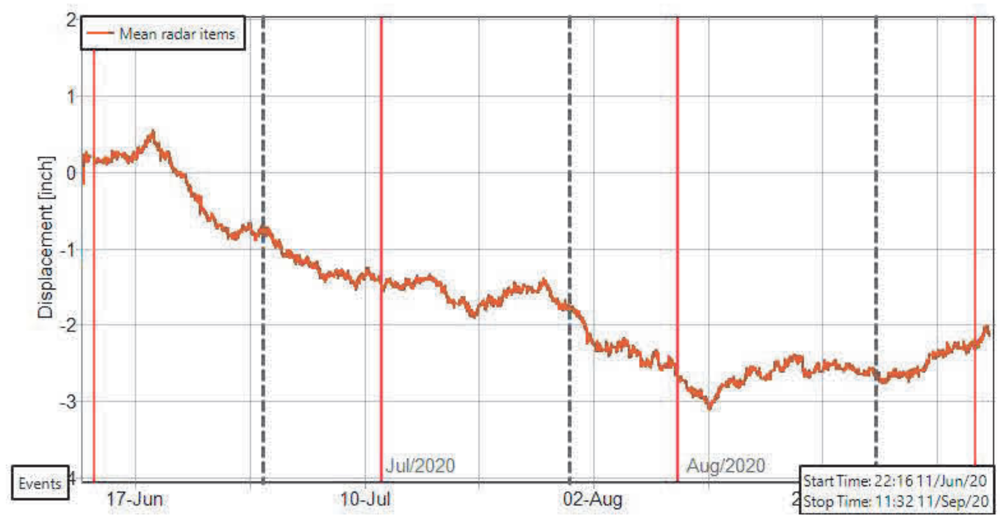
Mean radar items
2
1
0
-1
-2
-3
Displacement [inch]
Events
17-Jun
10-Jul
02-Aug
Jul/2020
Aug/2020
Start Time: 22:16 11/Jun/20
Stop Time: 11:32 11/Sep/20

M13 Movement Direction

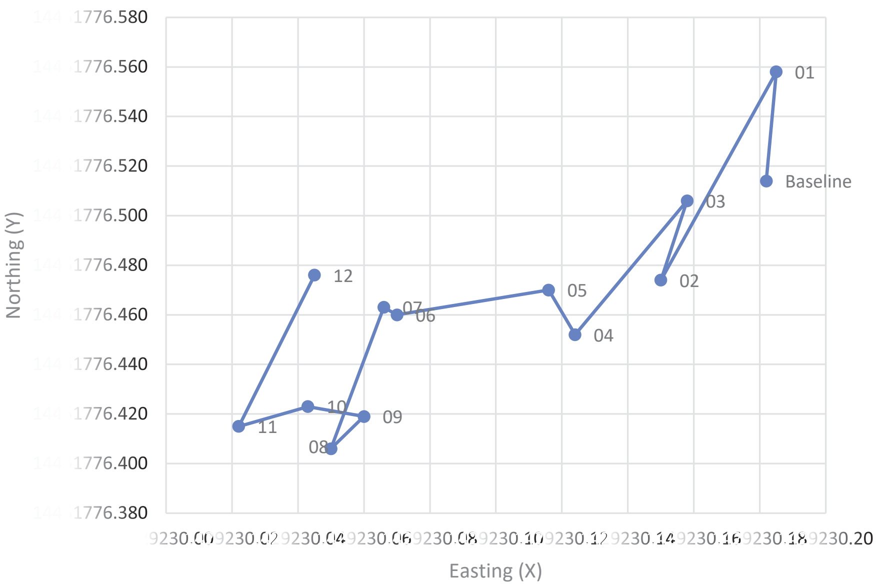

M13 Distance from Baseline (in.)

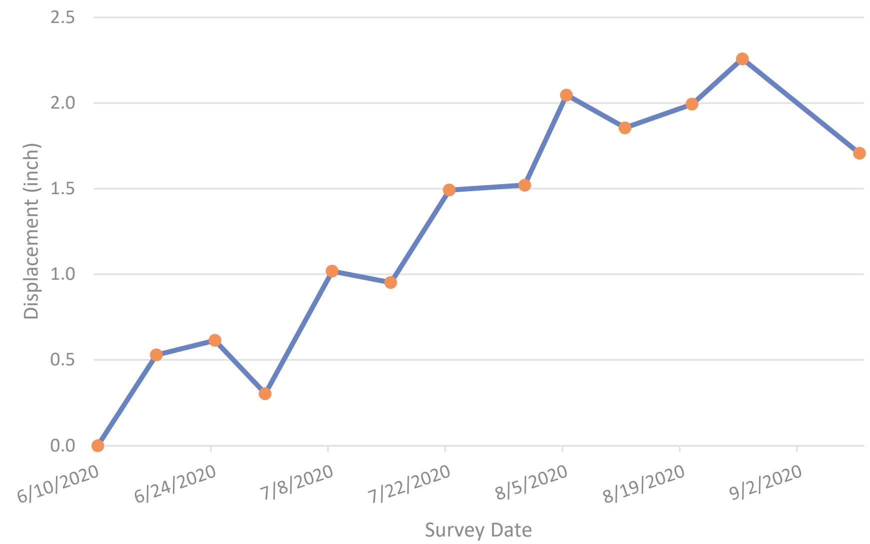

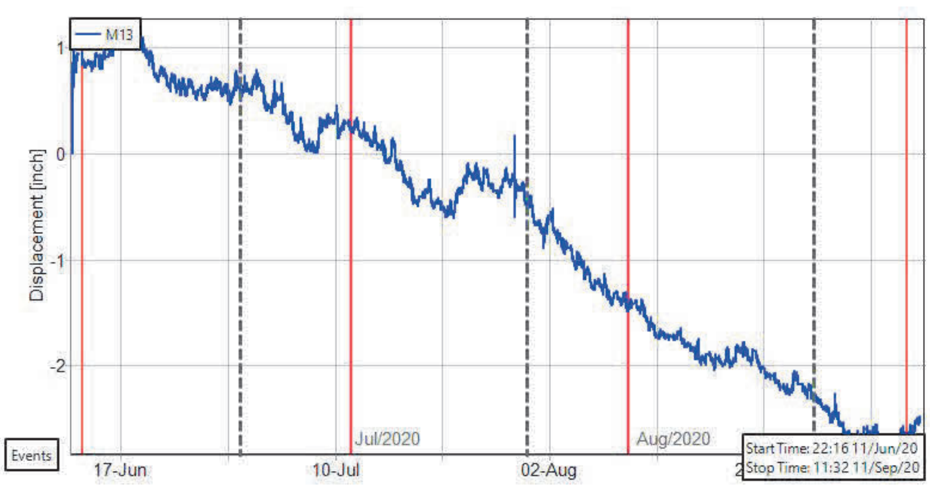

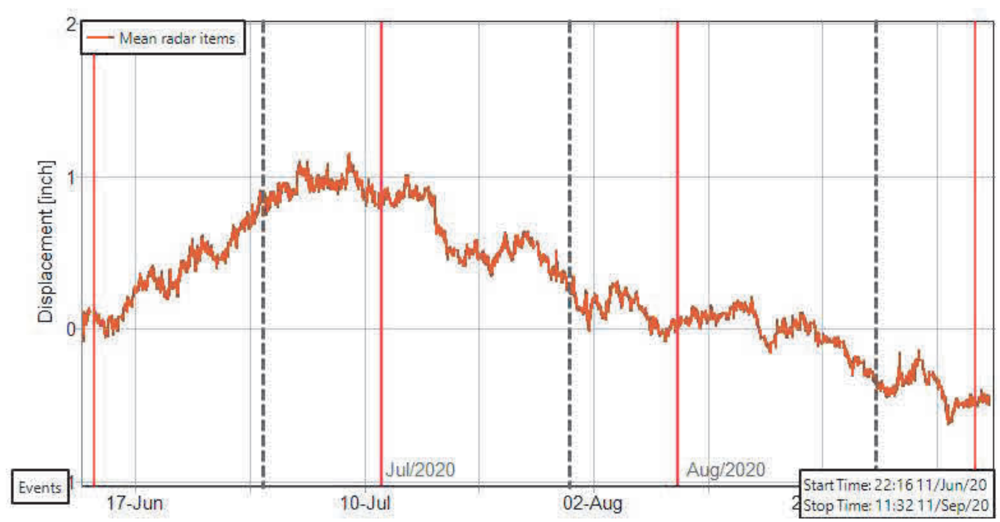

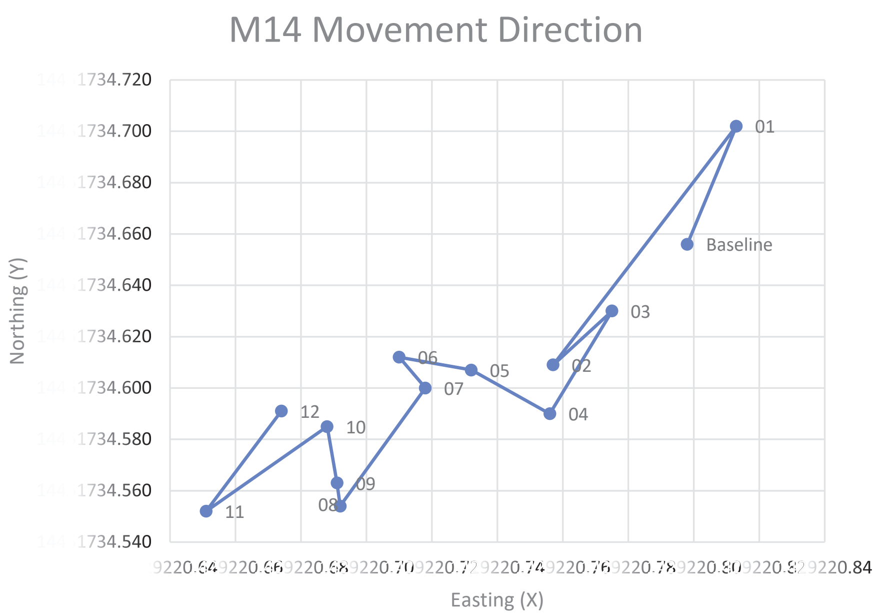
M14 Movement Direction
Northing (Y)
1734.720
1734.700
1734.680
1734.660
1734.640
1734.620
1734.600
1734.580
1734.560
1734.540
Easting (X)
01
Baseline
03
02
06
05
07
04
12
10
09
08
11

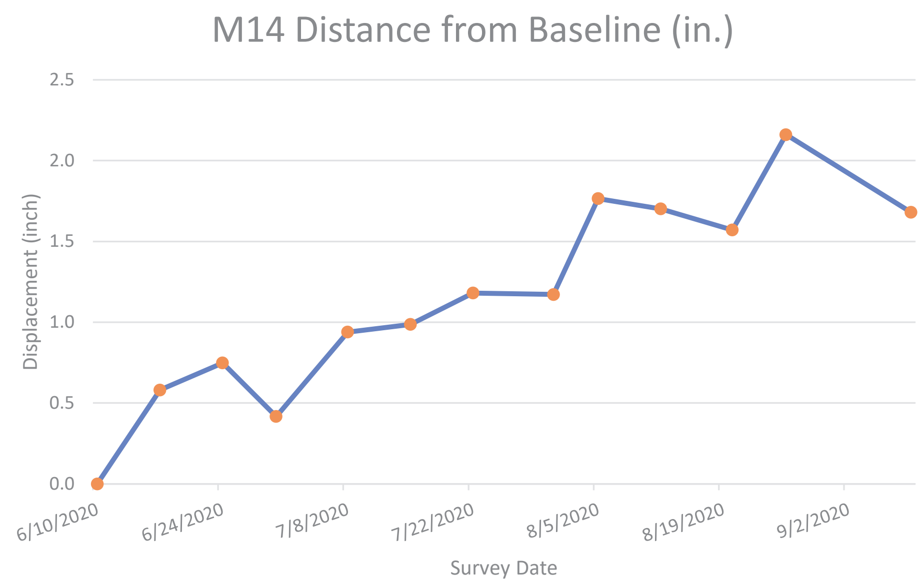
M14 Distance from Baseline (in.)
Displacement (inch)
2.5
2.0
1.5
1.0
0.5
0.0
6/10/2020
6/24/2020
7/8/2020
7/22/2020
8/5/2020
8/19/2020
9/2/2020
Survey Date

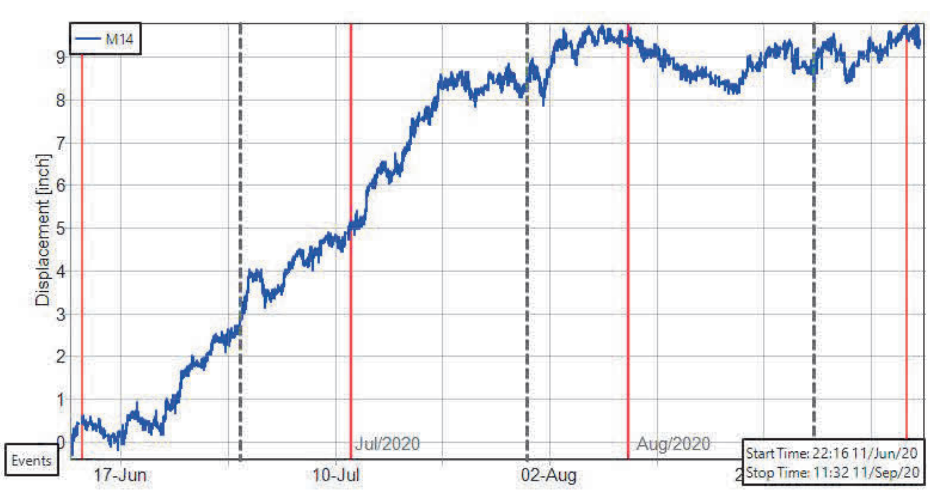
M14
Displacement [inch]
9
8
7
6
5
4
3
2
1
0
Events
17-Jun
10-Jul
02-Aug
Jul/2020
Aug/2020
Start Time: 22:16 11/Jun/20
Stop Time: 11:32 11/Sep/20

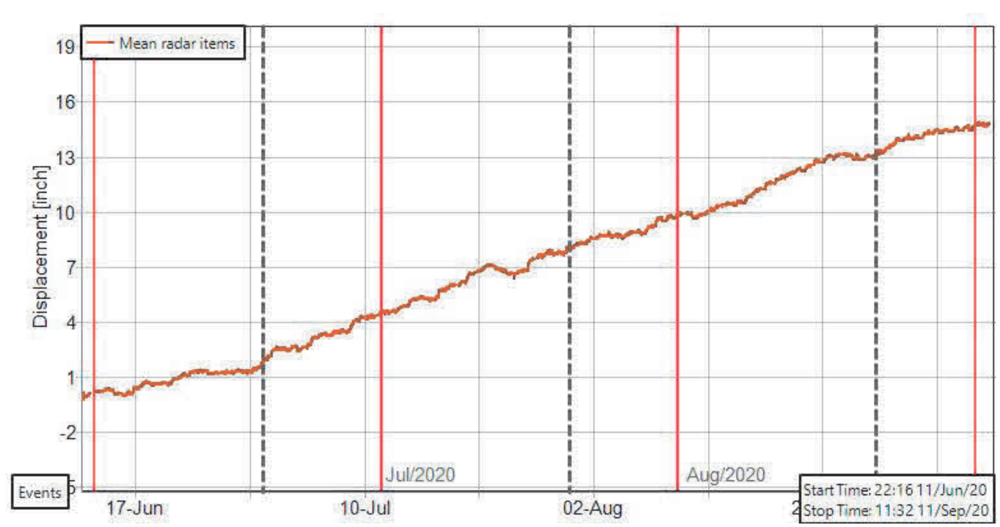
Mean radar items
Displacement [inch]
19
16
13
10
7
4
1
-2
-5
Events
17-Jun
10-Jul
02-Aug
Jul/2020
Aug/2020
Start Time: 22:16 11/Jun/20
Stop Time: 11:32 11/Sep/20

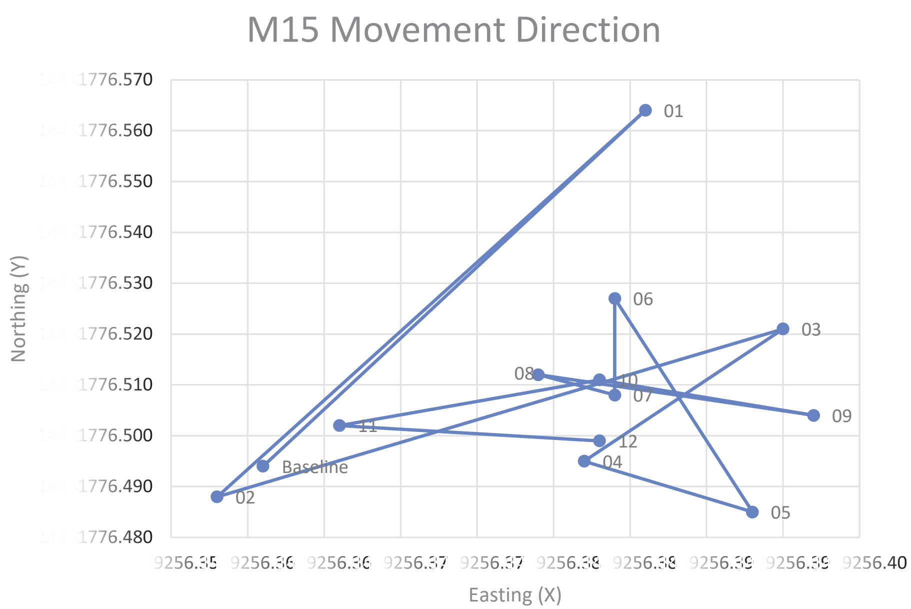
M15 Movement Direction
Northing (Y)
Easting (X)
1776.570
1776.560
1776.550
1776.540
1776.530
1776.520
1776.510
1776.500
1776.490
1776.480
9256.40
01
02
03
04
05
06
07
08
09
10
11
12
Baseline

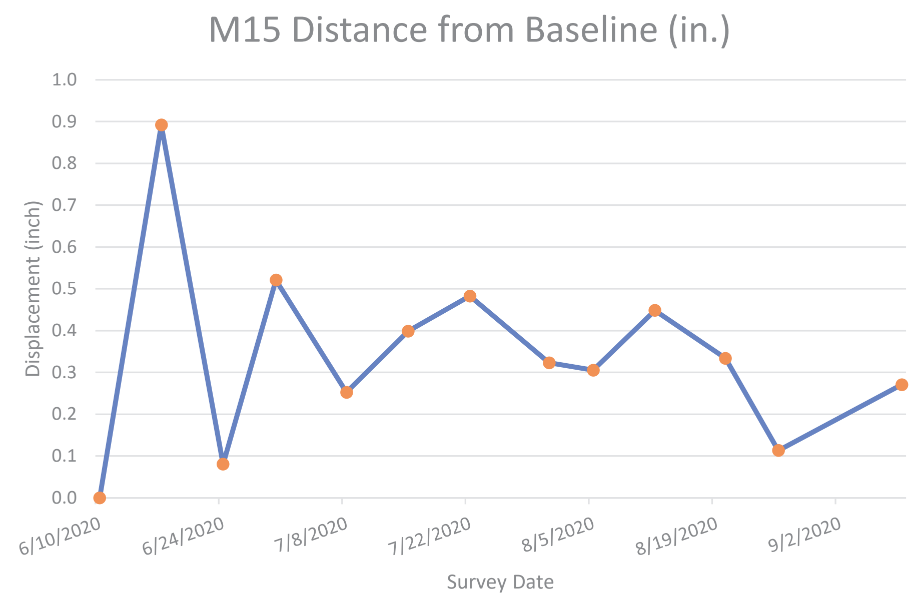
M15 Distance from Baseline (in.)
Displacement (inch)
Survey Date
1.0
0.9
0.8
0.7
0.6
0.5
0.4
0.3
0.2
0.1
0.0
6/10/2020
6/24/2020
7/8/2020
7/22/2020
8/5/2020
8/19/2020
9/2/2020

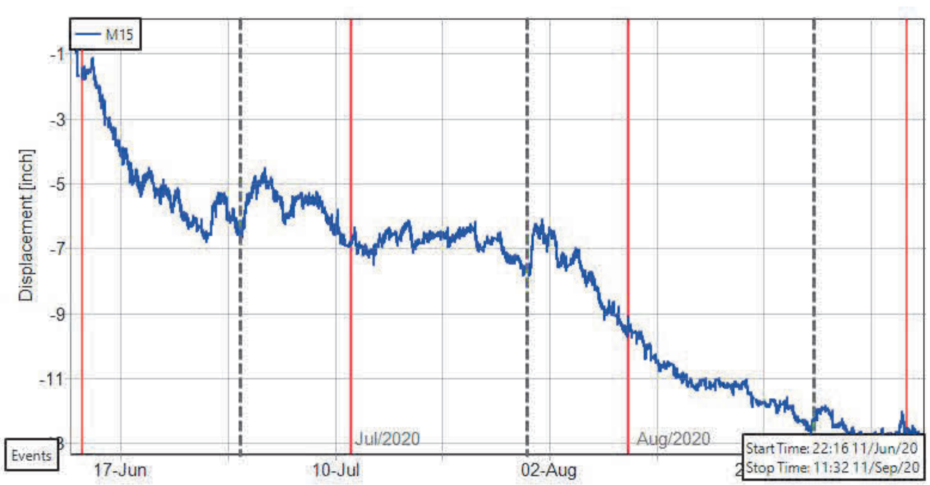
M15
Displacement [inch]
-1
-3
-5
-7
-9
-11
Jul/2020
Aug/2020
Events
17-Jun
10-Jul
02-Aug
Start Time: 22:16 11/Jun/20
Stop Time: 11:32 11/Sep/20

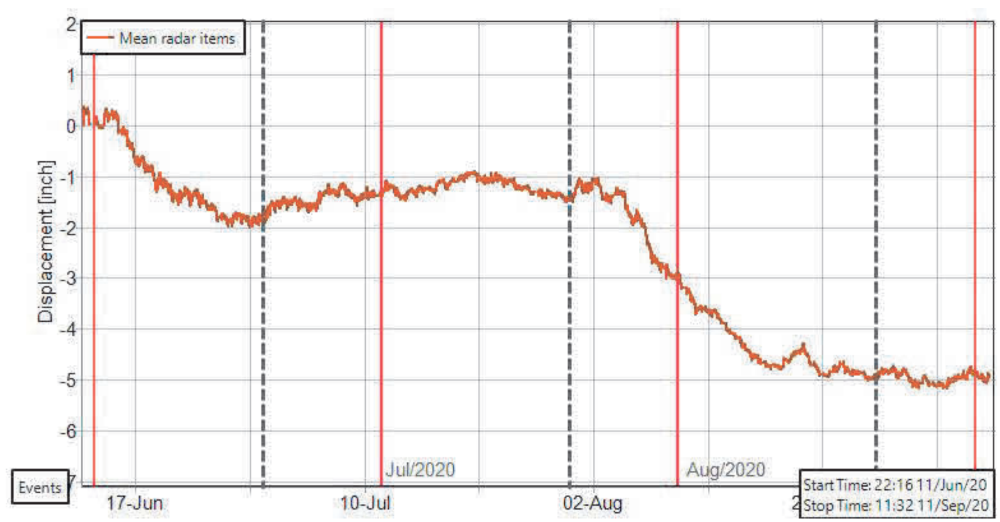
Mean radar items
Displacement [inch]
2
1
0
-1
-2
-3
-4
-5
-6
Jul/2020
Aug/2020
Events
17-Jun
10-Jul
02-Aug
Start Time: 22:16 11/Jun/20
Stop Time: 11:32 11/Sep/20

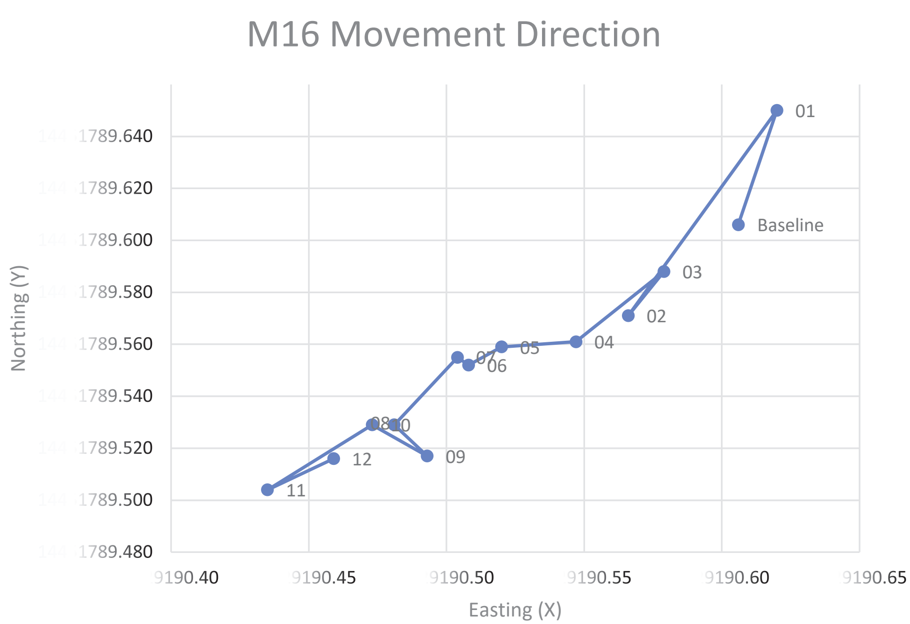
M16 Movement Direction
Northing (Y)
Easting (X)
1789.640
1789.620
1789.600
1789.580
1789.560
1789.540
1789.520
1789.500
1789.480
9190.40
9190.45
9190.50
9190.55
9190.60
9190.65
01
Baseline
03
02
04
05
06
09
12
11

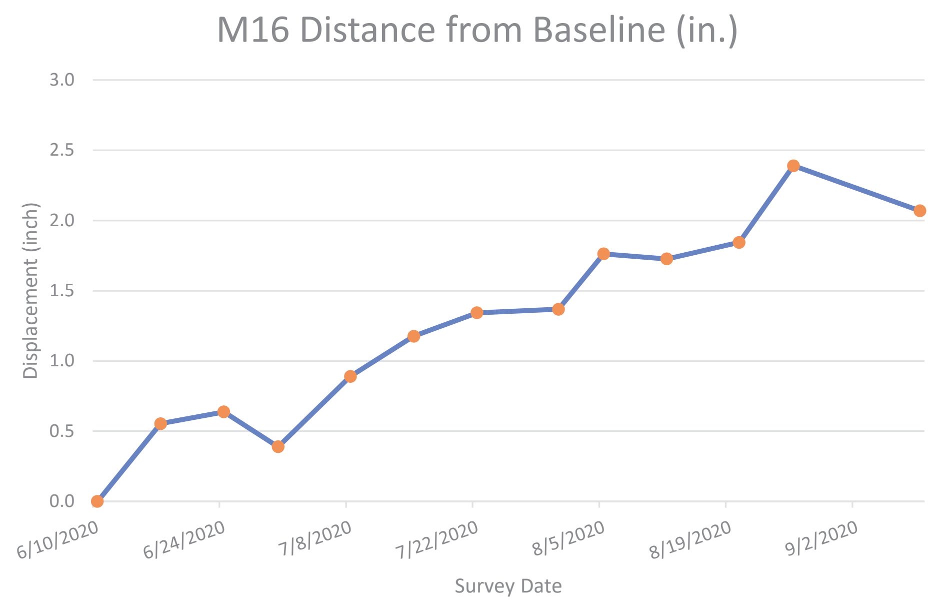
M16 Distance from Baseline (in.)
Displacement (inch)
Survey Date
3.0
2.5
2.0
1.5
1.0
0.5
0.0
6/10/2020
6/24/2020
7/8/2020
7/22/2020
8/5/2020
8/19/2020
9/2/2020

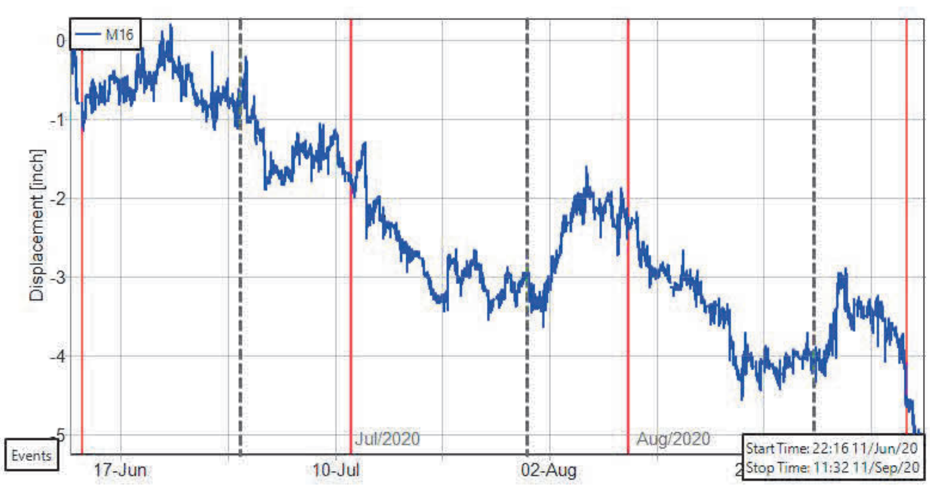
M16
Displacement [inch]
0
-1
-2
-3
-4
-5
Events
17-Jun
10-Jul
02-Aug
Jul/2020
Aug/2020
Start Time: 22:16 11/Jun/20
Stop Time: 11:32 11/Sep/20

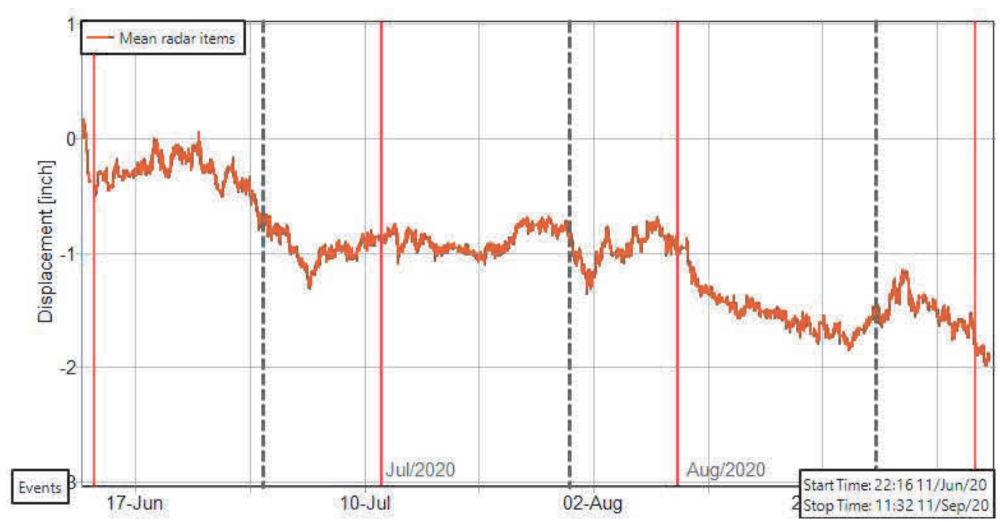
Mean radar items
Displacement [inch]
1
0
-1
-2
Events
17-Jun
10-Jul
02-Aug
Jul/2020
Aug/2020
Start Time: 22:16 11/Jun/20
Stop Time: 11:32 11/Sep/20

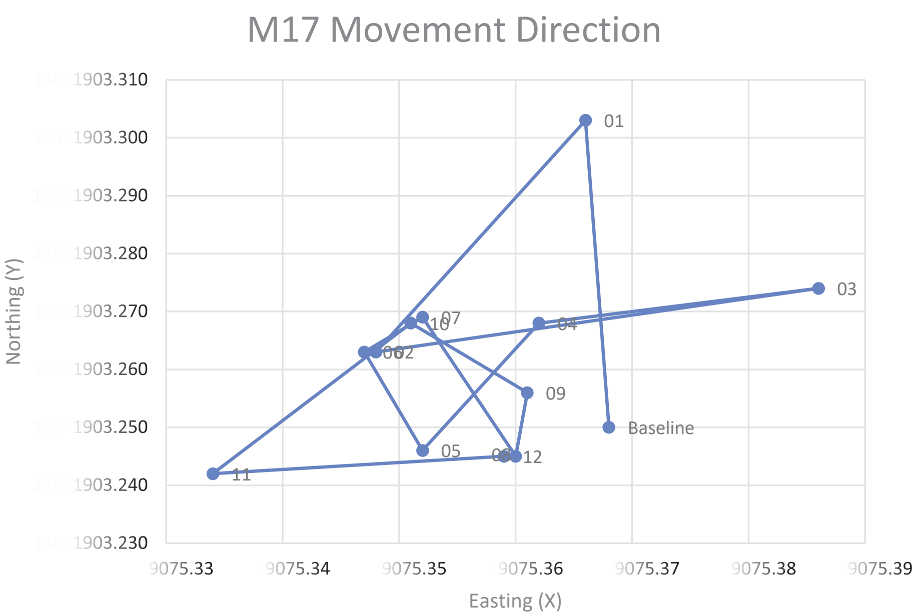

M17 Movement Direction
Northing (Y)
1903.310
1903.300
1903.290
1903.280
1903.270
1903.260
1903.250
1903.240
1903.230
9075.33
9075.34
9075.35
9075.36
9075.37
9075.38
9075.39
Easting (X)
01
03
04
07
10
06
02
09
Baseline
05
08
12
11

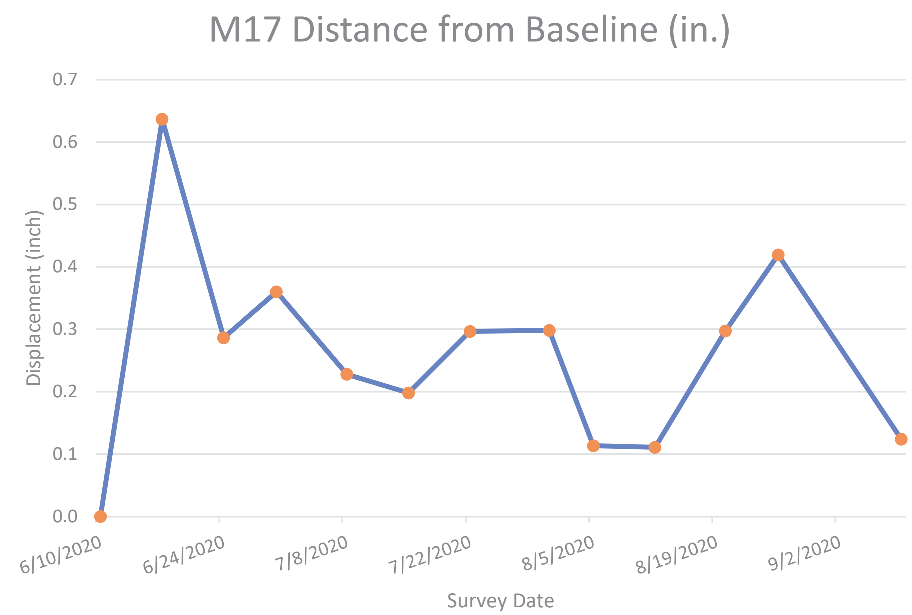

M17 Distance from Baseline (in.)
Displacement (inch)
0.7
0.6
0.5
0.4
0.3
0.2
0.1
0.0
6/10/2020
6/24/2020
7/8/2020
7/22/2020
8/5/2020
8/19/2020
9/2/2020
Survey Date

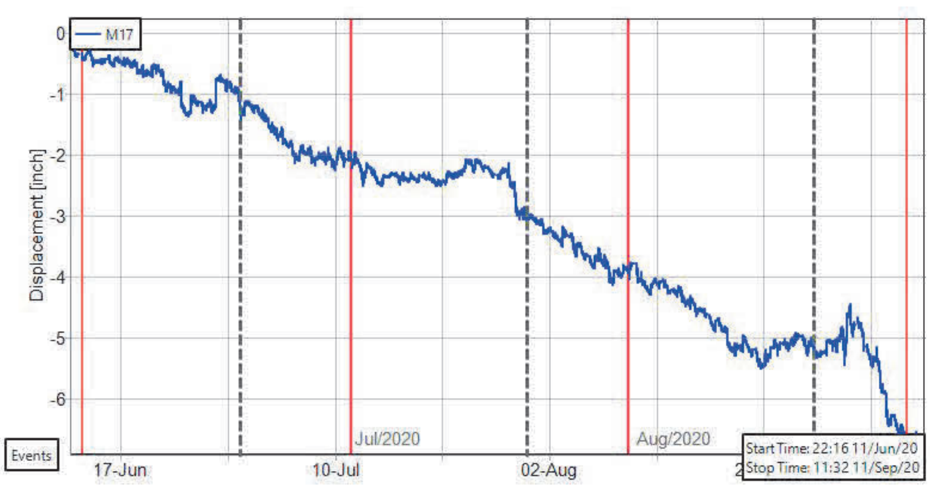

M17
Displacement [inch]
0
-1
-2
-3
-4
-5
-6
Events
17-Jun
10-Jul
02-Aug
Jul/2020
Aug/2020
Start Time: 22:16 11/Jun/20
Stop Time: 11:32 11/Sep/20

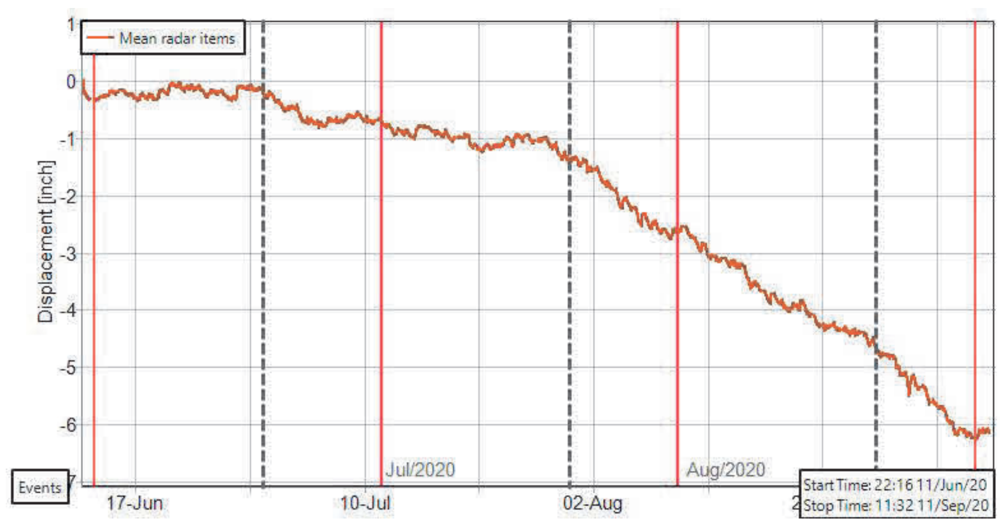

Mean radar items
Displacement [inch]
1
0
-1
-2
-3
-4
-5
-6
-7
Events
17-Jun
10-Jul
02-Aug
Jul/2020
Aug/2020
Start Time: 22:16 11/Jun/20
Stop Time: 11:32 11/Sep/20

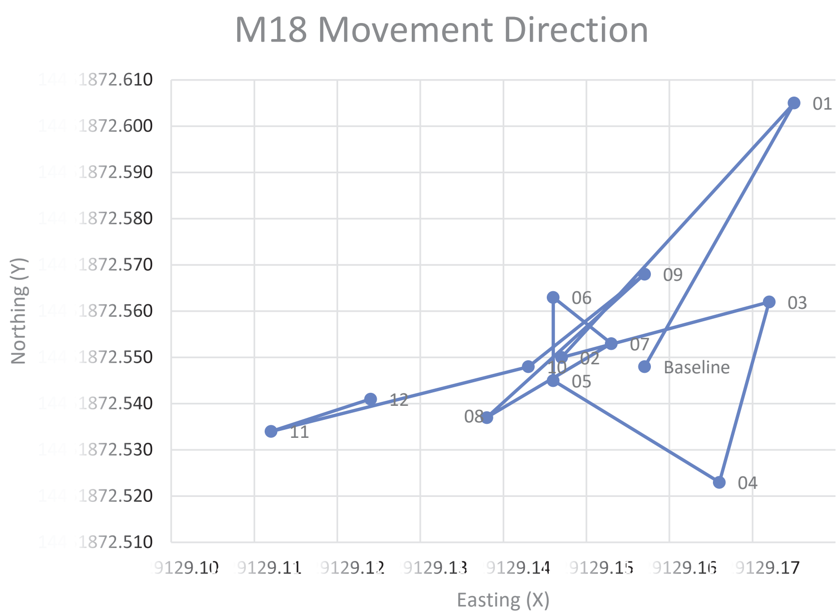
M18 Movement Direction
Northing (Y)
Easting (X)
1872.610
1872.600
1872.590
1872.580
1872.570
1872.560
1872.550
1872.540
1872.530
1872.520
1872.510
9129.10
9129.11
9129.12
9129.13
9129.14
9129.15
9129.16
9129.17
01
02
03
04
05
06
07
08
09
10
11
12
Baseline

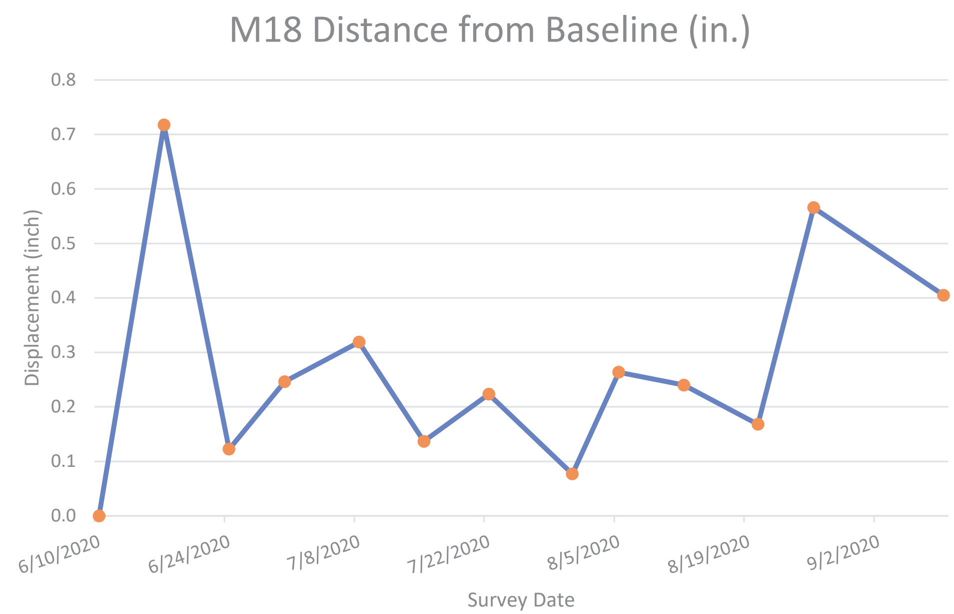
M18 Distance from Baseline (in.)
Displacement (inch)
Survey Date
0.0
0.1
0.2
0.3
0.4
0.5
0.6
0.7
0.8
6/10/2020
6/24/2020
7/8/2020
7/22/2020
8/5/2020
8/19/2020
9/2/2020

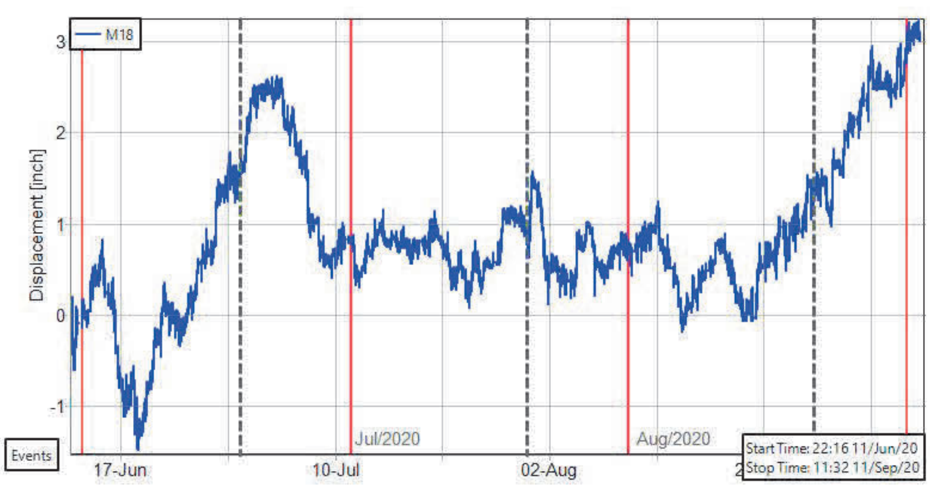
M18
Displacement [inch]
Events
17-Jun
10-Jul
02-Aug
Jul/2020
Aug/2020
Start Time: 22:16 11/Jun/20
Stop Time: 11:32 11/Sep/20

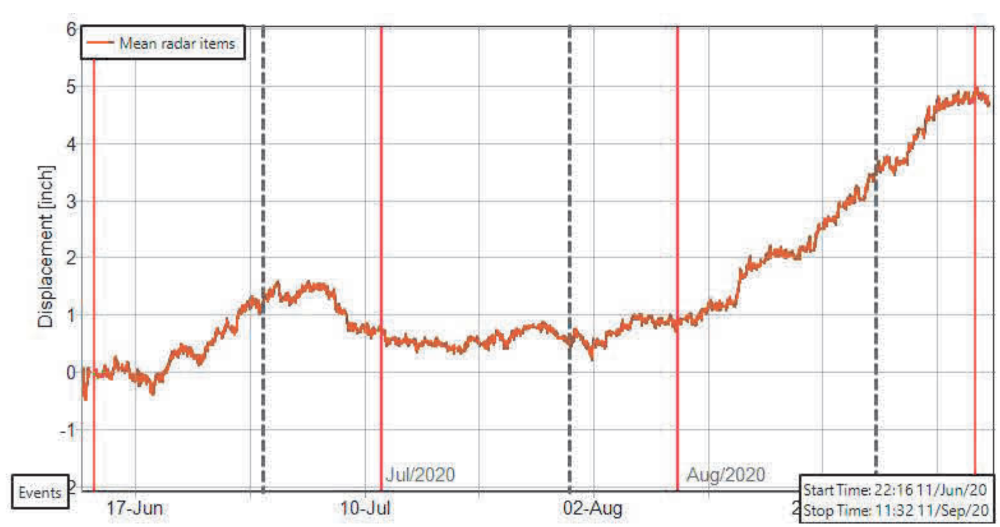
Mean radar items
Displacement [inch]
Events
17-Jun
10-Jul
02-Aug
Jul/2020
Aug/2020
Start Time: 22:16 11/Jun/20
Stop Time: 11:32 11/Sep/20

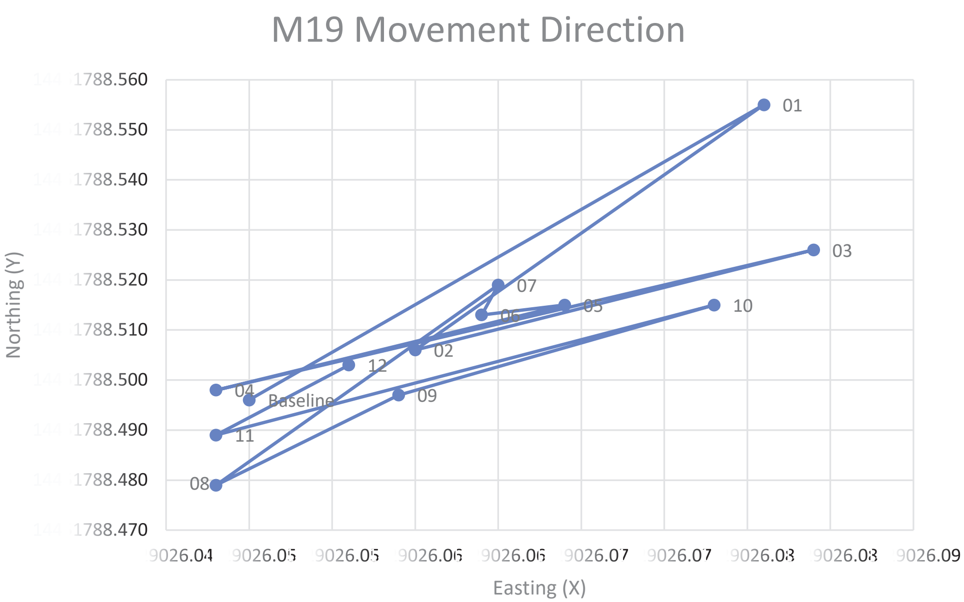
M19 Movement Direction
Northing (Y)
1788.560
1788.550
1788.540
1788.530
1788.520
1788.510
1788.500
1788.490
1788.480
1788.470
Easting (X)
9026.04
9026.05
9026.05
9026.06
9026.06
9026.07
9026.07
9026.08
9026.08
9026.09
01
02
03
04
05
07
08
09
10
11
12
Baseline

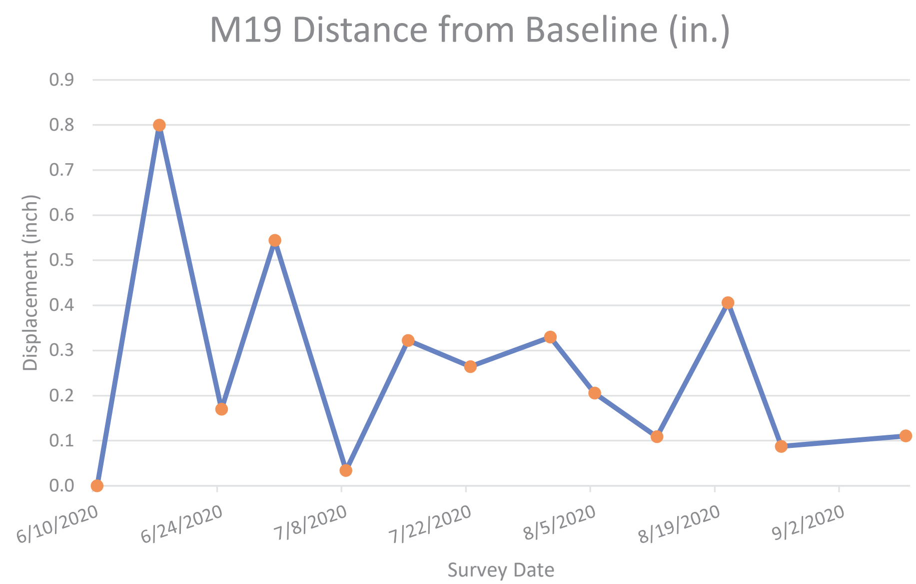
M19 Distance from Baseline (in.)
Displacement (inch)
0.9
0.8
0.7
0.6
0.5
0.4
0.3
0.2
0.1
0.0
6/10/2020
6/24/2020
7/8/2020
7/22/2020
8/5/2020
8/19/2020
9/2/2020
Survey Date

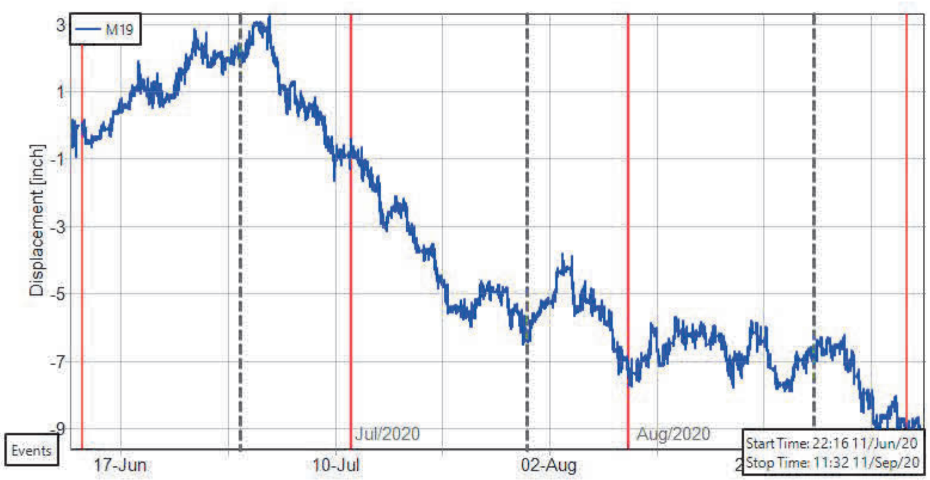
M19
Displacement [inch]
3
1
-1
-3
-5
-7
-9
Events
17-Jun
10-Jul
02-Aug
Jul/2020
Aug/2020
Start Time: 22:16 11/Jun/20
Stop Time: 11:32 11/Sep/20

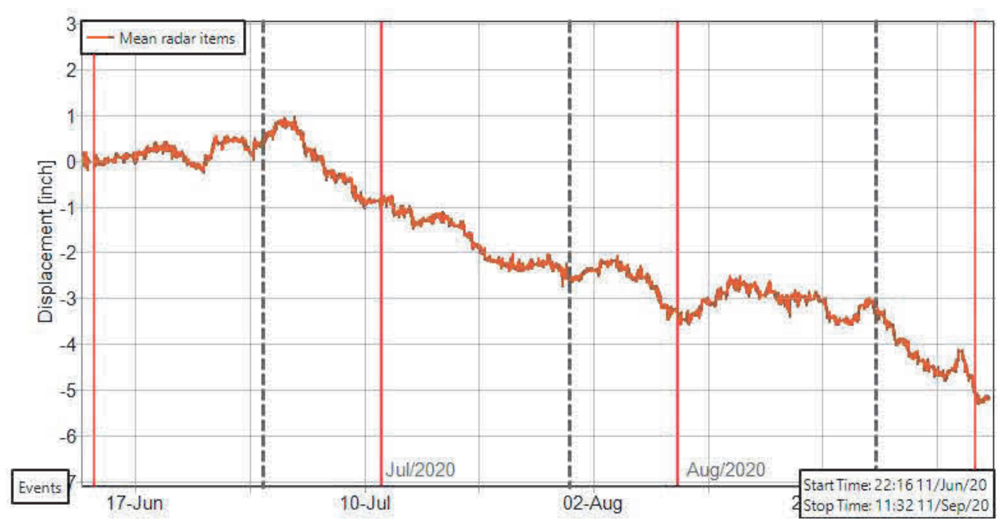
Mean radar items
Displacement [inch]
3
2
1
0
-1
-2
-3
-4
-5
-6
-7
Events
17-Jun
10-Jul
02-Aug
Jul/2020
Aug/2020
Start Time: 22:16 11/Jun/20
Stop Time: 11:32 11/Sep/20

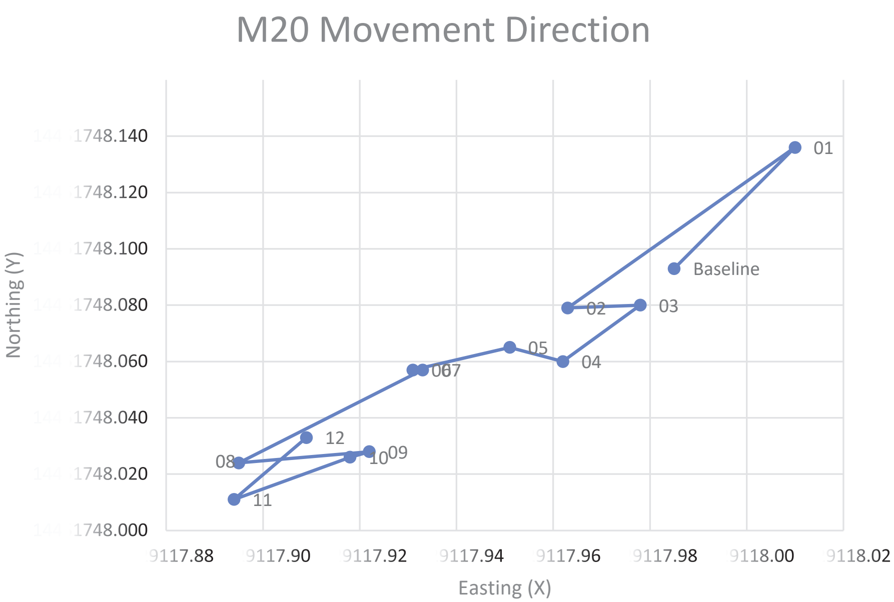
M20 Movement Direction
Northing (Y)
1748.140
1748.120
1748.100
1748.080
1748.060
1748.040
1748.020
1748.000
9117.88
9117.90
9117.92
9117.94
9117.96
9117.98
9118.00
9118.02
Easting (X)
01
Baseline
02
03
04
05
07
08
09
10
11
12

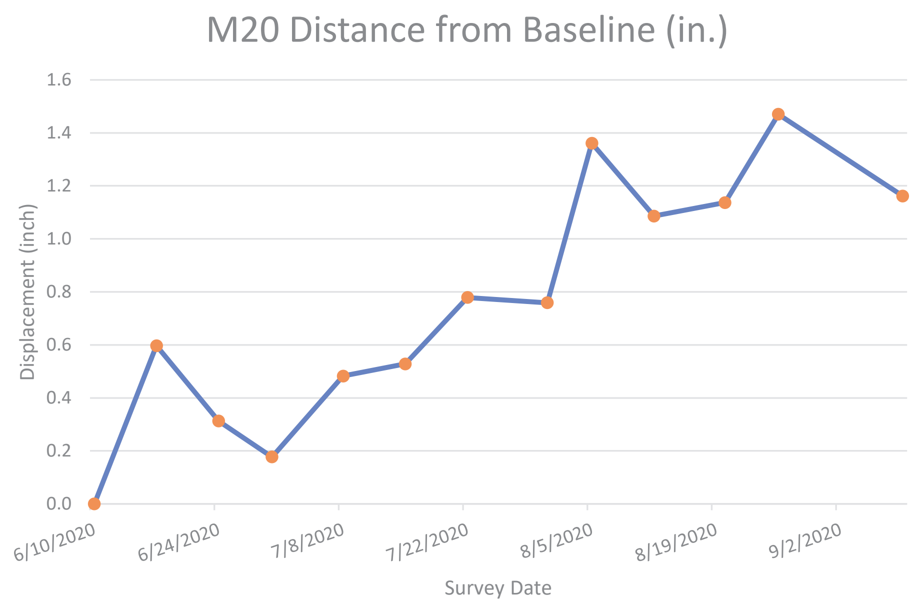
M20 Distance from Baseline (in.)
Displacement (inch)
1.6
1.4
1.2
1.0
0.8
0.6
0.4
0.2
0.0
6/10/2020
6/24/2020
7/8/2020
7/22/2020
8/5/2020
8/19/2020
9/2/2020
Survey Date

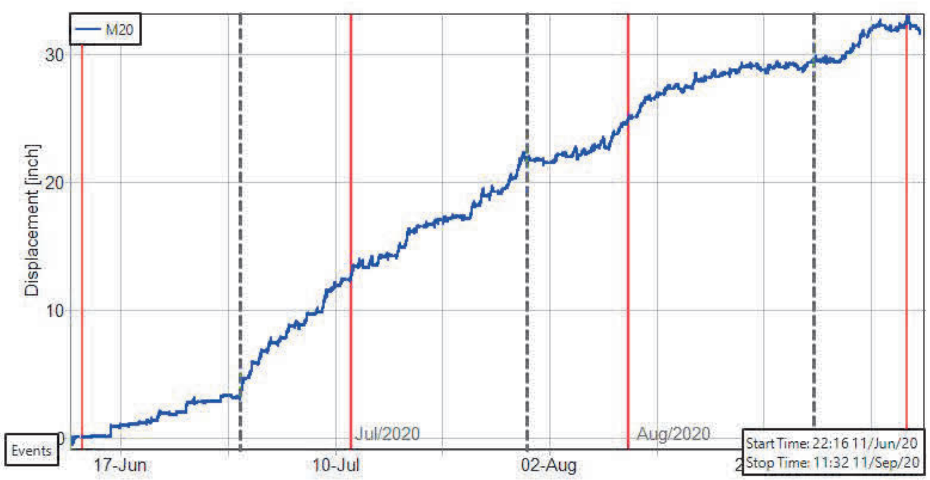
M20
Displacement [inch]
30
20
10
0
Jul/2020
Aug/2020
Events
17-Jun
10-Jul
02-Aug
Start Time: 22:16 11/Jun/20
Stop Time: 11:32 11/Sep/20

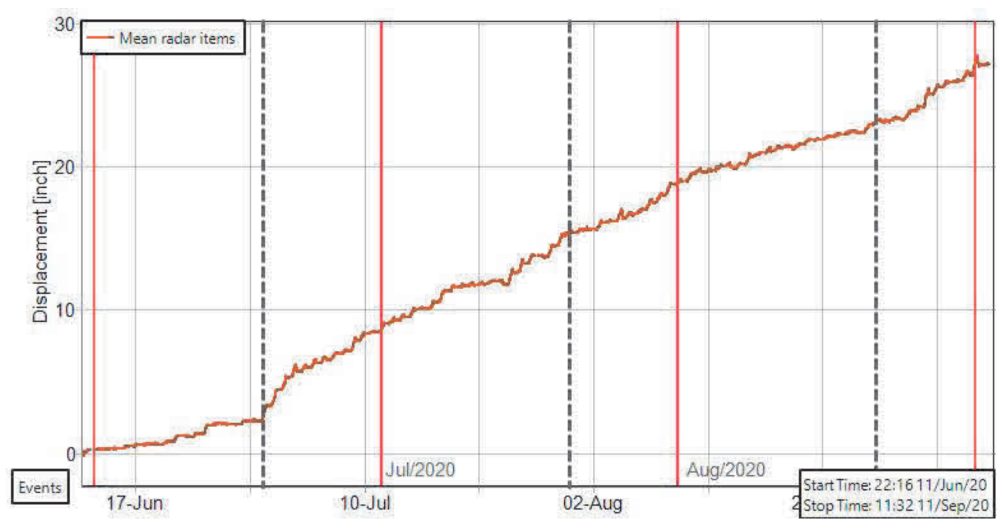
Mean radar items
Displacement [inch]
30
20
10
0
Jul/2020
Aug/2020
Events
17-Jun
10-Jul
02-Aug
Start Time: 22:16 11/Jun/20
Stop Time: 11:32 11/Sep/20

M21 Movement Direction

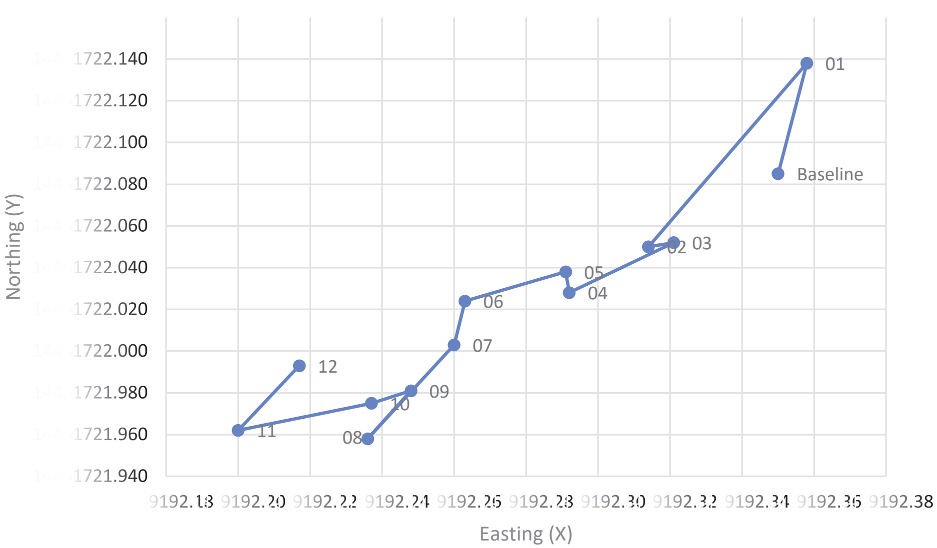

M21 Distance from Baseline (in.)

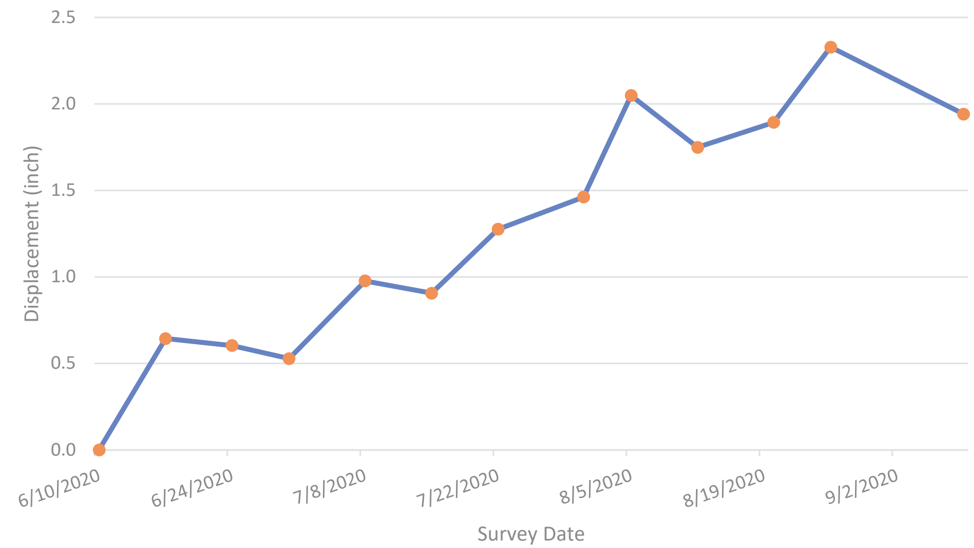

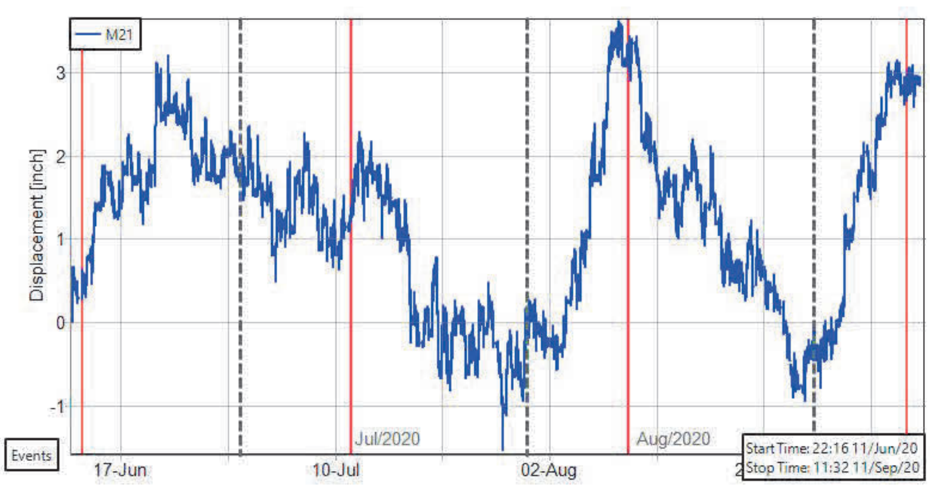

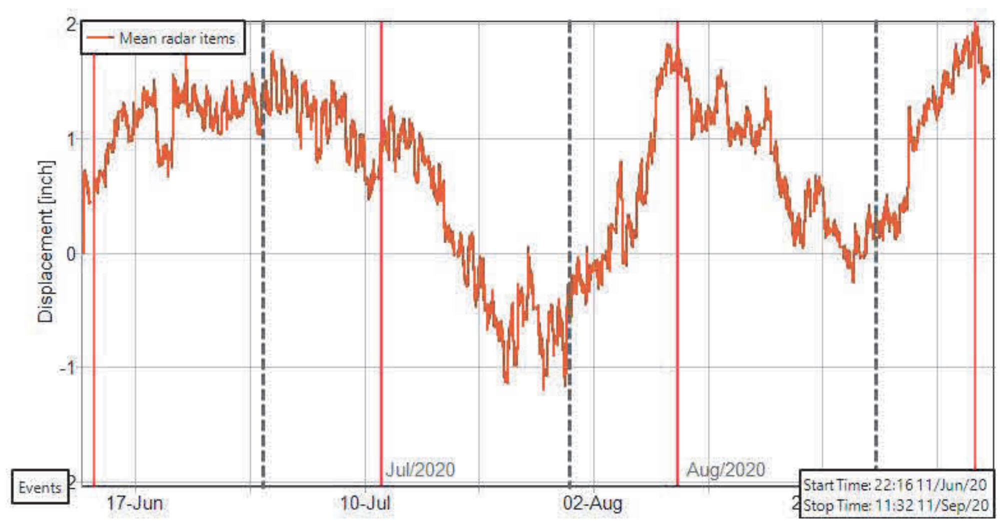

APPENDIX C POST-CONSTRUCTION RESULTS

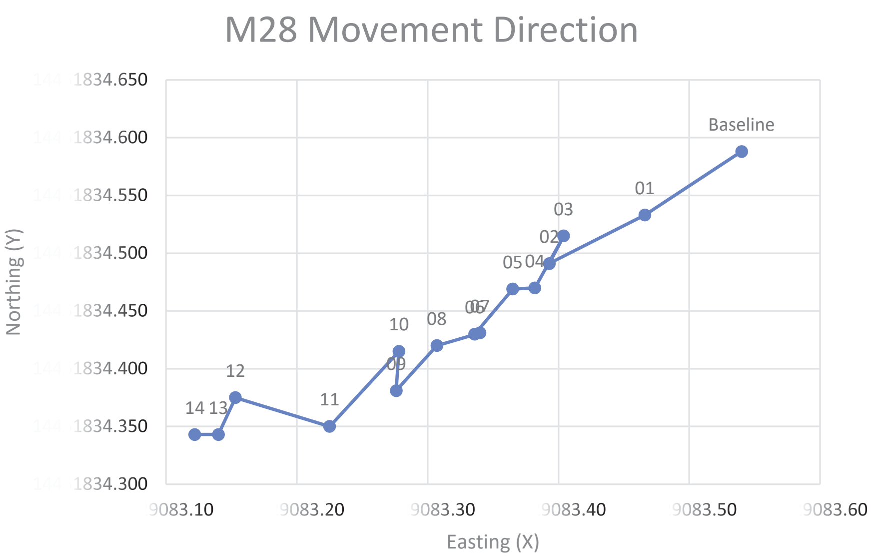
M28 Movement Direction
Northing (Y)
Easting (X)
Baseline
1834.650
1834.600
1834.550
1834.500
1834.450
1834.400
1834.350
1834.300
9083.10
9083.20
9083.30
9083.40
9083.50
9083.60

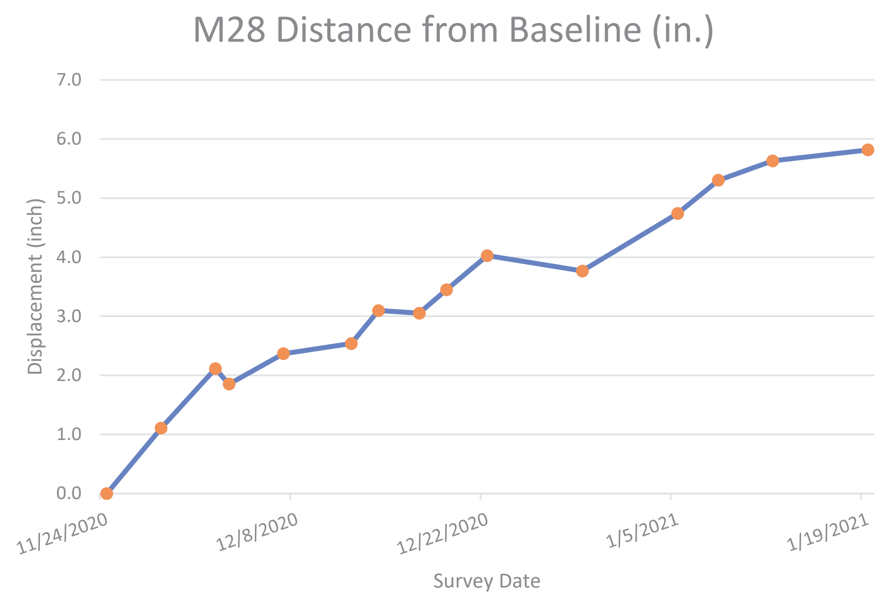
M28 Distance from Baseline (in.)
Displacement (inch)
Survey Date
11/24/2020
12/8/2020
12/22/2020
1/5/2021
1/19/2021

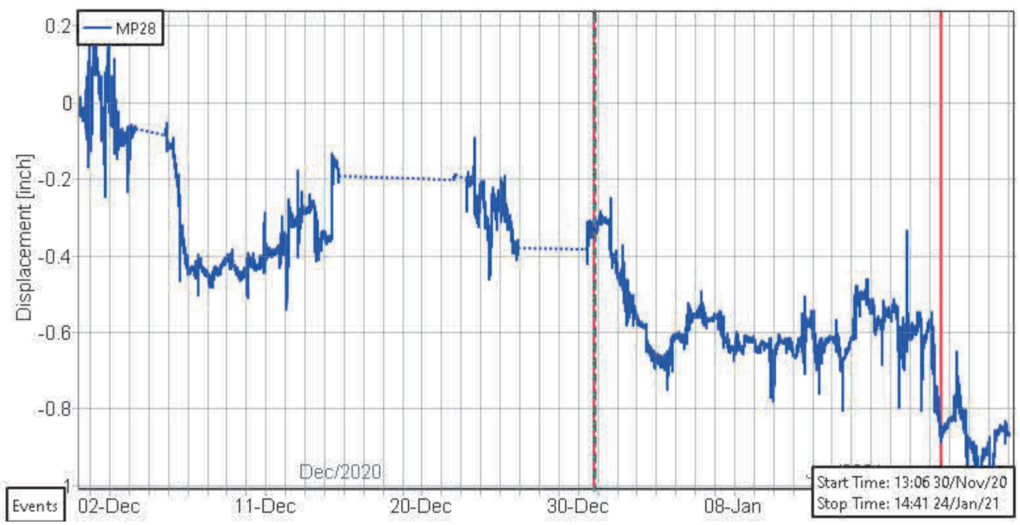
MP28
Displacement [inch]
Events
02-Dec
11-Dec
20-Dec
30-Dec
08-Jan
Dec/2020
Start Time: 13:06 30/Nov/20
Stop Time: 14:41 24/Jan/21

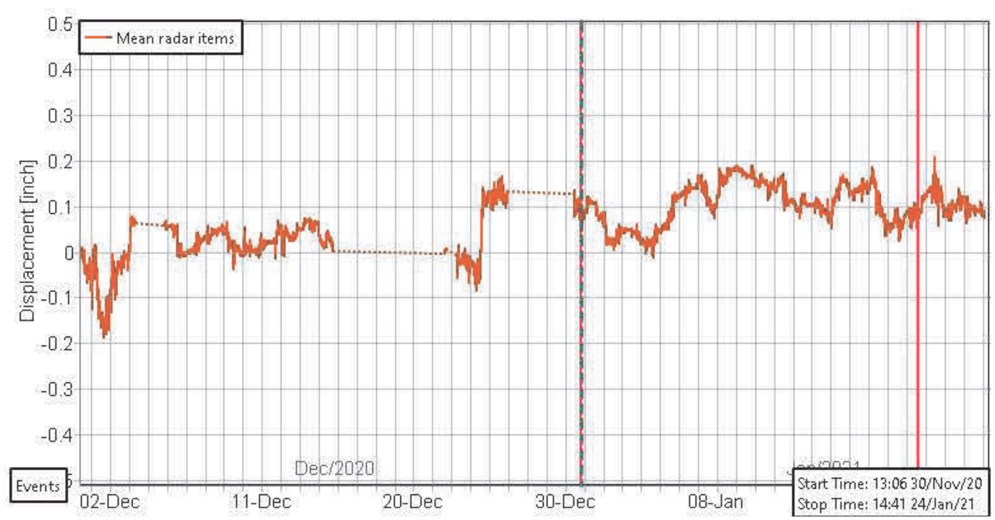
Mean radar items
Displacement [inch]
Events
02-Dec
11-Dec
20-Dec
30-Dec
08-Jan
Dec/2020
Start Time: 13:06 30/Nov/20
Stop Time: 14:41 24/Jan/21

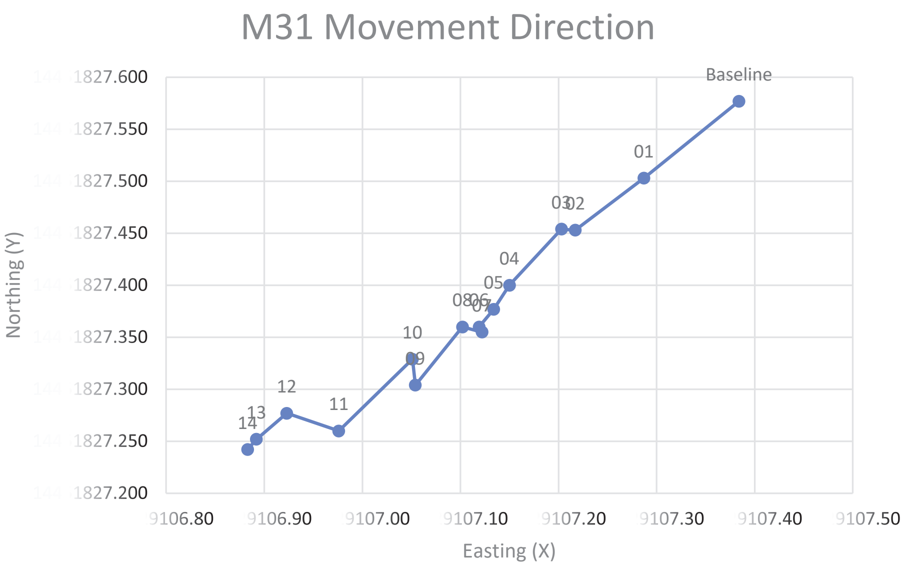
M31 Movement Direction
Northing (Y)
Easting (X)
Baseline
01
02
03
04
05
06
07
08
09
10
11
12
13
14
1827.600
1827.550
1827.500
1827.450
1827.400
1827.350
1827.300
1827.250
1827.200
9106.80
9106.90
9107.00
9107.10
9107.20
9107.30
9107.40
9107.50

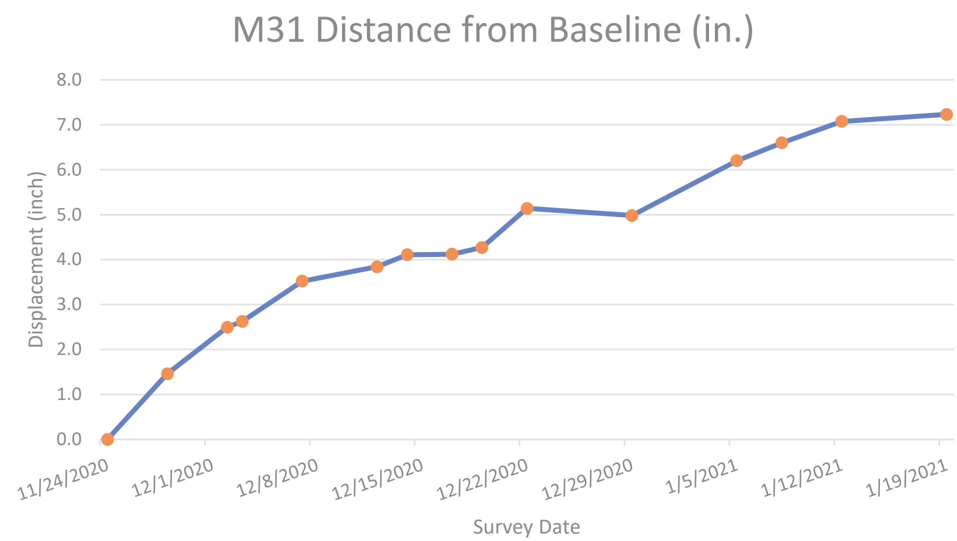
M31 Distance from Baseline (in.)
Displacement (inch)
Survey Date
8.0
7.0
6.0
5.0
4.0
3.0
2.0
1.0
0.0
11/24/2020
12/1/2020
12/8/2020
12/15/2020
12/22/2020
12/29/2020
1/5/2021
1/12/2021
1/19/2021


MP31
Displacement [inch]
Events
Dec/2020
02-Dec
11-Dec
20-Dec
30-Dec
08-Jan
Start Time: 13:06 30/Nov/20
Stop Time: 14:41 24/Jan/21

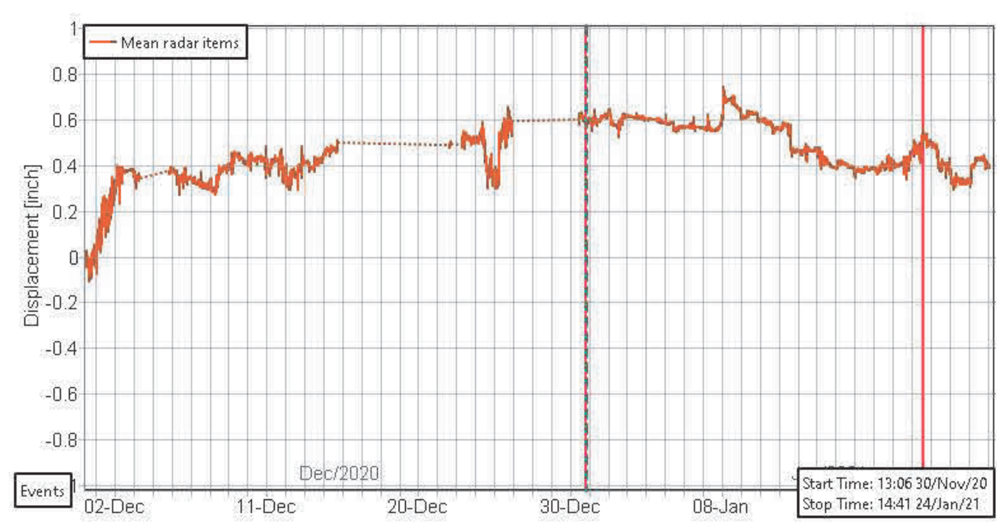
Mean radar items
Displacement [inch]
Events
Dec/2020
02-Dec
11-Dec
20-Dec
30-Dec
08-Jan
Start Time: 13:06 30/Nov/20
Stop Time: 14:41 24/Jan/21

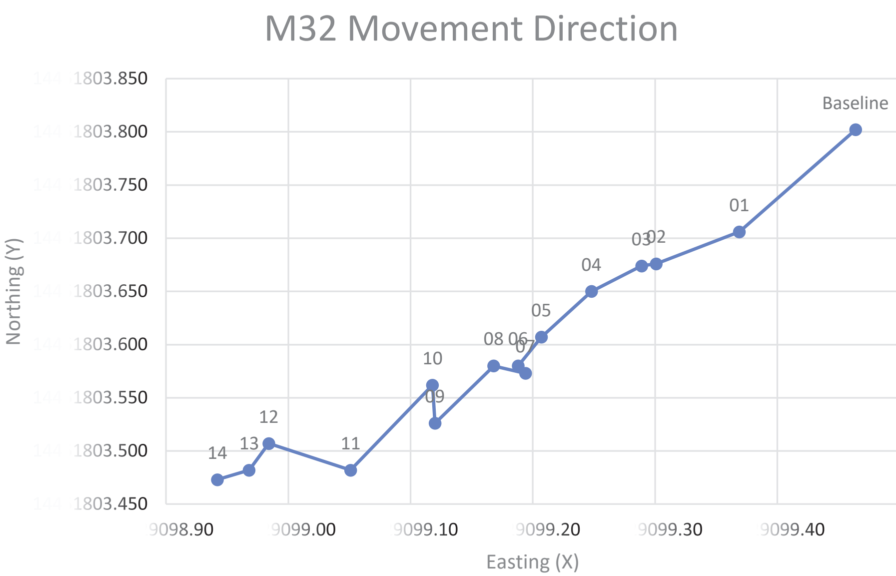

M32 Movement Direction
Northing (Y)
Easting (X)
1803.850
1803.800
1803.750
1803.700
1803.650
1803.600
1803.550
1803.500
1803.450
9098.90
9099.00
9099.10
9099.20
9099.30
9099.40
Baseline
01
02
03
04
05
06
07
08
09
10
11
12
13
14

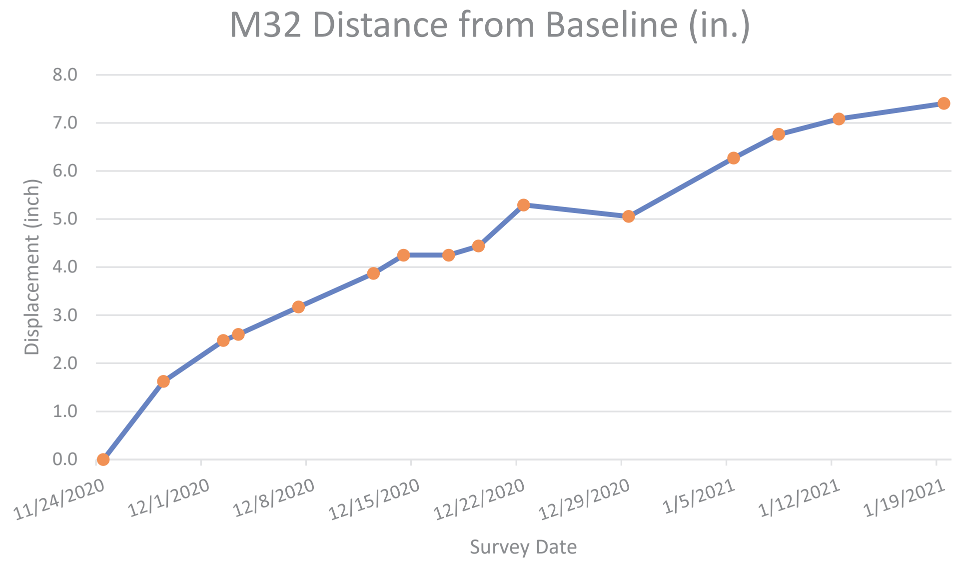

M32 Distance from Baseline (in.)
Displacement (inch)
Survey Date
8.0
7.0
6.0
5.0
4.0
3.0
2.0
1.0
0.0
11/24/2020
12/1/2020
12/8/2020
12/15/2020
12/22/2020
12/29/2020
1/5/2021
1/12/2021
1/19/2021

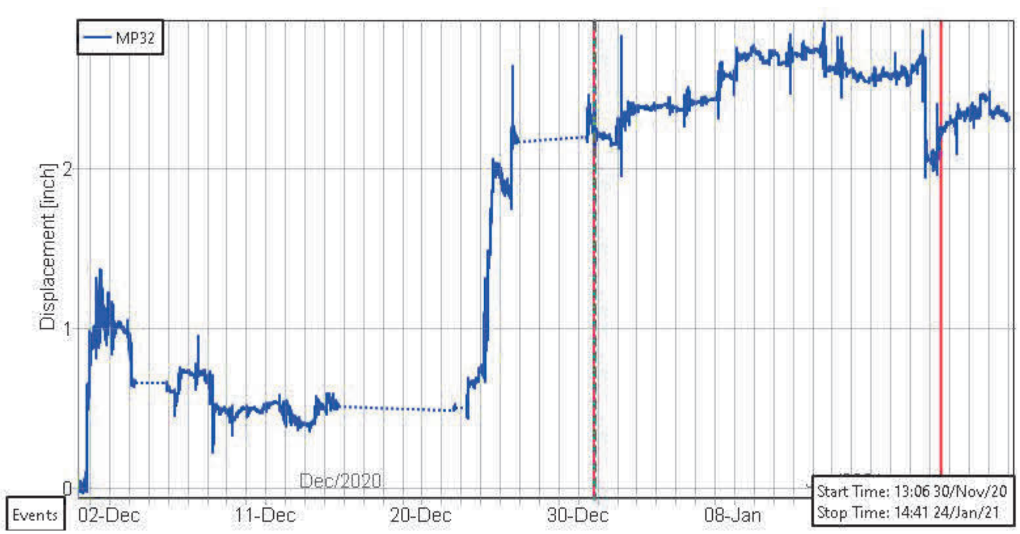

MP32
Displacement [inch]
2
1
0
Dec/2020
Events
02-Dec
11-Dec
20-Dec
30-Dec
08-Jan
Start Time: 13:06 30/Nov/20
Stop Time: 14:41 24/Jan/21

Mean radar items
Displacement [inch]
1
0.8
0.6
0.4
0.2
0
-0.2
-0.4
-0.6
-0.8
Dec/2020
Events
02-Dec
11-Dec
20-Dec
30-Dec
08-Jan
Start Time: 13:06 30/Nov/20
Stop Time: 14:41 24/Jan/21

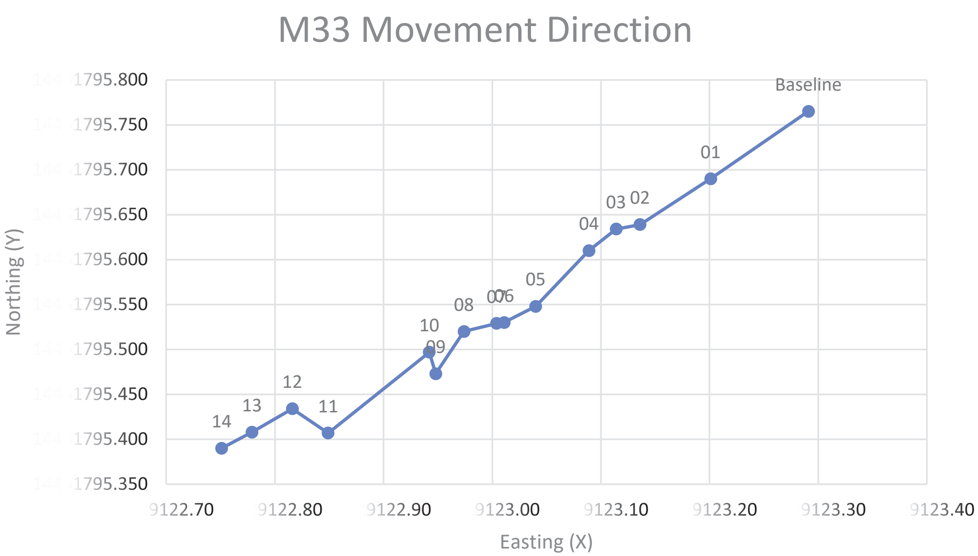
M33 Movement Direction
Northing (Y)
Easting (X)
1795.800
1795.750
1795.700
1795.650
1795.600
1795.550
1795.500
1795.450
1795.400
1795.350
9122.70
9122.80
9122.90
9123.00
9123.10
9123.20
9123.30
9123.40
Baseline
01
02
03
04
05
06
07
08
09
10
11
12
13
14

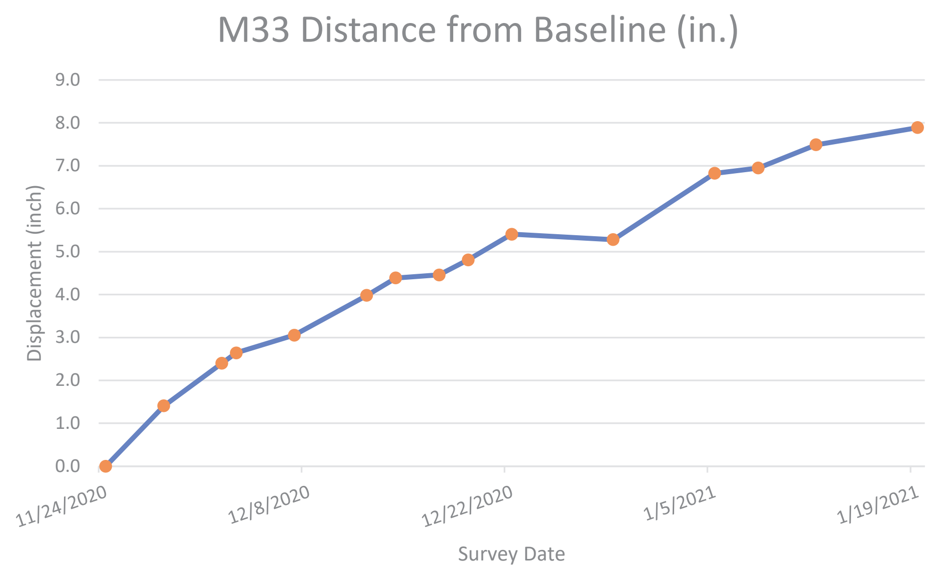
M33 Distance from Baseline (in.)
Displacement (inch)
Survey Date
9.0
8.0
7.0
6.0
5.0
4.0
3.0
2.0
1.0
0.0
11/24/2020
12/8/2020
12/22/2020
1/5/2021
1/19/2021

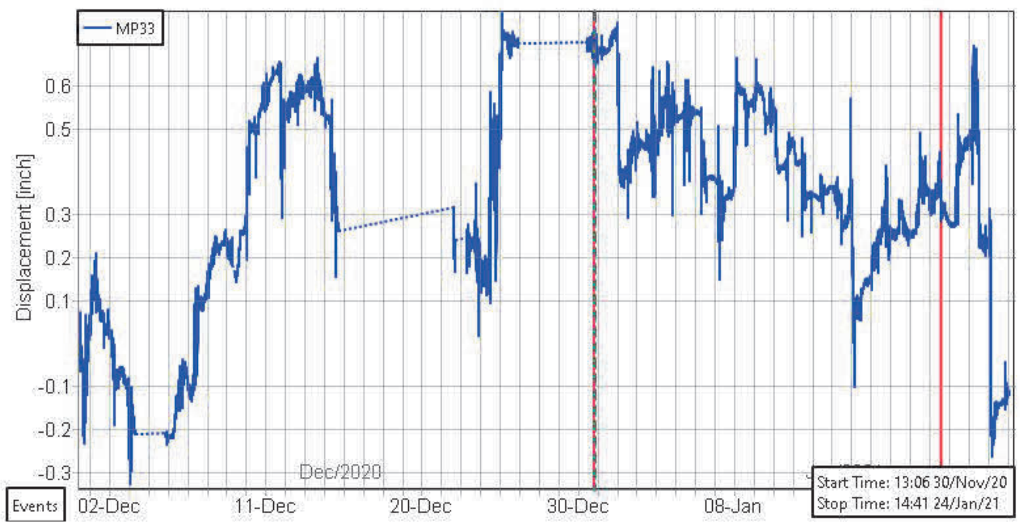
MP33
Displacement [inch]
0.6
0.5
0.3
0.2
0.1
-0.1
-0.2
-0.3
Dec/2020
Events
02-Dec
11-Dec
20-Dec
30-Dec
08-Jan
Start Time: 13:06 30/Nov/20
Stop Time: 14:41 24/Jan/21

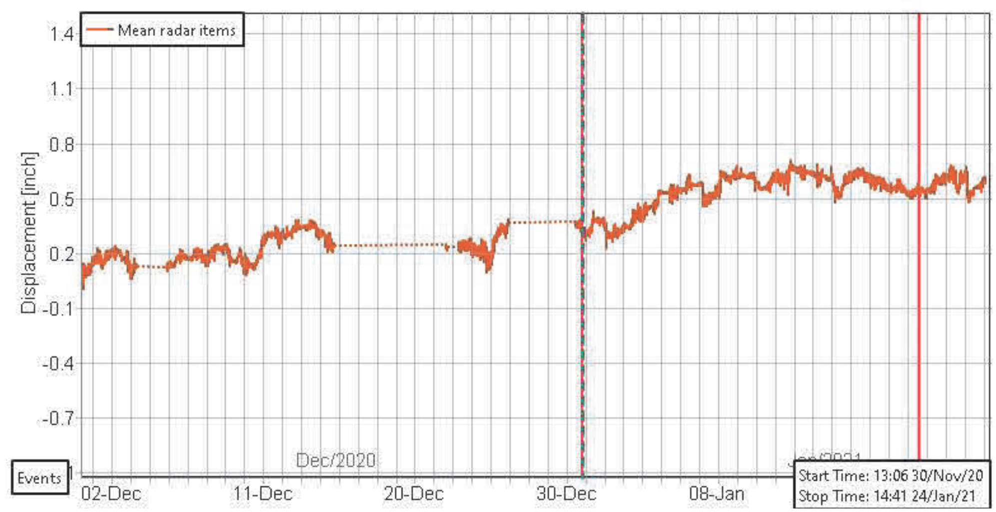
Mean radar items
Displacement [inch]
1.4
1.1
0.8
0.5
0.2
-0.1
-0.4
-0.7
Dec/2020
Events
02-Dec
11-Dec
20-Dec
30-Dec
08-Jan
Start Time: 13:06 30/Nov/20
Stop Time: 14:41 24/Jan/21

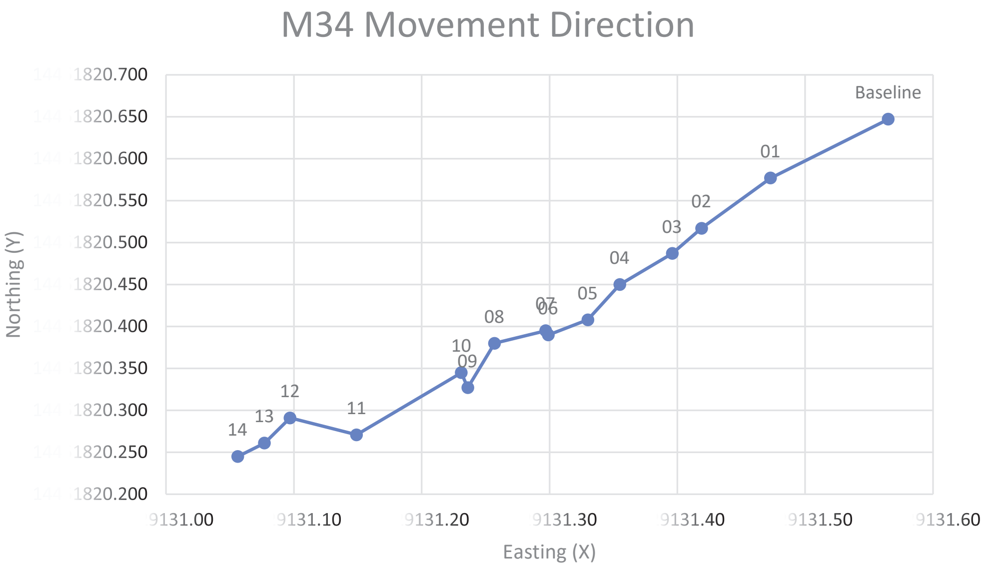
M34 Movement Direction
Baseline
01
02
03
04
05
06
07
08
09
10
11
12
13
14
1820.700
1820.650
1820.600
1820.550
1820.500
1820.450
1820.400
1820.350
1820.300
1820.250
1820.200
9131.00
9131.10
9131.20
9131.30
9131.40
9131.50
9131.60
Northing (Y)
Easting (X)

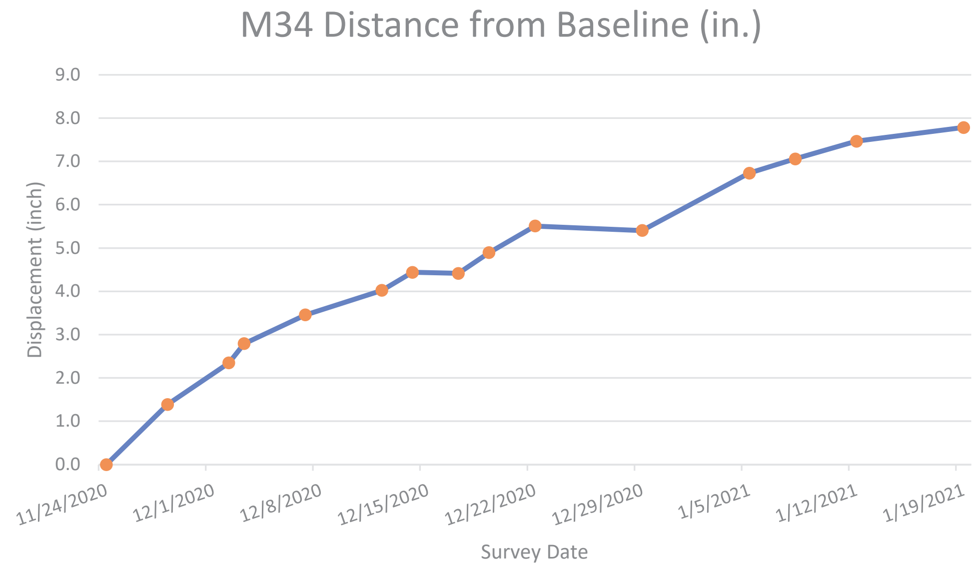
M34 Distance from Baseline (in.)
9.0
8.0
7.0
6.0
5.0
4.0
3.0
2.0
1.0
0.0
Displacement (inch)
11/24/2020
12/1/2020
12/8/2020
12/15/2020
12/22/2020
12/29/2020
1/5/2021
1/12/2021
1/19/2021
Survey Date

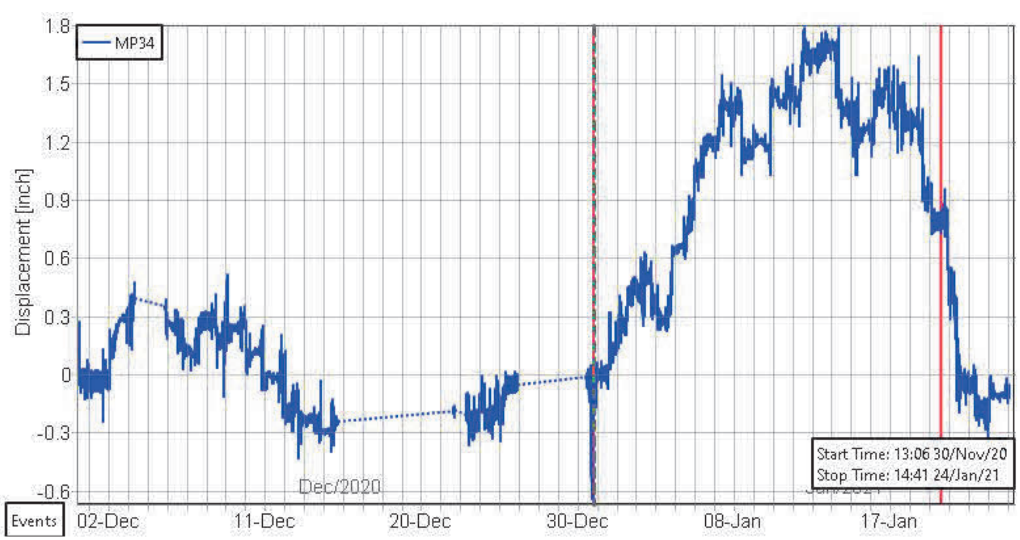
MP34
1.8
1.5
1.2
0.9
0.6
0.3
0
-0.3
-0.6
Displacement [inch]
Start Time: 13:06 30/Nov/20
Stop Time: 14:41 24/Jan/21
Dec/2020
Events
02-Dec
11-Dec
20-Dec
30-Dec
08-Jan
17-Jan

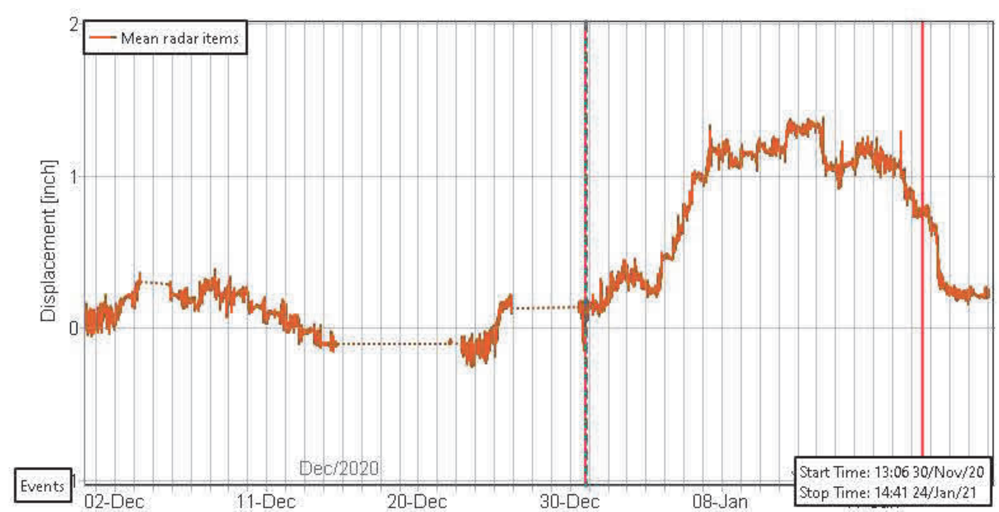
Mean radar items
2
1
0
Displacement [inch]
Dec/2020
Start Time: 13:06 30/Nov/20
Stop Time: 14:41 24/Jan/21
Events
02-Dec
11-Dec
20-Dec
30-Dec
08-Jan

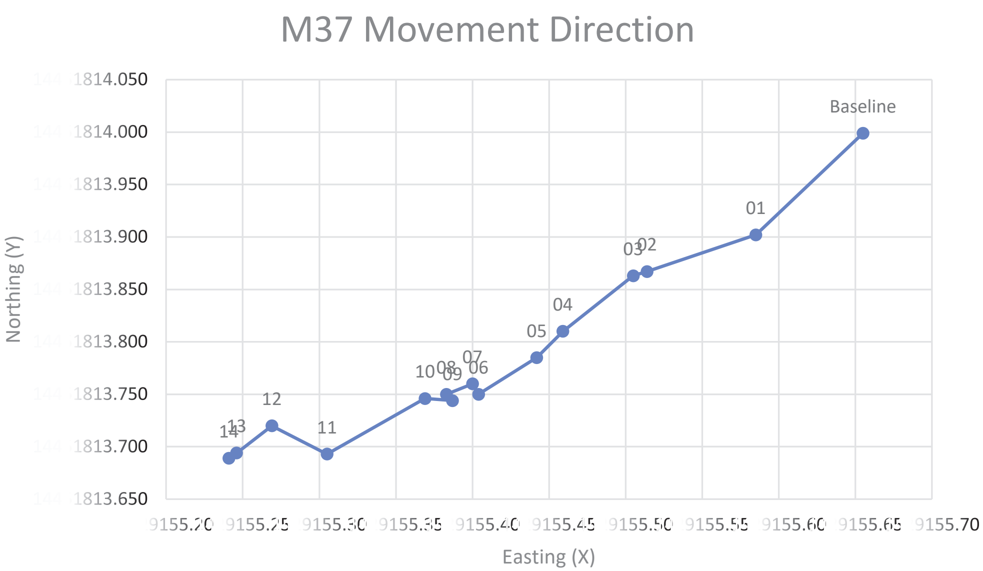
M37 Movement Direction
Northing (Y)
Easting (X)
Baseline
01
02
03
04
05
06
07
08
09
10
11
12
13
14
1814.050
1814.000
1813.950
1813.900
1813.850
1813.800
1813.750
1813.700
1813.650
9155.20
9155.25
9155.30
9155.35
9155.40
9155.45
9155.50
9155.55
9155.60
9155.65
9155.70

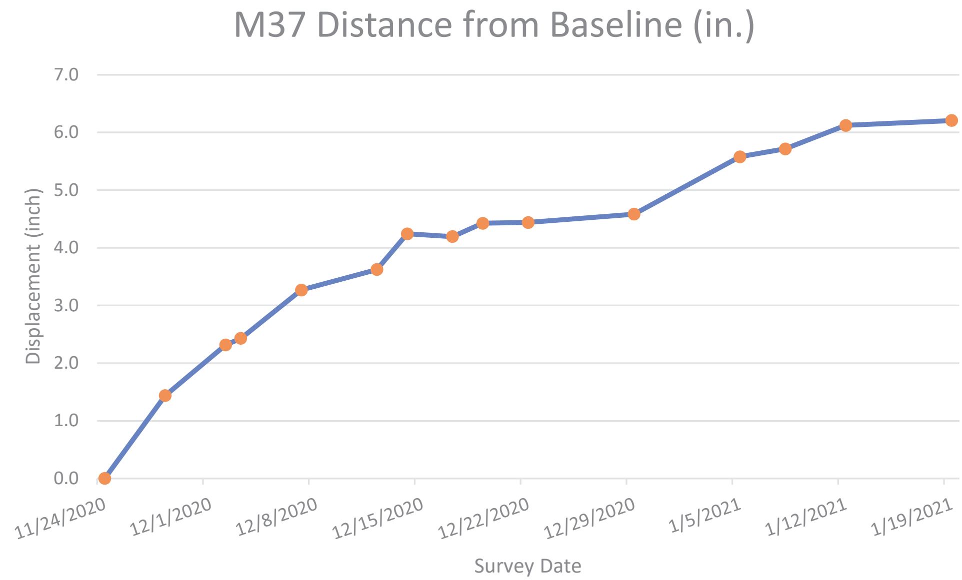
M37 Distance from Baseline (in.)
Displacement (inch)
Survey Date
7.0
6.0
5.0
4.0
3.0
2.0
1.0
0.0
11/24/2020
12/1/2020
12/8/2020
12/15/2020
12/22/2020
12/29/2020
1/5/2021
1/12/2021
1/19/2021


MP37
Displacement [inch]
0.5
0.3
0.1
-0.1
-0.3
-0.5
-0.7
-0.9
-1.1
-1.3
Dec/2020
Events
02-Dec
11-Dec
20-Dec
30-Dec
08-Jan
Start Time: 13:06 30/Nov/20
Stop Time: 14:41 24/Jan/21

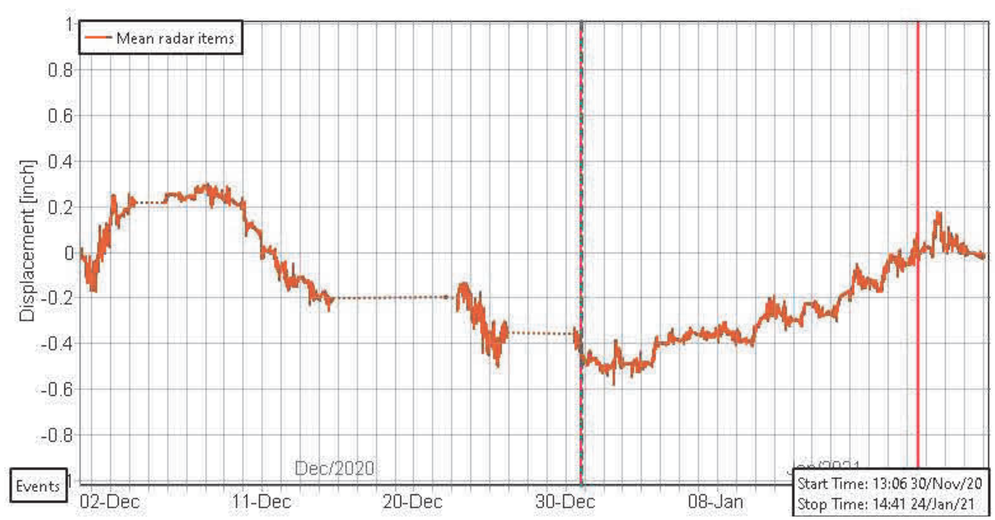
Mean radar items
Displacement [inch]
1
0.8
0.6
0.4
0.2
0
-0.2
-0.4
-0.6
-0.8
Dec/2020
Events
02-Dec
11-Dec
20-Dec
30-Dec
08-Jan
Start Time: 13:06 30/Nov/20
Stop Time: 14:41 24/Jan/21

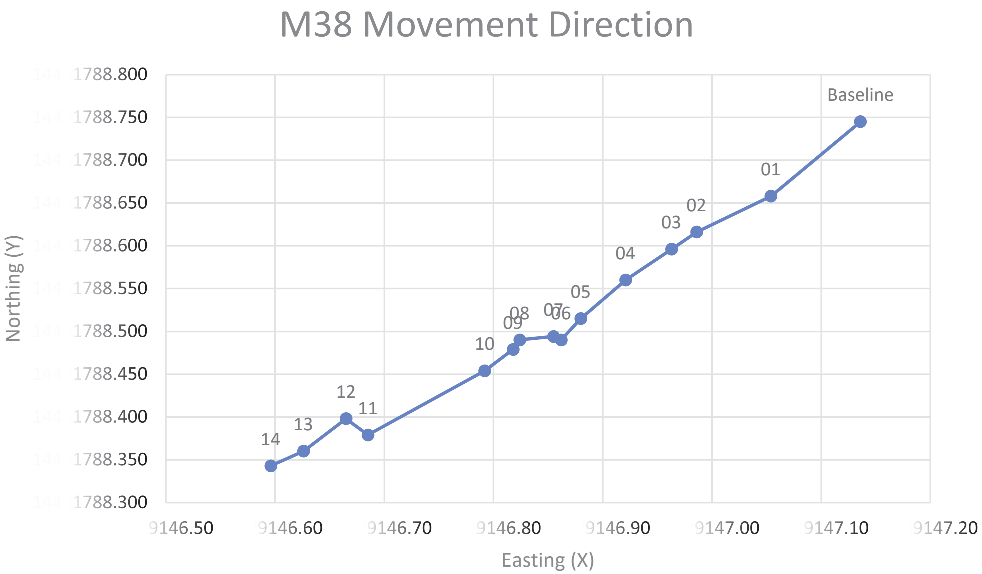
M38 Movement Direction
Northing (Y)
1788.800
1788.750
1788.700
1788.650
1788.600
1788.550
1788.500
1788.450
1788.400
1788.350
1788.300
Baseline
01
02
03
04
05
07
06
08
09
10
11
12
13
14
9146.50
9146.60
9146.70
9146.80
9146.90
9147.00
9147.10
9147.20
Easting (X)

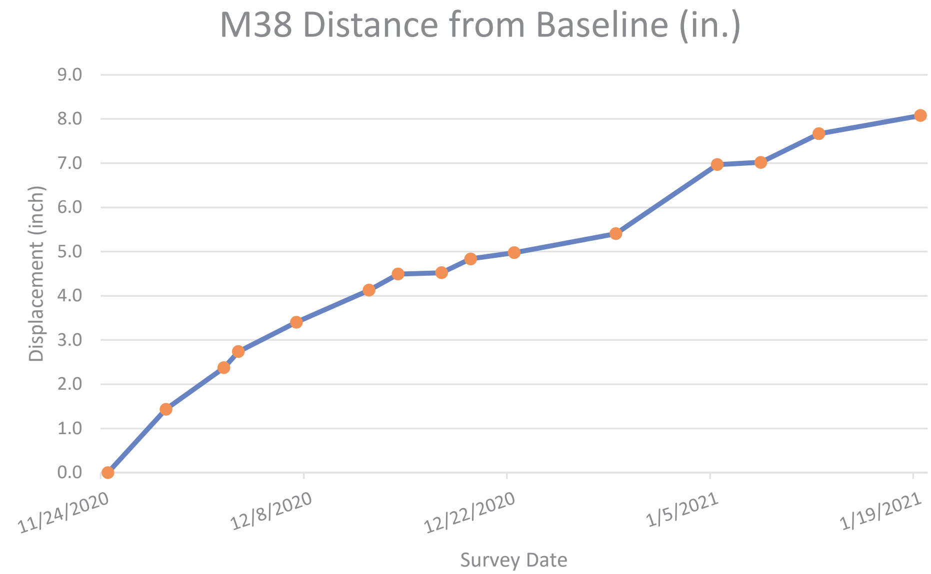
M38 Distance from Baseline (in.)
Displacement (inch)
9.0
8.0
7.0
6.0
5.0
4.0
3.0
2.0
1.0
0.0
11/24/2020
12/8/2020
12/22/2020
1/5/2021
1/19/2021
Survey Date


MP38
Displacement [inch]
0.3
0.1
-0.1
-0.3
-0.5
-0.7
-0.9
-1.1
Dec/2020
Events
02-Dec
11-Dec
20-Dec
30-Dec
08-Jan
Start Time: 13:06 30/Nov/20
Stop Time: 14:41 24/Jan/21

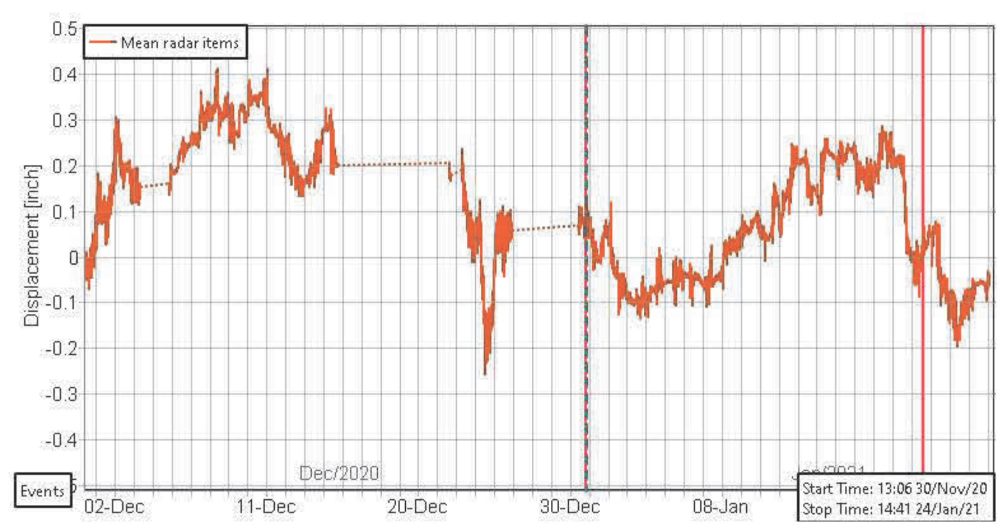
Mean radar items
Displacement [inch]
0.5
0.4
0.3
0.2
0.1
0
-0.1
-0.2
-0.3
-0.4
Dec/2020
Events
02-Dec
11-Dec
20-Dec
30-Dec
08-Jan
Start Time: 13:06 30/Nov/20
Stop Time: 14:41 24/Jan/21

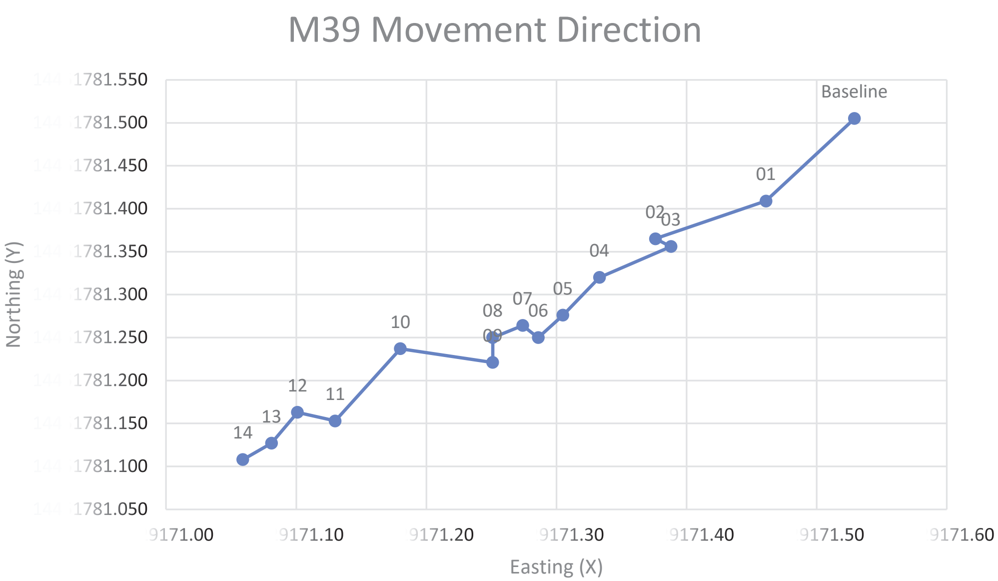

M39 Movement Direction
Baseline
01
02
03
04
05
06
07
08
10
11
12
13
14
1781.550
1781.500
1781.450
1781.400
1781.350
1781.300
1781.250
1781.200
1781.150
1781.100
1781.050
Northing (Y)
9171.00
9171.10
9171.20
9171.30
9171.40
9171.50
9171.60
Easting (X)

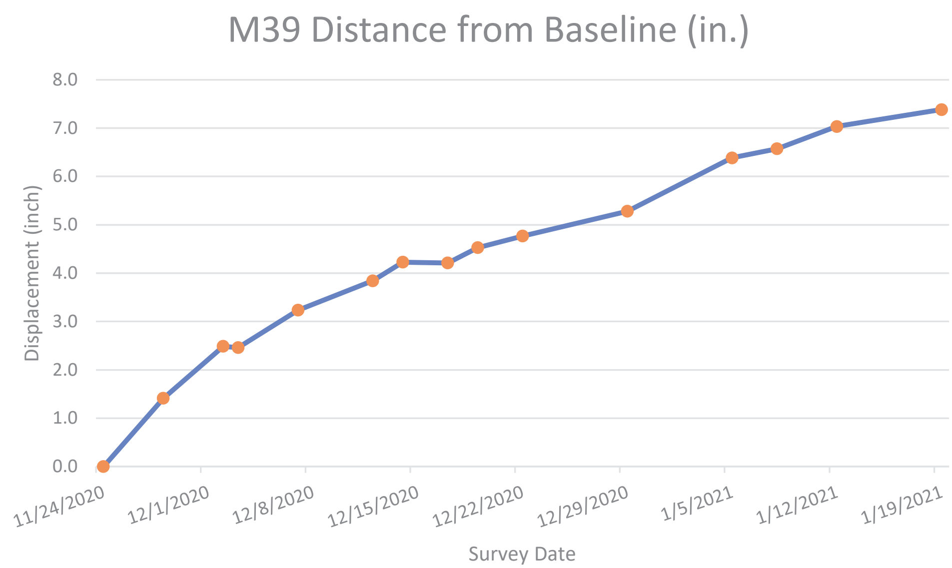

M39 Distance from Baseline (in.)
8.0
7.0
6.0
5.0
4.0
3.0
2.0
1.0
0.0
Displacement (inch)
11/24/2020
12/1/2020
12/8/2020
12/15/2020
12/22/2020
12/29/2020
1/5/2021
1/12/2021
1/19/2021
Survey Date

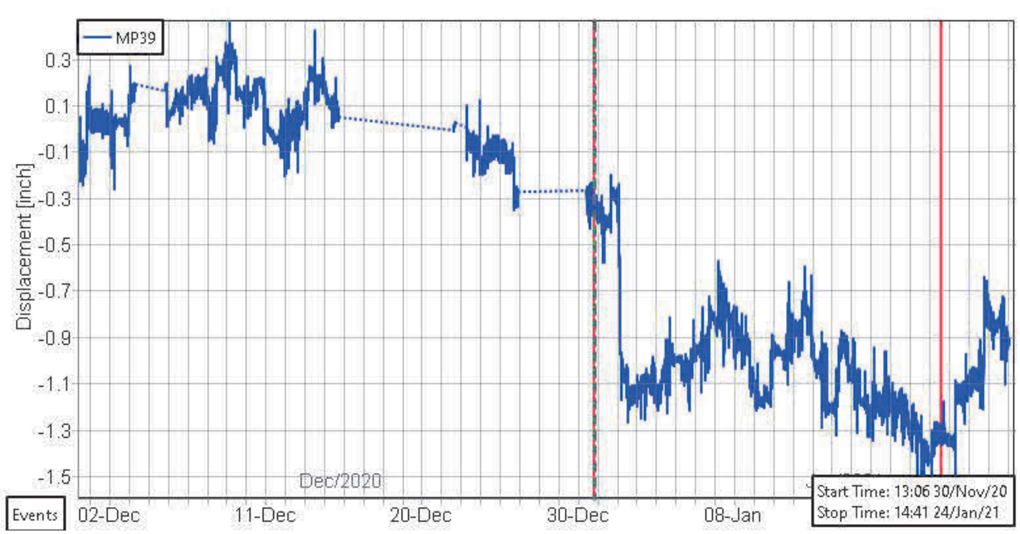

MP39
0.3
0.1
-0.1
-0.3
-0.5
-0.7
-0.9
-1.1
-1.3
-1.5
Displacement [inch]
Dec/2020
Events
02-Dec
11-Dec
20-Dec
30-Dec
08-Jan
Start Time: 13:06 30/Nov/20
Stop Time: 14:41 24/Jan/21

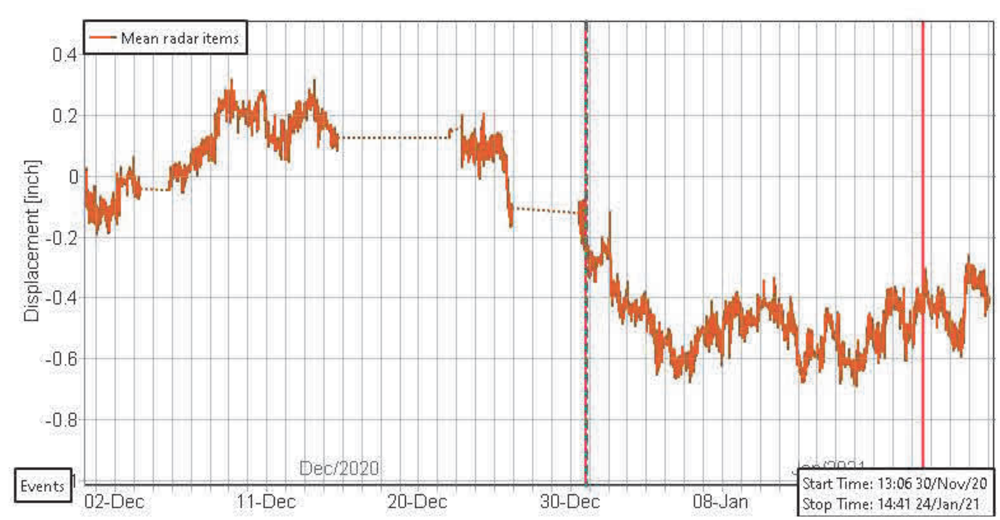

Mean radar items
0.4
0.2
0
-0.2
-0.4
-0.6
-0.8
Displacement [inch]
Dec/2020
Events
02-Dec
11-Dec
20-Dec
30-Dec
08-Jan
Start Time: 13:06 30/Nov/20
Stop Time: 14:41 24/Jan/21

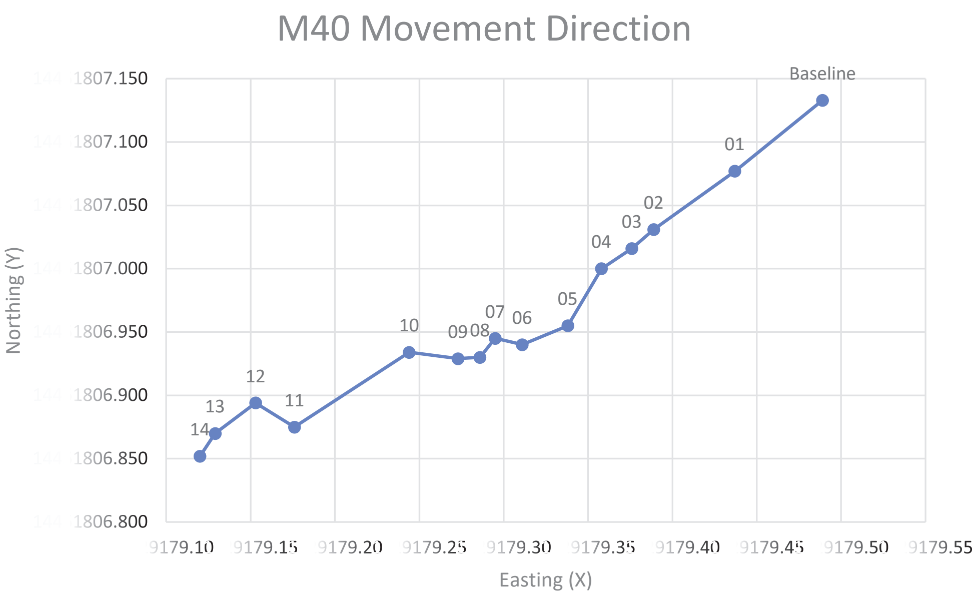
M40 Movement Direction
Baseline
01
02
03
04
05
06
07
08
09
10
11
12
13
14
Northing (Y)
1807.150
1807.100
1807.050
1807.000
1806.950
1806.900
1806.850
1806.800
9179.10
9179.15
9179.20
9179.25
9179.30
9179.35
9179.40
9179.45
9179.50
9179.55
Easting (X)

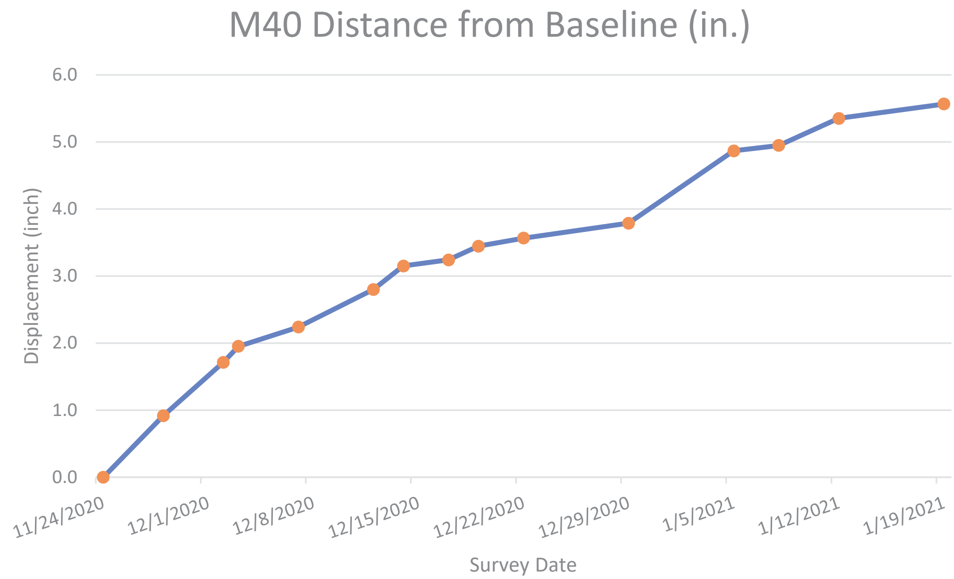
M40 Distance from Baseline (in.)
Displacement (inch)
6.0
5.0
4.0
3.0
2.0
1.0
0.0
11/24/2020
12/1/2020
12/8/2020
12/15/2020
12/22/2020
12/29/2020
1/5/2021
1/12/2021
1/19/2021
Survey Date

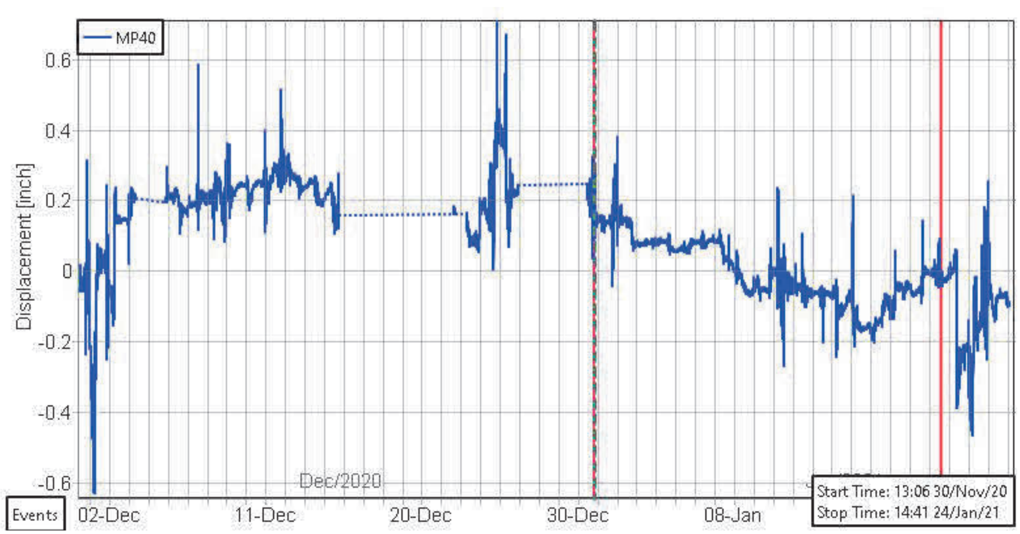
MP40
Displacement [inch]
0.6
0.4
0.2
0
-0.2
-0.4
-0.6
Dec/2020
Events
02-Dec
11-Dec
20-Dec
30-Dec
08-Jan
Start Time: 13:06 30/Nov/20
Stop Time: 14:41 24/Jan/21


Mean radar items
Displacement [inch]
1
0.8
0.6
0.4
0.2
0
-0.2
-0.4
-0.6
-0.8
Dec/2020
Events
02-Dec
11-Dec
20-Dec
30-Dec
08-Jan
Start Time: 13:06 30/Nov/20
Stop Time: 14:41 24/Jan/21

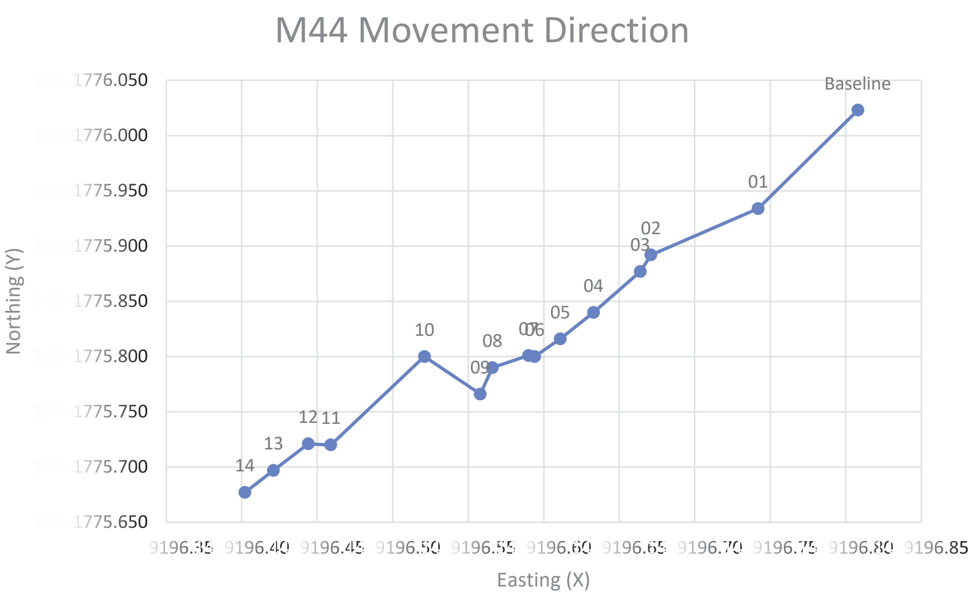

M44 Movement Direction
Baseline
01
02
03
04
05
07
06
08
09
10
12
11
13
14
1776.050
1776.000
1775.950
1775.900
1775.850
1775.800
1775.750
1775.700
1775.650
Northing (Y)
9196.35
9196.40
9196.45
9196.50
9196.55
9196.60
9196.65
9196.70
9196.75
9196.80
9196.85
Easting (X)

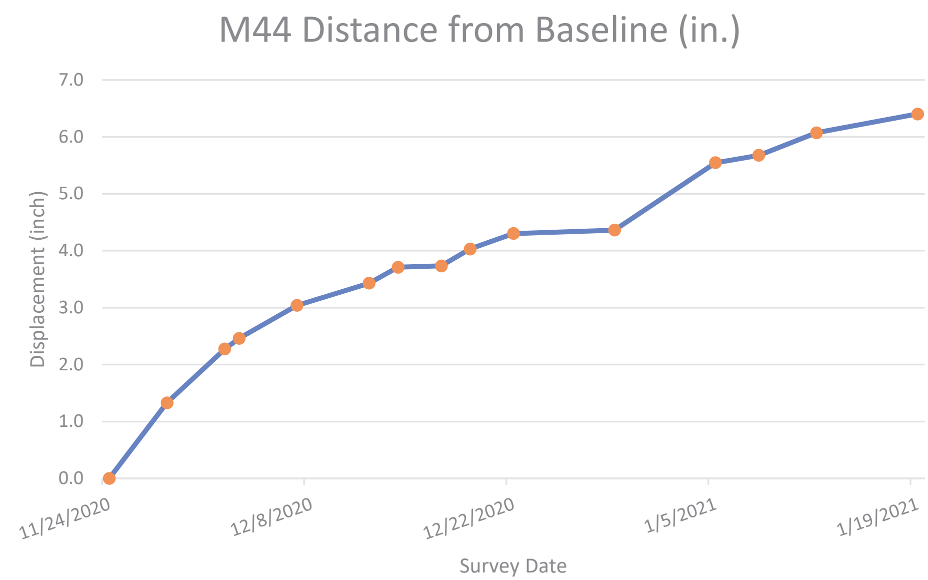

M44 Distance from Baseline (in.)
7.0
6.0
5.0
4.0
3.0
2.0
1.0
0.0
Displacement (inch)
11/24/2020
12/8/2020
12/22/2020
1/5/2021
1/19/2021
Survey Date

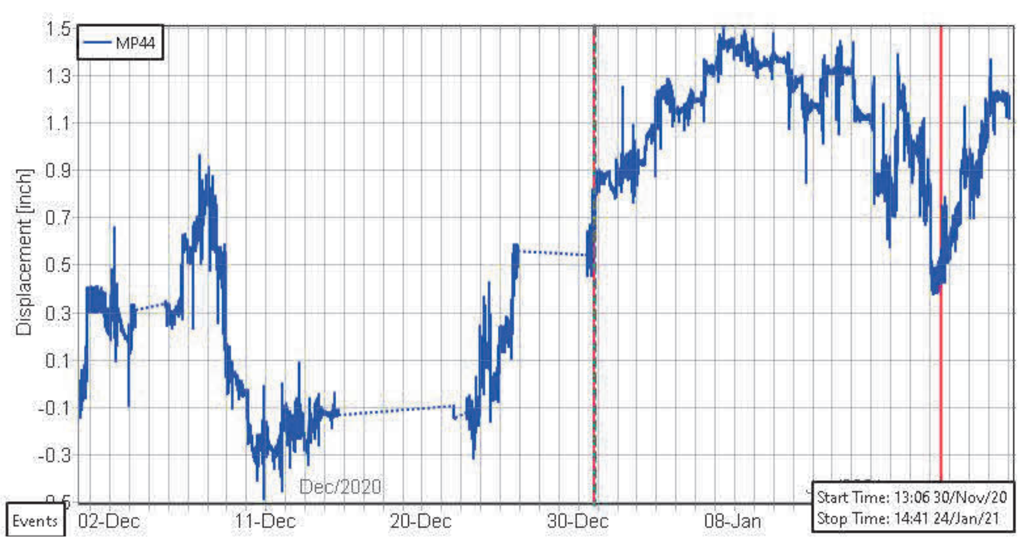

MP44
1.5
1.3
1.1
0.9
0.7
0.5
0.3
0.1
-0.1
-0.3
Displacement [inch]
Dec/2020
Events
02-Dec
11-Dec
20-Dec
30-Dec
08-Jan
Start Time: 13:06 30/Nov/20
Stop Time: 14:41 24/Jan/21

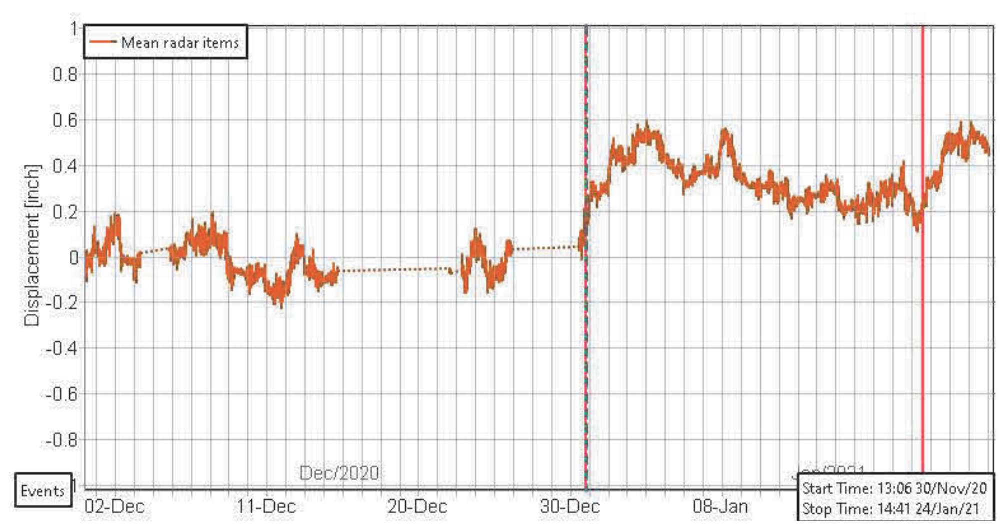

Mean radar items
1
0.8
0.6
0.4
0.2
0
-0.2
-0.4
-0.6
-0.8
Displacement [inch]
Dec/2020
Events
02-Dec
11-Dec
20-Dec
30-Dec
08-Jan
Start Time: 13:06 30/Nov/20
Stop Time: 14:41 24/Jan/21

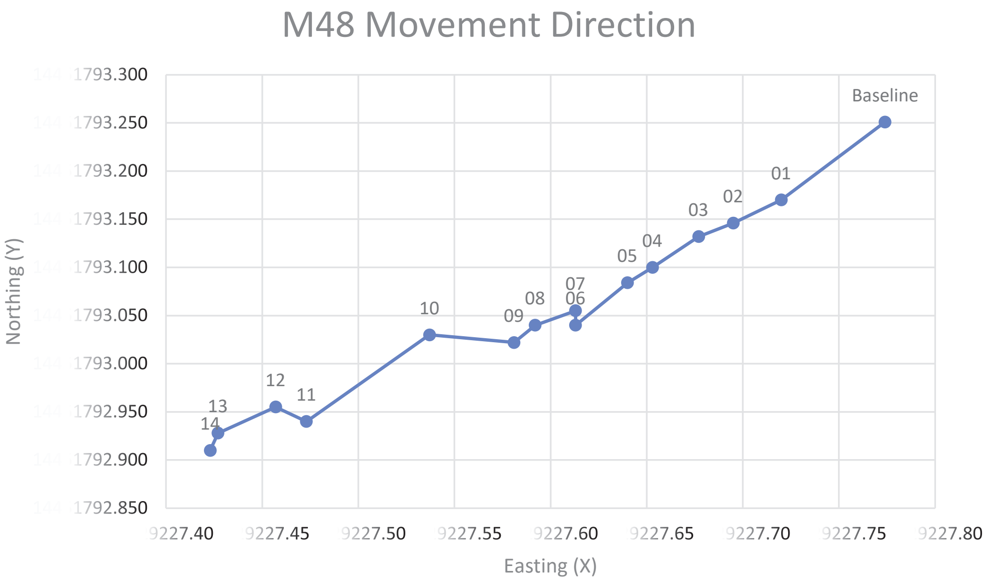
M48 Movement Direction
Baseline
01
02
03
04
05
06
07
08
09
10
11
12
13
14
1793.300
1793.250
1793.200
1793.150
1793.100
1793.050
1793.000
1792.950
1792.900
1792.850
Northing (Y)
9227.40
9227.45
9227.50
9227.55
9227.60
9227.65
9227.70
9227.75
9227.80
Easting (X)

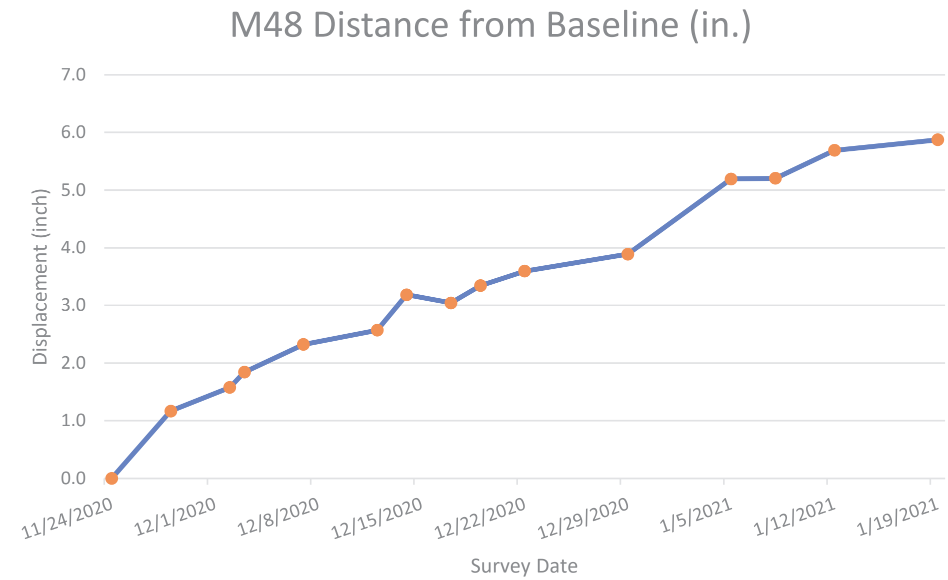
M48 Distance from Baseline (in.)
7.0
6.0
5.0
4.0
3.0
2.0
1.0
0.0
Displacement (inch)
11/24/2020
12/1/2020
12/8/2020
12/15/2020
12/22/2020
12/29/2020
1/5/2021
1/12/2021
1/19/2021
Survey Date

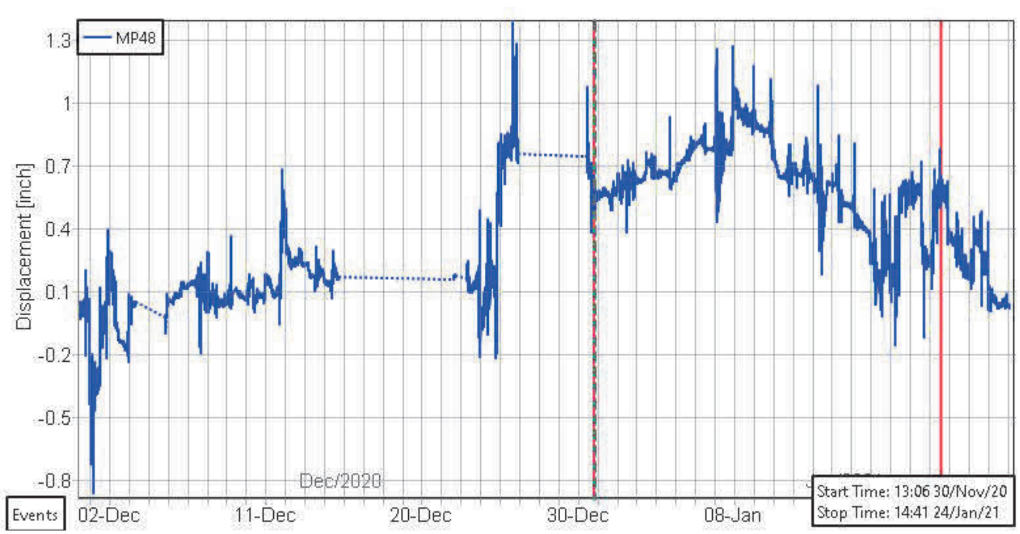
MP48
1.3
1
0.7
0.4
0.1
-0.2
-0.5
-0.8
Displacement [inch]
Dec/2020
Events
02-Dec
11-Dec
20-Dec
30-Dec
08-Jan
Start Time: 13:06 30/Nov/20
Stop Time: 14:41 24/Jan/21

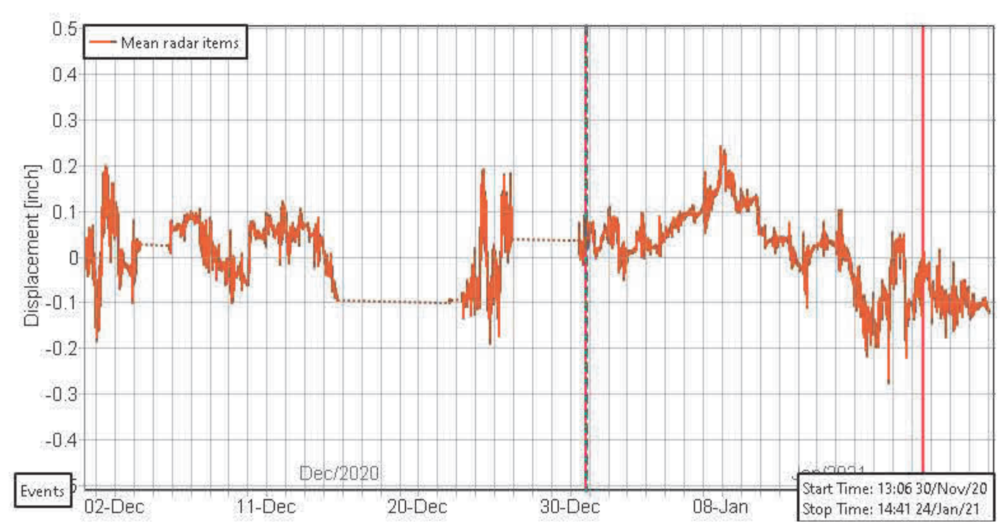
Mean radar items
0.5
0.4
0.3
0.2
0.1
0
-0.1
-0.2
-0.3
-0.4
Displacement [inch]
Dec/2020
Events
02-Dec
11-Dec
20-Dec
30-Dec
08-Jan
Start Time: 13:06 30/Nov/20
Stop Time: 14:41 24/Jan/21

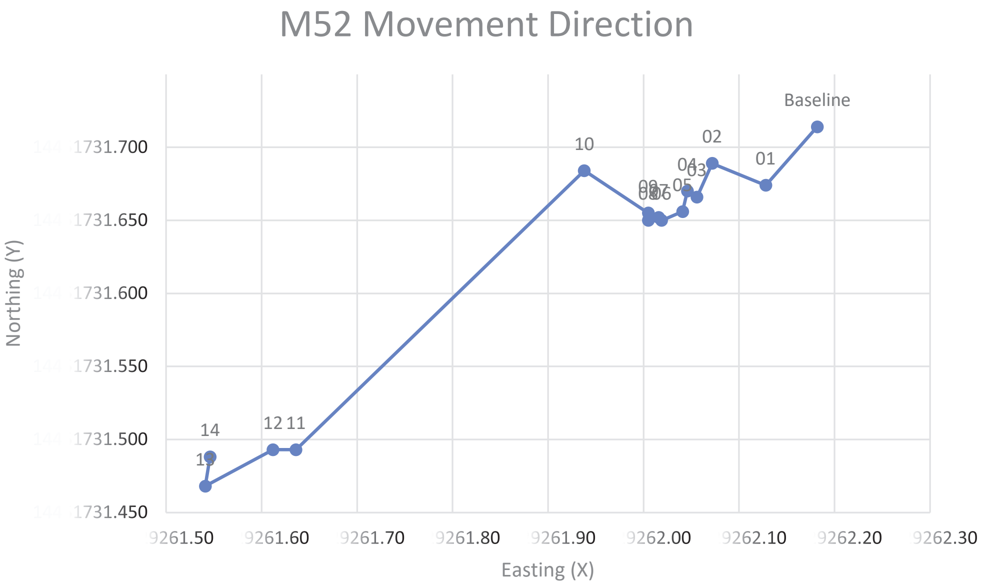

M52 Movement Direction
Northing (Y)
Easting (X)
Baseline
10
02
01
14
12 11
1731.700
1731.650
1731.600
1731.550
1731.500
1731.450
9261.50
9261.60
9261.70
9261.80
9261.90
9262.00
9262.10
9262.20
9262.30

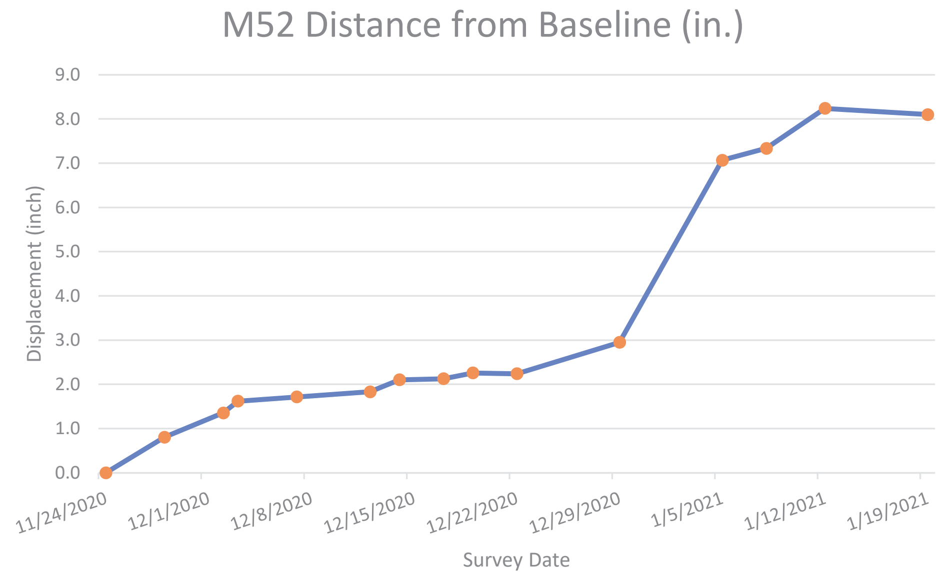

M52 Distance from Baseline (in.)
Displacement (inch)
Survey Date
9.0
8.0
7.0
6.0
5.0
4.0
3.0
2.0
1.0
0.0
11/24/2020
12/1/2020
12/8/2020
12/15/2020
12/22/2020
12/29/2020
1/5/2021
1/12/2021
1/19/2021

MP52
Displacement [inch]
1.4
1.2
1
0.8
0.6
0.4
0.2
0
Dec/2020
Events
02-Dec
11-Dec
20-Dec
30-Dec
08-Jan
Start Time: 13:06 30/Nov/20
Stop Time: 14:41 24/Jan/21

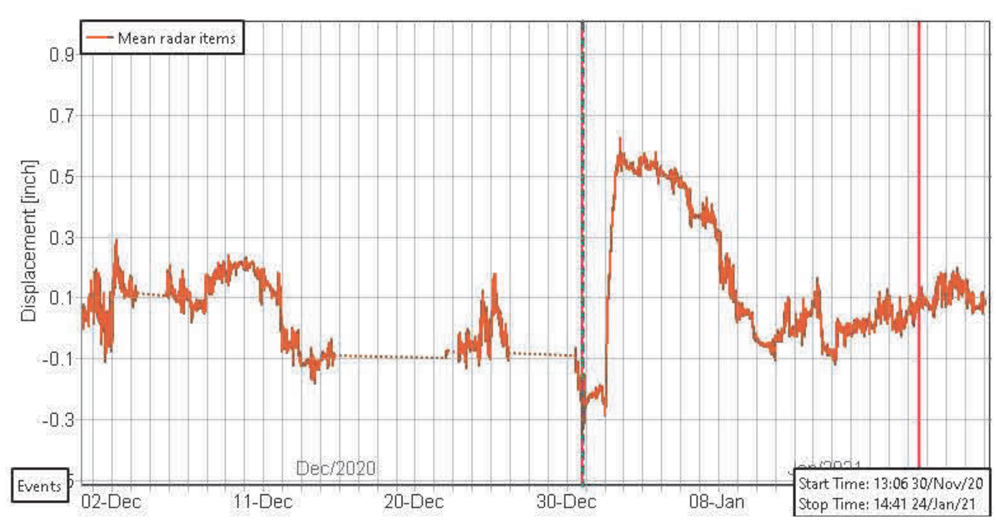

Mean radar items
Displacement [inch]
0.9
0.7
0.5
0.3
0.1
-0.1
-0.3
Dec/2020
Events
02-Dec
11-Dec
20-Dec
30-Dec
08-Jan
Start Time: 13:06 30/Nov/20
Stop Time: 14:41 24/Jan/21

APPENDIX D 3vGeomatics REPORT

3vGEOMATICS

Archive InSAR Analysis of Slope Displacement in Eastern Ohio

Prepared for Golder Associates and the Pipeline Research Council International

Prepared by 3vGeomatics Inc.

Authors:

Murray Down,

Jacob Brown

Release Date: July 9, 2021

Revision Date: September 14, 2021

Contents

List of Acronyms

ALOS-2	Advanced Land Observing Satellite - 2
in/yr	Inches per year (displacement rate)
CSV	Comma-separated values
DEM	Digital Elevation Model
InSAR	Interferometric Synthetic Aperture Radar
KML	Keyhole Markup Language
LiDAR	Light Detection and Ranging
LOS	Line of Sight (line from satellite to measurement location on th ground)
m	Meters
NOD	New Object Detection
ROW	Right of Way
SAR	Synthetic Aperture Radar
SNR	Signal-to-Noise Ratio

1 Executive Summary

Interferometric synthetic aperture radar (InSAR), a remote displacement monitoring technology, was used to monitor the stability of a west facing slope in eastern Ohio, USA. This analysis used 19 descending (west-looking) images acquired from March 2020 to May 2021, and 6 ascending (east-looking) images acquired from February 2021 to June 2021.

The displacement measurements were derived from the phase component of the satellite radar data through interferometric image processing. Unlike more traditional, ground-based methods of monitoring, InSAR does not require any deployment of people or resources to the area of interest (AOI). The quality of InSAR is reduced by thick vegetation, but this was ameliorated by using a satellite with a long wavelength (The Japanese ALOS-2 satellite).

Multiple delivery formats include 3vG's web interface called Motionary to facilitate efficient distribution of the InSAR results to all team members with secure login credentials.

Table 1.1: Summary of eastern Ohio InSAR and New Object Detection Analysis

Footprint name	**Eastern Ohio**
SAR satellite used	ALOS-2, long wavelength (~24 cm)
Landscape	Rolling hills in Ohio, with particular attention to a west facing slope
Product types	Displacement time series data (at 11,23,128 locations), average displacement rate maps, SNR confidence contours, and new object detection products using amplitude data.
Number of images	19 descending + 6 ascending
Reporting period	15 March 2020 – 19 June 2021

1 Introduction

The area of interest (AOI) for this study is located in Ohio, with rolling hills and vegetation, as shown in Figure 1.1.

Figure 1.1: The critical part of the monitoring area with the background showing the elevation model (left) and Esri optical imagery (right). The main displacement is on a west/southwest-facing slope near the middle of these figures.

InSAR is a satellite-based, remote monitoring technology that is ideally suited for measuring ground displacement over large geographic areas. Unlike other monitoring technologies, InSAR doesn't require any on-site instrumentation, human site visits, or aircraft. It is immune to cloud cover, time of day, land-use conflicts, site access obstacles and other logistical challenges. Each time a satellite passes over a defined AOI, typically every 4 to 14 days, a SAR image is acquired that is thousands of square miles in size (specific size depends on each satellite's footprint and the specified resolution). Algorithms analyze millions of data points across each image taken over time to precisely measure displacement of the ground and of infrastructure. InSAR is a mature, proven technology with numerous studies having been conducted comparing InSAR measurements to ground-based systems, with the results consistently corroborating the technology as being a precise and effective measurement tool.

Figure 1.2 illustrates a simplified example of a SAR satellite flying past an AOI on two different occasions several days apart. For simplicity, figure 1.2 illustrates reflections from two locations: location A remains stable between passes while location B is displaced between passes. When the satellite passes over a second time, the same locations are measured in the same way from the same satellite vantage point. At each location, the phase from the first pass is compared with the phase from the second pass to derive the change in distance from the satellite.

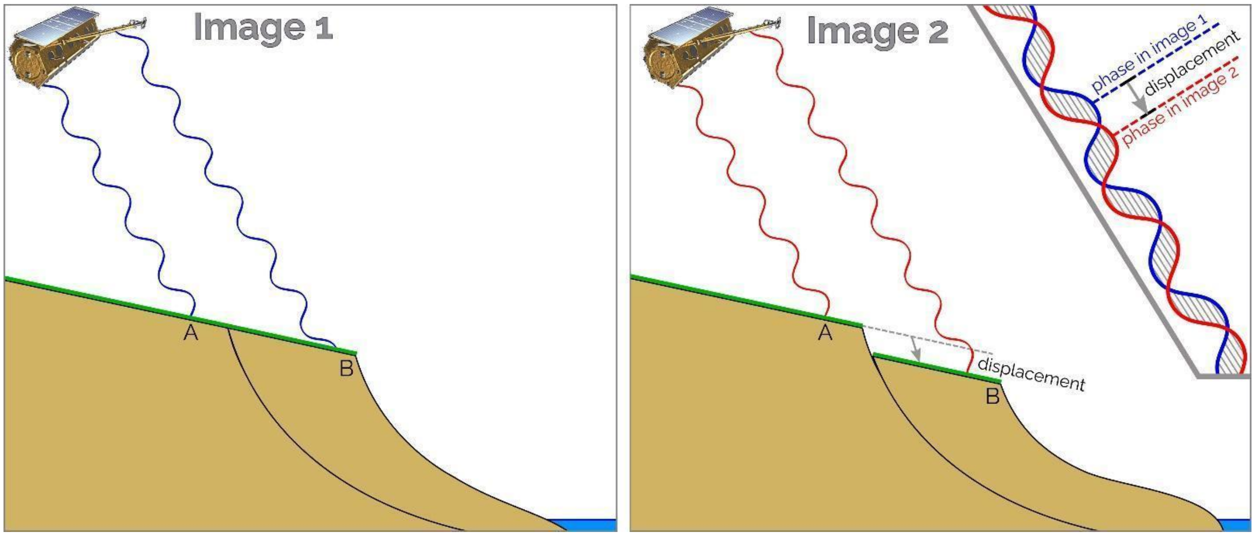

Figure 1.2: A simplified example of how InSAR measures displacement (point B) relative to stable reference locations (point A) by comparing the phase of reflected radio waves from the first pass (left image, blue lines) with the second pass (right image, red lines

The raw data for this analysis consists of synthetic aperture radar (SAR) images collected by a satellite. Ground displacement was measured by analysis of the interference patterns between the phase measurements of these images in a process called InSAR (Interferometric SAR). The displacement measurements were further refined through advanced filtering, signal modeling, noise removal, and spatial statistics to produce several product components such as displacement rate maps, SNR contours, and time series graphs of cumulative displacement. These components were delivered together in several product formats including SQLite databases

2 Synthetic Aperture Radar Data

The primary raw data used for this project consisted of SAR images collected by a satellite sensor called ALOS-2 (Advanced Land Observing Satellite-2) aboard a satellite called PALSAR-2 (Phased Array L-band SAR) which is owned and operated by JAXA (Japanese Space Exploration Agency). The raw data were purchased from JAXA by 3vGeomatics, and processing and analysis was completed by 3vGeomatics. Among the myriad commercially available SAR satellites, ALOS-2 was chosen for its long wavelength, which enables it to maintain coherent displacement measurements over heavily vegetated terrain, unlike most other satellites using shorter wavelengths. ALOS-2's wavelength of approximately 23.6 cm falls within a range of the electromagnetic spectrum called L-band (~15-30 cm). ALOS-2 was tasked in SM-1 mode, with a resolution of 3 m, a footprint of 69 km x 56 km, and a revisit time of 14 days. Acquisition dates of the 6 ascending (east-facing) radar images used in this analysis are shown in Table 2.1, and the 19 descending (west-facing) radar images are shown in Table 2.2. Figure 2.1 details all of the ascending and descending acquisition dates. The terrain covered by the radar image footprint is shown in figure 2.2.

Table 2.1: Dates of the 6 ascending ALOS-2 SAR images that were included in this analysis.

27 Feb 2021	10 Apr 2021	24 Apr 2021	22 May 2021	05 Jun 2021	19 Jun 2021

Table 2.2: Dates of the 19 descending ALOS-2 SAR images that were included in this analysis.

15 Mar 2020	12 Apr 2020	26 Apr 2020	24 May 2020	21 Jun 2020	02 Aug 2020
30 Aug 2020	13 Sep 2020	27 Sep 2020	11 Oct 2020	25 Oct 2020	08 Nov 2020
06 Dec 2020	03 Jan 2021	17 Jan 2020	31 Jan 2021	28 Feb 2021	11 Apr 2021
23 May 2021					

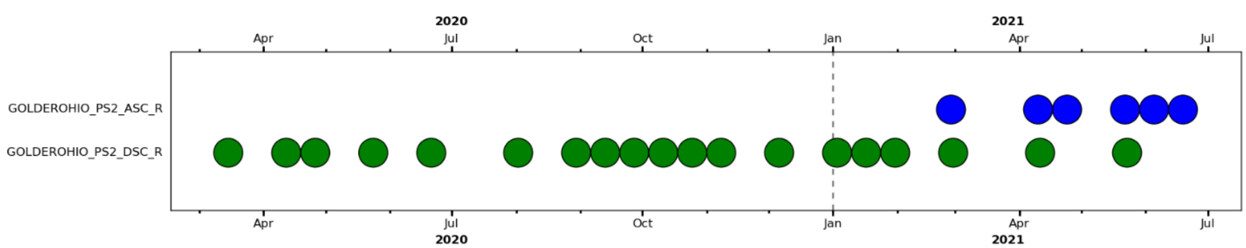

Figure 2.1: Timeline of the 6 ascending and 19 descending ALOS-2 SAR images that were included in this analysis. Each ascending image is represented by a blue circle, and descending images are indicated by a green circle. Touching circles indicate images acquired 14 days apart. Gaps indicate longer intervals.

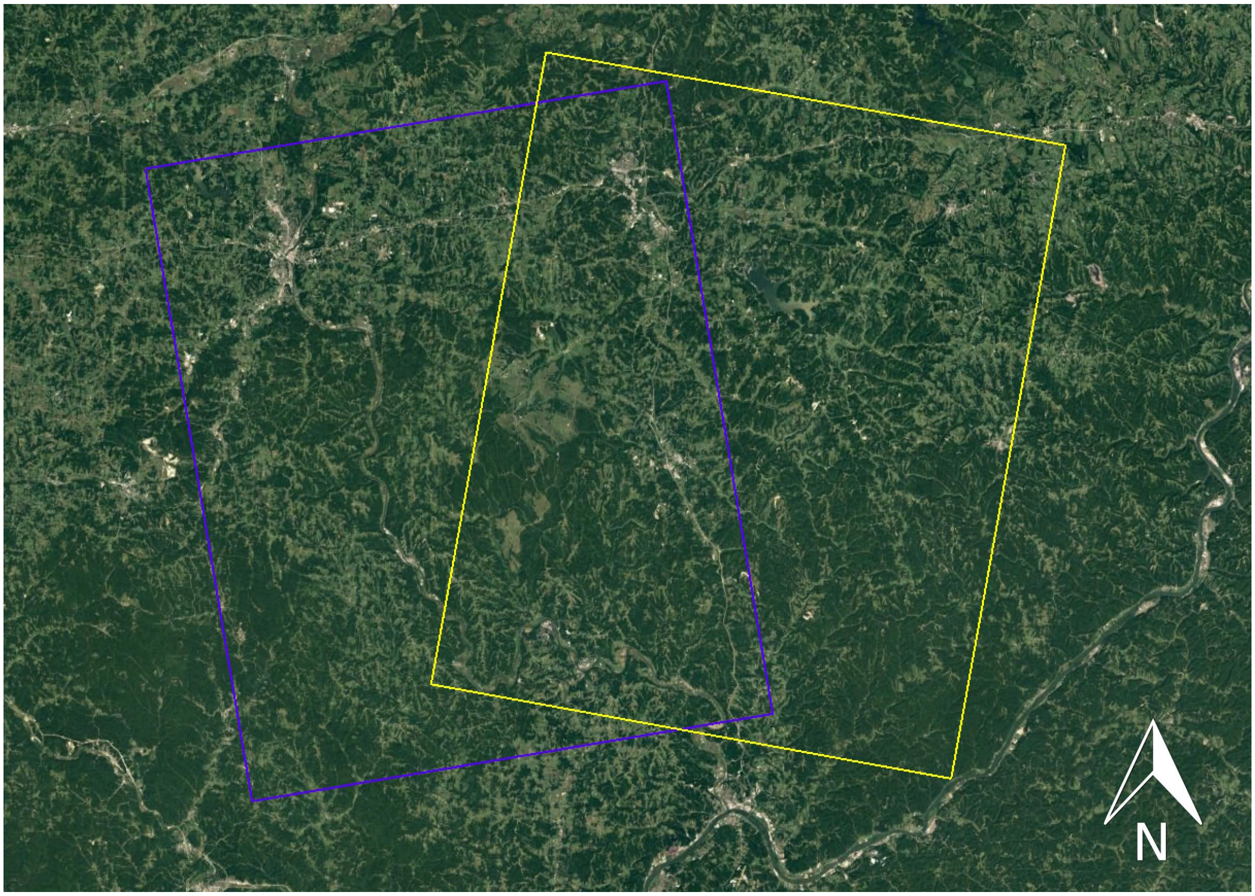

Figure 2.2: The ALOS-2 footprints (ASC in blue and DSC in yellow) over Ohio. The monitoring area is in the overlapping area of the two footprints..

3 InSAR Results

The InSAR results consist of three product components discussed in section 3.1:

- Displacement rate maps: Raster files showing the average displacement rate in all measurable parts of the AOI.
- SNR contours: Vector files showing the extent of high confidence displacement areas.
- Time series data: Histories of cumulative displacement as seen from the descending line-of-site over time for millions of measurement locations.

The report is presented in multiple file formats, including:

- Sqlite database with ArcMap MXD and toolbar
- Motionary, 3vG's web platform which is updated with the latest results after each comprehensive report, and the latest time series results are amalgamated with past comprehensive time series results to present a continuous history of displacement spanning multiple reports

3.1 Data Components

3.1.1 Displacement Rates

The displacement rate shows the average rate of displacement during the analysis period in units of cm per year (cm/yr) or inches per year (in/yr). For this analysis, several displacement rates were produced using different groups of SAR images. Figure 3.1 shows the single-look west-looking long time period displacement rate, scaled at +/- 10in/yr.

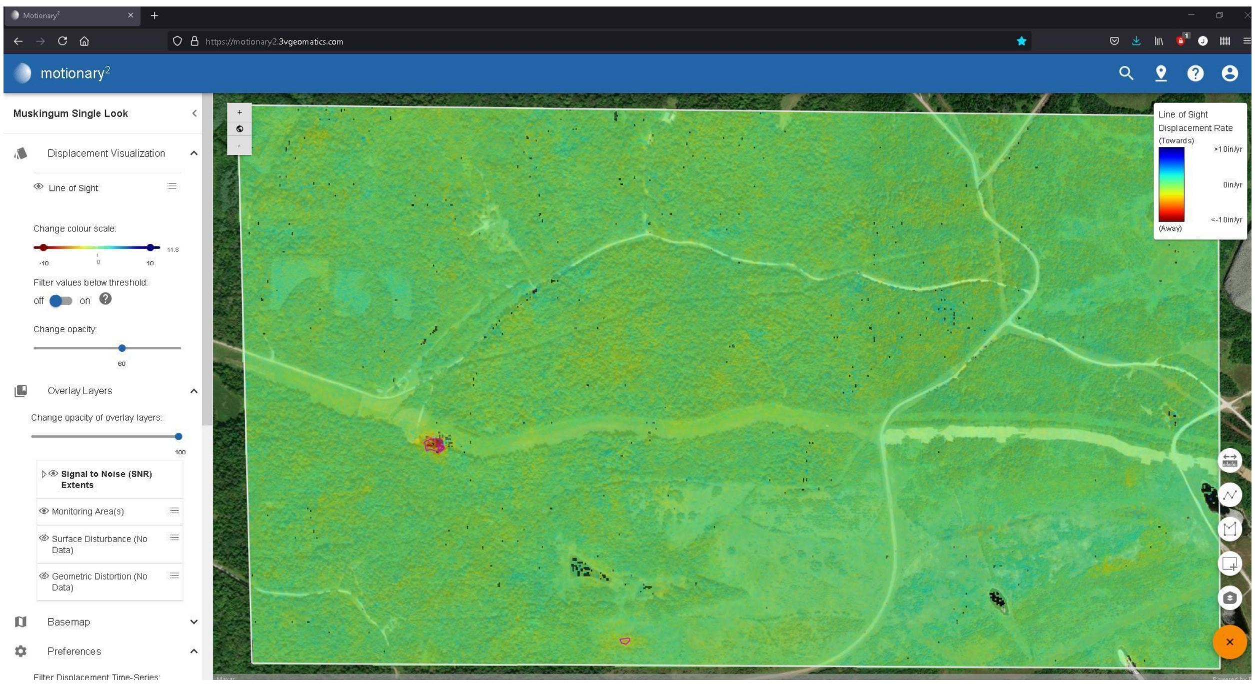

Figure 3.1: A semitransparent Motionary Heatmap of the single-look west-looking LOS displacement rate over the AOI, scaled at +/- 10 in/yr. SNR level 2.0 and 3.0 contours can be seen in white..

3.1.2 Signal to Noise Ratio Contours

Signal to noise ratio (SNR) contours were generated to highlight areas of significant displacement. SNR is the ratio of the displacement signal to the measurement noise. It is measured in standard deviations (sigma) and it varies spatially for a given dataset covering a set period of time. The SNR results are thresholded to produce contours at three different levels with the following qualitative interpretations:

- SNR 4.0 sigma: Indicate strong evidence for displacement, low chance of the signal in that area being caused by noise alone.
- SNR 3.0 sigma: Indicate reasonable evidence for displacement
- SNR 2.0 sigma: Indicates weak evidence for displacement and should be treated with caution.

Figure 3.2 shows SNR contours in white overlaid on the displacement rate map. The SNR contours include metadata that can be customized to include the closest distance from each contour to the closest operator-provided asset such as a pipeline centerline, however pipeline centerlines were not provided to 3vG for this project.

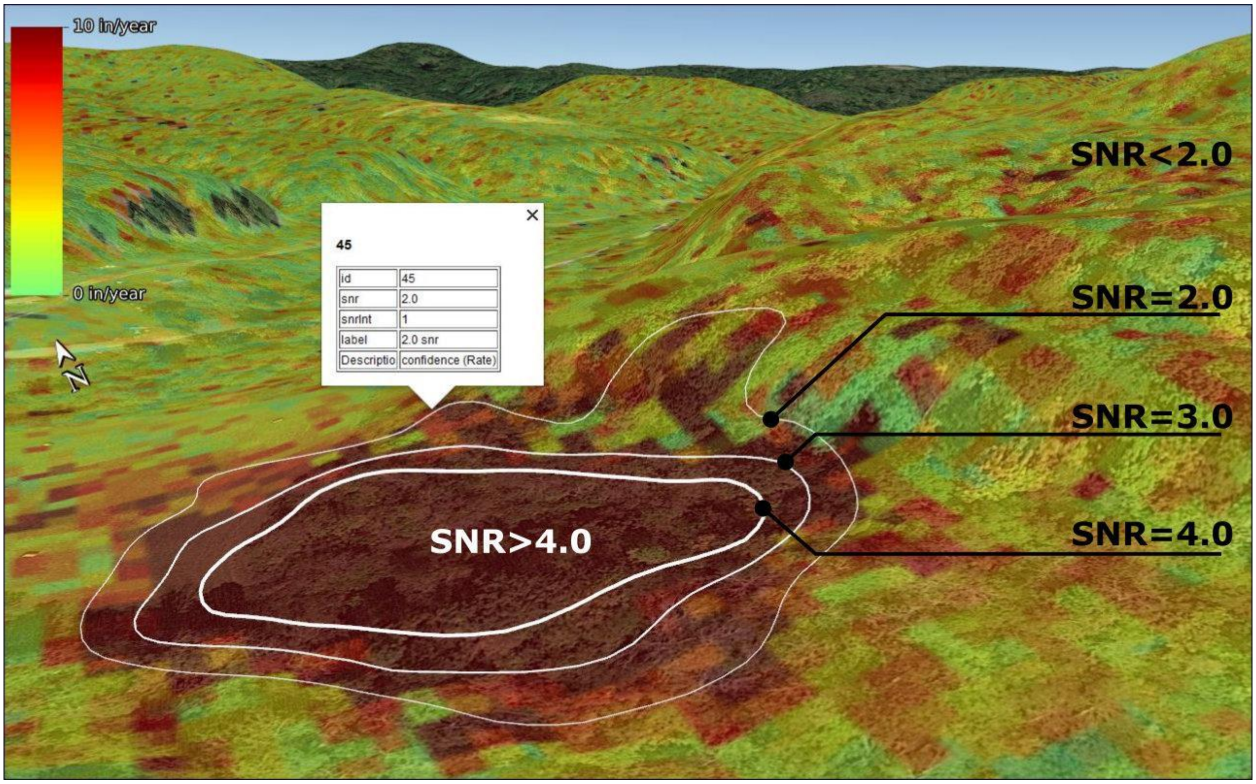

Figure 3.2: SNR contours in white indicating the extent of higher confidence displacement areas as a guide to interpreting the semitransparent displacement rate layer scaled at 10 inches/year. Just like this rate, these SNR contours were produced using images from both look directions over a short time period in 2021.

Several sets of SNR contours were generated for this project, with each set being specific to the time period and measurement dimensions of a specific group of images used in that analysis. SNR contours are designed to be used in conjunction with the appropriate matching rate layer corresponding to the same date range and images as the set of SNR contours; the noise level changes across the area of interest, so areas with low noise have a lower “detection threshold”. Thus, much smaller displacement rates are significant at the 3.0 and 4.0 sigma levels in locations where the noise is low relative to displacement magnitude. Figures 3.3 and 3.4 show three different sets of SNR contours and associated displacement rates, along with details of the images used and look directions of each set of products. Figure 3.5 shows a comparison of the west-looking SNR contours with the dual-look SNR contours over backgrounds showing the elevation model, and optical imagery.

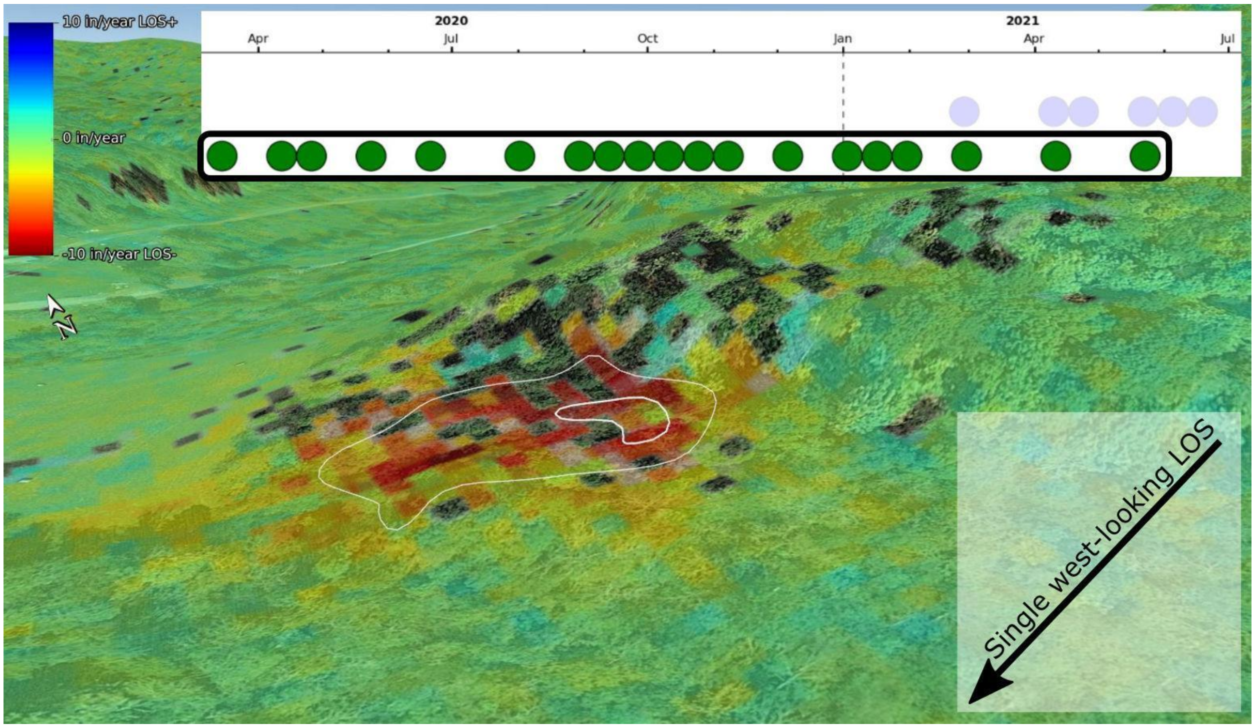

Figure 3.3: The displacement rate and SNR contours produced using all available descending (west-looking) images.

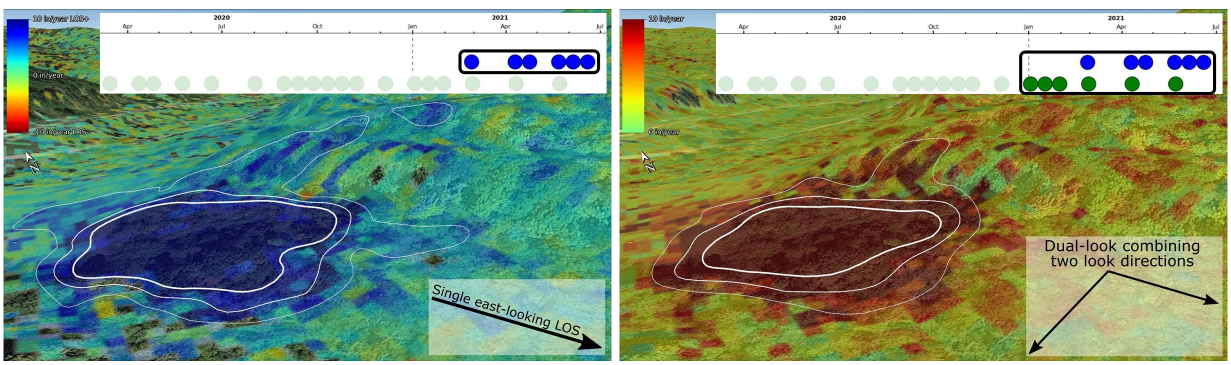

Figure 3.4: The displacement rate and SNR contours produced using all available ascending (east-looking) images (left) shows displacement towards the sensor (west in this case). The displacement rate and SNR contours produced using images from both look directions (right) could only be produced over a shorter time period when images were acquired from both directions..

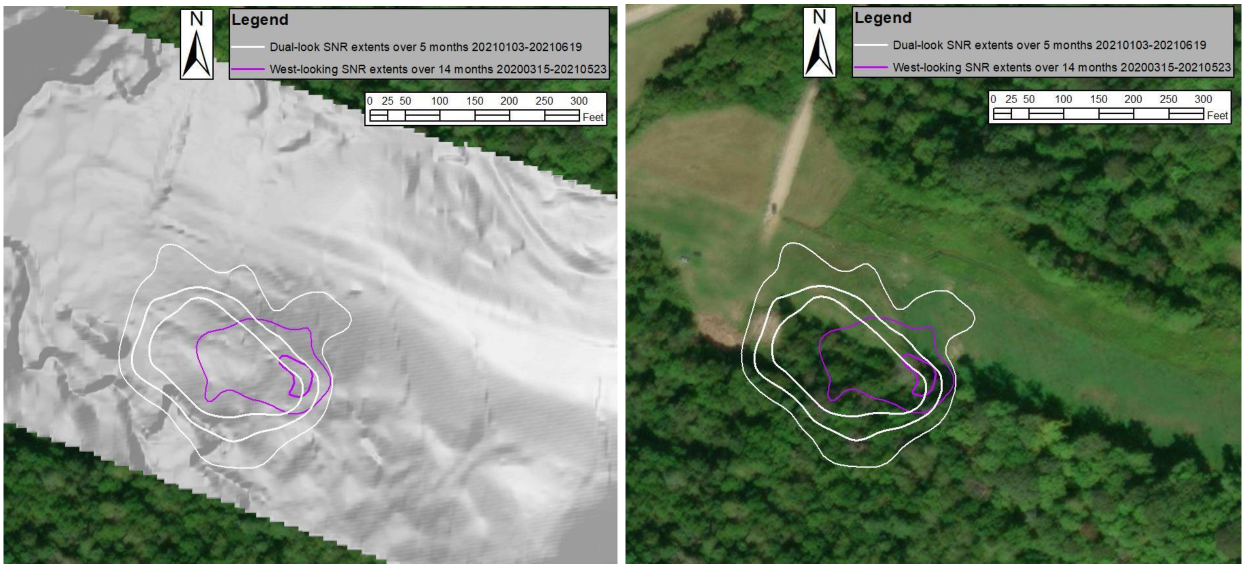

Figure 3.5: Comparison of the SNR extents from two different analyses. The purple contours represent displacement measured only by the west-looking data over 14 months, while the white contours represent displacement measured by both look directions but only over the most recent 5 months. The Background on the left shows the hill-shaded lidar DEM, while the right image shows optical from Esri.

The SNR extent contours are vector representations of values that vary between every pixel. Groups of adjacent pixels must all have an SNR value above a threshold in order to create an SNR contour. SNR depends on the ratio between the signal (measured displacement magnitude) and the noise (variability in that measurement). A noisy fast-moving pixel can sometimes have the same SNR value as a less-noisy but slower-moving pixel. Figure 3.6 illustrates four hypothetical histograms showing gaussian distributions of multiple displacement rate measurements. Each graph represents the distribution of rate measurements over different time periods in the same radar image pixel, with the displacement rate on the x axis and the frequency of that measurement in the y axis. Pixels where successive rate measurements are more consistent will have a pointier curve and a smaller standard deviation, while noisy inconsistent pixels that yield a wider range of displacement rate measurements will have a flatter curve and larger standard deviation. The SNR used in this report is the ratio of the average rate magnitude over the standard deviation.

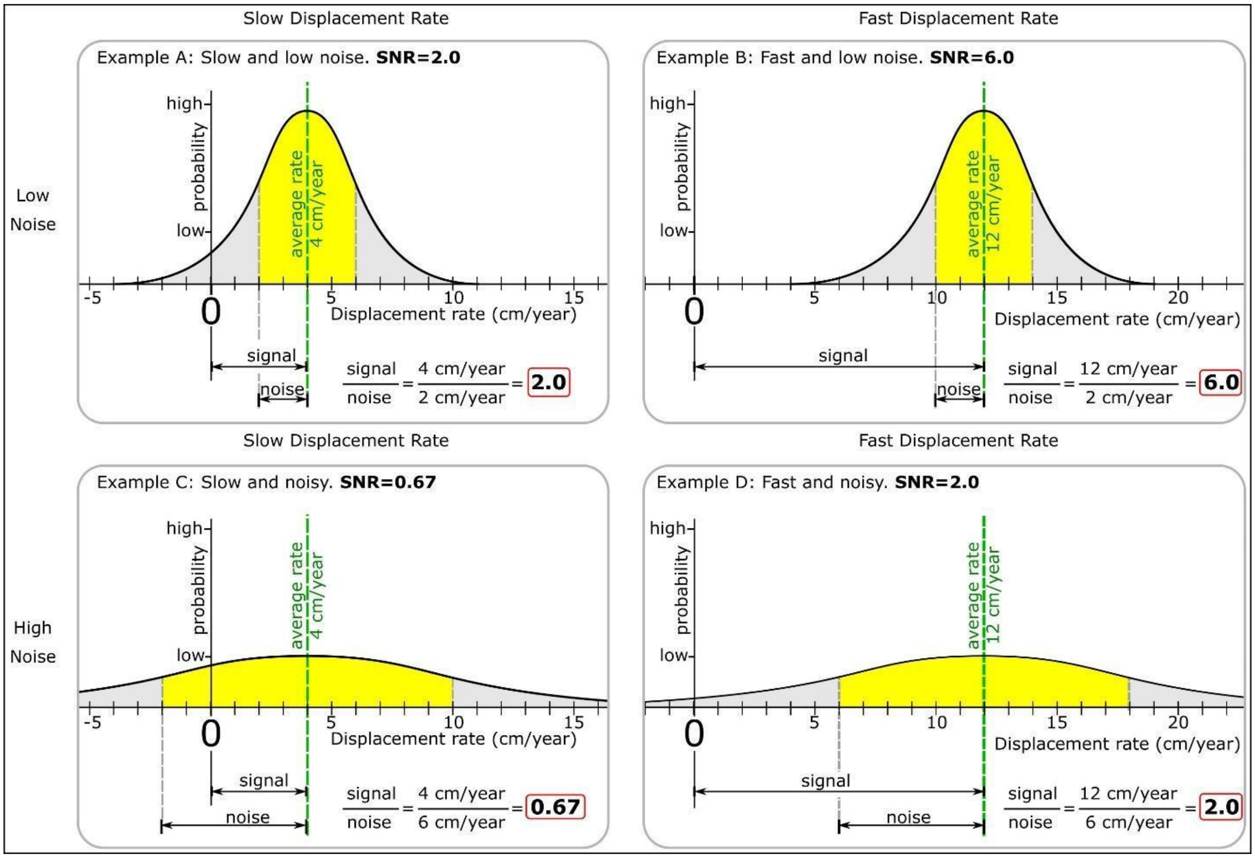

Figure 3.6: Illustration of various hypothetical rate measurement histograms with different values of SNR.

3.1.3 Point Time Series

Time series results have been produced for over 11 million points distributed throughout the AOI, each containing the history of that point during the study period. Each point contains cumulative displacement data for the analysis period, and multi-point selection and graphing is supported by Motionary (section 3.2.1) and the 3vG ArcMap toolbar (section 3.2.2).

3.2 Delivery Formats

The rate, contours and points are all delivered in several formats.

3.2.1 Motionary Product Format

The most accessible delivery format is 3vG's internally developed web platform called Motionary, which has improved substantially over the last year. Motionary has nearly all of the features of the ArcMap product, but it doesn't require any special software other than a web browser. Access is regulated through usernames and passwords specific to the site.

Figures 3.8 through 3.14 show screenshots of Motionary. The displacement rate map's scale can be adjusted on the fly to any arbitrary value. The rate map can be filtered to show only areas moving faster than a chosen value, as shown in Figure 3.10, making areas transparent if they're moving slower than this threshold.

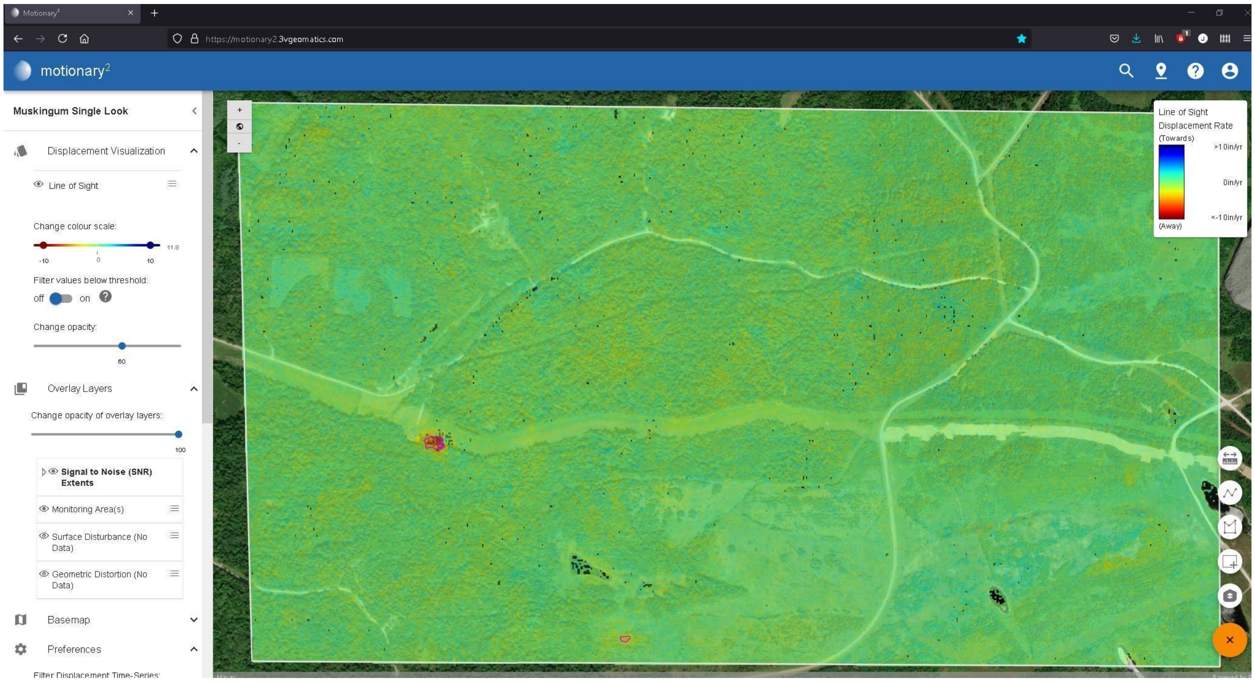

Figure 3.8: Motionary screenshot showing the full footprint rate (adjustable scale) and SNR contours in purple.

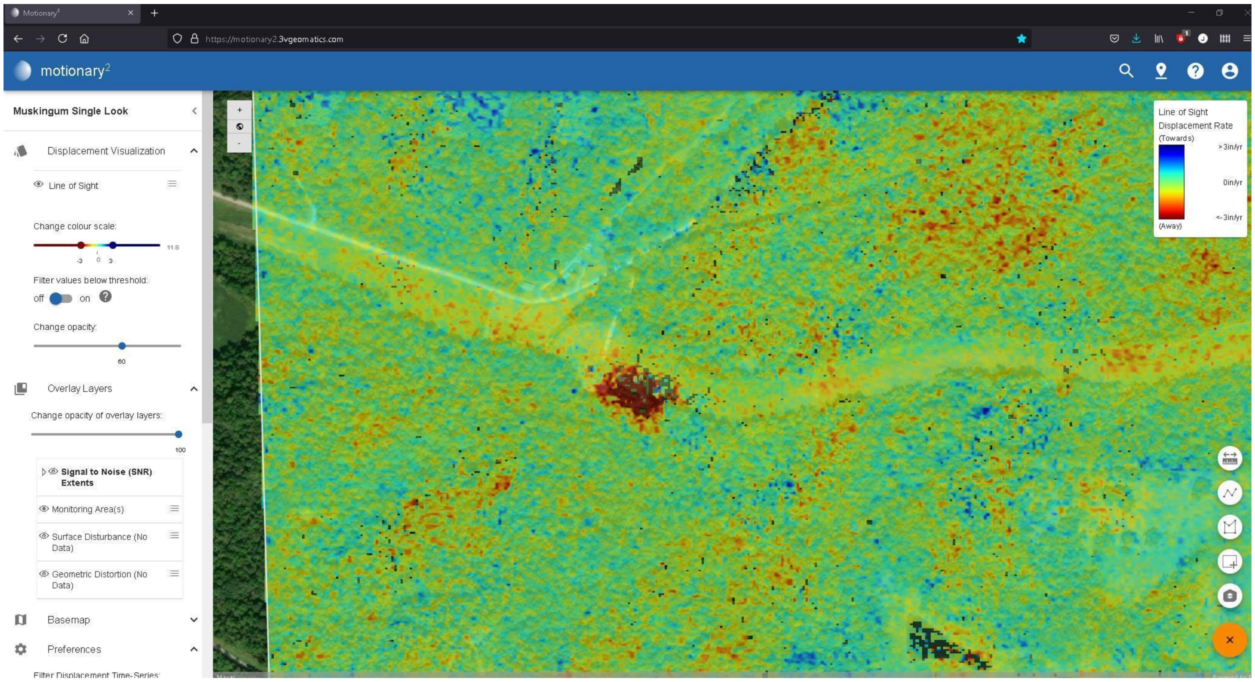

Figure 3.9: Motionary screenshot showing a closeup view of the rate map with the SNR contours toggled off and the rate arbitrarily adjusted to 3 in/yr in the left side control panel.

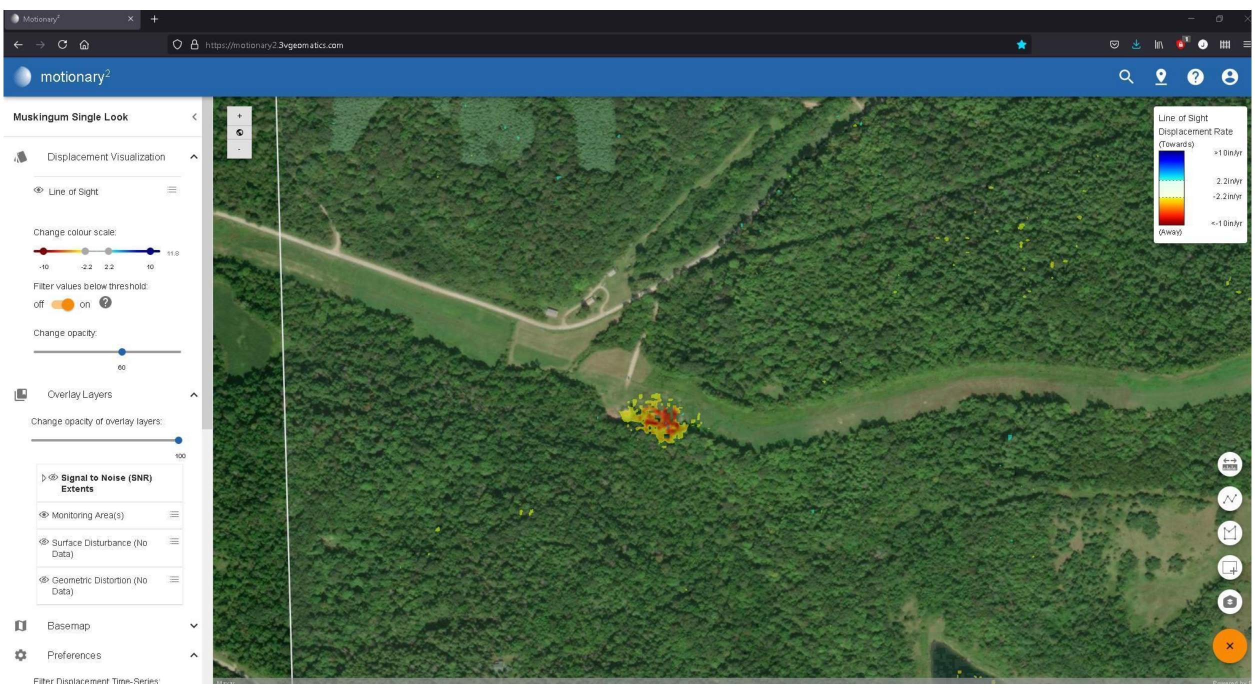

Figure 3.10: Motionary screenshot showing a closer view of the rate map with a feature activated to filter rate values below an adjustable threshold (2.2 in/yr in this example). The rate scale is adjusted to 10 in/yr.

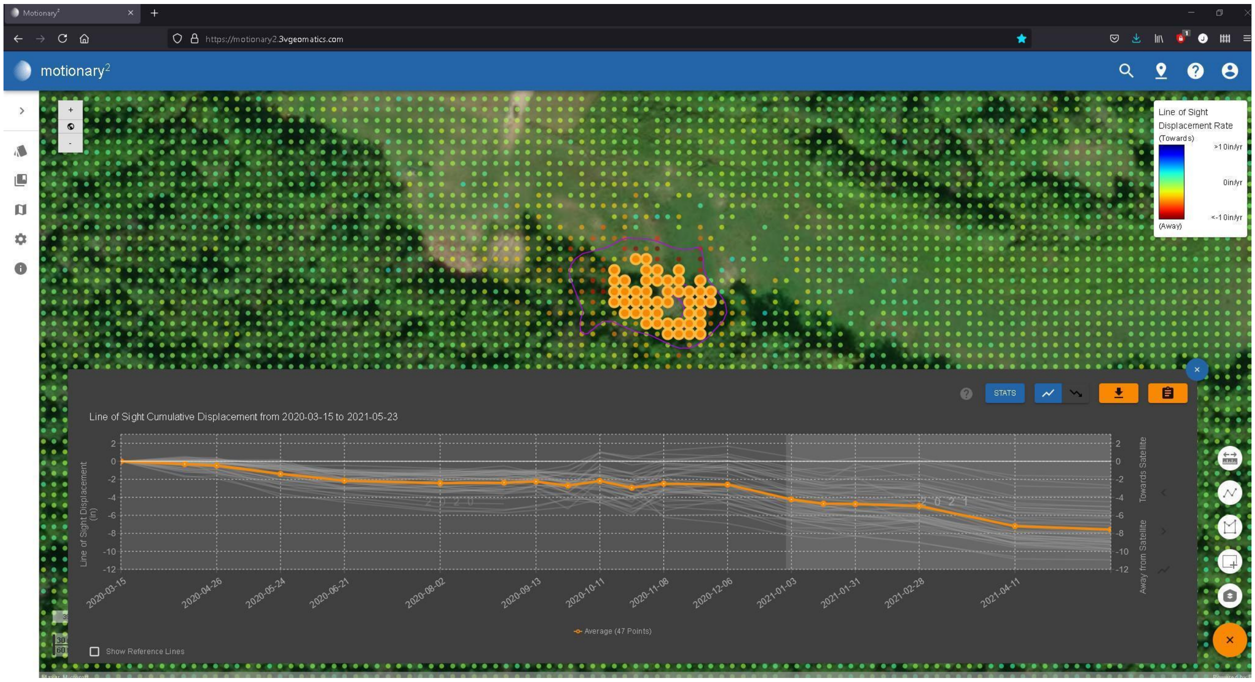

Figure 3.11: Motionary screenshot showing a graph of multiple selected points, with the SNR contours shown in purple.

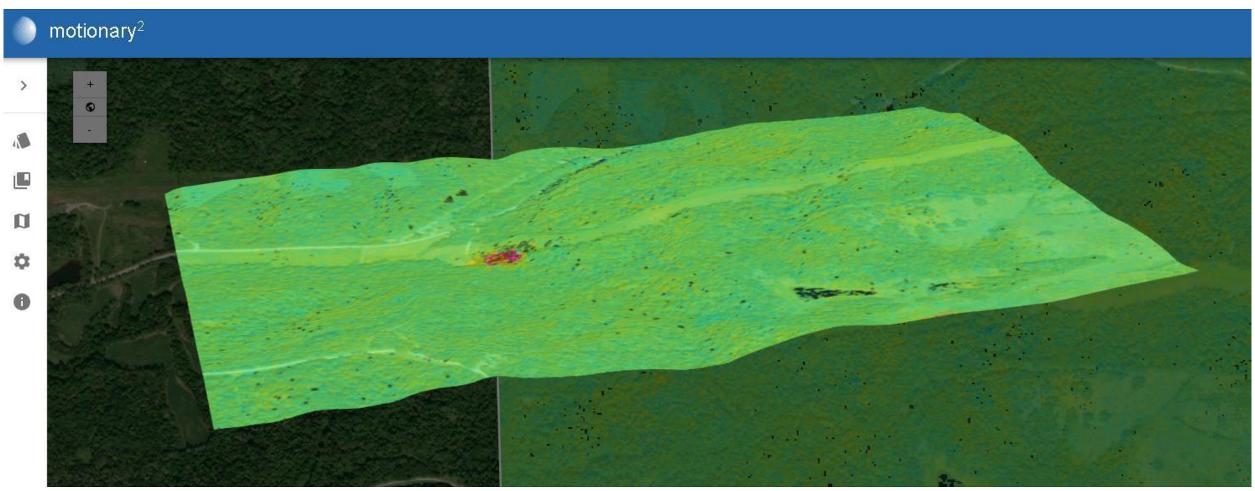

Figure 3.12: Motionary screenshot showing the rate and contours in 3-D view mode to put the displacement in the context of the topography.

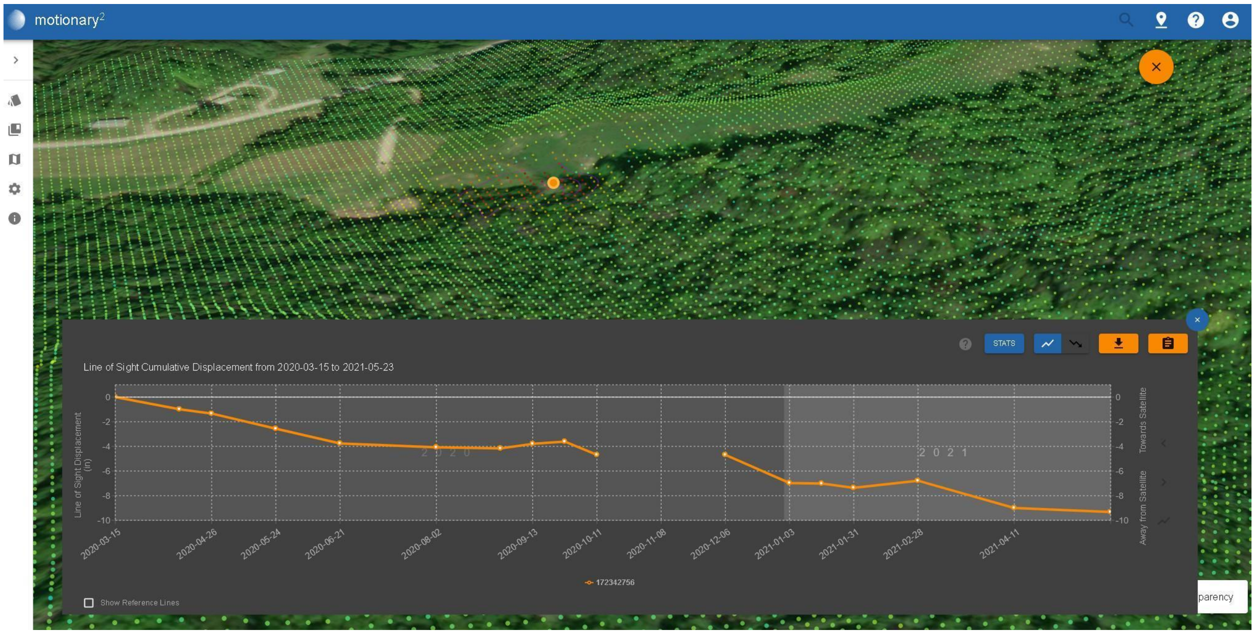

Figure 3.13: Motionary screenshot showing a graph of a point in 3-D view mode, with information about a specific date being shown as the mouse is hovered over that point on the graph.

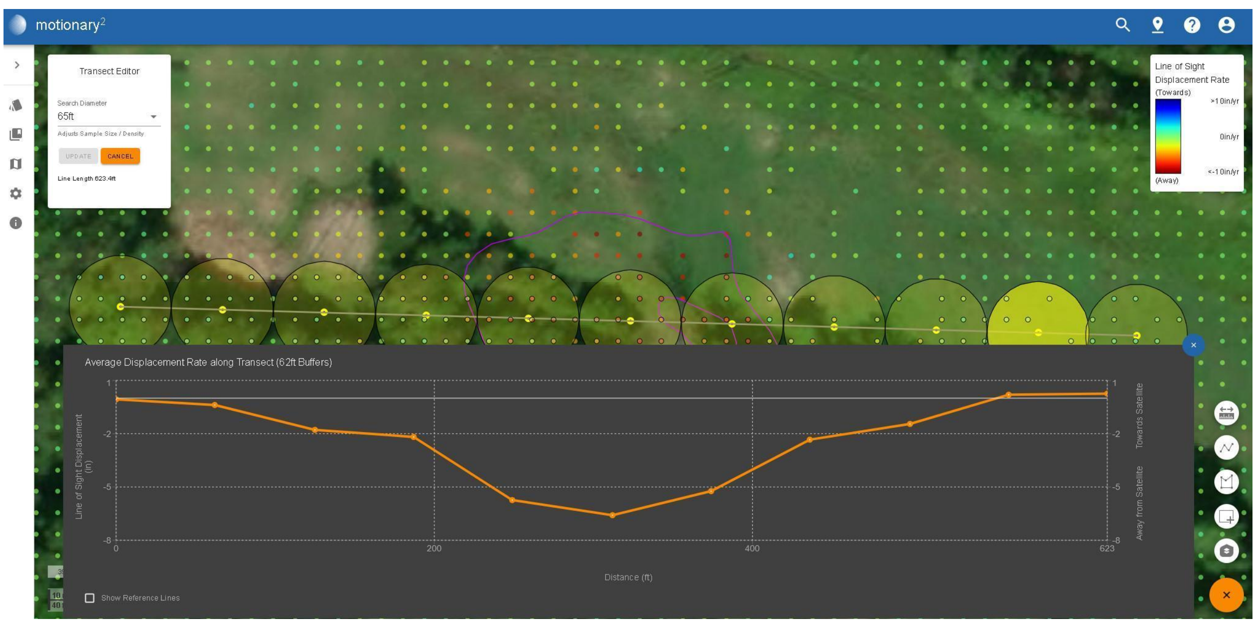

Figure 3.14: Motionary screenshot showing a transect graph of displacement rate vs distance along the transect line. The adjustable sampling radius is shown in the top left panel, with the sampling circles highlighted in semitransparent yellow in the map (top).

3.2.2 ArcMap and SQLite database Product Format

The ArcMap product includes the complete dataset saved in an SQLite database along with a companion MXD file and custom ArcMap toolbar for investigating the results. Figure 3.15 shows screenshots of the archive results in ArcMap with the 3vG ArcMap toolbar.

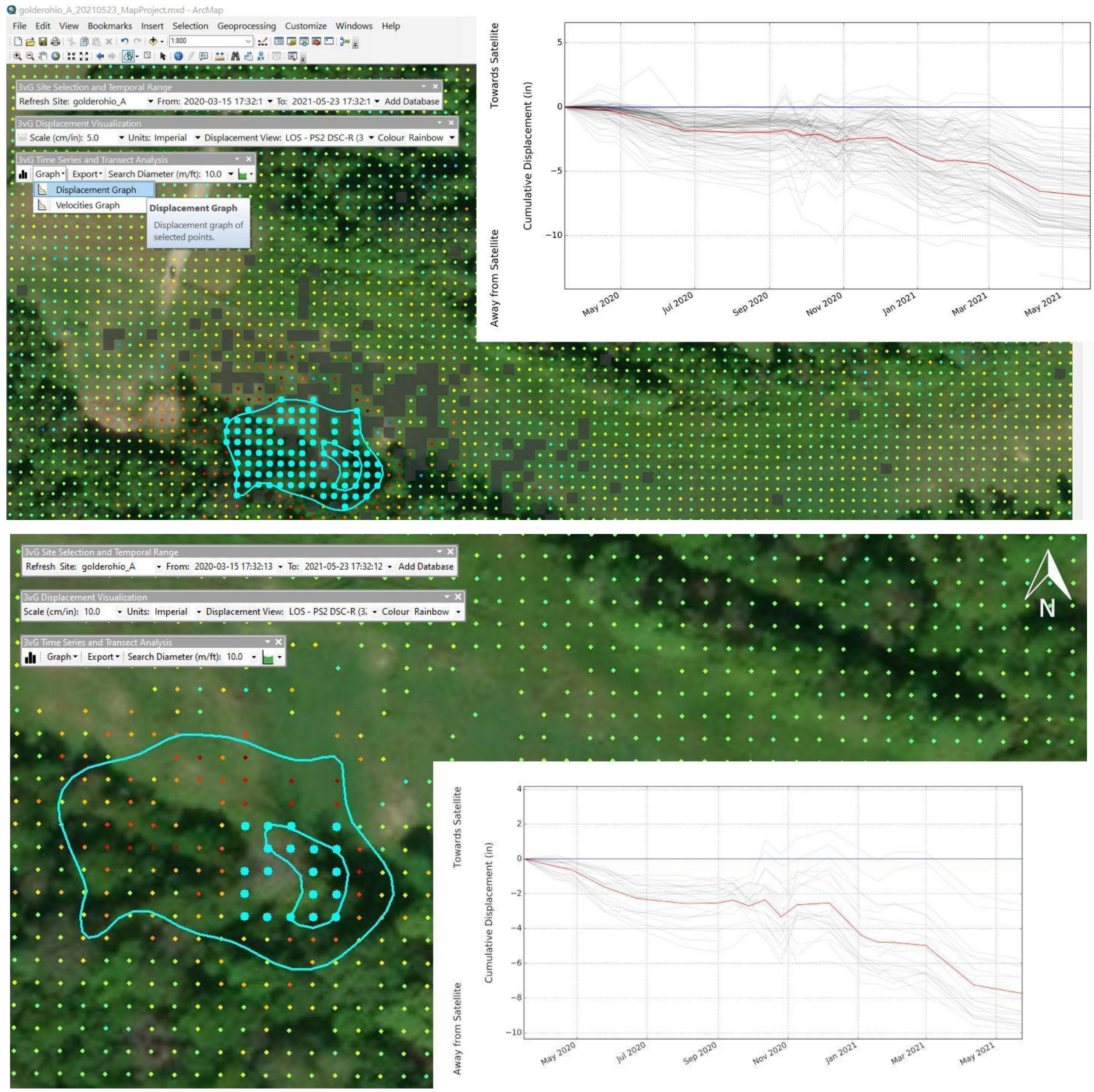

Figure 3.15: Screenshots of ArcMap showing time series graphs produced with the 3vG ArcMap toolbar from groups of selected points (cyan). The SNR contours also appear cyan because they are selected but they don't affect the graphs. The red line shows the average displacement of all the selected points.

4 Discussion

4.1 Dual-Look Geometry

With the availability of both ascending and descending SAR images, the individual look directions were combined into a dual-look product which has additional features compared to the single look products. Unlike the native LOS geometry of single look products, dual-look products contain combined measurements that are projected onto a displacement vector field. This results in more accurate displacement estimates and better coverage over the area of interest.

From these two independent LOS measurements, a direction of displacement can be solved in the east-west-up-down plane. The ascending and descending displacement vectors can then be co-projected along the solved vector, not only providing directional information, but also increasing the displacement magnitude appropriately. Note that the north-south direction is not considered because this is nearly the flight path of the satellite and there is no displacement sensitivity along this axis. Figure 4.1 demonstrates how the two LOS measurements are combined to derive the displacement vector directions in the plane.

Due to the difference in time-frame that the ascending and descending stacks span, the dual-look products have only been generated from January 2021. In addition, the products do not include the point time series due to the higher noise that is present in such a short time-frame; all other displacement rate products have been generated.

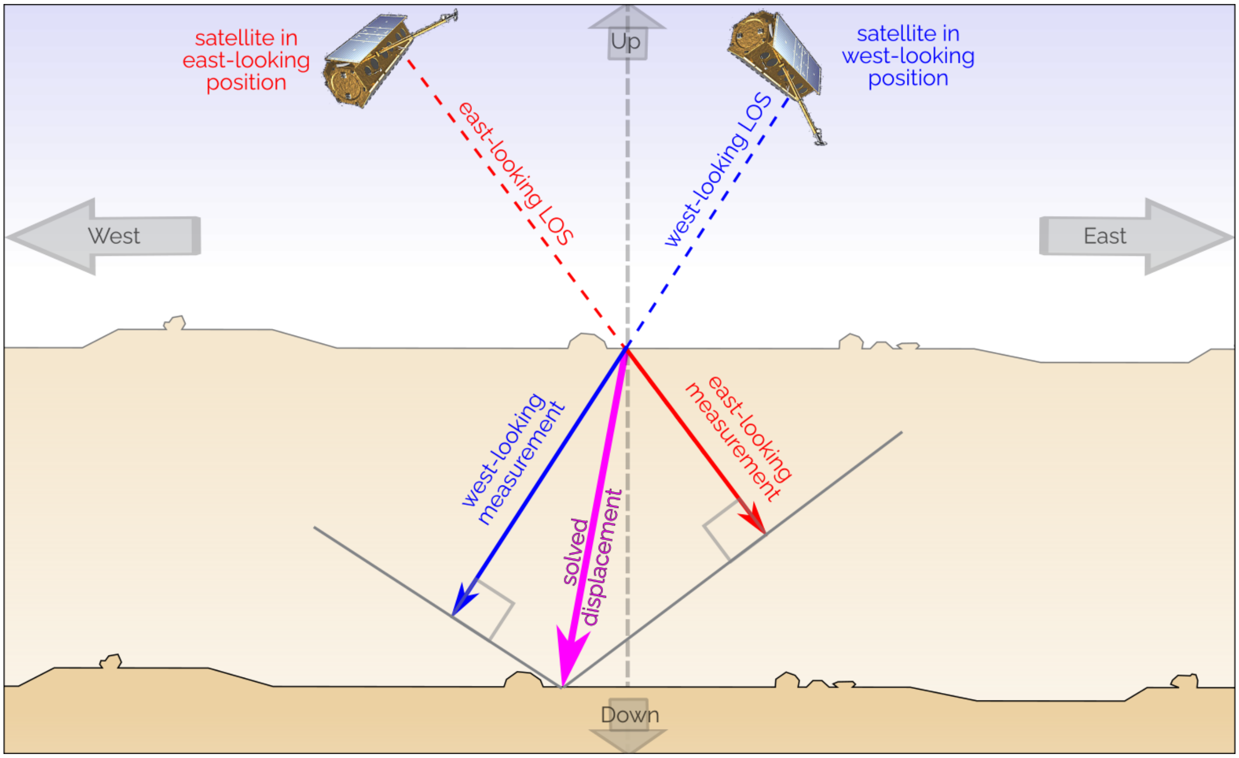

Figure 4.1: Using both ascending and descending satellite acquisitions, it is possible to solve for the displacement vector. This includes up-down components as well as the east-west components

4.2 Displacement characteristics on the slope

Within the AOI provided by Golder to 3vGeomatics was a slope that underwent remediation efforts in September 2020. The full archive analysis from March 2020 revealed a steady rate of displacement on the slope face, as seen by both the times series LOS displacement and velocity (see Figure 4.2). Coverage over the slope appears to slightly lower due to the remediation efforts.

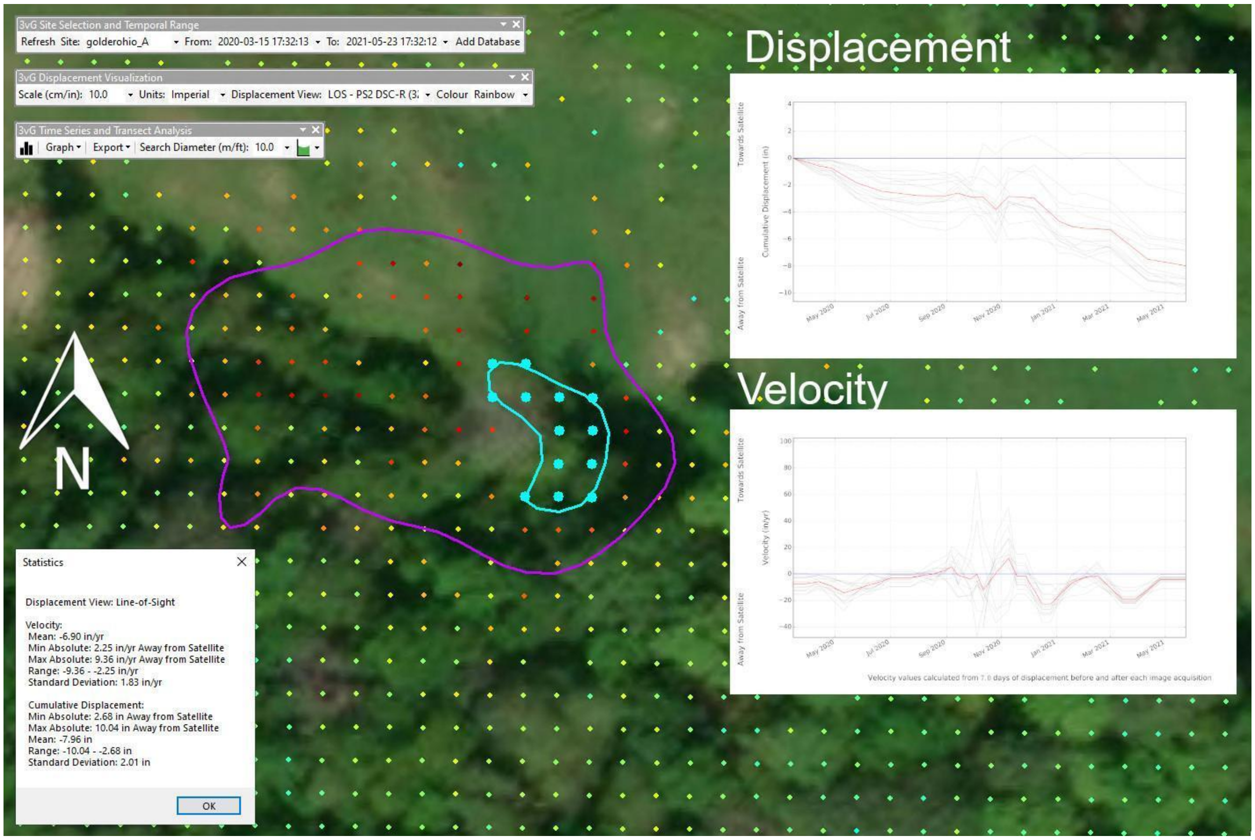

Figure 4.2: Statistics and time-series graphs for points within the SNR 3 contour identified in the DSC LOS comprehensive product. The selected points have an average displacement rate of 6.9 in/yr away from the satellite.

Analysis of the time series data for this slope reveals that this movement remains consistent even after the remediation efforts. This continued movement is supported by the identification of an SNR 4 (high confidence) contour from the dual-look analysis which only incorporated data after January 2021. Due to the limited number of images available to derive this dual-look product, and the small time-frame of the analysis, noise is significantly higher than in the LOS DSC product.

5 Amplitude Results

In addition to InSAR displacement data, which are primarily based on the phase component of the SAR data, other insight can be gleaned by analysing the amplitude component of the same SAR data. Samples of this amplitude data have been produced over a subset of the study area.

New Object Detection

The amplitude (brightness) of pixels in the images can be specially processed to pinpoint locations and times where large objects appear near a pipeline or other infrastructure. This method is particularly adept at detecting the appearance of large machinery such as excavators, heavy trucks, and drill rigs. If such machinery is operating in the area without proper permits and knowledge of buried pipelines, it could lead to utility strikes rupturing the pipeline. While new object detection products can't differentiate between types of machinery or other similar objects, they can highlight locations of new activity quickly and guide investigations to quickly address potential utility strike threats.

Radar images use electromagnetic radiation with a much longer wavelength (typically 3 cm - 24 cm) than visible light (400-700 nm), which changes the way it bounces off of surfaces. Certain objects can appear much brighter or darker in radar images than they would in visible light images. Among many factors affecting brightness, dense metallic objects with many corners and chunky parts can create a large radar cross section, which can vary significantly as they change orientation. These properties can be exploited to detect anomalies that suggest machinery might be active near pipelines.

After the first eight radar images are collected over an area of interest and the images are aligned with each other to match pixels covering the same locations, the average brightness of each pixel is stored. For most radar satellites in standard mode, these pixels are spaced 3 m (10 feet) apart. When the next image is collected, the brightness of each pixel is compared to the temporal average brightness of that same pixel during all of the previous image dates. Statistical analysis highlights pixels that became significantly brighter in the last image than the average. This ensures that pre-existing bright targets are not flagged unless they move a few meters to occupy a different pixel, or change their orientation to become much brighter. This comparison is done at every pixel located within a user-defined distance from the client's assets. The brightness increase threshold is fine tuned to achieve a balance that aims to ignore small inconsequential changes while catching the most significant changes that are more likely to be heavy machinery.

These results are presented for several recent dates, with the points color-coded by date of first appearance. This highlights clusters of points with ongoing change, suggesting ongoing activity. appearance of each identified point. The graph in the right of figure 5.1 shows the target brightness history at a dark orange point with a sharp brightness increase on October 11th, which indicates the first appearance of this data point..

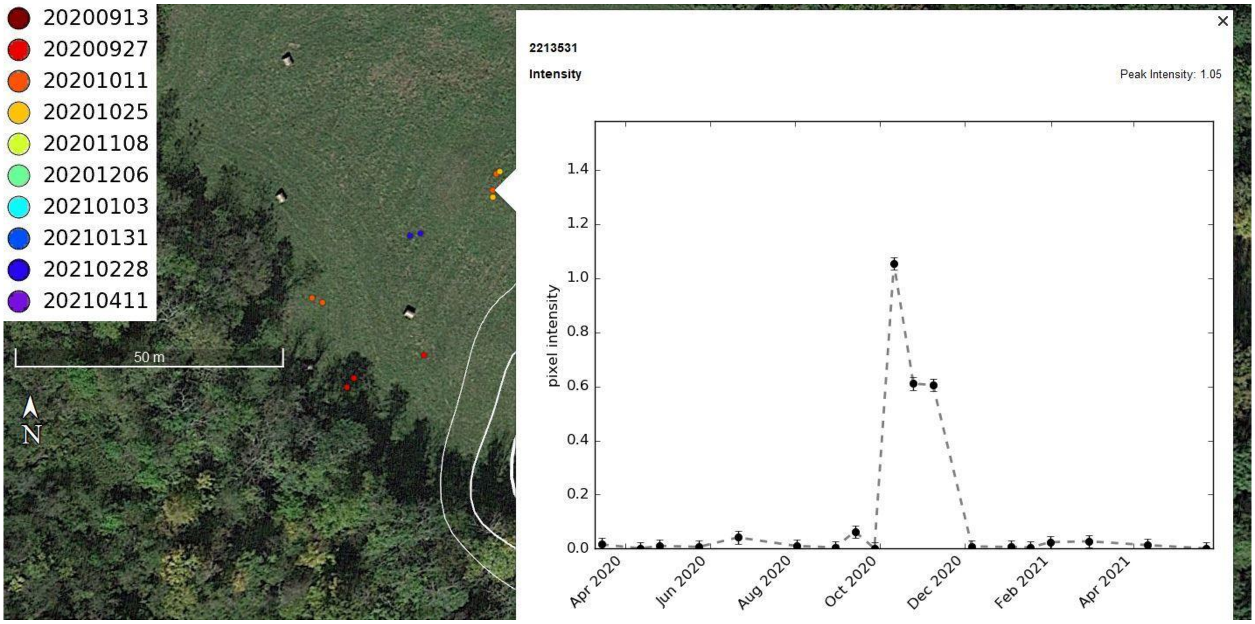

Figure 5.1. A screenshot showing a New Object Detection data point. The point color indicates the date of first appearance as shown in the legend in the top left with dates in YYYYMMDD format.

In addition to the point data, the raster (or heatmap) data shows the radar brightness of areas of interest at each image date (figure 5.2).

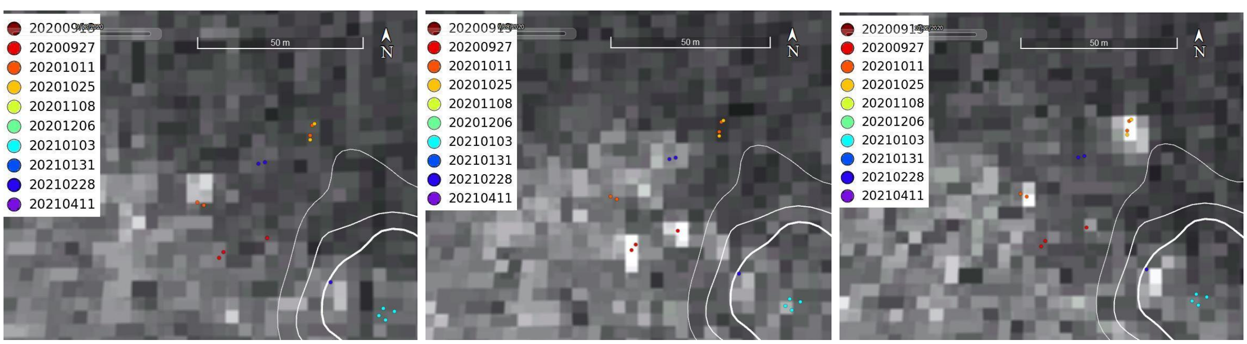

Figure 2. A small section of the amplitude images acquired on September 13th (left), September 27th (middle), and October 11th (right). The clusters of white pixels that appear suddenly are highlighted by the points associated with the image in which those pixels first became much brighter than the average of the past eight images.

6 Conclusions

InSAR shows strong displacement on the slope of interest has been occurring since at least early 2020 and is continuing into 2021. While the dual-look data is sensitive to displacement in more directions, it could only be produced for a shorter time period when images were available from both look directions. The single-look west-looking analysis, while dimensionally restricted in displacement direction sensitivity, has measurements from earlier in 2020 and has a sufficient amount of quality data to produce time series graphs of cumulative displacement over time.

7 Appendix A: Considerations for Monitoring Pipelines with InSAR

This section briefly outlines some concepts that facilitate use of InSAR for geohazard monitoring.

7.1 Resolution

For optical imagery, spatial resolution is defined by the smallest resolvable object. For InSAR however, it is better defined as the minimum distance between adjacent pixels. Spatial resolution of this dataset is 3 m in the raw data as they are acquired, but effective resolution is reduced by necessary processing such that the results are delivered with 4 m pixel spacing. Several adjacent pixels must show displacement together in order to be properly interpreted as displacement by the InSAR algorithms, and to show up in the SNR contours.

7.2 Orbit Revisit Period

Revisit period indicates how long before the satellite can collect data over the same position on the ground. The ALOS-2 satellite used in this analysis revisits the site every 14 days per look direction, however it isn't able to collect data every time due to conflicts with other collection targets.

7.3 Wavelength

A SAR satellite's wavelength is proportional to its tolerance of vegetation. Longer wavelengths like L-band (23.6 cm, used by ALOS-2) have high tolerance to vegetation, maintaining reliable measurements even in forested areas, but they are still limited in very thick forests. The tradeoff is that wavelength is inversely proportional to precision of the displacement measurements. Short wavelengths such as X-band (3.1 cm) and C-band (5.6 cm, used by Sentinel) can produce more precise displacement measurements than L-band, at the cost of sparser coverage in vegetation. Short wavelengths are best suited to arid areas with minimal vegetation and urban areas with abundant hard surfaces such as buildings, bridges, and pavement.

7.4 Look Directions and Displacement Sensitivity

InSAR is inherently one dimensional; displacement is measured in the line of sight (LOS) of the satellite. Displacement for a target moving down a slope that happens to exactly coincide with the look direction, can be fully captured. In general, however, this will rarely be the case, and InSAR will underestimate the real displacement. Figures 7.1 and 7.2 illustrate the issue with simplified scenarios representing a landslide and subsidence. With some exceptions, slopes that face away from the look direction tend to more often provide better opportunities for InSAR monitoring.

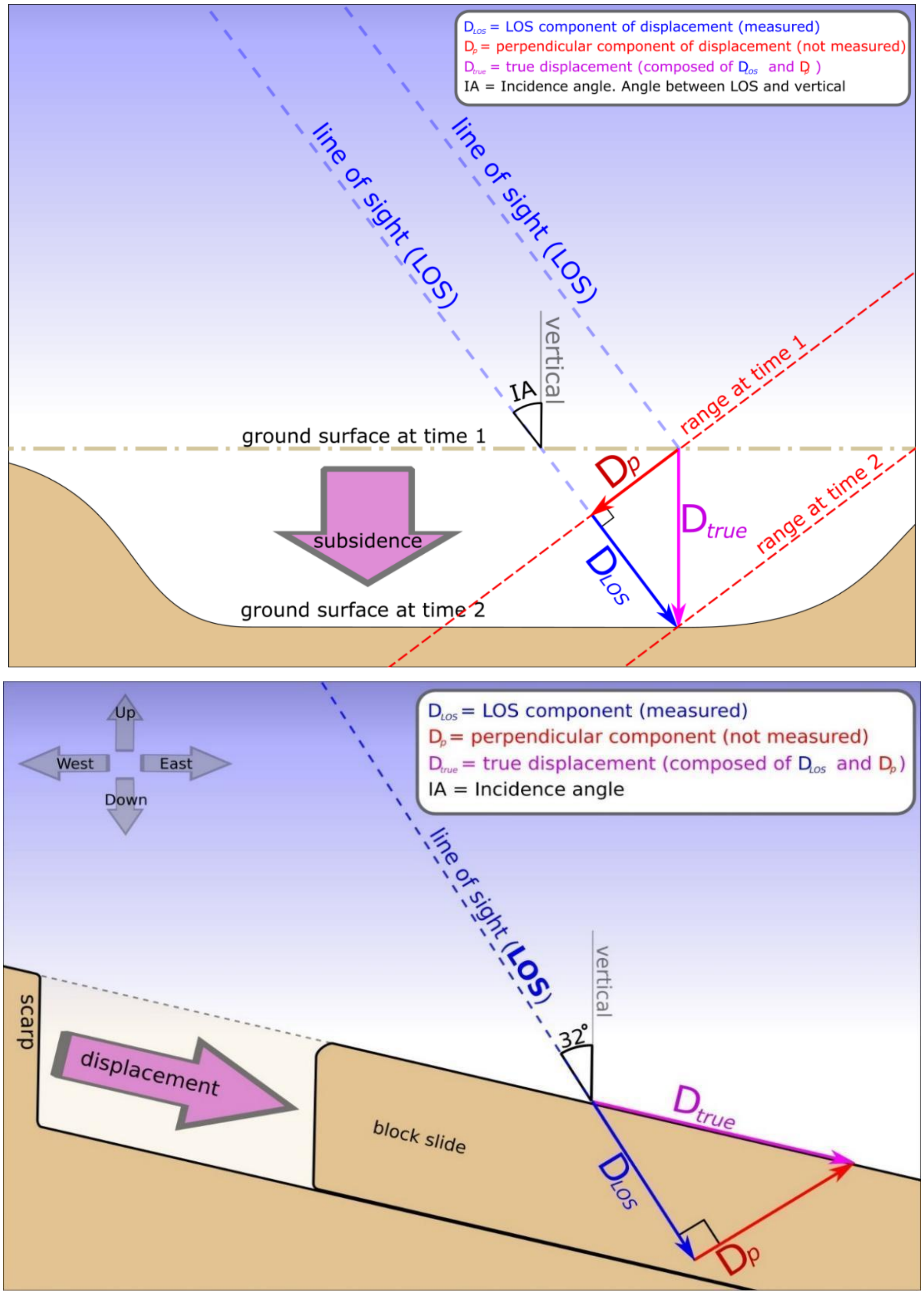

Figure 7.1: Simplified scenarios of vertical subsidence (top) and a block slide on a hill facing away from the satellite (bottom). InSAR underestimates the actual displacement, because it only captures the component that is along the LOS.

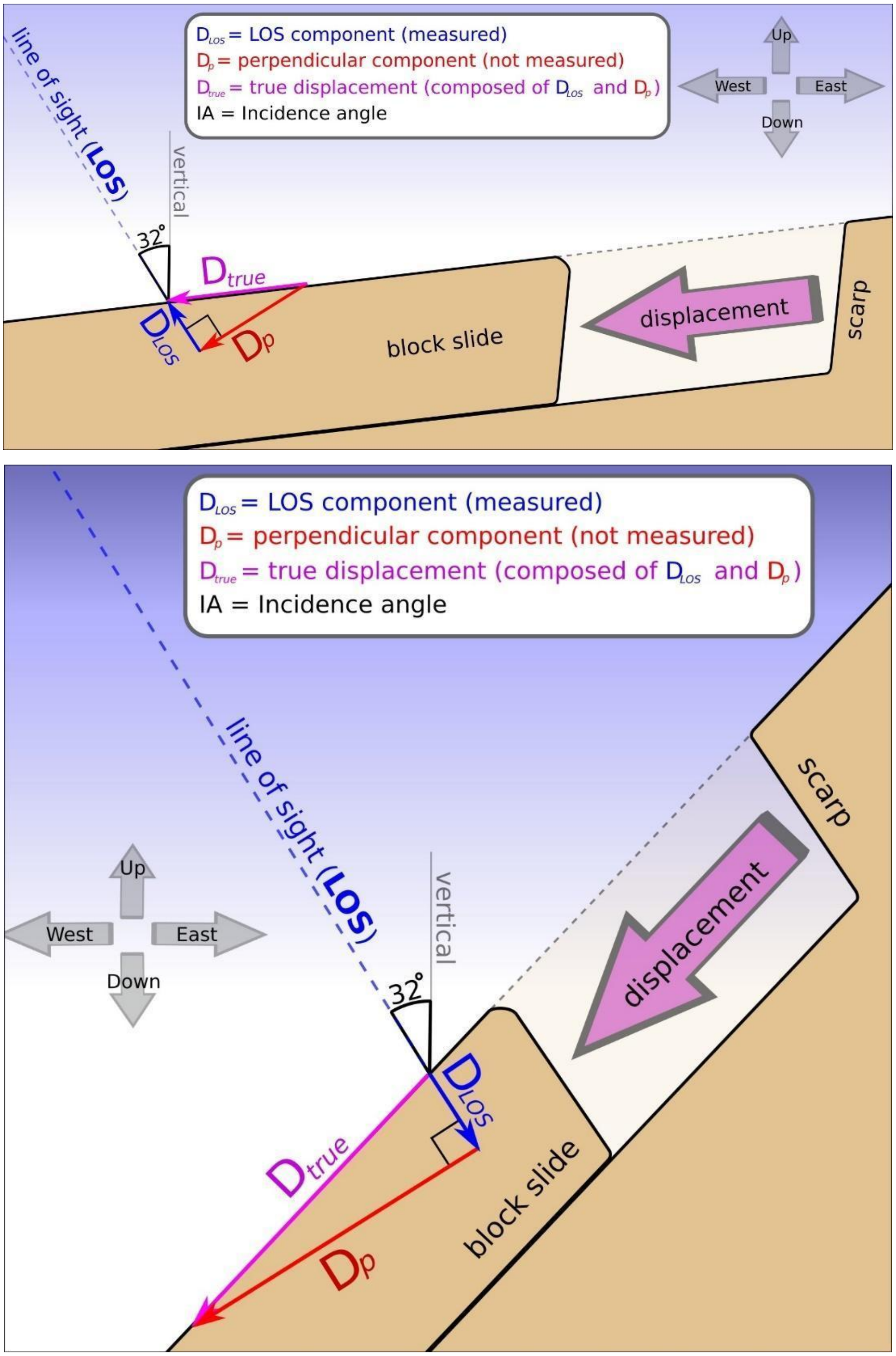

Figure 7.2: Simplified scenarios of displacement on slope aspects oriented facing the satellite. East-facing InSAR has low sensitivity to these slopes so west-facing InSAR should be used.

InSAR only measures the component of displacement that is aligned with the line of sight (LOS) of the satellite. The LOS is a line between the measurement target and the satellite position at the time of measurement. The LOS can be interpreted as the direction that the satellite “looks”, and it can differ between footprints.

All displacement measurements only show the component of displacement that is aligned with the LOS. This geometry means the sensor is insensitive to the north-south component of displacement. Consequently, the full displacement magnitude is often higher than that measured by InSAR, as discussed further in the subsection “Look Directions and Displacement Sensitivity”.

In the displacement rate products, blue areas indicate displacement towards the satellite, referred to as positive displacement. The sideways-looking nature of SAR sensors means that positive displacement is not necessarily moving upwards. The more likely cause of positive displacement signal is a strong lateral displacement component in a specific direction. Further details are explained in the 3vG InSAR Guide, included with this report.